The nanotoxicology of a newly developed zero-valent iron nanomaterial for groundwater remediation and its remediation efficiency assessment combined with *in vitro* bioassays for detection of dioxin-like environmental pollutants

Von der Fakultät für Mathematik, Informatik und Naturwissenschaften der RWTH Aachen University zur Erlangung des akademischen Grades eines Doktors der Naturwissenschaften genehmigte Dissertation

vorgelegt von

Diplom-Biologe
Andreas Herbert Schiwy

aus Tarnowitz (Polen)

Berichter: Universitätsprofessor Dr. rer. nat. Henner Hollert
Universitätsprofessor Dr. rer. nat. Andreas Schäffer

Tag der mündlichen Prüfung 28. Juli 2016

To my wife and my children

Summary

The assessment of chemicals and new compounds is an important task of ecotoxicology. In this thesis a newly developed zero-valent iron material for nanoremediation of groundwater contaminations was investigated and *in vitro* bioassays for high throughput screening were developed. These two elements of the thesis were combined to assess the remediation efficiency of the nanomaterial on the groundwater contaminant acridine. The developed *in vitro* bioassays were evaluated for quantification of the remediation efficiency.

Within the NAPASAN project developed iron based nanomaterial showed in a model field application its nanoremediation capabilities to reduce organic contaminants in a cost effective way. The ecotoxicological evaluation of the nanomaterial in its reduced and oxidized form was conducted with various ecotoxicological test systems. The effects of the reduced nanomaterial with field site resident dechlorinating microorganisms like *Dehalococcoides sp.*, *Desulfitobacterium sp.*, *Desulfomonile tiedjei, Dehalobacter sp.*, *Desulfuromonas sp.* have been investigated in batch und column experiments. A short-term toxicity of the reduced nanomaterial was shown. However, in a prolonged investigation the NZVI did not show any chronic toxic effects to dechlorinating microorganisms in a time-frame up to 300 days. The contribution of this thesis was the toxicological assessment of the oxidized nanomaterial with ecotoxicological model organisms like *Desmodesmus subspicatus*, *Daphnia magna*, *Danio rerio* and *Salmonella typhimurium*. The oxidized NZVI showed a toxicity at elevated concentrations of >100 mg/L. The most sensitive test system was the Daphnia acute toxicity test with an EC_{50} value of 163 mg/L. All other test systems showed a lower or no toxicity of the nanomaterial. Therefore, the nanomaterial can be applied in nanoremediation applications without comprehensive constrains. Especially, as these elevated concentrations will only occur at the contaminated hot spots during the application of this technology as it has been shown that a transport away from the remediation site is not probable.

As a second element of this thesis the development of *in vitro* bioassays to elucidate toxicity in high throughput applications have been conducted. Therefore, the micro-EROD bioassay to determine the CYP1A-inducing potential of samples was developed. Recently, its protocol to investigate environmental sample was presented in *Nature protocols* in detail. This protocol can be applied to a multitude of samples types (feed and food, chemicals, sediments etc.) und has the advantage of sensitivity and ready to use methodology. Evolving this bioassay new cell lines in a serum-free animal component-free chemically defined medium and suspension culturing conditions have been developed. The investigations with reference compounds like TCDD showed that these newly developed cell lines were highly comparable to the established adherent cell lines. The EC_{50} value for the newly developed H4IIE-S cell lines was 11 pM, which was comparable to the adherent H4IIE cell line. The adherent cell line was presented in

literature with EC_{50} values ranging from 5 pM to 47 pM. The newly developed system showed the feasibility of high throughput with clear financial benefits in comparison to the established technology, as the cultivation in suspension is more cost efficient. In this cultivation mode the whole volume is used for cultivation compared to adherent cell lines for which only the surface of a culturing vessel can be used.

As synthesis the effect of the newly developed NZVI on a model compound in co-exposure has been investigated. The heterocyclic polyaromatic hydrocarbon acridine was applied as a model contaminant as it showed in literature mechanism specific toxicity. It was selected to evaluate the application of bioassays for the assessment of the remediation efficiency of the newly developed nanomaterial. At first the co-exposure of the iron nanomaterial with acridine was evaluated in the fish embryo toxicity test with accompanying instrumental analysis. The results showed a toxicity of acridine with an EC_{50} value of 1 mg/L, which was comparable to results obtained in literature. The newly developed NZVI did not show any effects on acridine in the fish embryo toxicity test and the instrumental analysis. Additionally, the micro-EROD bioassay did not indicate any dioxin-like potential for this compound. These results were not expected as acridine showed dioxin-like activity and NZVI were applied for remediation of heterocyclic polyaromatic hydrocarbons like acridine in literature. Various factors like passivation of the nanomaterial or a high stability of the model compound could have influenced the outcome of the investigations. For the *in vitro* investigations of the dioxin-like potential of acridine a substrate inhibition or a species related low receptor affinity could have caused this results. Both elements should be investigated in follow-up studies. The application of a dioxin-like activity monitoring *in vitro* bioassay to elucidate the remediation efficiency was not successful. Therefore, another compound should be applied as the model groundwater pollutant. Possible candidate substances are PAHs or β-naphthoflavone or TCDD as they are more potent CYP1-inducer. Nevertheless, *in vitro* bioassays can be applied as monitoring tools for remediation applications. Especially, for effect directed analysis *in vitro* bioassays are suitable to elucidate the fraction with a specific toxicity. For this application the newly developed cell lines in suspension are especially beneficial. They can be used to investigate extracts of environmental samples with reduced handling effort and thus improve the analytical throughput significantly

Zusammenfassung

Die Bewertung von Chemikalien und neuen Substanzen ist eine wichtige Aufgabe der Ökotoxikologie. Thema dieser Dissertation ist die Bewertung eines neu entwickelten eisenbasierten Nanomaterials zur Remediation von Grundwasserschadensfällen und die Entwicklung von bioanalytischen *In vitro*–Verfahren, um die Toxizität von Substanzen im Hochdurchsatz zu untersuchen. Diese beiden Untersuchungsschwerpunkte wurden in der vorliegenden Arbeit kombiniert. Anschließend sollte mit Hilfe des Schadstoffs Acridin die Anwendung von Bioassays zur Bewertung der Remediationsleistung erprobt werden.

Das im NAPASAN Projekt neuentwickelte nullwertige Eisennanomaterial zeigte das Potential organische und anorganische Umweltgifte auf eine kostengünstige Art zu beseitigen. Dies wurde am Beispiel einer Nanoremediationsanwendung an einem Modellfeldstandort gezeigt. Die ökotoxikologische Untersuchung des Materials wurde mit unterschiedlichen ökotoxikologischen Tests in der reduzierten und oxidierten Form durchgeführt. Als Testorganismen für die Untersuchung des reduzierten Materials wurden Vertreter ausgewählt, die im Feldstandort heimisch sind. Zu diesen gehören die dechlorierenden Mikroorganismen *Dehalococcoides sp.*, *Desulfitobacterium sp.*, *Desulfomonile tiedjei*, *Dehalobacter sp.* und *Desulfuromonas sp.*. Diese wurden in Batch- und Säulenversuchen untersucht. Darüber hinaus wurden Modellorganismen wie *Desmodesmus subspicatus*, *Daphnia magna*, *Danio rerio* und *Salmonella typhimurium* zur ökotoxikologischen Bewertung des oxidierten Eisennanomaterials verwendet. Die Ergebnisse zeigten eine kurzzeitige Toxizität des reduzierten Nanomaterials gegenüber den Mikroorganismen. Jedoch wurde in Langzeitstudien über einen Zeitraum von 300 Tagen keine chronische Toxizität des Nanomaterials gegenüber den dechlorierenden Mikroorganismen beobachtet. Das oxidierte Material zeigte eine Toxizität nur bei Konzentrationen >100 mg/L. Die empfindlichsten Organismen waren die Daphnien mit einem EC_{50}-Wert von 163 mg/L. Alle weiteren Testsysteme zeigten eine geringere Toxizität des oxidierten Nanomaterials. Aus diesem Grund kann das Nanomaterial ohne große Einschränkungen angewendet werden, besonders da solche erhöhten Konzentrationen nur in Rahmen einer gezielten Remediationsanwendung vorkommen und nur sehr lokal auftreten. Ein Transport des Materials in ökotoxikologisch relevanten Konzentrationen ist nicht wahrscheinlich.

Im zweiten Teil der vorliegenden Arbeit lag der Fokus auf der Entwicklung eines *In vitro*-Verfahrens. Dazu wurde der Micro-EROD Bioassay zur Bewertung des CYP1A-Induktionspotentials entwickelt. Das in *Nature Protocols* veröffentlichte Protokoll des Mikro-EROD Bioassays bietet eine detaillierte Beschreibung der Methode. Mit dieser neu entwickelten Methode kann eine Vielzahl von Probentypen (Lebensmittel, Chemikalien, Sedimente etc.) untersucht werden. Zusätzlich bietet die Methode den Vorteil einer hohen Sensitivität und leichten Zugänglichkeit selbst für Personal mit wenigen Erfahrungen im Bereich der zellbasierten Analytik. Aufbauend auf diesem Bioassay wurden neue Zelllinien entwickelt, die in einem serumfreien chemisch definierten Medium in Suspension kultiviert werden. Die Untersuchungen mit Standardsubstanzen wie TCDD zeigten für die

neuentwickelten Zelllinien eine hohe Vergleichbarkeit zu den etablierten Zelllinien. Der ermittelte EC_{50}-Wert gegenüber TCDD betrug mit der neu entwickelten H4IIE-S Zelllinie 11 pM und war damit vergleichbar mit adhärenten H4IIE Zellen für die in der Literatur ein EC_{50}-Werte zwischen 5 pM und 47 pM publiziert wurde. Dabei überwiegen die ökonomischen Vorteile des neu entwickelten Systems, da die Kultivierung der Zellen in Suspension effizienter und kostengünstiger ist. In diesem Modus kann das gesamte Volumen eines Kulturgefäßes für die Kultur der Zellen verwendet werden, während bei adhärenten Zellen nur die Grundfläche zur Verfügung steht.

Als Synthese wurde der Effekt des neuentwickelten Nanomaterials mit dem Schadstoff Acridin in Ko-exposition untersucht. Da Acridin in bereits publizierten Studien eine Mechanismus-spezifische Aktivität zeigte, wurde es als Modellschadstoff ausgewählt, um mit diesem Schadstoff die Anwendung von *In vitro*-Testverfahren bei Ko-exposition des Acridins mit dem Nanomaterial zu untersuchen. Zunächst wurde die Ko-exposition des Eisennanomaterials mit Acridin im Fischembryotoxizitätsassay mit dem Zebrafisch *Danio rerio* mit begleitender instrumenteller Analytik untersucht. Die Ergebnisse zeigten eine Toxizität von Acridin gegenüber Fischembryonen mit einem ermittelten EC_{50}-Wert von 1 mg/L, was mit bereits publizierten Daten übereinstimmte. Das neu entwickelte Eisennanomaterial zeigte weder im Fischembryotoxizitätstest noch bei den Ergebnissen der instrumentellen Analytik einen Effekt auf den Modelschadstoff. Zusätzlich zeigte die Untersuchung im Mikro-EROD Bioassay keine dioxin-ähnliche Wirksamkeit für Acridin. Diese Ergebnisse entsprachen nicht den Erwartungen, da Acridin als dioxin-ähnlich wirksam und nanoskaliges Eisen als geeignet für die Remediation von heterozyklischen polyaromatischen Kohlenwasserstoffen in der Literatur beschrieben wurden. Diverse Faktoren wie eine Passivierung des Nanomaterials oder zu hohe Stabilität des Modelschadstoffs könnten hierbei eine Rolle gespielt haben. Für die I*n vitro*-Untersuchung zur dioxin-ähnlichen Aktivität von Acridin könnte eine Substrathemmung oder eine speziesabhängige Rezeptoraffinität zu den Ergebnissen geführt haben. Beide Elemente sollten in Folgestudien untersucht werden.

Zusammenfassend lässt sich sagen, dass die Kombination von *In vitro*-Bioassays zur Bewertung der Remediationsleistung noch nicht vollständig ausgereift ist. Es besteht noch dringender Forschungsbedarf in diese Richtung. Außerdem sollte die Modelsubstanz noch mal angepasst werden und die Studie mit z.B. einem PAH oder Substanzen wie β-Naphthoflavon oder TCDD wiederholt werden. Erst dann kann abschließend beurteilt werden inwieweit sich *In-vitro* Bioassays eignen, um die Remediationsleistung zu untersuchen. Die Anwendung der neu entwickelten Zelllinien in Suspension ist jedoch für die Bewertung von unbekannten Altlastenstandorten vielversprechend und sollte in Folgestudien weiterentwickelt werden. Besonders in der Kombination mit instrumenteller Fraktionierung und Analytik können die neu entwickelten Suspensions-Zelllinien helfen im Hochdurchsatz eine effektdirigierte Analytik zur Identifikation der für die Effekte verantwortlichen Schadstoffe durchzuführen.

Table of Content

List of Abbreviations

°C	Degree Celsius
µm	Micrometre
1D	One dimensional
2-AA	2-Aminoanthrancene
2D	Two dimensional
3D	Three dimensional
3Rs	Reduction, Refinement and Replacement
4-NOPD	4-nitro-o-phenylendiamin
AhR	Aryl hydrocarbon receptor
ATCC	American Type Culture Collection
AU	Absorbance units
AZA	5-Azacytidine
BCA	Bicinchoninic acid
bioTEQs	Bioassay derived TCDD equivalent quotients
BMBF	Federal Ministry of Education and Research in Germany
BRK-Medium	Bringmann and Kühn medium
BSE	Bovine spongiform encephalopathy
CCD	Charge-coupled device
cDCE	Cis-1,2-dichloroethene
CDM	Chemically defined media
CHCs	Chlorinated hydrocarbons
CNTs	Carbon nano tubes
CO_2	Carbon dioxide
CV	Coefficient of variation
CYP1A	Cytochrome enzyme subfamily 1A
D	Diffusion coefficient
D/I	Dimethylsulphoxide and isopropanol
DAD	Diode array detector
DCF	2',7'-dichlorofluorescein
DCFDA	2′,7′-dichlorodihydrofluorescin diacetate
DCFH	2',7'-dichlorodihydrofluorescin
d_H	Hydrodynamic diameter
DIN	Deutsches Institut für Normung

DLCs	Dioxin-like chemicals
dl-PCBs	Dioxin-like PCBs
DLS	Dynamic light scattering
DLVO	Derjaguin-Landau-Verwey-Overbeek
DMEM	Dulbecco/Vogt modified Eagle's minimal essential medium
DMSO	Dimethylsulphoxide
DMSO+I	Dimethylsulphoxide + isopopanol
DNA	Deoxyribonucleic acid
DPBS	Dulbecco's Phosphate-Buffered Saline
EC	European Commission
EC_X	Effect concentrations
EDA	Effect directed analysis
EDL	Electrical double layer
EDX	Energy dispersive x-ray analysis
EELS	Electron energy loss spectroscopy
ELS	Electrophoretic light scattering
ENM	Engineered nanomaterials
EROD	7-ethoxyresorufin-*O*-Deethylase
ETX	7-ethoxyresorufin
FAU	Formazine Attenuation Units
FBS	Fetal bovine serum
FCS	Fetal calf serum
Fe(0)	Zero-valent iron
Fe(II)	Ferrous iron
Fe(III)	Ferric iron
Fe(IV)	Ferryl iron
FET	Fish embryo toxicity test
FU	Fluorescence units
g/L	Gramm per litre
h	Hour or hours
H_2O_2	Hydrogen peroxide
HCl	Hydrochloric acid
HEPES	2-[4-(2-hydroxyethyl)piperazin-1-Yl]ethanesulfonic acid
hetero-PAHs	Heterocyclic polyaromatic hydrocarbons

hpf	Hours post fertilization
HPLC	High performance liquid chromatography
hr	Hours
ISO	International Organization for Standardization
k_B	Boltzmann constant
LABO	Bund/Länder-Arbeitsgemeinschaft Bodenschutz
LC50	Lethal concentration with 50 % effect
LOD	Limit of detection
LOQ	Limit of quantification
mg/L	Milli gramm per litre
min	Minute
ms	Millisecond
MSDS	Material Safety Datasheet
NADPH	Nicotinamide adenine dinucleotide phosphate
NaOH	Sodium hydroxide
NAPASAN	Nano Particles For Groundwater Damage Repair
NC	Negative control
NF	Nitrofurantoin
nm	Nanometre
NOM	Natural organic matter
NSO	Nitrogen, sulphur and oxygen
NZVI	Nanoscale zero-valent iron
OD	Optical density
OECD	Organization for Economic Co-Operation and Development
p.a.	Pur analysis
PBS	Phosphate buffered saline
PC	Positive control
PCBs	Polychlorinated biphenyls
PCDD/Fs	Dibenzo-*p*-dioxins and dibenzo furans
PCE	Perchloroethene
PCE	Perchlorethylene
PCR	Polymerase Chain Reaction
PDI	Polydispersity index

pH	Negative of the logarithm to base 10 of the activity of the hydrogen ion
POPs	Persistent organic pollutants
PP	Polypropylene
PS	Polystyrene
PSE	Pressurized solvent extraction
PSL	Polystyrene latex
PTFE	Polytetrafluoroethylene
QC	Quality Control
REACH	Registration, Evaluation, Authorisation and Restriction of Chemicals
RFU	Relative fluorescence unit
ROS	Reactive oxygen species
rpm	Revolutions per minute
SEM	Scanning Electron Microscope
SFM	Serum-free medium
SME	Small and medium sized enterprises
SOP	Standard operating procedure
T	Absolute temperature
TC	Treatment control
TCDD	2,3,7,8, tetrachlorodibenzo-*p*-dioxin
TCE	Trichloroethylene
TEM	Transmission Electron Microscopy
TEQs	TCDD equivalent quotients
TiO2	Titanium dioxide
TPP	Techno Plastic Products
UBA	Environmental Protection Agency
UFPs	Ultrafine particles
UV	Ultra violet
VC	Vinyl chloride
WING	Materials innovations for industry and society
XDLVO	Extended Derjaguin-Landau-Verwey-Overbeek
Z-Average	Cumulated mean of DLS size measurements
ZVI	Zero-valent iron

ζ-potential	Zeta potential
η_0	Viscosity

List of Figures

List of Tables

Chapter 1
Introduction

1.1. Introduction

Nanotechnology is regarded as the most important technology for the 21st century. It is a source of new products and processes. The annual world consumption of nanoscale chemicals and materials is estimated to be 11 million tons with an approximate value of 20 billion Euros (EC, 2012c). The estimated market volume of nanotechnology is estimated to range from 0.3 to 2.6 trillion dollar for the year 2015 (Kovalev, 2013).The two most dominant products in the market are carbon black with 9.6 million tons and synthetic amorphous silica with 1.5 million tons (EC, 2012c). Newly developed engineered nanomaterials (ENMs) like carbon nano tubes (CNTs), silver, titanium dioxide nanoparticles or nanoscale zero-valent iron (NZVI) account only for a small percentage of the production volume (Schlag et al., 2011). However, in small volumes these ENMs are already available in many consumer products like sports clothing (silver), water proof clothing, electronics and personal care products like suntan lotions (titanium dioxide) (Chen and Mao, 2007; DTU Environment, 2014; Maynard and Michelson, 2006; Seitz et al., 2013; Volker et al., 2013b). Furthermore, these materials are applied at medical applications and will be in future used for therapy and diagnosis of diseases (Mahapatra et al., 2013; Nel et al., 2009; Singh et al., 2010). In environmental technology ENMs will be applied for remediation technologies called nanoremediation like water treatment and *in situ* remediation (Bhawana and Fulekar, 2012; Karn et al., 2009; O'Carroll et al., 2013). NZVI are a very promising material for remediation applications (Yan et al., 2013b; Zhang, 2003; Zhang and Elliott, 2006). To sum up an increased exposition of the environment as well as human exposure to ENMs is expected (Gottschalk and Nowack, 2011; Klaine et al., 2012; Lin et al., 2010; Mueller and Nowack, 2008; Scheringer, 2008). Handy et al. (2008b) expect that many of the engineered and natural nanomaterials will have the aquatic compartment as their final sink. Hence, aquatic organism will be particularly exposed to nanomaterials (Joner et al., 2007; Moore, 2006).

1.1.1 Nanotechnology and engineered nanomaterials

The scientific term nanotechnology is defined as the controlled and focused manipulation or modification of matter at the atomic and molecular scale. This technology creates new materials with remarkably varied and new physico-chemical properties (Handy et al., 2008b; Roco, 2003). It is a rapidly expanding area of research with huge potential in many sectors. This technology has evolved over the last decades and the term nanotechnology was first applied to the manipulation of atoms and molecules to obtain macroscale products by Prof. Dr. Taniguchi (1974). Following, the term has been extended by the National Nanotechnology Initiative to

include all research concerning matter with one dimension below 1 to 100 nm (Roco, 1999b). This defined scale includes the quantum mechanical effects that are the source of the materials new properties. Hence, the extended definition includes not only a particular technology but a research category (Roco, 1999a; Schummer, 2004).

However, not only the definition by Rocco is used in the scientific community but many different coexist for the term nanotechnology and nanomaterial (Joachim, 2005; Maynard, 2011; Taniguchi, 1974). These definitions try to include the size, the shape and the production origin of a nanomaterial. The shape of nanomaterials is categorized into different groups: nanoparticles are spherical, nano rods have a rod like shape and nano fibres have a fibre like structure. There are many more structure categories according to Oberdörster et al. (2005).

It has to be mentioned that particles smaller than 100 nm are already categorized by (eco)toxicologist as ultra fine particles (UFPs). This is the toxicological term for materials smaller than 100 nm that were produced in uncontrolled conditions and hence includes also some nanomaterials. The release of these particles into air, terrestrial, marine and aquatic systems is from natural and anthropogenic sources. Natural sources for UFP are volcanic dust (Ammann et al., 1990), colloidal particles in water (Lead and Wilkinson, 2006) and particles originating from ground erosion (Hasegawa et al., 2007). Furthermore, this category accounts also for particles that are released into the environment unintended for example by incineration or corrosion of functionalized surfaces (Christian et al., 2008; Oberdörster et al., 2005). Therefore nano sized particles are not a novelty for the environment (Oberdörster et al., 2007). Animals should have adapted in the long period of evolution to these particles (Handy et al., 2008a). ENMs deviate from the other UFPs as they have unique physico-chemical properties. These properties originate from their size, homogenous chemical composition, special surface properties, solubility, form and agglomeration (Colvin, 2003; Handy et al., 2008b; Nel et al., 2006). However, the most influential aspect onto the properties of ENMs is their size. The ratio between the surface and the volume increases with decreasing size. Hence, the surface of ENMs is bigger when compared to larger objects and results in an increased reaction surface (Handy et al., 2008b). For objects with a diameter below 100 nm the surface increases exponentially. Nel et al. (2006) reported that within this increase also the number of surface defects in the crystal structure may accumulate. These structural defects lead to a modified electron configuration and at last to an increased reactivity. The occurrence of surface defects is related to the chemical composition of an ENM (Kong et al., 2011). ENMs have different layers and are differentiated by their structure (Ghosh Chaudhuri and Paria, 2012). The core is in the centre, followed by the mantle in its surroundings and the outer shell. The material composition

of the core is often used to categorize an ENM. This categorization can be further graduated. For example titanium dioxide nanomaterials can be further graduated into their mineral phases like anatase and rutil (Chen and Mao, 2007). The mantle is the second layer which can differ in its properties from the core. As an example NZVI have after contact with an oxygen atmosphere an oxide layer as a mantle (Grosvenor et al., 2004). Over this mantle a coating can be applied. This coating can be engineered or formed via interaction with biological molecules in the surrounding medium (von der Kammer et al., 2012). The coating modulates the reactivity as well as the bioavailability of an ENM (Nel et al., 2006; Nel et al., 2009). Additionally, showed Handy et al. (2008a), that ENMs have a longer half-life than its ultrafine analogues. Therefore, ENMs are positioned between atomic and molecular structures and the bulk material. To account for this special intermediate position and its specials behaviour in the aquatic environment Handy et al. (2008b) suggested that nanomaterials should have an extended definition. Henceforth, a definition of nanomaterials was proposed that included materials that are in at least one dimension smaller than 500 nm. With this pragmatic definition it shall be account for the phenomenon that nanomaterials at concentration ≥ 10 mg/L tend in natural water to form agglomerates and sediment (Petosa et al., 2010; Phenrat et al., 2009). These agglomerates reach up to µm dimensions but still consist of individual particles that comply with the original definition (Handy et al., 2008b). This definition is still under discussion, as nanomaterials, after agglomeration, loose often their specific optical and chemical properties.
Finally, the European Commission proposed in 2011 a definition for the term nanomaterial which includes natural and incidental materials (EC, 2011): ‘Nanomaterial’ means a natural, incidental or manufactured material containing particles, in an unbound state or as an aggregate or as an agglomerate and where, for 50 % or more of the particles in the number size distribution, one or more external dimensions is in the size range 1 nm-100 nm. In specific cases and where warranted by concerns for the environment, health, safety or competitiveness the number size distribution threshold of 50 % may be replaced by a threshold between 1 and 50 %. By derogation from point 2, fullerenes, graphene flakes and single wall carbon nanotubes with one or more external dimensions below 100 nm should be considered as nano-materials (EC, 2011). The European Commission implemented provisions to review this definition to include experience and scientific and technological developments. (EC, 2012d). However, after some recommendations and a further review from the European Joint Research Centre the definition could not be completely reviewed in the year 2014. Of special interest for this review is the number size distribution threshold of 50 % and wheatear it should be increased or decreased. An update is expected for 2016 (EC, 2016).

1.1.2 Nanotoxicology

The investigation of ENMs toxicity has been widely initiated for a careful and sustainable handling of nanomaterials (Falkner and Jaspers, 2012; Roco, 2007). As an example the Organization for Economic Co-operation and Development (OECD) has founded a program to evaluate the existing toxicity test system for chemicals for the application with ENMs (Kearns et al., 2009; Kühnel and Nickel, 2014). This has been initiated as the toxicity of ENM cannot be concluded from its bulk material. For example, show mainly inert materials like titanium dioxide toxic properties as ENMs (Handy et al., 2008b; Nel et al., 2006). These aspects are accounted for by the establishment of a new branch of ecotoxicology the nanoecotoxicology (Behra and Krug, 2008; Kahru and Dubourguier, 2010; Krug and Wick, 2011; Oberdörster et al., 2005). Many scientific groups investigate the effects of nanomaterials *in vivo* and *in vitro* (Behra and Krug, 2008; Kahru and Dubourguier, 2010; Kahru and Ivask, 2013; Scheringer, 2008). Since 1995 the number of publications was steadily increasing (cf. Figure 1.1). Especially, from the year 2005 onward the number of publications gained momentum and culminated in the years 2014 and 2015. The year 2015 was the first with a lower publication number than the preceding year. Nevertheless, these numbers show how important this field had become.

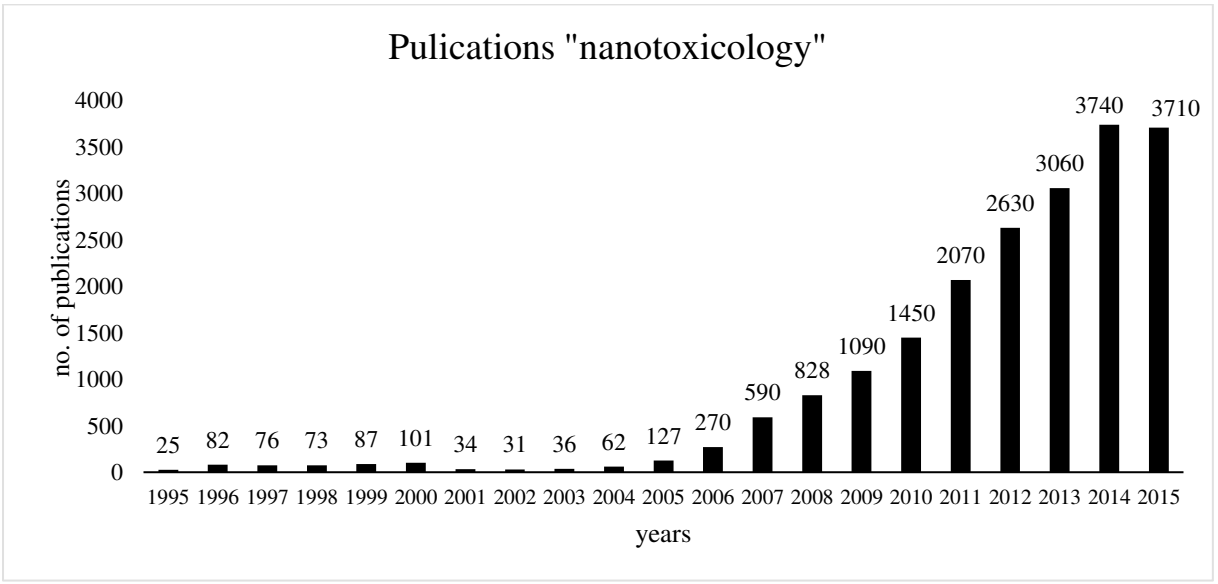

Figure 1.1: Number of publications including the term “nanotoxicology” from the year 1995 to 2015. Source: Google Scholar accessed 06.01.2016

Within these studies different toxic effects like generation of reactive oxygen species, cytotoxicity and mortality are reported for nanomaterials (Colvin, 2003; Handy et al., 2008a; Pan et al., 2013; Rana and Kalaichelvan, 2013).

It is an area of scientific research to elucidate if nanomaterials are more toxic than their micro-sized counterparts (Karlsson et al., 2009; Wyrwoll et al., 2016). Therefore, a size independent toxicity is proposed (Choi and Choy, 2011) and the surface of the materials is brought into focus (Warheit et al., 2007).

1.1.3 Behaviour of engineered nanomaterials in the aquatic environment

Different factors modulate the interaction possibilities of ENMs with biological interfaces and determine their toxicity (cf. Figure 1.2). On the one hand the attributes of ENMs are determined by the material itself like its size, chemical composition, surface modification, form, surface curvature, porosity, roughness and solubility. On the other hand has the surrounding environment influence on the properties of nanomaterials (Petosa et al., 2010). Examples of these interdependences are the ζ (zeta) potential, the particle agglomeration, degradation and solubility (Nel et al., 2009). Various counter measures can be applied to maintain the materials in suspension but most of these methods are tailored to a specific medium. Thus, if ENMs come into contact with the environment new interactions with the aquatic media occur that have an effect on the stability of the suspension.

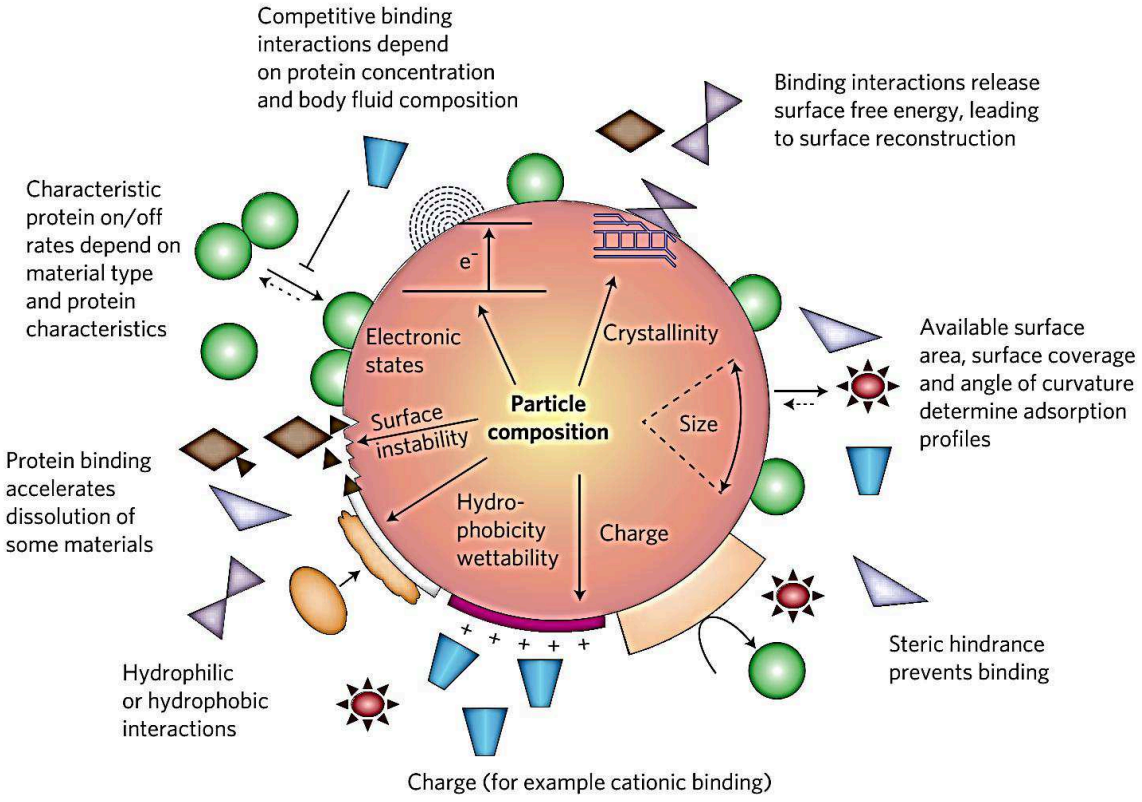

Figure 1.2: Interactions of an engineered nanomaterial (ENM) with biological interfaces– figure re-drawn from Nel et al. (2009)

These interaction with aquatic media often results in agglomeration of the nanomaterial and a sedimentation process (Baalousha, 2009; Handy et al., 2008a; Nichols et al., 2002; Sorensen and Baun, 2015; Zhou et al., 2014). These interaction result for different forces and can be calculated by colloidal chemistry. The forces that have to be taken into account between two particles follow the same principles like all colloid particles. These includes the van der Waals forces, solvation, solvophobic and depletion forces. However, the calculations have to be adjusted to the specific effects of nanomaterials (Handy et al., 2008b; Nel et al., 2009). The interaction with biological materials is much more complex than between particles and makes the calculation even more complex especially as biological systems are constantly undergoing changes (Nel et al., 2009). The described forces and effects are summed up according to their discoverer as the Derjaguin, Landau, Verwey and Overbeek theory (DLVO) theory. This theory describes the stability of lyophobic dispersions by summarizing the repulsive electrostatic and attractive van der Waals forces between the colloid particles (cf. Figure 1.3). It assumes that the surfaces of the particles are planes that have a homogenous and not changing charge density. The surrounding medium influences only the dielectric constant (Cao, 2004). However, this simple DVLO theory is not sufficient to describe the interactions of ENMs in aquatic media. This is due to the unique ENM shape and compositions. Therefore, an extended DVLO (XDVLO) theory was introduced (Gatica et al., 2005). This theory includes also steric repulsion forces originating from absorbed polymer, polyelectrolyte coating or natural organic matter (NOM; cf. Figure 1.3). It can be even further extended to included additional forces like bridging, osmotic, steric, hydrophobic acid-base and magnetic properties. (Hotze et al., 2010).

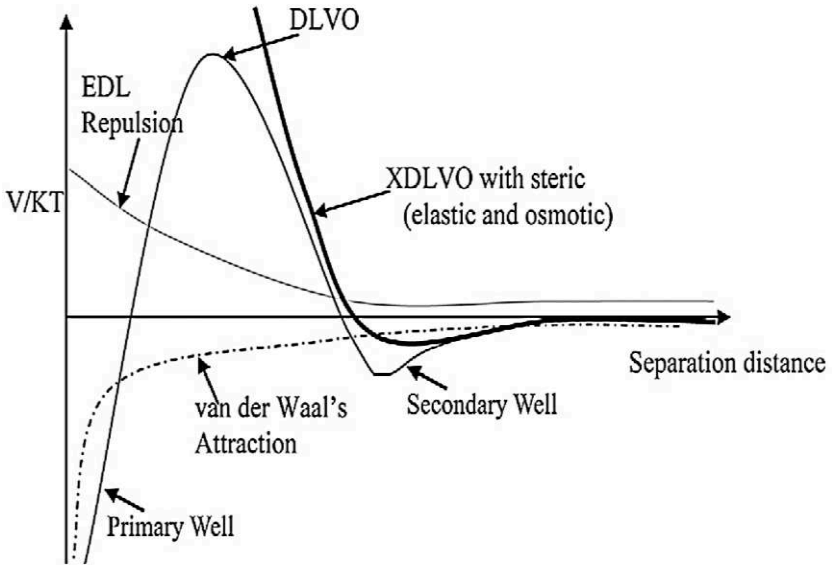

Figure 1.3: The Derjaguin-Landau-Verwey-Overbeek (DLVO) and extended XDLVO theory for nanomaterials figure re-drawn from Hotze et al. (2010), V/KT, potential energy divided by Boltzmann's constant and absolute temperature

The Figure 1.3 shows the different calculated energies that result from the interplay of the different forces and the distance between two particles. If designed properly a configuration can be achieved in which an energy barrier is formed against aggregation. Additionally, with this theory the state of aggregation can be calculated. In Figure 1.3 the two wells are of special importance as they estimate the spatial distance between two particles that result in the primary well in an irreversible aggregation and in the secondary well in a reversible aggregation. However, the study by Phenrat et al. (2007) showed that by including magnetic force into the XDLVO this force dominates the interaction energy and thus no predicted energy barrier to aggregation and wells can be calculated.

1.1.4 Toxic reactions at the surface of engineered nanomaterials

On the surface of a nanomaterial a multitude of reactions can occur (cf. Figure 1.4). The factors affecting the reactions are: material composition, electronic structure, surface coatings, solubility and environmental factors like ultraviolet (UV) light. These reaction include Fenton chemistry, dissolution, redox reactions and generation of reactive oxygen species (ROS) (Nel et al., 2006). Especially, for one component and transition metal nanomaterials the generation of ROS can be a source of toxicity. This reaction is caused by the coincidence of electron acceptors or donors with molecular oxygen. The underlying mechanisms for ROS are a disproportionation or a Fenton reaction. In the presence of transition metal compounds a Fenton reaction with hydrogen peroxide (H_2O_2) can also lead to the formation of ROS (Rodrigo-Moreno et al., 2013). Iron and iron oxide nanomaterials are a good example of a transition metal compounds. These compounds if incorporated can disturb the cellular redox reactions (Auffan et al., 2008; Nel et al., 2006). Some nanomaterials like titanium dioxide induce cytotoxic stress via ROS in reaction to the excitation with UV light (Amiano et al., 2012; Wyrwoll et al., 2016). A further mode of toxicity is the direct interaction with biomolecules which lead to a cleavage of covalent bounds (Nel et al., 2006).

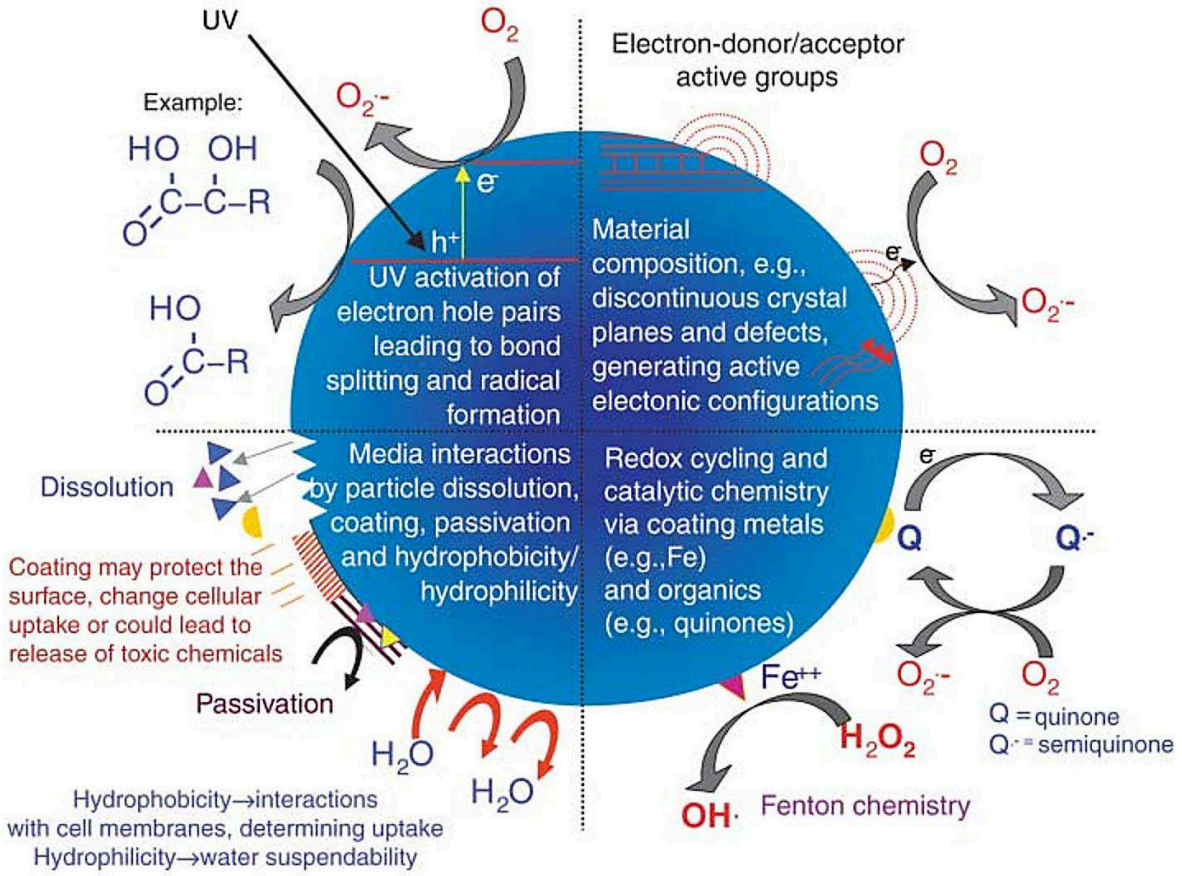

Figure 1.4: Possible reactions at the surface of an engineered nanomaterial (ENM) – figure re-drawn from Nel et al. (2006)

1.2. NAPASAN – Nanoparticles for ground water remediation

Several investigations within this thesis (Chapter 2 and 3) were conducted within the joint research project founded by the federal ministry of education and research of Germany (BMBF) entitled “NAPASAN – Nanoparticles for ground water remediation” grant number 03X0097A. The following paragraph will introduce the scientific, social and economic topics of this project. An important challenge of the 21st century is the sustainable development of our society. Nanotechnology is promising to aid in this difficult task by enabling an industrial development with a reduced demand of resources and facilitating new applications within many disciplines (BMBF, 2003; Corbett et al., 2000).However, sustainability is not limited to do better in the future but means as well to take responsibility for our legacy. In the federal republic of Germany 313,853 (2012) suspected polluted sites were registered and annually 1.1 billion (2004) euro were invested for remediation actions (LABO, 2012; United States International Trade Commission, 2004). Till the year 2012 27,337 sites have been declared as remediated and on further 4,442 sites remediation was ongoing. Another 14,409 sites were declared as

contaminated sites which have to remediated (LABO, 2012). These legacy sites are a global problem with enormous costs. The European Union estimated a remediation cost of 109 billion for all its member states (EC, 2002a). These legacies also reduce the available area for urban development and led to contamination of groundwater. This is of special concern for Germany as 64% of its drinking water is supplied by groundwater. It is Germany´s most import drinking water resource. (Laasch and Laasch, 2013).

Therefore, the development of novel remediation techniques is important to find new and better ways to secure or even restore groundwater aquifers. The BMBF supported the development and application of new nano-based remediation technologies within its WING program (materials innovations for industry and society; BMBF 2003). Within this program the joint project NAPASAN developed a novel cost-effective nanoremediation tool for contaminations with chlorinated dense non aqueous phase liquids (DNAPLs) like chlorinated hydrocarbons (CHCs). These contaminants are important in the context of groundwater remediation. The widespread distribution and high application volumes of CHCs resulted in many environmental contaminations. In a study by Stupp et al. (2007) evaluating 110 groundwater remediation projects elucidated that 62 % of the ongoing remediation actions in Germany in the year 2006 were in the context of CHCs. Due to the high density of CHCs deep aquifer zones are reached by accidental leakages, contaminating large groundwater volumes with long plumes and long lasting source zones (Cohen et al., 1993; Jackson and Dwarakanath, 1999; Stroo et al., 2003). Depending on the conditions of the aquifer the degradation of CHCs can be significantly slower compared to other compounds (Borden et al., 1997; Wiedemeier et al., 1996). Additionally, to achieve a successful remediation both the source and the plume have to be cleaned up (Pankow and Cherry, 1996). Therefore, a cost-effective tool is needed to remediate this contaminant.

The technical approaches for source and plume remediation can be categorized into two groups:

In the first category named pump and treat include technologies that remediate the contaminants as a phase (mobilization) or in a soluble form (solubilization) from the aquifer. This category included the classic pump & treat approach in which groundwater is pumped from the subsurface and treated in facilities on the surface (Heron et al., 1998; Todd and Mays, 1980). Additionally, innovative treatments like the introduction of thermic energy as steam or solid heat sources, and the application of solubilizers like surfactants or alcohols are summarized in this category (Heron et al., 1998; Londergan et al., 2001; Parkinson et al., 2004). The challenges of this category are the long remediation durations (>10 years). Additionally, they often do not meet the remediation goals within a reasonable timeframe and thus create incalculable operating costs (Mackay and Cherry, 1989). Furthermore, the risk of an

uncontrolled mobilization of the contaminants through the reduction of cohesive forces or through displacement of the contaminant has to be accounted for (Baviere et al., 1997; Pennell et al., 1994; Scherer et al., 2000).

The second category consists of technologies that transform the contaminants directly with biological or chemical processes. These technologies are categorized as *in situ* remediation. Natural attenuation or enhanced natural attenuation via microbial degradation, oxidative processes like the application of permanganate or Fenton reagent and reductive processes are summed up in this category (Patil et al., 2013; Schmidt and Tiehm, 2008; Tiehm and Schmidt, 2011; Tiehm et al., 2007; Yeh et al., 2013; Yuan et al., 2013; Zhao et al., 2013). The challenge of these techniques is the technical solution for the contact of the contaminant with the treating agents (Khan et al., 2004). One solution are permeable reactive barriers (Karn et al., 2009). This are constructions within the ground that contain the treating agents and are perfused by the groundwater aquifer (Cantrell et al., 1995). However, these permeable reactive barriers are often difficult to construct as the area on the surface is densely built and the required depths in the subsurface cannot be reached (Grieger et al., 2010). The alternative are injections of the remediation agents - often in large amounts – into the subsurface (Karn et al., 2009). The drawback of this technique is that it can cause unwanted modifications of the aquifer (Müller and Nowack, 2010).

The work within this thesis is a new addition to the second category as nanomaterials can be applied as for *in situ* remediation. This approach is called nanoremediation. Various nanoscale materials like carbon nanotubes, aluminium or zero-valent iron are promising to diminish environmental pollutants directly in the source (Patil et al., 2015). For zero-valent iron the application of nanoscale materials is a advancement of the technology as granulated zero valent iron in permeable reactive barriers has shown the potential to remediate plumes of CHCs (Gillham and O'Hannesin, 1994). However, with these permeable reactive barriers only the plume could be treated and with NZVI the source can be treated. NZVI can be injected *in situ* into the contaminants source and are effective for remediation of various pollutants (Fu et al., 2014a; Köber et al., 2014; Yuan et al., 2013; Zhang, 2003). This nanomaterial can reduce problematic substances like polychlorinated biphenyls (PCBs), dioxins, heterocyclic polyaromatic hydrocarbons (hetero-PAHs) and CHCs (Chang et al., 2005; Gosu and Gurjar, 2013; Gosu et al., 2016; Li et al., 2006; McGeough et al., 2007; Schmidt et al., 2011; Wang and Zhang, 1997; Yan et al., 2013b; Zhang, 2003; Zhang and Elliott, 2006). Furthermore, it can reduce and immobilize heavy metals like chromium and arsenic (Gheju, 2011; Nemecek et al., 2014; O'Carroll et al., 2013; Patil et al., 2015; Ponder et al., 2000; Singh et al., 2012). The

nano-size´s advantage is its enormous specific surface which leads to a very rapid reaction with the contaminants (Bokare et al., 2007; Cantrell et al., 1995; Gillham and O'Hannesin, 1994; Wang and Zhang, 1997). Moreover, they can be injected into permanent or temporal injection wells as well as via cost effective drilling methods directly into the source of contaminants (Dietrich and Leven, 2006; O'Carroll et al., 2013). This aspect is a major benefit as it results in reduced costs as no expensive construction measures have to be applied for remediation. However, the production of NZVI with sufficient transportation range in the underground is still a challenge (de Boer, 2007; De Boer, 2006; Hotze et al., 2010; Kim et al., 2012; Müller et al., 2006a; Müller et al., 2006b; Phenrat et al., 2007). To ensure sustainability of this technology the interactions between microbial and abiotic dechlorination and potential ecotoxicological effects have to be investigated (Baun et al., 2008; Caliman et al., 2010; Flecken et al., 2012; Grieger et al., 2010; Kalin, 2004; Schell et al., 2013; Schiwy et al., 2012; Schmidt et al., 2013; Tiehm et al., 2009; Tiehm et al., 2010). In the NAPASAN project NZVI produced in a cost-effective top down milling process were developed and assessed as a new CHCs´ remediation tool.

1.2.1 Scientific contribution of the NAPASAN project

The main focus of the NAPASAN project was the advancement of a new technology for environmental protection, especially for CHC source zone treatment with NZVI. A cost effective production of suitable nanomaterials and their behaviour in sediment-water-contaminant-system was described in detail. The aim was to improve the manufacturing process of the nanomaterial. On the one hand the NZVI have to be modified with coating or additives to ensure their transport in the saturated aquifer zone and on the other hand their reactivity towards the contaminants needed to be maintained. Biological investigations have analysed the effects of the nanomaterial on the environment. The particles were evaluated concerning their toxic potential and their synergistic or antagonistic effects on the microbial communities of the aquifer. Monitoring techniques for the quantitative detection of nanomaterials based on magnetic susceptibility were developed. The nanomaterial chemical modifications were confirmed in flow, transport and reactivity experiments in various scaling (1D, 2D). For a successful planning and dimensioning of a field application a detailed exploration and a numeric model of the groundwater and contaminant flow, and transport processes were conducted. The mathematic model is based on the results of the experiments. Finally, a pilot application with a 500 kg NZVI injection was conducted at a pilot site (cf. Figure 1.5). This injection was conducted on a site that is difficult to remediate with conventional remediation

techniques. Its location on a parking lot that is accessible only via a narrow street that additionally is closely surrounded by buildings can be seen in Figure 1.5. For this major milestone the pilot site was surveyed and the contamination distribution was modelled. Following, the NZVI injection was prepared with the help of a numeric model and conducted with state of the art injection techniques. Thereafter, the contaminants concentrations as well as the distribution of the NZVI were monitored with various techniques. Through the cooperation of research partners with small and medium sized enterprises (SME) we gained knowledge and the necessary tools for the production, modification, application and monitoring of NZVI.

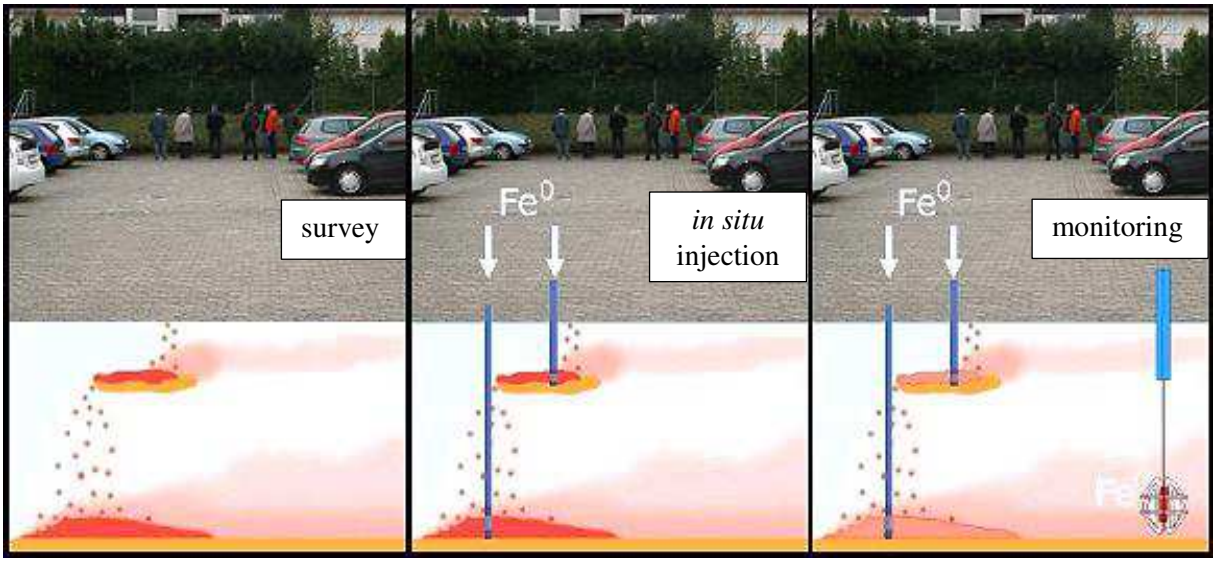

Figure 1.5: Three phases within the field application of the NAPASAN project – Figure redrawn from http://www.napasan.de/ (2011)

1.2.2 Structure of the NAPASAN project

The joint research project NAPASAN was structured into five packages with the following partners:

- **VEGAS** – University of Stuttgart, Institute for Modelling Hydraulic and Environmental Systems, VEGAS - Research Facility for Subsurface Remediation, Stuttgart
- **CAU** - University of Kiel, Institute for Applied Geology - Aquatic Geochemistry and Hydrogeology, Kiel
- **KWI** - DECHEMA e.V., Karl-Winnacker-Institute (KWI), Frankfurt am Main
- **Fugro** – Fugro Consult GmbH, Brunswick
- **IBL** - Umwelt- und Biotechnik GmbH, Heidelberg
- **ITE** – University of Stuttgart, Institute of Theory of Electrical Engineering (ITE), Stuttgart
- **Hermes Messtechnik**, Stuttgart

- **RWTH** – RWTH Aachen University, Institute for Environmental Research, Department of Ecosystem Analysis, Aachen
- **TU Berlin** - Technical University of Berlin, Institute of Environmental Technology, Chair of Water Quality Control, Berlin
- **TZW** – Scientific Association for Gas and Water's (DVGW) Water Technology Centre, Department of Environmental Biotechnology, Karlsruhe
- **UVR-FIA** – UVR-FIA GmbH, Verfahrensentwicklung-Umweltschutztechnik-Recycling, Freiberg

1) Manufacturing and characterization of the NZVI

This work package contained the cost-effective production as well as the modification and characterization of the nanomaterial. In addition to this the potential ecotoxicological effects of NZVI were investigated.

Partner: TU Berlin, UVR-FIA, KWI, TZW, RWTH

2) Introduction and transport of the NZVI in the sub surface

In this module the injection and transport behaviour of the nanomaterial in soil was evaluated. Possible synergism with biological dechlorination was investigated.

Partner: VEGAS, CAU, TU Berlin, TZW, IBL

3) *In situ* monitoring of contaminants and of the NZVI in the aquifer

The development of a field NZVI and contaminant monitoring technique that proved the distribution of the nanomaterials and the degradation of the contaminant in the aquifer was successfully developed in this module.

Partner: VEGAS, ITE, TU Berlin, Fugro, Hermes Messtechnik

4) Numeric modelling of the project site, particle injection and monitoring-system

The numeric modelling was founded on the input parameters of all parties participating. The parameters included the reactivity and transportability of the NZVI. Its output was used for the planning of the pilot project.

Partner: CAU, Fugro

5) Implementation and field application

The work packages one to four cumulated in the second project phase - the field application. It was performed in three phases (survey, injection, monitoring; cf. Figure 1.5) to showcase the benefits and possible problems of the technology. An extensive on-site monitoring for biological and chemical parameters was conducted.

Partner: Fugro, IBL, VEGAS

1.2.3 Nanotoxicology within the NAPASAN project

In this thesis different ecotoxicological aquatic and mechanistic test systems were applied to investigate the environmental impact of the newly developed NAPASAN nanomaterial as our contribution to work package 1 – Manufacturing and characterization of the NZVI – within the joint research project NAPASAN. An extensive characterization was conducted for this nanomaterial to elucidate the state of the nanomaterial and to gain insight about nanospecific toxicity. In the following paragraph these characterization and toxicity assessment methods are introduced.

1.3. The characterization of engineered nanomaterials

A detailed characterization of ENMs is crucial for the understanding of the specific nano effects and to distinguish them from the effects of the bulk material (Powers et al., 2006; Warheit, 2008). Therefore, many techniques have to be applied to investigate ENMs (Joshi et al., 2008; Powers et al., 2006). Also new techniques have been developed to gain further insight (Carr and Malloy, 2006). However, these techniques are cost intensive and require some special sample treatment (Powers et al., 2006). This treatment can have an influence on the sample and make it difficult to interpret the results (Jiang et al., 2009; Powers et al., 2006). To investigate ENMs an applied technique should distinguish objects smaller than 10 nm. Hence, classical light microscopy is not applicable as it cannot overcome the Abbe-Limit (<200 nm) (Heintzmann and Ficz, 2006; Stelzer, 2002). Below this limit inevitable aberrations and diffraction phenomena occur. Techniques that detect structures below this limit have been developed. However it was a challenging task as even transmission electron spectroscopy, a microscopic technique applying smaller than light electrons, was not able to overcome this limit till the 1960s (Ruska, 1987). Therefore, only elaborate techniques can give information in the nanoscale and not all of them can be widely applied. Some of these techniques have only a narrow working range within only are few magnitudes and other are only applicable to ENMs with distinct properties (Powers et al., 2006). To sum up, a ready to use technique to investigate different sized nano and non nano materials that is transportable and easily to use without sample preparation in real life situations is still missing. The techniques applied in this thesis included dynamic light scattering (DLS), transmission electron microscopy (TEM) with energy dispersive x-ray analysis (EDX), and x-ray diffractometry (XRD).

1.3.1 Dynamic light scattering

Dynamic light scattering (DLS) is a non-invasive technique, which is used for the size characterization of dispersions in the sub-micrometre range (Nickel et al., 2014). It is also known as photon correlation spectroscopy or quasi-elastic light scattering (Mattison et al., 2003). The basic principle of DLS is the scattering of light by particles in a suspension. DLS measures the intensity fluctuation of scattered light caused by the Brownian motion of particles leading to constructive/destructive interferences. According to the Stokes-Einstein equation (Equation 1.1), the diffusion coefficient D is inversely proportional to the hydrodynamic diameter of the particles.

$$d_H = \frac{k_B T}{3\pi\eta_0 D} \quad \text{Stokes-Einstein equation}$$

Equation 1.1: Stokes-Einstein equation; d_H = hydrodynamic diameter, k_B = Boltzmann constant, T = absolute temperature, η_0 = viscosity and D = diffusion coefficient

This means that small particles show relatively large and larger particles a small diffusion coefficient. From this, it follows that smaller particles move more rapidly than larger particles. By observing the motion and determining the diffusion coefficient of particles in liquid media, fluctuations of scattered light intensities over time, it is possible to determine their hydrodynamic size, via an autocorrelation function G (cf. Equation 1.2) (Hassellov et al., 2008; Mattison et al., 2003; Xu, 2001).

$$G = \int_0^\infty I(t)I(t+\tau)dt = B + Ae^{-2q^2 D\tau}$$

Equation 1.2: Intensity correlation function G; B = baseline, A = amplitude, D =translational diffusion coefficient (Mattison et al., 2003)

The intensity correlation function of the signal, G, decays at an exponential rate which is dependent upon the diffusion of the particles being measured (ISO, 1996). The particles size calculations hold only for spherical particles if they are significantly smaller than the wavelength of the laser light (i.e. below 250 nm). Only then, the Rayleigh scattering is applicable. Polydisperse samples measurements should be performed at different angles, and DLS is not recommended for unstable or drifting systems. The result is a scattering intensity weighted particle size distribution. Larger particles typically dominate the size results, as the intensity of the scattered light generally increases with particle size. For small particles below 100 nm, the Rayleigh approximation postulates that the intensity is proportional to size by the power of six (Hahn, 2006). For example, the scattered intensity of a 100 nm particle is one million times higher as the scattered light of a 10 nm particle of the same composition, leading to a shadowing of smaller particles. Therefore, small particles or any weak scatterers are

underestimated or even not detected in a polydisperse suspension using DLS. This technique is ready to use as only a suspension is measured in a cuvette. However, various prerequisites have to be fulfilled for a measurement that is meaningful and can be shared with the scientific community (Tiede et al., 2008). Hence, its applicability with environmental samples that include interfering factors is limited.

1.3.2 Transmission electron microscopy and energy dispersive x-ray analysis

The transmission electron microscopy (TEM) uses a beam of electrons to depict ultra-thin samples. The image is formed through the interaction of the electrons with the specimen. It is magnified and focused on a fluorescent screen or a CCD camera. This microscopy technique is capable to investigate samples at significantly higher resolution than light microscopy. The reason for this higher resolution is the much smaller de Broglie wavelength of electrons. Hence, transmission electron microscopy can resolve objects that are thousands of times smaller than light microscopy (Williams and Carter, 2009). This analysis method is applied in a wide range of scientific fields in physics and biologic science. The first TEM was built by Max Knoll and Ernst Ruska in 1931 (Ruska, 1987). However, this device was not able to reach a higher resolution than light microscopy. Its successor was able to overcome this resolution limit in 1933. A first commercial successful TEM was available in 1939. It had a 30,000-fold magnification (Williams and Carter, 2009). Subsequent development led to instruments that were able to magnify a specimen 100,000-fold in 1954 (Ruska, 1987). The development of TEMs had to overcome difficulties that were closely connected to the advantages of this technology. For example, the short material wavelength - a prerequisite for good resolution - is the reason for specimen damage because of the high electron energy. The deflectability of electrons in the magnetic field – a precondition for lens imaging – is also the cause of problems and limited the resolution as this magnetic field, within the microscope, has to be effectively shielded against magnetic fields in the surrounding environment (Ruska, 1987). With technical development some of these problems were solved. Additional benefits of a TEM are that it is possible to add other analytic technologies like energy dispersive x-ray spectroscopy or electron energy loss spectroscopy into the analytical setup (Reimer, 1984). This development led to devices that can investigate not only small objects but combined with other technologies can give qualitative and quantitative answers on the species and structure of samples. The energy dispersive x-ray spectroscopy investigates the interaction of x-ray excitation with a sample (Cao, 2004). The source of the x-ray excitation can be an electron beam or an x-ray beam. The x-ray emissions of a sample are characteristic for its atomic composition as each element has a

unique atomic structure. Therefore, by detecting and measuring the x-ray emission the elemental composition of a sample can be determined with this analytic technique (Shindo and Oikawa, 2002).

1.3.3 X-ray diffraction spectrometry

The x-ray diffractometry is an analytical technique that can identify the atomic and molecular structure of crystals (Snyder, 2006). The underlying principle is the diffraction of x-ray beams caused by atoms within a crystal. These diffracted beams are analysed concerning their angel and intensity to obtain a three dimensional picture of the electron density within a crystal. With this information the positions, the chemical bonds, the disorder and many other information of the crystal atoms are calculated. Finally, the crystal structure is elucidated. This technique can be applied to investigate metals, salts, minerals and various organic and biological molecules. The x-ray diffractometry was crucial for the understanding of many biological molecules like vitamins, drugs, proteins and nucleic acids (Franklin and Gosling, 1953; Watson and Crick, 1953). An x-ray diffractometry measurement requires the sample to be placed on a goniometer. Then the sample is rotated while being exposed to an x-ray radiation source from a fixed angle. The diffraction pattern is recorded into a 2D image. It consists of reflections that can be described as spaced spots. A series of 2D pictures taken at different angels is then mathematically converted into a 3D model of the electron density through Fourier transforms. Limiting factors in the quality of the analysis are the size and the composition of the crystals. Various diffraction methods have been developed that can be categorized concerning their scattering. Methods that use the same wavelength as the incoming are called elastic (Birkholz, 2006). Here only the change in the direction/angel of the x-ray is recorded. The other method is called inelastic scattering (Birkholz, 2006; Cao, 2004). With this method the alternation of the incoming x-ray energy by the sample is recorded. The result is a loss of energy and, hence, an increased wavelength. This technique obtains no information about the distribution of atoms but gives insight into the excitation states of the investigated sample. The wide application of x-rays lies in their physical properties. X-rays exist in the wavelengths of 0.01 to 10 nm. For x-ray diffractometry often the 0.1 nm wavelength is applied. This wavelength is in the same dimension as a covalent bond and the radius of an atom. Hence x-rays can be applied to determine atomic-resolution structures (Powers et al., 2006).

1.4. Aquatic toxicity of the nanoscale zero-valent iron

Within the NAPASAN project different standardized toxicity test systems were applied to investigate the nanotoxicity of the newly developed NZVI nanomaterial. The test systems were

the algae growth inhibition test with *Desmodesmus subspicatus* (DIN; OECD), the crustacean immobilization test with *Daphnia magna* (DIN; OECD), the fish embryo toxicity test with *Danio rerio* (DIN; OECD) and as a mechanistic bioassay the Ames fluctuation test with *Salmonella typhimurium* (ISO; OECD). All tests were conducted referring to guidelines provided by the German Institute for Standardization (DIN), the Organization for Economic Cooperation and Development (OECD) and the International Organization for Standardization (ISO). The OECD evaluated its test guidelines for the application with nanomaterials (Kearns et al., 2009). This OECD program was called "safety of manufactured nanomaterials" (OECD, 2014a). In an expert meeting in the year 2013 different aspects of the test guidelines and their applicability for testing of ENM were discussed. A conclusion was that many test guidelines are applicable for nanomaterials. However, as in this thesis special regard shall be taken for the characterization of the ENM introduced (Kühnel and Nickel, 2014).

1.4.1 Fresh algae and cyanobacteria growth inhibition test with *Desmodesmus subspicatus*

The algae growth inhibition test evaluates the influence of a test sample on the growth rate of algae and cyanobacteria species (DIN, 2010b; OECD, 2011). In this thesis the green algae *Desmodesmus subspicatus* was applied. This species has a worldwide distribution (Forró et al., 2008). At the base of the food chain it is an important food source for zooplankton and fish. It can be used as an indicator for nutrient conditions of lakes. Furthermore, it is a model organism in plant physiology, ecology and evolutionary studies. Many of the algae cells features are visibly by light microscopy but scanning electron microscopy is necessary to elucidate the attributes of the cell wall. The algae reproduce primarily asexually by autospores. The autospores are released by fracture of the lateral cell wall (Altenburger et al., 2008). The form of *Desmodesmus* as colony or unicellular morph is related to its environmental conditions. The unicellular morph is a reaction to good nutrition and light conditions. It is preferred at high growth rates whereas the colony morph has the benefit to provide more security against predators. With its position in the aquatic food web *Desmodesmus* is an important organism for ecotoxicological assessment as harmful effects at this level multiply into the following tropic levels. Therefore, tests with algae have been standardized to investigate negative effects of chemicals, pharmaceuticals, waste waters and extracts of environmental samples like sediments (Cleuvers, 2003; Hafner et al., 2015; Nagai et al., 2013). This test system has been recommended for the investigation of soils within the ERNTE project (Römbke et al., 2006). Ecotoxicological studies with algae are required for the environmental risk assessment within

the scope of the registration of substances and products like Reach or GHS (EC, 2006a; UN, 2015). This tests have also been conducted to elucidate nanomaterial toxicity (Hund-Rinke and Simon, 2006; Kulacki and Cardinale, 2012; Marsalek et al., 2012; Masarovičová and Kráľová, 2013; Quigg et al., 2013; Schwab et al., 2011; Voelker et al., 2015; Wang et al., 2011). Within the OECD meeting on suitability of standardized toxicity test for the assessment of nanomaterials it was concluded that this test can be generally be applied. The recommendation included no specific amendments. However, several critical points were identified that should be considered within the guidance document (GD) and the guidance document on sample preparation and dosimetry (GSPD) (Kühnel and Nickel, 2014; OECD, 2011; OECD, 2012; OECD, 2014b).

1.4.2 Crustacean immobilization test with *Daphnia magna*

The crustacean immobilization test assesses any negative effects of a test sample on the mobility of the organisms. The endpoint of this test is the number of immobile daphnids. They are recorded as immobile when no movement is visible within 15 sec after the test vessel has been gently shaken (DIN, 2010a; OECD, 2004). *Daphnia magna* was the investigated the crustacean species in this thesis. It is a sensitive sentinel species in the freshwater ecosystems which inhibit most types of standing freshwater with a mostly pelagic habitus. The most striking morphologic features are flattened leaf-like legs which are used to create a water current for its filtering apparatus and an uncalcified shell called the carapace (Ebert, 2005). This feeding apparatus is so efficient that bacteria can be collected but the food mainly consists of planktonic algae (Carvan et al., 2000). The best food sources are green algae and many laboratory experiments are conducted with *Desmodesmus* as feed (Siehoff et al., 2009). Their reproduction is characterized by an asexual mode that occurs during the growth season. In this asexual mode the females produce parthenogenetic eggs that result in genetic clones (Ebert, 2005). A sexual reproduction is only introduced under predator stress and changing environmental factors. *Daphnia magna* has been the subject of intense biological investigations for over 100 years. It has been used to investigate a multitude of research topics like inheritance and development, cellular function, physiological systems, immunity response, disease, macromolecular structure/function relationships and the genetic basis of complex phenotypic traits. It can be also applied to monitor online water quality (Knie, 1978). Furthermore, it has been implemented into standardized ecotoxicity tests and became a worldwide applied biotest (DIN, 2010a; OECD, 2004). Testing procedures are established for acute and chronic exposure conditions within OECD and DIN guidelines. Like the algae test it is applied to investigate chemical

compounds like pharmaceuticals or pesticides as well as environmental samples like waste waters or sediment extracts (Baumann et al., 2013; Carvalho et al., 2014; Cleuvers, 2003; Hafner et al., 2015; Persoone et al., 2009; Tatarazako and Oda, 2007; von der Ohe et al., 2012). Additionally, studies with crustaceans are required for the risk assessment of substances and products for the registration within REACH or GHS (EC, 2006a; UN, 2015). Studies have also been conducted to elucidate nanomaterial toxicity (Baumann et al., 2014; Hund-Rinke and Simon, 2006; Marsalek et al., 2012; Romer et al., 2013; Voelker et al., 2015; Volker et al., 2013a; Wyrwoll et al., 2016). The OECD meeting on the suitability of tests systems for investigation of nanomaterials concluded for this test system that it is suitability for nanomaterial testing and the same recommendations as for the algae test were proposed (Kühnel and Nickel, 2014; OECD, 2004; OECD, 2012; OECD, 2014b).

1.4.3 Fish embryo toxicity test with *Danio rerio*

The fish embryo toxicity (FET) test investigates negative effects like mortality of developmental abnormities of a test compound on fish embryos of different fish species. A commonly applied species is *Danio rerio* (Strahle et al., 2012). This fish species common name is zebra fish and it is endemic to the tropical fresh waters of the Himalayan region. Streams, canals, ditches, ponds and stagnant water bodies are the commonly inhabited waters. *Danio rerio* belongs to the family of cyprinidae. It has an approximate generation time of three to four months and adult female zebrafish spawn every two to three days without an annual cycle. During each spawning a female may lay hundreds of eggs (Westerfield, 2000). Its common name zebrafish is derived from the five blue horizontal stripes on the side of the body that resemble the body colour of a zebra (Westerfield, 2007). The zebrafish are relatively small when compared to other fish with an approximate body length of 3 cm (Wixon, 2000b). A main advantage of this model organism is its rapid embryonic development which is easily observable as the chorion and the embryo is transparent (Lammer et al., 2009). This developmental processes are representative for vertebrate-specific tissue and organs like neural crest and parts of the hearth (Hill et al., 2005; Scholz et al., 2008; Wixon, 2000a). Additionally, the genome of the diploid *Danio rerio* has been extensively studied and compared to the human genome (Howe et al., 2013). The research with this organism has yielded advances in many scientific fields of biology like developmental biology, oncology and environmental sciences (Strahle et al., 2012). Tests with this organism have been standardized within the OECD and DIN guidelines (DIN, 2008; OECD, 2013). In aquatic toxicology it is a standard organism to test potentially toxic chemicals, wastewaters, sediments or environmental sample extracts

(Braunbeck et al., 2005; Di Paolo et al., 2015; DIN, 2008; Hafner et al., 2015; Hollert et al., 2003; Keiter et al., 2006; OECD, 2013; Schiwy et al., 2015b).In this test procedures it is applied either as adult (OECD 203), juvenile (OECD 210) or embryos (OECD 236, DIN EN ISO 15088). It has been shown that the zebrafish acute embryo toxicity test correlates well with the fish acute toxicity test (r=0.9) for industrial chemicals, plant protection products, surfactants, pharmaceuticals and biocides (Belanger et al., 2012; Belanger et al., 2013). This correlations can be also extended to adult fish and the embryos (Braunbeck et al., 2005). In consequence, the fish embryo toxicity test replaced adult fish in waste water testing in Germany since 2005 (DIN, 2008; Scholz et al., 2008). Additionally, an implementation of the fish embryo toxicity test OECD 236 is expected to be included into the REACH guidance on aquatic toxicity (ECHA, 2016; Halder et al., 2014). Finally, this test system has also been applied to investigate ENM toxicity in various studies (Fako and Furgeson, 2009; Felix et al., 2013; Krysanov et al., 2010; Simon et al., 2014a). Its suitability for testing of nanomaterials has not been discussed within the working party on nanomaterials of the OECD. However, studies have been conducted with nanomaterials like titanium dioxide following the OECD 236 guidelines with no restrictions presented (Wyrwoll et al., 2013).

1.4.4 Ames fluctuation test with *Salmonella typhimurium*

The Ames fluctuation test with *Salmonella typhimurium* is a mechanistic bioassay to detect mutagens (Ames et al., 1975; Maron and Ames, 1983). It is an artificial system to predict from mutagenicity in bacteria to mutagenicity and even carcinogenicity in mammals. The investigation of potential carcinogens is based on the assumption that many carcinogens are mutagens and most mutagens are carcinogens (Griffiths, 2005). The Ames test was developed with the aim to have an inexpensive and rapid method to test many different compounds under many conditions (Griffiths, 2005). It uses sensitized *Salmonella typhimurium* bacteria to quantify the mutagenic activity of a sample (Ames et al., 1975). This mutagenicity towards the bacterium does not translate directly into mutagenicity in laboratory animals and finally humans (Kirkland et al., 2014). However, there is a high predictive value that compounds that were detected as mutagens in the test are rodent carcinogens (McCann et al., 1975; Zeiger, 1998). In a study by Dunkel et al. (1985) it has been shown that 75 % of chemicals that were positive in the Ames test were also confirmed as carcinogens for rodents. However, not all rodent carcinogens are mutagenic in the Ames bioassay. As a screening assay with its strengths in ease, rapidity and cost effectiveness it is an important tool for chemical assessment (Mortelmans and Zeiger, 2000; Reifferscheid et al., 2012).

For the assessment of mutagens several strains of *Salmonella typhimurium* are used. All of them are specially selected mutants that are defective in the gene for synthesizing the essential amino acid histidine (Ames et al., 1975). Hence, these strains can only grow in medium that is supplemented with histidine. These strains differ in the genetic mutation as some of them have a base-pair substitution, frameshift mutations or transitions/transversions in the histidine gene (Tejs, 2008). In contact with a mutagenic compound these defective strains can undergo a reverse mutation that leads to a gain of function mutation. As a result these revertant bacteria can grow in medium without histidine (Maron and Ames, 1983). Several chemicals are not mutagenic in their native form but are transformed into mutagens by the mammalian liver metabolism. As bacteria do not have the same metabolic processes as mammals a test protocol with external metabolic activation was added. Liver enzyme extracts (S9) of rats or hamsters are used to simulate mammalian metabolic conversion of the test compound (Ames et al., 1973). This test can be conducted a plate or in a suspension format. In this thesis the bacterial suspension also known as Ames fluctuation assay was conducted where the number of revertants is indicated by the change of colour form purple to yellow in the assay plate (ISO, 2012). The results of the Ames test showed at high concentrations often a linear correlation between the concentrations of the test compound and the observed number of revertants. The conclusion is that this mutagenic action cannot be controlled by a threshold concentration and so no dose is risk free (Auerbach, 1949; Ehling et al., 1983). However, this conclusion is under discussion as the test are often performed at high concentrations and cells a capable to defend against genetic modifications (Ames and Gold, 1997; Upton, 1989). Therefore, mutagenicity specific pathways are proposed (Upton, 1989). Under consideration of theses pathways dose-response relationships can be determined (Clewell and Andersen, 2016; Crebelli, 2000; Kirsch-Volders et al., 2000; Upton, 1989). This test has been incorporated into national and international guidelines like US EPA, DIN, OECD and ISO. It is a recommended test within the REACH regulations for chemicals produced at volumes of 1 tonne or more per year (Annex VI and VII) as well as higher production volumes (Annex VIII) (EC, 2006a). This method is also recommended for the investigation of water and waste water (ISO, 2012). It has been applied for the investigation of nanomaterials (Barzan et al., 2014; Di Sotto et al., 2009; Hasegawa et al., 2012; Kumar et al., 2011; Landsiedel et al., 2009; Pan et al., 2010; Szalay et al., 2012). In studies the suitability of the Ames test for nanomaterial testing has been discussed (Landsiedel et al., 2009; Ng et al., 2010; Singh et al., 2009). Especially, the bacterial cell wall was seen as a problem (Landsiedel et al., 2009; Singh et al., 2009). This aspect was investigated by Clift et al. (2013) and they reported that various nano-objects were able overcome the

bacterial cell wall. However, the results of study for the Ames assay showed no mutagenicity for various materials which were mutagenic in a mammalian cell proliferation assays (Clift et al., 2013; Landsiedel et al., 2009).

1.5. Additional investigations complementing the view on the nanoscale zero-valent iron

Complementing the tests within the NAPASAN project investigations were conducted with *in vitro* bioassays to assess the interaction of the NZVI nanomaterial with a groundwater contaminant. The model contaminant PCE applied in the NAPASAN project was not suitable for the investigations as it does not show any mechanism specific toxicity like dioxin-like activity and it is volatile. Hence, the investigations with bioassays would be limited to cytotoxicity and the procedure would require laborious adaptations to minimize and quantify the substance loss through volatility. Therefore, the hetero-PAH acridine was selected as model compound to investigate the co-exposure of NZVI and an environmental contaminant (cf. Figure 1.6). These environmental contaminants are of special interest as they contribute significantly to the ecotoxicological hazard of water, sediment and soil samples. An important factor that affects their toxic potential to the environment is that many of these hetero-PAHs have a high polarity and water solubility when compared to PCBs and dioxins. Thus, these compounds are more widespread in the environment than their unsubstituted homologous polycyclic aromatic hydrocarbon (PAHs) counterparts (Brinkmann et al., 2014a).

1.5.1 Model compound Acridine

Hetero-PAHs have been recognized as a widespread environmental pollutant in various compartments (Blum et al., 2011; Brinkmann et al., 2014a; Brinkmann et al., 2014b; Mundt and Hollender, 2005; Peddinghaus et al., 2012). An important source of these compounds originate in creosote the product of the industrial process of coal tar-oil distillation as well as pharmaceutical processes, oil shale, petroleum refinery (Brinkmann et al., 2014a; Brinkmann et al., 2014b; Gosu and Gurjar, 2013; Peddinghaus et al., 2012). The first industrial applications date back to the 19th century (Wiersum, 1996). A main application of this process was to obtain chemical synthesis precursors for textile dyes. Hence, high environmental concentration originate from tar oil contaminated sites from where it can be distributed into groundwater (Blum et al., 2011; Neuwoehner et al., 2009; Schlanges et al., 2008). These compounds were reported to show various toxic effects including acute toxicity to fish as well as endocrine or dioxin-like toxicity in cell lines (Brinkmann et al., 2014a; Brinkmann et al., 2014b; Hinger et al., 2011; Peddinghaus et al., 2012). One of these hetero-PAHs is acridine (Figure 1) that is

known to exhibit toxicity to the aquatic environment (Eisentraeger et al., 2008; Feldmannova et al., 2006; Parkhurst et al., 1981; Peddinghaus et al., 2012). Additionally, mechanistic modes of toxicity like dioxin-like activity, endocrine activity or genotoxicity have been reported for this compound (Brinkmann et al., 2014a; Brinkmann et al., 2014b; Hinger et al., 2011; Moir et al., 1997). Due to its chemical properties presented in Table 1.1 acridine can be found in elevated concentrations in the environment (Blum et al., 2011). Finally, NZVI are proposed as a tool to remediate this compound and other similar heterocyclic PAHs (Gosu and Gurjar, 2013; Gosu et al., 2016; Wang and Zhang, 1997; Zhang and Elliott, 2006).

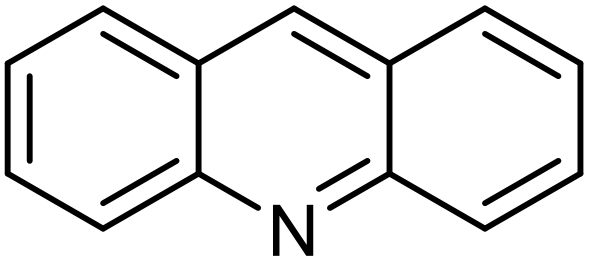

acridine

Figure 1.6: Chemical structure of acridine

Table 1.1: Chemical properties of acridine

CAS Number	000260-94-6
Chemical Name	Acridine
Molecular Formula	C13H9N
Molecular Weight	179.22
Melting Point.	108 °C
Boiling Point	345.5 °C
Water Solubility, 25 °C, exp. (Banwart et al., 1982)	38.4 mg/L
Log P (octanol-water), exp. (Hansch et al., 1995)	3.4
Vapour Pressure, 25 °C, exp. (Perry and Green, 1984)	0.000135 mm Hg
pKa Dissociation Constant, 15°C, exp. (Perrin, 1965)	5.45
Henry's Law Constant, 25 °C, est. (Meylan and Howard, 1991)	3.97 10^{-9} atm-m^3/mol
Atmospheric OH Rate Constant, 25 °C, est. (Meylan and Howard, 1993)	0.275 10^{-12} cm^3/molecule-sec

(SRC PhysProp Database accessed 11.01.2016); est. : estimated; exp. : experimental

1.5.2 *In vitro* bioassays for the determination of dioxin-like activity

In vitro bioassays with analytical cell lines help to replace animal testing. Therefore, they play an important role for the implementation of the 3Rs principle. This principle aims to implement humane animal research by replacement, reduction and refinement of animal experiments (Flecknell, 2002; Russell et al., 1959; Wittevrongel, 2013). The 3R framework has been implemented into national and international legislation. Thus, reliable and defined cell and tissue culturing methods with quality criteria are crucial.

In this thesis *in vitro* bioassays were selected that focused on dioxin-like activity as final endpoint. This mode of action of a compound is characterized by the fact that the toxicity is mediated via the aryl hydrocarbon receptor (AhR) (Bittner et al., 2006; Eichbaum et al., 2014; Olsman et al., 2007). The AhR receptor is a cytosolic receptor with a helix-loop-helix domain (Goldstein and Safe, 1989). In a signalling cascade a transcriptional activation is started which cumulates in the synthesis of P4501A cytochrome enzymes (CYP1A) (Delescluse et al., 2000;

Hilscherova et al., 2000; Hu et al., 2007). Cytochromes belong to a multigene family of heme-containing proteins that are expressed in the liver, kidney, gastrointestinal tract, gills and other tissue of many organisms (Hammond and Strobel, 1992; Rodrigo et al., 2001). They belong to the phase-I-reactions that oxidize, hydrolyse or reduce xenobiotics (Burke and Mayer, 1974; Schiwy et al., 2015b). These reactions can detoxify xenobiotics but in some cases can also lead to a bioactivation (Arlt et al., 2015; Donato et al., 1998). This process results in an increased toxicity of an xenobiotic after interaction with the enzymes (Castell et al., 1997; Ioannides and Lewis, 2004). To sum up, dioxin-like activity is a receptor mediated toxicity that acts toxic to organisms that have this receptor. The prolonged enzymatic upregulation leads to cellular damage as the enzymes cannot detoxify the compounds and in their high abundance harm the cells (Roos and Kaina, 2006). This activity can lead to cell death or the formation of cancerous cells (Nebert et al., 2004; Park et al., 1996; Roos and Kaina, 2006).

Dioxin-like chemicals are ubiquitous compounds with hydrophobic and lipophilic attributes (Eichbaum et al., 2014; Giesy et al., 1994; Hilscherova et al., 2000). Furthermore, their fate in the environment is characterized by persistence as they are resistant to biological and chemical degradation (Fiedler, 2003). They tend to bio-accumulate and bio-magnify (Giesy and Kannan, 1998). Dioxin-like chemicals do not occur in large numbers and still policies were introduced to reduce their release into the environment (Lallas, 2001). The most prominent compounds in this class are the dibenzo-*p*-dioxins and dibenzo furans (PCDD/Fs) with 2,3,7,8, tetrachlorodibenzo-*p*-dioxin (TCDD) as the most prominent compound (Longnecker et al., 1997; Schecter et al., 2006). It is a very potent dioxin-like activity inducer and a very toxic compound (Longnecker et al., 1997; Schecter et al., 2006). Moreover, other compounds with a planar or coplanar geometry show this mode of toxicity like dioxin-like PCBs, polycyclic aromatic hydrocarbons (PAHs) including hetero-PAHs, and a multitude of known and unknown compounds (Hankinson, 1995; Tue et al., 2013).

An example for a mechanistic bioassay to detect dioxin-like activity is the micro-EROD bioassay with H4IIe cells (Schiwy et al., 2015a; Schwirzer et al., 1998; Thiem et al., 2014). This cell line originates from *Rattus norvegicus* and is a rat liver tumour cell line (Pitot et al., 1964). With this *in vitro* bioassay it is possible to investigate dioxin-like chemicals (DLCs) in different samples (Benedict et al., 1973; Bradlaw and Casterline Jr, 1979; Schiwy et al., 2015a; Thiem et al., 2014). The dioxin-like potential is quantified by determining the induction of the CYP1A monooxygenase 7-Ethoxyresorufin-*O*-deethylase (EROD) (Tillitt et al., 1991b). The enzyme activity can be determined and correlated to TCDD which is used as a positive control. As a result TCDD equivalent quotients (TEQs or bioTEQs) can be calculated (Ahlborg et al.,

1994; Hädrich et al., 2012; Safe, 1990; Van den Berg et al., 1998; Van den Berg et al., 2006; van den Berg et al., 2013). This value expresses the AhR inducing potential in a sample as the amount of TCDD that would cause the same effect. The micro-EROD bioassay is a good example of the state of the art technology for analytic cell lines. Similar elements can be found in various bioassay investigating different cellular pathways (Escher et al., 2014). These bioassays are sometimes complemented with genetic modification of the cell lines to improve sensitivity of the assay by introducing luciferase based reporters (Brennan et al., 2015; Kojima et al., 2015). These reporters show the advantage that they do not show substrate inhibition and that luminescence is a more sensitive endpoint (Eichbaum et al., 2014; Schipper et al., 2013). These bioassays have in common that they are conducted with adherent cell lines that are maintained in a medium supplemented with fetal calf serum.

However, the application of fetal calf serum (FCS) as a supplement is problematic for this technology as it has many ethical and technical problems. First of all, it is a very complex mixture of different factors and components like proteins, growth factors, vitamins, trance elements, hormones and many more (Gstraunthaler, 2003). Hence, it is not defined and varies between production charges (Hawkes, 2015; Honn et al., 1975). Furthermore, it is obtained from unborn calf and, thus, does not complete replace animals in the toxicity assessment (Gstraunthaler, 2003; van der Valk et al., 2004). Another problem is that as an animal product it can be contaminated with diseases like bovine spongiform encephalopathy (BSE) or viruses like bovine viral diarrhea (BVD) (Bolin et al., 1991; van der Valk et al., 2004; Wessman and Levings, 1998). Therefore, it cannot be used for the production of new biological medical products (van der Valk et al., 2004). Especially, for this purpose another factor plays an important role as the availability of this resource is limited and a maximum production capacity is expected which negative consequence for the cost of *in vitro* techniques (Brindley et al., 2012). The next step in *in vitro* technology is the substitution of FCS with more reliable, sustainable, economical, safer, tailor-made and more ethical serum-free, chemically defined media (SFM/CDM) (van der Valk et al., 2010). The advantages of serum-free media result in chemically-defined and controlled culture conditions (Gstraunthaler, 2003). As a result of the reduced variability in medium composition sources for microbial and biological contaminations are eliminated (van der Valk et al., 2004). Furthermore chemically defined media offer advantages in down-stream process like a facilitated isolation of cell culture products (van der Valk et al., 2004). Another aspect of *in vitro* cell culturing is whether the cells are grown adherent to the bottom of a vessel or free in suspension (Biaggio et al., 2015; Chu and Robinson, 2001). The culturing as suspension cell culture has the benefit that the cells can be cultivated at

much higher densities than adherent cells and allow for multiple new applications (Biaggio et al., 2015). To sum up, these improvements lead to a higher throughput, with minimized variation and cost efficiency.

1.6. The aims of this thesis

In this thesis the toxicity of an iron based nanomaterial was investigated within the joint research project NAPASAN. This project aimed to develop a cost effective zero-valent iron nanomaterial for the *in situ* remediation of chlorinated hydrocarbons in groundwater aquifers. A classical chemicals assessment was conducted including test from different trophic levels like algae, crustacean, early life stages of vertebrates and a mechanism specific test for mutagenicity (Chapter 3). To gain insight into the source of toxicity of the nanomaterial a thoroughly material characterization was conducted. The investigations included methods that elucidate the nanomaterial size as well as the material composition. Additionally, the generation of reactive oxygen species during exposure to the nanomaterial was investigated in a cell free assay. The following questions were addressed:

a. What is the material composition and morphology of the aged nanomaterial?
b. Is the nanomaterial toxicity mediated through ROS generation?
c. Are the newly developed zero valent iron flakes in their aged state a threat to the aquatic environment?

In the second part of the thesis *in vitro* bioassays were optimized and developed to investigate the dioxin-like activity of environmental samples. It included the development of a robust and widely applicable bioassay protocol for the micro-EROD bioassay (Chapter 4). Additionally, analytic cell lines H4IIE, H4IIE-Luc and HEPG2 were adapted to an animal component free medium and suspension cell culture (Chapter 5). Research was focused on:

a. Development of a widely applicable license free protocol for the determination of the CYP1A-inducing potential
b. Adaptation of analytical cell lines to a chemically defined medium and suspension culturing conditions
c. Initial evaluation of the newly developed cell lines
d. Investigation of the co-exposure of NZVI and acridine with bioassays

To combine the two elements of the thesis, the effect of the newly developed nanomaterial for groundwater remediation on the dioxin-like active groundwater contaminant acridine was investigated (Chapter 6). The *in vitro* bioassay was applied as monitoring tools to determine the remediation activity. These investigations were complemented with the FET test, in combination with instrumental HPLC analysis for the compound acridine. The structure of the thesis is presented in Figure 1.7.

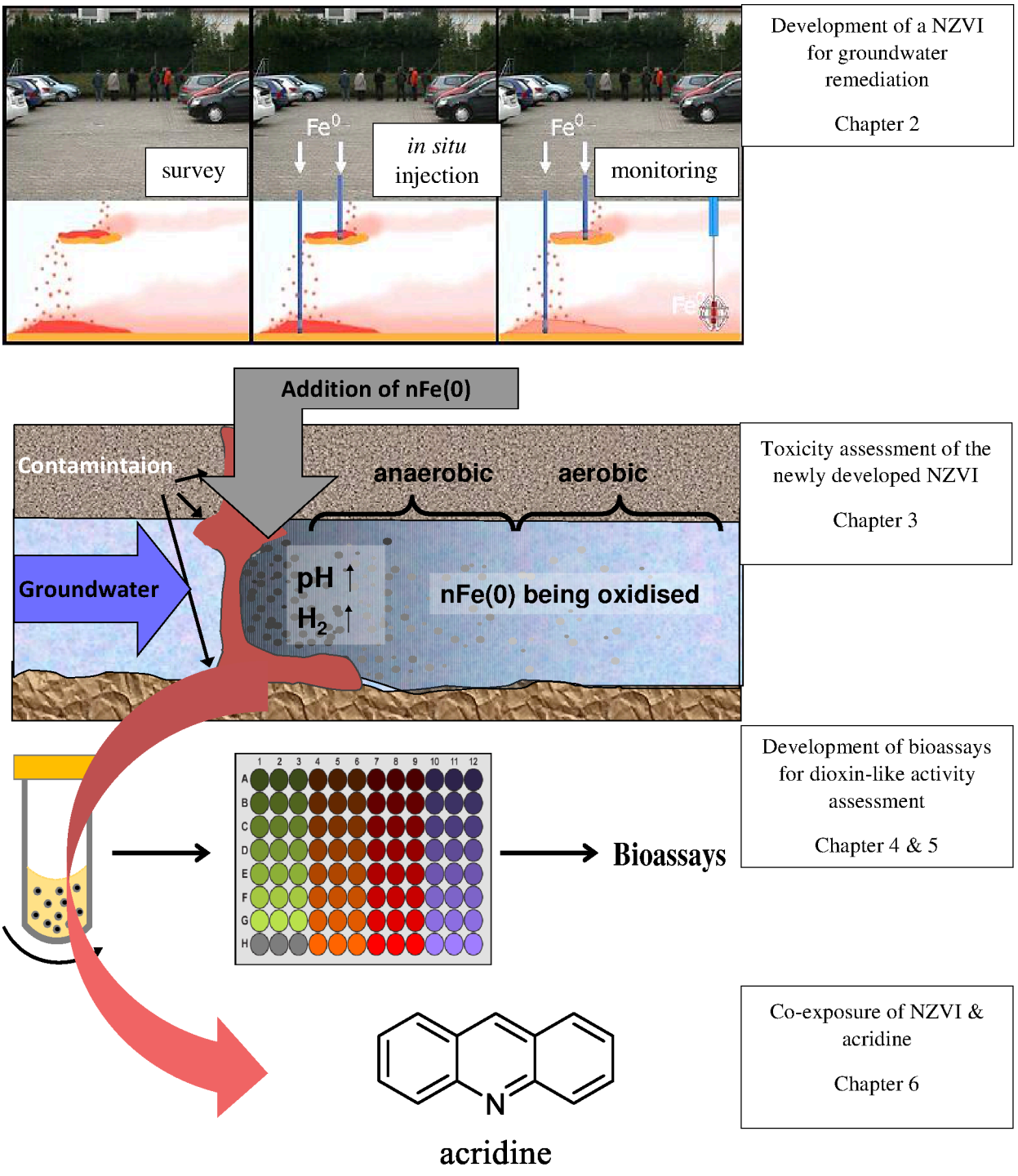

Figure 1.7: Graphical abstract of the study design

Chapter 2
Nanoscale zero-valent iron flakes for groundwater treatment

This chapter has been published in the peer-reviewed article:
Köber, R., Hollert, H., Hornbruch, G., Jekel, M., Kamptner, A., Klaas, N., Maes, H., Mangold, K.M., Martac, E., Matheis, A., Paar, H., Schäffer, A., Schell, H., Schiwy, A., Schmidt, K.R., Strutz, T.J., Thümmler, S., Tiehm, A., Braun, J., 2014. Nanoscale zero-valent iron flakes for groundwater treatment. *Environmental Earth Science* 72, 3339-3352. DOI: 10.1007/s12665-014-3239-0

Abstract

Even today the remediation of organic contaminant source zones poses significant technical and economic challenges. Nanoscale zero-valent iron (NZVI) injections have proved to be a promising approach especially for source zone treatment. We present the development and the characterization of a new kind of NZVI with several advantages on the basis of laboratory experiments, model simulations and a field test. The developed NZVI particles are manufactured by milling, consist of 85 % Fe(0) and exhibit a flake-like shape with a thickness of <100 nm. The mass normalized perchloroethylene (PCE) dechlorination rate constant was 4.1 x 10^{-3} L/g h compared to 4.0 x 10^{-4} L/g h for a commercially available reference product. A transport distance of at least 190 cm in quartz sand with a grain size of 0.2–0.8 mm and Fe(0) concentrations between 6 and 160 g/kg (sand) were achieved without significant indications of clogging. The particles showed only a low acute toxicity and had no long-term inhibitory effects on dechlorinating microorganisms. During a field test 280 kg of the iron flakes was injected to a depth of 10–12 m into quaternary sand layers with hydraulic conductivities ranging between 10^{-4} and 10^{-5} m/s. Fe(0) concentrations of 1 g/kg (sand) or more [up to 100 g/kg (sand)] were achieved in 80 % of the targeted area. The iron flakes have so far remained reactive for more than 1 year and caused a PCE concentration decrease from 20,000–30,000 to 100–200 µg/L. Integration of particle transport processes into the OpenGeoSys model code proved suitable for site-specific 3D prediction and optimization of iron flake injections.

Keywords Nanoscale zero-valent iron; Reactivity; Mobility; Ecotoxicology; Microbiology: Field test; Numerical model

2.1. Introduction

During the last 10–15 years there has been an increasing number of scientific publications investigating different characteristics and capabilities of nanoscale zero-valent iron (NZVI) particles with most of them showing NZVI to be a promising substance for groundwater and in particular source remediation e.g. (Henn and Waddill, 2006; Kuiken, 2010; Phenrat et al., 2011). Major advantages in this technology are the injectability of the particles in immediate vicinity of the contaminant source, high reaction rates due to the large surface area and a large number of relevant contaminants which are treatable, especially chlorinated hydrocarbons (CHCs) as, e.g. per- or trichloroethylene. Despite these advantages and promising results of laboratory and field studies, NZVI still do not represent standard technology for source treatment of CHCs or other contaminants. This is mainly due to the low availability in Europe

and to the high costs. Today, NZVI is typically produced by reductive precipitation of Fe(0) from solutions containing Fe^{2+} using strong reductants like borohydride or hydrogen. Further developmental opportunities of this production technology are so far limited due to the relatively high costs of the required chemicals.

With this contribution, we want to introduce a new kind of NZVI particles produced for source remediation by grinding of macroscopic raw materials of elementary iron to the micrometre and nanometre scale without the need of expensive chemicals. Besides particle production, the properties and functionality of the new particles as well as their field applicability are described. The development was an iterative process between particle production on the one hand and verification of reactivity, mobility and ecological sustainability on the other. In addition to the testing of different raw materials, grinding additives and grinding procedures, the development of coatings to prevent early sedimentation caused by aggregation (Phenrat et al., 2008; Phenrat et al., 2007) was investigated and the size, shape, surface area, structure and Fe(0) content of the particles were characterized.

Reactivity characteristics of NZVI must fulfil two requirements. First, immediate reactivity has to be high to achieve short treatment times and second, long-term reactivity has likewise to be sufficiently high to provide reactivity over several weeks or even months. Such periods are essential since not all of the contaminant mass will be affected by NZVI particles directly after injection, due to the heterogeneous distribution of aquifer permeability, contaminant mass and NZVI transport. For a successful source treatment with NZVI, which means removal of the bulk contaminant mass, a sufficiently high Fe(0) concentration and a particle distribution as homogeneous as possible are important. The Fe(0) demand would be 28 g/kg (sand) for a PCE contamination with a residual saturation of 5 %. However, so far lab or field experiments including a quantification of Fe(0) mass could verify appropriate Fe(0) concentrations only up to a distance of a few decimetres from the injection point (Phenrat et al., 2010; Taghavy et al., 2010). Even if relatively short distances of, for example, 2 m between injection points can be covered using advanced injection technology like direct-push, it has to be ensured that the injected NZVI can be transported such distances at sufficient concentrations. Besides the improvement of application-oriented aspects, a further goal was to promote confidence in the transferability from lab to field scale and in the ecotoxicological and microbial innocuousness of the new particles. A systematic and quantitative evaluation of NZVI applicability as a remedial approach for CHC contaminants in soil and groundwater under field-relevant conditions has been reported only recently (Phenrat et al., 2011). Henn and Waddill (2006) supplied evidence that NZVI effectively degraded contamination and reduced the mass flux

from the source as a critical metric identified for source treatment. Many early studies were reported as successes with limited discussion addressing challenges associated with NZVI application at a field scale (Elliott and Zhang, 2001; Zhang, 2003). Zhang and Zhao (2013) provides a good review of NZVI application for CHC remediation, underlining the lack of systematically built up experience under field conditions. O'Carroll et al. (2013) point out a significant need for field studies that demonstrate rigorous site characterization, optimization of on-site injection infrastructure, design of injection fluid properties and reporting methods to reduce the unreliability associated with NZVI delivery. Our field scale pilot study aimed to provide answers to these questions. To optimize NZVI injection and distribution for field applications, the particle development was accompanied by the adaption of a numerical model. While the classical filtration theory (Yao et al., 1971) was shown to be inappropriate to explain NZVI transport in porous media in many cases, studies considering more complex approaches like blocking, ripening and straining processes have proven to be able to describe transport behaviour under different hydraulic and geochemical boundary conditions (Bradford et al., 2003; Bradford et al., 2009; Bradford et al., 2011; Bradford et al., 2002; Johnson and Elimelech, 1995; Johnson et al., 1996; Ko and Elimelech, 2000; Loveland et al., 2003; McDowell-Boyer et al., 1986; Sun et al., 2001b; Tiraferri et al., 2010; Tosco and Sethi, 2009; Tosco and Sethi, 2010). However, more-dimensional model applications considering transport behaviour of NZVIs for field conditions are quite rare (Cullen et al., 2010; Kanel et al., 2008; Sun et al., 2001ac). Therefore, the objectives of the reactive transport modelling part were (1) to identify and parameterize governing transport processes under different injection conditions and (2) to transfer and apply these findings to the field scale using more-dimensional simulations including model verification by field investigations. Although there are already various studies showing only low acute toxicity for NZVI materials (El-Temsah and Joner, 2012; Marsalek et al., 2012; Phenrat et al., 2009; Wang et al., 2012), these findings cannot directly be transferred to newly developed particles, since different chemical composition, coatings or shape of NZVI can have an influence on the toxicity. Since microbial degradation can additionally contribute to the removal of main target contaminants like chlorinated ethylenes (Aktas et al., 2012; Tiehm and Schmidt, 2011), inhibition of the microbial degradation by NZVI should be excluded. Moreover, reductively dechlorinating and also other hydrogenotrophic bacteria can act as a sink for the hydrogen produced during anaerobic NZVI corrosion and thus mitigate the potential for clogging. The suspending agents and stabilization materials of NZVI formulations can function as an additional source of electron donors for biological dechlorination. Thus, the combination of abiotic dechlorination with NZVI and biological dechlorination can have synergetic effects.

All these topics are needed for the throughout evaluation of the characteristics and capabilities of this new and promising type of NZVI. This paper will therefore summarize all of these aspects for the developed particles to give a brief overall view. More detailed and extended presentations of the individual topics will be part of subsequent publications.

2.2. Methods

2.2.1 Particle production

To develop a method to produce nanoparticles of elementary iron in a two-stage top-down process, various commercial iron powders (carbonyl iron, sponge iron, cast iron and iron powder) were tested. Within the project various grinding equipment, grinding additives and milling times were investigated (Table 2.1). The focus was set on grinding tests with different mills, such as vibrating mills, ball mills and stirred ball mills in a laboratory as well as on a semi-industrial scale. The selection of the grinding media was a challenge because of the formation of hydrogen in an aqueous agent (tap water, deionized water; pH value controlled). Different organic media were tested; in the end mono ethylene glycol (MEG) was selected. Consequently, the iron particles were produced in a two-stage procedure. The first step involved dry grinding with inhibitors as corrosion protection up to a particle size <40 µm. Wet fine grinding, the second process step, was realized with MEG as the grinding liquid and addition of a surfactant. Sponge iron (Höganäs, NC100.24) was used as the raw material for production batches A1–A4 and Atomet 57 or 58 (Rio Tinto, Quebec Metal Powders Ltd) for batches B1–B5 which also included the particles for field applications selected by reactivity and mobility investigations.

Table 2.1: Particle production batches with associated conditions

Batch	Raw material	Pre-milling		Wet milling			Code
		Aid	Unit	Aid	Unit	Media	
A1	Sponge iron; (Höganäs)	-		Additive 3	5 L stirred ball mill	Ethylene glycol	V 71
A2	Sponge iron; (Höganäs)	-	Vibrating cup mill	Additive 3	5 L stirred ball mill	Ethylene glycol	V 72
A3	Sponge iron; (Höganäs)	-	Vibrating cup mill	Additive 4	5 L stirred ball mill	Ethylene glycol	V 73
A4	Sponge iron; (Höganäs)	2 % Activated carbon	Ball mill	Additive 3	5 L stirred ball mill	Ethylene glycol	V 80
B1	ATOMET 57 (Rio Tinto)		Ball mill	Additive 3	5 L stirred ball mill	Ethylene glycol	V 84b
B2	ATOMET 57 (Rio Tinto)	Additive 2	Ball mill	Additive 3	5 L stirred ball mill	Ethylene glycol	V 89
B3	ATOMET 58 (Rio Tinto)	Additive 2	Ball mill	Additive 3	200 L ball mill	Ethylene glycol	ZAB01
B4	ATOMET 58 (Rio Tinto)	Additive 2	Ball mill	Additive 3	200 L ball mill	Ethylene glycol	ZAB04
B5	ATOMET 57 (Rio Tinto)	Additive 2	Ball mill	Additive 3	2 x 500 L ball mill	Ethylene glycol	MMA01

2.2.2 Coatings

To study the effect of coatings on the size and agglomeration of iron particles at first, a series of experiments were performed using freshly prepared nanoparticles, as long as no grinded

particles were available. Afterwards the results were transferred to grinded particles. According to the procedure described by Bonder et al. (2007) iron nanoparticles are formed by chemical reduction of iron(II) salts using boron hydrate as a reducing agent. Iron(II) sulphate $FeCl_2$ x 4 H_2O (Fluka), sodium borohydride $NaBH_4$ (Sigma Aldrich), polyethylene glycol PEG 400 (Fluka, linear molecule; molecular weight 380–420 g/mol) and sodium dodecyl sulphate SDS (Merck) used for the preparation of preliminary test particles were of analytical grade and were used as received. Iron nanoparticles were synthesized by reduction of $FeCl_2$ in ethanol (96 %). 25 ml of 6 mM $NaBH_4$ was drop-by-drop added to a stirred solution of 1.8 mmol $FeCl_2$ and a PEG concentration between 0.5 and 2 mmol in 250 mL cooled (0 °C) ethanol. Because of the air-sensitivity of the iron particles, the solution was kept in an inert gas atmosphere (N_2). After 2 h stirring the particles precipitated. The supernatant solvent was poured off and the particles suspended in de-ionized water (18 MΩcm). The reduction was accomplished in the presence of different polyethylene glycols (PEGs), which enclose the freshly formed iron particles. This procedure leads to small particles with narrow size distribution. Particle size distribution used for the coating development was determined with a Zetasizer Nano ZS (Malvern).

2.2.3 Particle characterization

The Fe(0) content of the milled particles was determined by measuring the hydrogen production in relation to the total amount of dissolved iron in acidic conditions (sulphuric acid). Dissolved iron concentrations were determined by Atomic Absorption Spectroscopy (AAS). Depending on the iron concentration of the sample either graphite furnace— AAS (GF-AAS, SpectrAA-400 Varian) or flame—AAS (F-AAS, GBC 906AA) was used. Furthermore, the concentration of dissolved iron was determined by the photometric method according to DIN 38401-E1.

To analyse the size distribution of particle batches a Mastersizer 2000 system (Malvern) was used. This technique is based on laser diffraction and measures the intensity of light scattered as a laser beam passes through a dispersed particulate sample. Calculations of the size distribution use the created scattering pattern and assume a spherical shape of the particles.

The specific surface area (BET) is an important parameter for the characterization of NZVI particles. The determination is based on the measurement of the adsorption of nitrogen on the surface according to (9227:1995). The measurement was performed using the areameter Area-Max 1 (CIS Seifert). Since the particles must be in a dry state, the suspension was first removed and the particles were coated with methanol to prevent oxidation. Before each BET measurement, the surface of the samples had to be de-gased to avoid contamination with

oxygen. The degassing took place in a separate thermostat-controlled heating device at a temperature of 105 °C until methanol evaporated. For the analysis of the particle size, shape, surface and structure, a Phenom electron microscope was used.

2.2.4 Reactivity comparison of different particle batches

To compare the particles produced under different milling conditions, reactivity tests were conducted in degassed and demineralized water in a 0.5-L gas-proof reactor. The solution was continuously stripped with nitrogen to achieve anaerobic conditions. The aquatic NZVI suspension was stirred at 200 rpm to minimize mass transport effects of contaminants on the reactivity. During the reaction the pH was controlled by titro-processors which kept the pH constant at 7 by adding hydrochloric acid. The start concentration of iopromide solutions for the reactivity comparison of different particle batches was 2 g/L (2.5 mmol/L). Dehalogenation rates were estimated by measuring the contaminant concentration and the dissolved iodide as a function of experimental time during the deiodination of iopromide (iodinated X-ray contrast media). Iopromide was quantified by LC–ESI-MS/MS (HP 1100, Agilent, Waldbronn, Germany; Quattro-LC, Micromass, Manchester, UK).

NZVI from NanoIron s.r.o. (N25) was used as a reference material. N25 particles have an average BET surface area of 20–25 m^2/g and an average particle size of 50 nm (Zhuang et al., 2012). However, in aqueous solution the particles aggregate to clusters of >1 µm (determined by dynamic light scattering, DLS). The particle shells consist of a thin iron oxide layer (Fe_3O_4, FeO) which encloses the Fe(0) core (core–shell-structure). Before each batch test the Fe(0) content of the nanoparticles was determined by measuring the hydrogen production under acidic conditions.

2.2.5 Longterm reactivity

The central part of the stand-alone column setup system was a syringe pump which is controlled by a Siemens Logo, controlling the switches of the solenoid valves to change between refilling and pump action of the syringes. Moreover it operated a membrane pump which supplies degassed water to a storage container. The water quality was monitored while the degassed water was pumped into a PCE mixing container to supply the syringe pump with a PCE solution with concentrations between 80 and 120 mg/L, comparable to the concentrations in a source zone. A total amount of 725 mg PCE were used for the longterm reactivity column test with the particle production batch B2. The syringe pump assured a continuous and almost pulse-free discharge of the PCE solution through the columns. It was possible to take water samples from sampling ports before and after each column to measure PCE concentration, the degradation

products chloride and metabolites, and pH. Outflow boundaries were controlled via a constant-head tank. The overflow rate of the constant-head tank was measured to confirm the flow rates from the syringes. The columns were made of glass, had a length of 200 cm and an inner diameter of 3.6 cm. Quartz sand was used as a porous medium (grain size 0.3–0.8 mm) with a bulk density of 1.67 g/cm^3, a corresponding porosity of approx. 0.36 and a pore volume (PV) of approx. 700 cm^3. Each column was controlled by an allocated syringe pump with flow rates about 175 cm^3/days resulting in seepage velocities of 0.5 m/days. To insert the NZVI particles (B2) in the column, 700 mL of a suspension with an Fe(0) concentration of 10.4 g/L (1 PV) was injected from the top of the vertically positioned column, which resulted in a total ZVI mass of 7.3 g within the first 0.5 m of the column and a maximum Fe(0)-concentration of 16 g/kg sand. To compare the newly developed with other NZVI particles, N25S was used in a separate column as a reference material. The Fe(0) concentration of this suspension during the injection was 20 g/L. The total mass of ZVI inside the column was 14 g (within 700 mL suspension), distributed along the 2 m column. The maximum ZVI concentration reached was 17 g/kg. First-order reaction rate constants, calculated from the PCE inflow and outflow concentrations of each column, were normalized to the respectively injected ZVI mass. The normalized rate by the mass of ZVI per unit aqueous phase volume (km) was calculated according to Taghavy et al. (2010).

2.2.6 Transport investigations

Transport investigations were performed in horizontal column experiments (L 2 m, ID 8 cm, quartz sand 0.2–0.8 mm, *n* approx. 0.35). To determine the best particle production batch, the different particle batches were injected at similar injection conditions with Fe(0) concentrations of about 10 g/L and filter velocities (*vf*) of 0.5 m/h. In this study, only the results of the two best batches with the best transport characteristics (B1 and B4) were represented. To compare the developed particles with commercial particles, an experiment with same injection conditions and N25S particles was performed additionally. To investigate if a particle distribution range of approximately 2 m or more and a sufficient Fe(0) concentration in the sand can be achieved, an experiment with the batch A4 was performed at similar injection conditions (filter velocity: 0.5 m/h, Fe(0): 9 g/L, quartz sand 0.25–1.0 mm, porosity: 0.36) but with a considerably greater injected Fe(0) mass. During injection the magnetic susceptibility was measured using a core sensor (Co. Bartington, Core Scanning Sensor Type MS2C) to quantify the concentration of total Fe(0) (Fe^0_{tot}) which indicates the sum of mobile and immobile Fe(0). The mass of retained

Fe(0) in the sand was the best variable for comparing the experiments because it could be determined exactly from Fe^0_{tot}.

2.2.7 Particle transport modeling

As an extensive basis for the present study, column tests conducted with commercial NZVI particles N25S under variable injection velocities (0.5–4.5 m/h), particle concentrations (5–17 g/L), and initial permeabilities (K = 6E-09–5E-11 m^2) were simulated using the matlab-based code E-MNM1D (Tosco and Sethi, 2010), considering blocking and straining as governing deposition processes. Because of a similar transport behavior of N25S and the developed particles (B4), both deposition processes were also considered and parameterized by simulations of a column test with the developed particles in preparation for the preliminary injection test at the field site and for simulations at field scale. For these field-scale simulations, the multi-component, multi-dimensional flow and transport code OpenGeoSys (OGS) (Kolditz et al., 2012) was used and modified (Hornbruch et al., in prep.). The mass transport is described in the following Equation 2.1, where C_i and S_i are the concentration of dissolved and attached species *i*, respectively, *t* is the time, *vf* the Darcy velocity, *n* the water filled porosity, and *D* the diffusion–dispersion tensor.

$$\frac{\partial(nC_i)}{\partial t} + \sum_i \rho_b \frac{\partial(S_i)}{\partial t} = -\nabla\left(v_f C_i\right) + \nabla\left(nD_i \nabla C_i\right)$$

Equation 2.1: Mass transport of NZVI

The OGS code was extended regarding the derived deposition processes for the exchange of species between water and solids according to E-MNM1D by Equation 2.2 and Equation 2.3,

$$\frac{\partial S_1}{\partial t} = \frac{n}{\rho_b} k_{a,1}\left(1 + A S_1^{\beta_1}\right) C_i - k_{d,1} S_1$$

Equation 2.2: Blocking

$$\frac{\partial S_2}{\partial t} = \frac{n}{\rho_b} k_{a,2}\left(1 + \frac{x}{d_{50}}\right)^{\beta_2} C_i - k_{d,2} S_2$$

Equation 2.3: Straining

where S is the attached concentration in the solid phase for each interaction site i, p_b the bulk density, $k_{a,i}$ and $k_{d,i}$ the attachment and detachment rate constants, respectively, and A the excluded area parameter according to Johnson et al. (1996) as the negative inverse value of a maximum sediment retention capacity $S_{max,}$ x the travel distance, d_{50} the mean soil diameter and β_i an exponent controlling attachment dynamics.

For field simulations, a homogeneous radial model was used considering a decreasing flow velocity with increasing distance from injection. The permeability was chosen to be 1E-12 m^2 based on direct-push investigations, while the effective porosity was assumed to be 20 %. The smallest grid spacing at the injection point was 0.10 m due to high flow velocities in the vicinity of the injection well using an injection rate of 13 L/min and an injection concentration of 2.5 g/L.

2.2.8 Field test

A field-scale pilot test was vital for assessing and validating the applicability of the newly developed NZVI particles, concepts and methodologies. NZVI field application was implemented at the demonstration site Breite St. in Braunschweig, Germany. The site was formerly used as a dry cleaning facility and is highly contaminated with PCE between 10 and 14 m below ground. The rather moderate hydraulic conductivity fine sands (1–5 x 10^{-5} m/s) exhibit PCE aqueous concentrations between 20 and 50 mg/L.

A proper dimensioning of the field-scale pilot-test in terms of spatial configuration, injection strategy and setup of the monitoring system cannot be achieved without a preliminary field-scale injection experiment. Injection relevant parameters were investigated during direct-push (DP) injection of 2 m^3 NZVI slurry (2.5 g/L) through pressure-activated injection probes at about 13 L/ min under a pressure of 5–6 bar. These preliminary test injections were performed at two different injection points depth oriented into horizons with similar characteristics to the pilot-test target area. Monitoring of the spatial NZVI distribution around injection points was carried out through DP-Liner sampling at the same depths followed by lab analytics through calibrated magnetic susceptibility measurements on the liner-based soil samples. Based on these findings, a full field-scale pilot application was designed (spacing of injection wells, injection rates, injection pressure, depth and type of injection, NZVI concentration) and implemented in summer 2012. Five newly developed NZVI *in situ* monitoring systems were installed in July 2012 prior to the injection. The multilevel ports for monitoring the NZVI spatial distribution through online metering of the magnetic susceptibility were equipped with additional multilevel groundwater sampling devices. To monitor the reaction zone in terms of

upgradient background, respectively downgradient effects, multilevel monitoring well groups (1″ inner diameter monitoring wells installed in a nested setup with depth-oriented screened intervals) were installed prior to the NZVI injection. 280 kg of iron was injected as slurry (10 g/L) at 14 injection points during the first 2 weeks of August 2012 at 4 depths between 10 and 12 m below ground. For each injection target horizon, 500 L slurry was injected in an omni-directional setup. Following the injection, the NZVI radius of influence was investigated by liner-based soil sampling. Spatial distributions of contaminants of concern and milieu parameters within the reaction zone and neighboring up- and downgradient areas were monitored over 1 year through a series of groundwater sampling events and analysis.

2.2.9 Investigation of the biological activity during field application

For the investigation of biological activities during the field application of NZVI, dechlorinating organisms were assessed by nested PCR. Investigated organisms were *Dehalococcoides sp.* (Smits et al., 2004), *Desulfitobacterium sp.* (Smits et al., 2004), *Desulfomonile tiedjei* (El Fantroussi et al., 1997a; El Fantroussi et al., 1997b), *Dehalobacter sp.* (Smits et al., 2004) and *Desulfuromonas sp.* (Loffler et al., 2000). The occurrence of these halorespiring microorganisms at a given site can be taken as an indicator for the degree of dechlorination occurring at this site (Schmidt et al., 2006). For the assessment of acute toxicity, the inhibition of luminescent bacteria was measured according to 11348-1 (2009).

2.2.10 Toxicity investigations

Aged NZVI were evaluated with standardized acute aquatic and mechanism-specific ecotoxicological tests. The nanomaterials were investigated in a worst-case scenario as ultrasonicated suspensions. The particle suspensions were dried in an oven over night at 80° C under air circulation. The powder weighed in with a maximal variance of 1 % and introduced into the corresponding aquatic media. The concentration range for of the aquatic test was up to 1000 mg/L. As acute toxicological tests, the *Daphnia magna* acute immobilization test according to DIN (2010a), the prolonged fish embryo toxicity test (96 h) according to DIN (2008) with *Danio rerio* (Braunbeck et al., 2005), the algae growth inhibition test DIN (2010b) with *Desmodesmus subspicatus* and as a mechanism-specific test the Ames fluctuation test according to ISO (2012) with *Salmonella typhimurium* (Reifferscheid et al., 2012) were applied.

2.3. Results and discussion

2.3.1 Particle characterisation

After milling, the particles were stored in ethylene glycol to avoid oxidation. On average fresh particles in suspensions consisted of 85 % Fe(0) (±2; $n = 3$). Investigations of the Fe(0) stability showed a reduction of about 10 % during 4-month storage. Figure 2.1 displays the measured particles size distribution of the final particle suspension after the two-step milling process [particle size: $d_{10}/d_{50}/d_{90}$ = 1.63/4.53/16.21 µm]. The BET analysis of the particles suspension shows a specific surface area of 18 m^2/g (raw material: 0.1 m^2/g; intermediate product: 0.7 m^2/g).

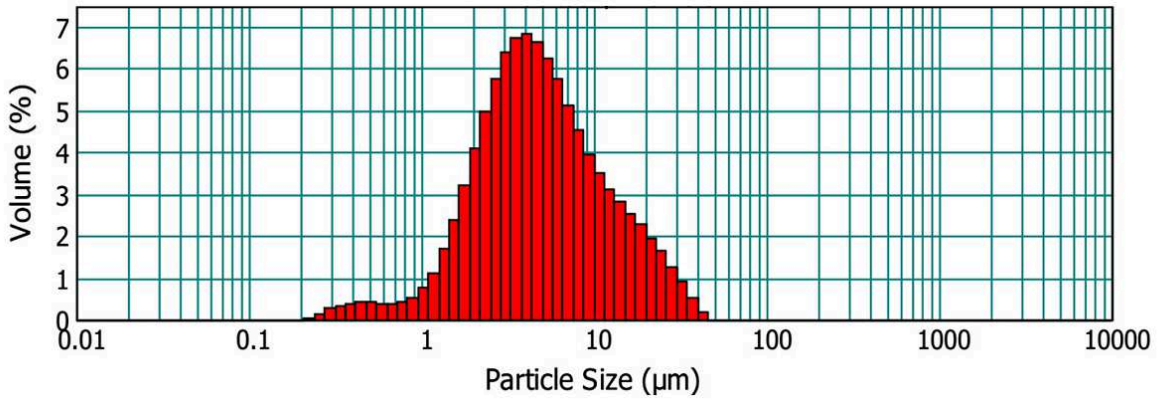

Figure 2.1: Particle size distribution of particle batch B4

Due to the milling process the particle suspension contained different agglomerates, probably causing a wide particle distribution. The largest measured agglomerates were 45 µm in size, the smallest 200 nm.

This was confirmed by a scanning electron microscopy (SEM) image of dried particles (Figure 2.2). The SEM image shows that larger particles can consist of several layers of small particles.

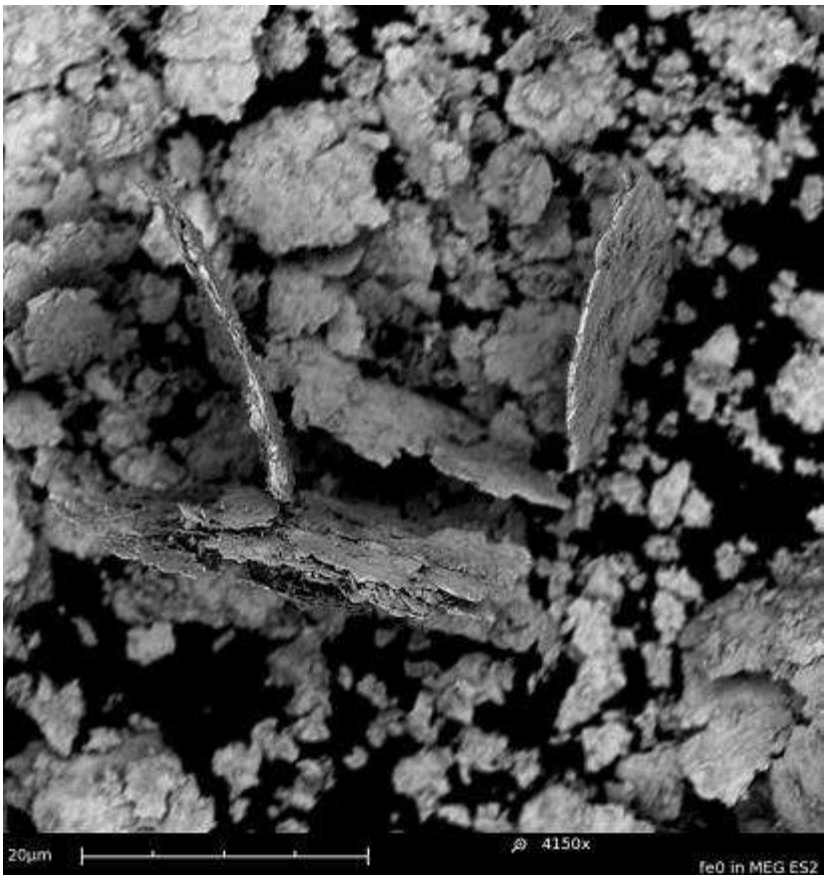

Figure 2.2: SEM image of ground particles (B4) after two-step milling process

Furthermore, the final iron particles can be described as a flake shape resulting from the milling process. While the lateral size of the flake is approximately several micrometers, the particle thickness is less than 100 nm. This stands in contrast to the mathematical model of the mastersizer 2000 system and has to be considered. The mathematical model of the mastersizer assumes a spherical shape of a particle for its calculation. Furthermore, it predicts a larger particle size when the laser beam hits a particle in front instead of side.

2.3.2 Coating effects

Utilizing PEG 400, a size distribution between 24 and 164 nm was found 6 h after synthesis. 18 h later the size distribution had increased (33–255 nm). Particles stored in nitrogen atmosphere for many days exhibit no significant precipitation. Synthesis of NZVI also was made in aqueous solution (pH between 9 and 10) without addition of PEG. In this case, iron particles precipitated within a few hours. Hence, PEG is able to diminish agglomeration if it is added during synthesis of nanoparticles. Similar practice is advantageous if iron particles are made by milling. Ethylene glycol is an alternative to PEG 400. In the presence of ethylene glycol, suspensions of milled iron are stable for many days even if diluted with deionized water

(1:100). However, addition of oxygen results in agglomeration and complete precipitation within 18 h. Ethylene glycol coatings are hydrophilic and permeable for oxygen (Bonder et al., 2007). Fe(II) ions are formed during the oxygen-induced corrosion process of iron particles. We assume, that Fe(II) ions play a vital role in agglomeration. The addition of small amounts of sodium dodecyl sulfate (SDS, 10 mM) inhibits precipitation in the presence of oxygen appreciably. A possible explanation is the formation of Fe(II)–SDS complexes, which form a protective layer on the iron particles inhibiting the corrosion process (Rajendran et al., 2002). Agglomeration induced by ions also is observable while adding drinking water. Two samples of ethylene glycol-coated milled iron particles were diluted with potable water under inert gas atmosphere in a glove box. Without SDS a spontaneous precipitation occurred. The sample containing 10 mM SDS also showed initiation of precipitation. However, after 4 h the supernatant solution was still a dark suspension. In this experiment, calcium and magnesium ions in potable water might be responsible for agglomeration.

2.3.3 Reactivity comparison of different particle batches

The present study investigates the reactivity of NZVI in batch experiments depending on varying parameters of the milling process. The production batches of NZVI differ with regard to basic material, milling duration, and type of dispersant chemicals used: in all degradation experiments, iopromide is subject to a pseudo-first-order rate kinetics. The concentration of iopromide decreases exponentially over time with a very good correlation (Figure 2.3, Table 2.2). Degradation of iopromide is verified by an increase of the iodide concentration. Furthermore, a constant DOC concentration throughout experimental time excludes a decrease in iopromide concentration caused by adsorption onto the reactor surface in addition to dehalogenation. This is in accordance with results of Stieber et al. (2011). Apparent dehalogenation rates during experiments with tested milled particles are comparable (except A1) to the rate which is observed during experiments with the reference nanoparticles N25.

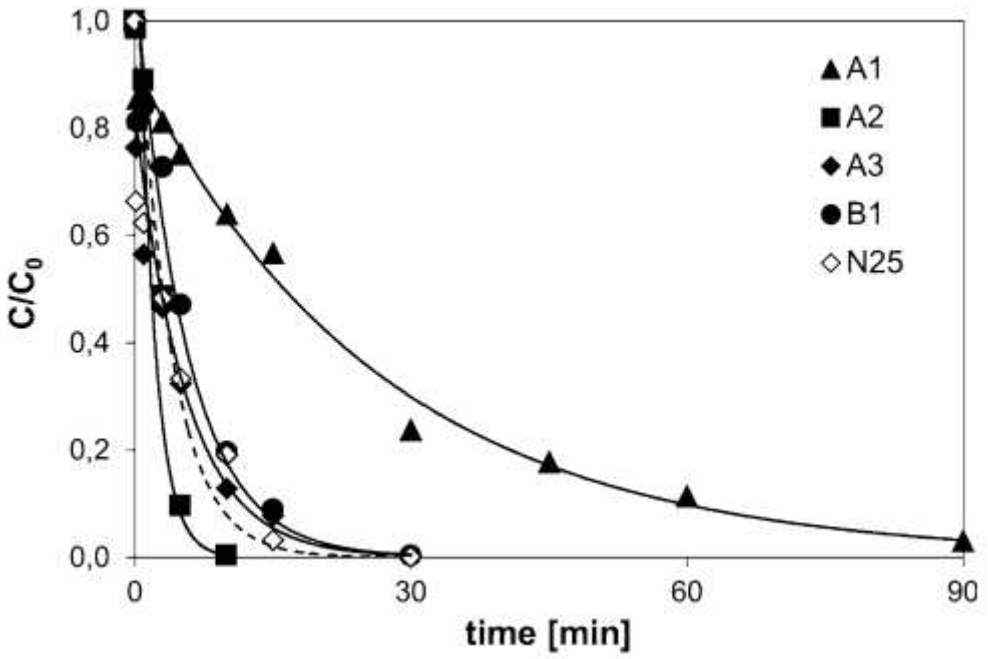

Figure 2.3: Normalized concentration of iopromide as a function of time during degradation by different particles. See Table 2 for degradation rate constants

Table 2.2: Observed first-order rate constants (K_{obs}) and used Fe(0) masses for the batch tests shown in Figure 2.3

	$n_{Fe0,start}$ (mmol)	K_{obs}(1/s) (degradation Iop.)
A1	7.0	6.21 x 10^{-4}, R^2=99
A2	10.0	9.59 x 10^{-3}, R^2=97
A3	6.9	3.03 x 10^{-3}, R^2=99
B1	8.0	3.02 x 10^{-3}, R^2=99
N25	7.2	4.41 x 10^{-3}, R^2=97

The particle batch A1 shows a significantly lower degradation rate of iopromide because of a lower surface area available for the reaction. The shorter milling duration of A1 (only one milling step) probably results in larger particles and a lower surface area of the particle suspension. In experiments with fine-milled Fe(0), Matheson and Tratnyek (1994) report that the dehalogenation performance is a linear function of the iron surface area concentration. In the present study, higher Fe(0) amounts correspond to higher iron surfaces available in the batch reactor which might be the reason for the slightly higher degradation rate of the particle batch A2. Within the present batch system, the organic contaminant (iopromide) is effectively de-halogenated by the milled iron particles. Further experiments will focus on the reactivity of NZVI particles in conditions comparable to the aquifer (sand columns).

2.3.4 Longterm reactivity

Column experiments have been performed to simulate remediation of PCE solution in a source zone with NZVI particles. Within the first 12 days (3 pore volumes), the particles showed the highest reactivity resulting in a decrease of the dissolved PCE concentrations of up to 90 % (95.9 mg/L). Thereafter, the reaction decelerated and leveled off at a constant PCE reduction of approx. 50 % (Figure 2.4). This change in reactivity is probably the result of mineralogical transformations on particle surfaces. Stoichiometric chloride formation showed an almost complete degradation of the reduced PCE mass. Furthermore, throughout the experiments, only a small amount of 13.5 mg TCE total mass and no other metabolites were detected. The particles showed a persistent and stable reaction for more than 40 days (10 pore volumes) without any significant changes of pH due to dechlorination or anaerobic corrosion.

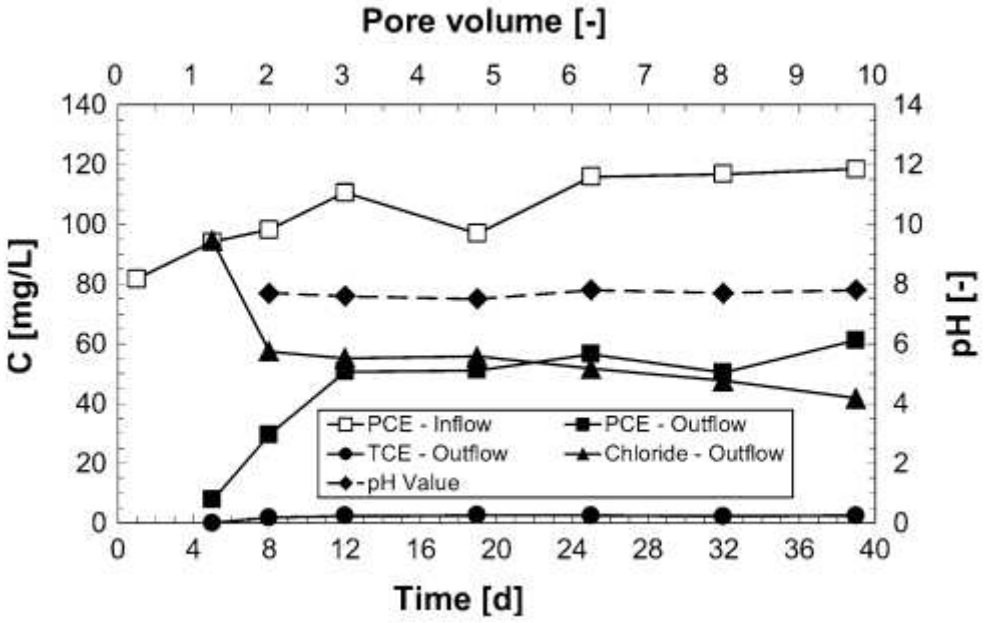

Figure 2.4: Concentrations of PCE, TCE, chloride and pH during the column experiment (B2)

Within the first PV, a PCE reduction rate constant (k_{obs}) of 1.1 x 10^{-1} L/h was observed, after 10 PV the k_{obs} had an average of 4.3 x 10^{-2} L/h. Under the same experimental conditions, N25S and B2 particles were directly compared (Fig. 5). When normalized by the mass of ZVI per unit aqueous phase volume (k_m), the B2 particles showed approximately one magnitude larger rate constants than the reference particles N25S (Figure 2.5). The average value of this rate constant was 4.1 x 10^{-3} L/g h for B2 particles and 4.0 x 10^{-4} L/g h for N25S. The better performance of the newly developed particles is probably caused by the mechanical activation of the surface during the milling process resulting in a flake shape with a highly reactive non-stabilized

surface. N25S particles are deactivated by part-oxidation of the surface to enhance their stability against reactions like anaerobic corrosion.

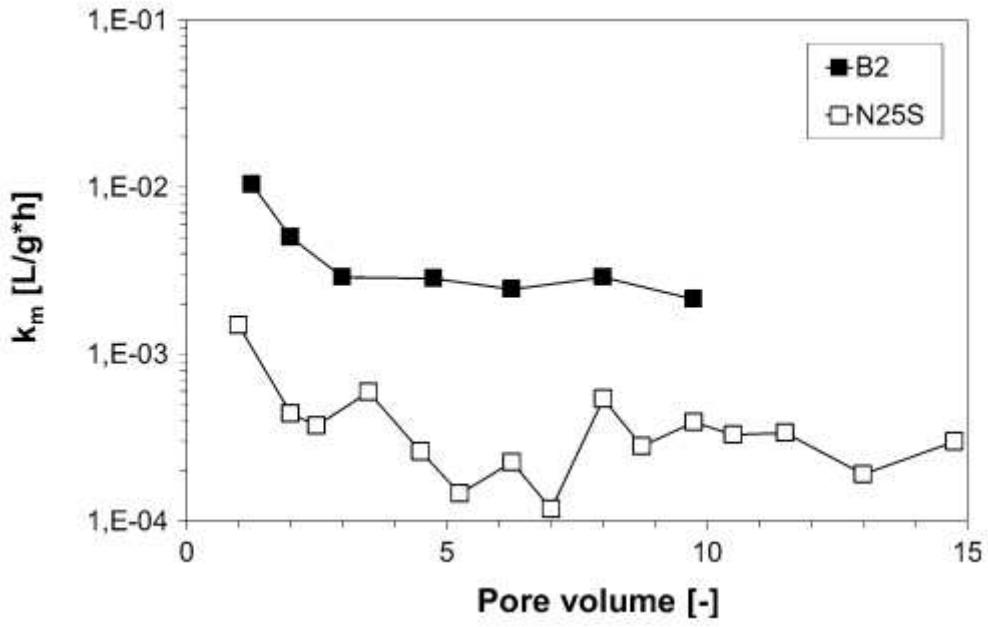

Figure 2.5: Comparison of PCE reduction rate constants normalized by Fe(0) mass for B2 and N25S particles

The ZVI mass normalized rate constant of the B2 particles is consistent with the magnitude of the normalized rate constant for RNIP particles (NZVI by TODA) as reported by Liu et al. (2005). In comparison to the mass normalized rate constant of micron-sized iron powder of 4.8 x 10^{-4} L/g h measured by Doong and Lai (2006), B2 shows a one-order magnitude larger rate constant (average 4.1 x 10^{-3} L/g h). For field application, a longer contact time between the reactive surface and the dissolved contaminants is needed to improve the efficiency of the degradation.

2.3.5 Transport

At comparable retained Fe(0) masses of 33–40 g, B4 particles had the greatest distribution range of 90 cm if $Fe(0)_{tot}$ >1 g/kg (sand) is taken as a reference compared to 35 cm for N25S and 24 cm for B1 (Fig. 6). Besides the longer transportation length of batch B4, these particles additionally showed the lowest Fe(0) concentration gradients and the most homogenous distribution. The lack of additives during the pre-milling process for batch B1 is assumed to be responsible for its relatively low transportability. The used grinding additives as well as the Fe(0) content and iron impurities seemed to be the controlling factors for the distribution range. The flake-like shape resulting from the grinding process is assumed to be the reason for slower sedimentation and better transport characteristics compared to the chemically precipitated N25S particles with a more spherical shape (Komar and Reimers, 1978). NZVI particles in the

experiment with the higher injected volume of A4 suspension could be transported throughout the whole column producing Fe(0)tot concentration of at least 27.5 g/kg (sand) up to 1.7 m flow path (Figure 2.6). $Fe(0)_{tot}$ concentrations near the injection point accounted for 100 g/kg (sand) and more. To our knowledge, the results presented here are the first proof that NZVI particles can be spread over 2 m with resulting Fe(0) concentrations sufficiently high for source treatment.

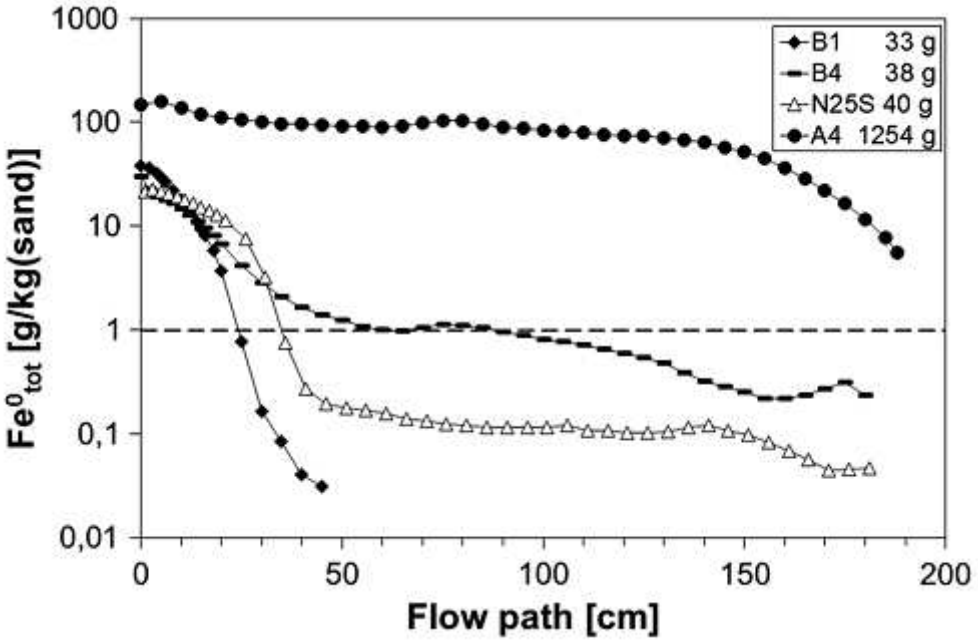

Figure 2.6: $Fe(0)_{tot}$-concentration profiles along the flow path at comparable injected Fe(0) masses for the particle batches B1, B4 and N25S and for a higher injected Fe(0) mass for the batch A4

2.3.6 Field test

During the preliminary field injection tests, the proof of NZVI presence and persistence achieved through liner-soil sampling indicated a radius of influence (ROI defined by the 0.5 g/L NZVI iso-concentration) of about 1 m. Following the field-scale pilot-test injection, liner-based soil sampling validated the previous findings in terms of NZVI ROI and confirmed DP direct injection as a NZVI subsurface delivery method being able to achieve a quasihomogeneous coverage of the reaction zone (Figure 2.7).

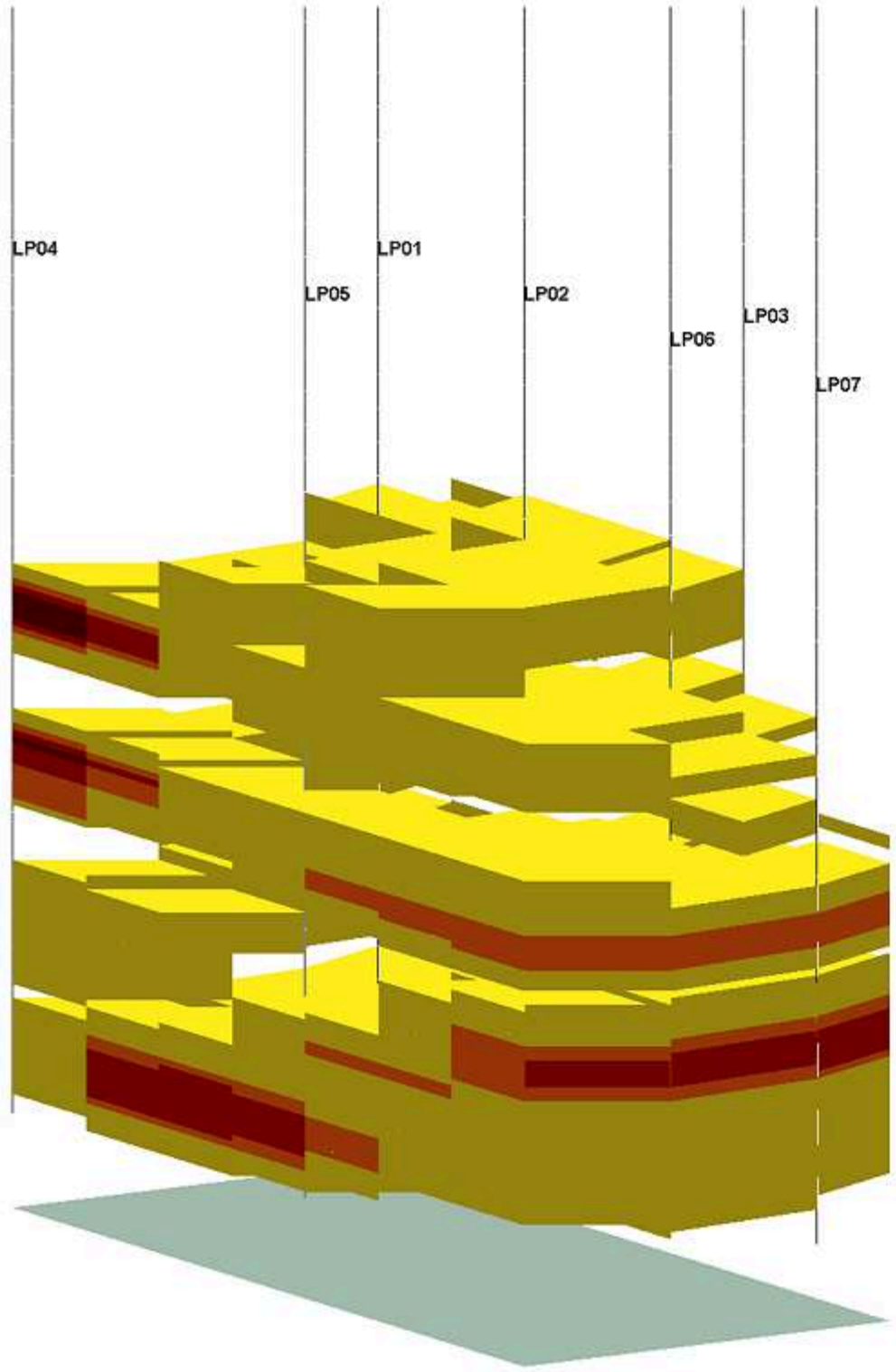

Figure 2.7: Quasi-homogeneous NZVI spatial distribution in soil (light shading >1 g/kg, dark shading >5 g/kg)

Groundwater monitoring for 1 year following the fieldscale pilot-test injection in August 2012 revealed a drastic decrease of the PCE concentrations from 20–30 mg/L down to 100–200 µg/L both in the source area and downgradient plume (Figure 2.8). The increase of the PCE concentrations immediately after the NZVI injection is probably due to mechanical

mobilization from neighboring NAPL bodies. A typical initial increase of degradation products (TCE, cis-DCE) followed by a decrease was observed. VC was detected only in concentrations below 4 µg/L. Ethene was produced in high concentrations both in the source area (up to 21 mg/L) and in the downgradient plume (up to 3.5 mg/L). Such ethene concentrations suggest initial PCE concentrations of about 120 mg/L. The increase of chloride from 60 to 200 mg/L further supports the conclusions about high initial PCE concentrations indicating an additional input from the PCE-NAPL. Despite the temporary accumulation of cis-DCE pointing to additionally occurring biological degradation processes, the fast production of high amounts of ethene indicates iron-mediated abiotic reductive dechlorination. Further groundwater monitoring is planned and an additional liner-soil sampling campaign should reveal the present NZVI spatial distribution as well as NZVI consumption during 1 year, as important steps towards mass balance and efficiency estimations.

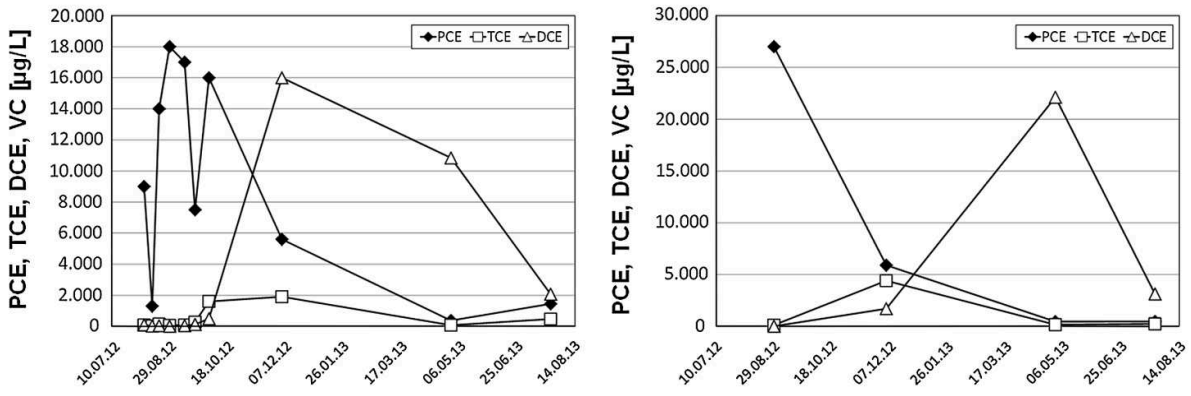

Figure 2.8: Chlorethene concentrations in groundwater samples (left source area, right downgradient plume)

2.3.7 Biological activity during field application

Dechlorinating microorganisms were detected by PCR in the source area and in the downgradient plume at all sampling times. Furthermore, formation and accumulation of cis-DCE point to the occurrence of biological dechlorination. Thus, there was no sustained inhibition of the naturally occurring dechlorinating microorganisms by injection of NZVI. Rather biological dechlorination was stimulated by the organics introduced during NZVI application, despite transient unfavorable pH values due to fermentation. Decreasing sulfate concentrations indicated a microbial sulfate reduction. Both dechlorination as well as sulfate reduction consume hydrogen, thus avoiding gas clogging. At some measurement points, a transient inhibitory effect on luminescent bacteria up to a maximum LID (Lowest ineffective dilution) of 16 was measured, which returned to no effective toxicity in the course of monitoring. Comparative studies in the laboratory using soil and groundwater from the site

confirmed the findings of the field application and showed a stimulation of biological dechlorination by injection of NZVI suspension.

2.3.8 Modeling

Using the fitted parameterization reported in Table 2.3, the measurement data of the particle concentration profile in the column test and its simulation with E-MNM1D as well as with the extended OGS are in satisfactory agreement (Figure 2.9), showing mainly a typical shape of strained particles (Bradford et al., 2002; Tosco and Sethi, 2010). Even though the variances of the measurements of the sediment cores, probably caused by unknown inhomogeneous permeability distributions, are partially severe (Figure 2.9), the simulation is quite similar to the measured mean particle distribution indicating the suitability of the developed model and the parameterization for supporting application design. For 0.5 g/kg (sand) as a concentration used to define the transport length of $Fe(0)_{tot}$, the predicted particle spreading is about 0.7 m. To consider pore clogging effects due to particle deposition, the OGS model approach is actually applied with a permeability–porosity relationship.

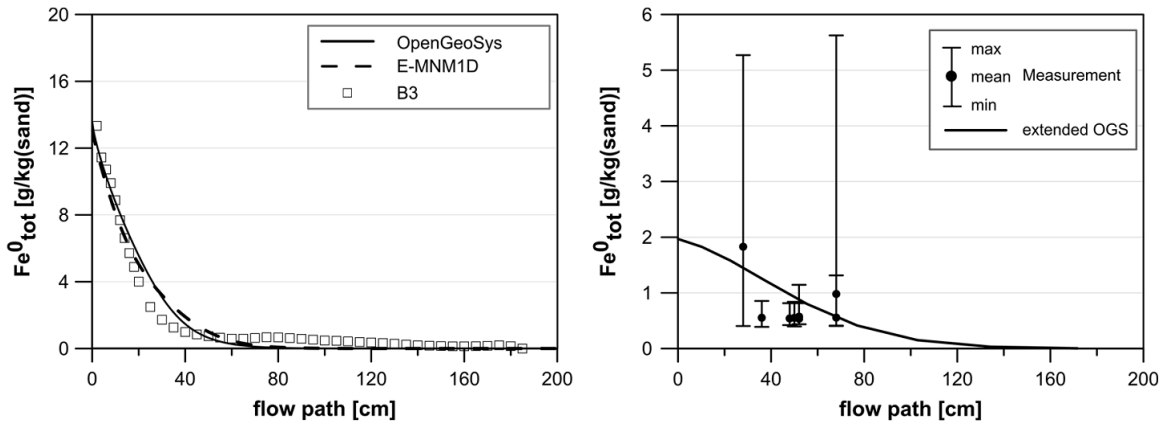

Figure 2.9: Observed and simulated particle distribution along the column at the end of the injection (left). Comparison of the simulation results with measurmeants from the preliminary field test (right)

Table 2.3: Deposition parameters fitted on a column experiment(c_{inj} 10 g/L, vf 0,5 m/h, K 2E-11 m^2)

Blocking		Straining	
$k_{a,1}$ [s^{-1}]	1.1E-02	$k_{a,2}$[s^{-1}]	3.5E-03
$k_{d,1}$ [s^{-1}]	1.0E-03	$k_{d,2}$ [s^{-1}]	1.6E-04
β_1 [-]	9.4E-01	β_2 [-]	-2.0E-02
S_{max} [kg/kg]	2.0E-02		

2.3.9 Ecotoxicity

Since the aquatic tests use aerobic organisms, only oxidized NZVI were tested. In the environment, NZVI are transformed into oxides thus being a more realistic object of investigation. The particles agglomerated within minutes and were deposited at the bottom of the test vessels in the presence of oxygen. In the *Daphnia magna* immobilization test, the particles caused immobility at concentrations below 1000 mg/L. An attachment of the particles to the body of the animals was observed which was counteracted by additional movement. After molting, these particles were shed and only minor consequent attachment was observed. The samples were not mutagenic in the Ames fluctuation test. The fish embryo toxicity test was the most sensitive assay in the applied biotest battery. The embryos of *Danio rerio* showed both lethal and sublethal (delayed hatching) effects at concentrations below 100 mg/L. The nanomaterials associated with the chorion of the fish eggs and impacted the evaluation. Any unhatched fish eggs were opened at the end of the test. The algae growth inhibition test was not applicable as the algae clogged between the particles, thus resulting in shading and a growth inhibition by physical means. Within the Ames fluctuation test, the bacterial density measurement was affected by deposited nanomaterials in the exposure vessels. As a solution, a multi-point measurement was suggested to overcome this problem. We compared our results with studies on iron oxide nanomaterials and aged zero-valent nanomaterials. The low toxicity is in agreement with results of Filser et al. (2013) and Sun et al. (2011) for iron oxide nanoparticles and of Marsalek et al. (2012) and Phenrat et al. (2009) for aged zero-valent iron nanomaterials. However, a study by Li et al. (2009) on adult medaka fish using iron oxide nanoparticles reported deleterious changes on gills and intestine filament at concentrations of 5 mg/L and suggested oxidative stress as the mode of action. Moreover, El-Temsah and Joner (2012) reported an effect on reproduction of earthworms in concentrations <100 mg/kg for aged NZVI.

Based on these results, aged NZVI can be classified in aquatic acute category 3 following the globally greed system of classification and labeling of chemicals (EC, 2008). Consequently, with regard to ecotoxicity, the use of NZVI can be recommended for remediation purposes. However, both the effects of a prolonged or chronic exposure and interactions with other chemicals are unknown.

2.3.10 Concluding remarks

As a result of the research activities presented, a new type of NZVI particles with advantages over preexisting NZVI particles concerning reactivity, transportability and economy (<50 €/kg)

was developed for groundwater remediation. The relatively high reactivity of the iron flakes may originate from the specific shape of the particles exhibiting higher specific surface area compared to more spherical shapes. The manufacturing process and the resulting shape may also enable the development of pits and edges favoring pitting corrosion and thus enhancing electron transfer. Furthermore, corrosion and electron transfer are increased by impurities in the ZVI, the amount of which is higher in the iron flakes due to the raw materials used than in relatively pure precipitated nanoiron particles.

The newly developed iron flakes are the only NZVI material for which transportability in relevant concentrations for up to 1 m and more could be confirmed by solidphase analysis in the lab and the field. These comparatively good transport characteristics with a relatively homogeneous particle distribution and low-permeability decreases are probably also the result of the flake-like shape decreasing the particle sedimentation rate and pore plugging since thin particles retained in pore throats allow higher water flow compared to spherical particles.

These practical important advantages together with the measured low acute toxicity of the particles, the observed synergies with microbial dechlorination and the developed possibility for numerical optimization of field applications illustrate that the iron flakes have a significant potential for source treatment of CHCs and other contaminants. The iron flakes are at present produced for research purposes and on demand.

Acknowledgments

This work is part of the joint project NAPASAN (Nanoparticles for ground water remediation) which was funded by the German Federal Ministry for Education and Research (BMBF) under the Grant Number 03X0097 within the research program NanoNature (Nanotechnologies for Environmental Protection—Value and Impact) which is part of the framework program WING (Material Innovations for Industry and Society).

Chapter 3
The ecotoxic potential of a new zero-valent iron nanomaterial, designed for the elimination of halogenated pollutants, and its effect on reductive dechlorinating microbial communities

This chapter is based on a publication in the peer-reviewed journal:
Schiwy, A., Maes, H.M., Koske, D., Flecken, M., Schmidt, K.R., Schell, H., Tiehm, A., Kamptner, A., Thümmler, S., Stanjek, H., Heggen, M., Dunin-Borkowski, R.E., Braun, J., Schäffer, A., Hollert, H. 2016. The ecotoxic potential of a new zero-valent iron nanomaterial, designed for the elimination of halogenated pollutants, and its effect on reductive dechlorinating microbial communities. *Environmental Pollution*. DOI: 10.1016/j.envpol.2016.05.051

Abstract

The purpose of this study was to assess the ecotoxicological potential of a new zero-valent iron nanomaterial produced for the elimination of chlorinated pollutants at contaminated sites. Abiotic dechlorination through the newly developed nanoscale zero-valent iron material and its effects on dechlorinating bacteria were investigated in anaerobic batch and column experiments. The aged, i.e. oxidized, iron material was characterization with dynamic light scattering, transmission electron microscopy and energy dispersive x-ray analysis, x-ray diffractometry and cell-free reactive oxygen measurements. Furthermore, it was evaluated in aerobic ecotoxicological test systems with algae, crustacean, and fish, and also applied in a mechanism specific test for mutagenicity. The anaerobic column experiments showed co-occurrence of abiotic and biological dechlorination of the common groundwater contaminant perchloroethene. No prolonged toxicity of the nanomaterial (measured for up to 300 days) towards the investigated dechlorinating microorganism was observed. The nanomaterial has a flake like appearance and an inhomogeneous size distribution. The toxicity to crustacean and fish was determined and the obtained EC_{50} values were 163 mg/L and 458 mg/L, respectively. The nanomaterial showed no mutagenicity. It physically interacted with algae, which had implications for further testing and the evaluation of the results. Thus, the newly developed iron nanomaterial was slightly toxic in its reduced state but no prolonged toxicity was recorded. The aquatic tests revealed a low toxicity with EC_{50} values $\geq$ 163 mg/L. These concentrations are unlikely to be reached in the aquatic environment. Hence, this nanomaterial is probably of no environmental concern not prohibiting its application for groundwater remediation.

Keywords: nZVI, nanoremediation, ecotoxicology

3.1. Introduction

The ecotoxicological evaluation of new technologies in their early developmental stages is beneficial to identify any negative ecological consequences (Baun et al., 2009; Hund-Rinke et al., 2015; Kühnel et al., 2014; Maynard et al., 2006; Nel et al., 2006; Nowack et al., 2014; Oberdörster et al., 2007). This proactive approach is more and more welcomed by founding bodies and is included in promotional programs for new technologies. A recent example is the founding of the WING program of the federal ministry of education and research in Germany. This program aimed to promote new material science developments like nanotechnology and includes ecotoxicological assessments.

Nanotechnology was described as the manipulation of single atoms or molecules (Roco, 1999a; Taniguchi, 1974). In material science, it is the most prominent development in the last century. It started in the 1960s and led to an increased development of new materials with astonishing properties (Cao, 2004; Feynman, 1960). Their application bears the promise to advance our society at an accelerated speed (Roco et al., 2011). It promises to improve many production processes and to enable new ones (Hannink and Hill, 2006). The annual world consumption of nanoscale chemicals and materials is estimated to be 11 million tons with an approximate value of 20 billion Euros (EC, 2012c). The two most dominant products in the market are carbon black (9.6 million tons) and synthetic amorphous silica (1.5 million tons, EC 2012). Newly developed engineered nanomaterials (ENMs) like carbon nanotubes (CNTs), silver, titanium dioxide nanoparticles or nanoscale zero-valent iron (NZVI) account only for a small percentage of the production volume (Schlag et al., 2011). However, in small volumes these ENMs are already available in many consumer products like clothing (silver), electronics (CNTs), and personal care products like suntan lotions (titanium dioxide) (Chen and Mao, 2007; DTU Environment, 2014; Hund-Rinke and Schlich, 2014; Maynard and Michelson, 2006; Schlich et al., 2013; Seitz et al., 2013; Volker et al., 2013b; Wyrwoll et al., 2016). Furthermore, these materials will be used in the medical field for therapy and diagnostics of disease in the near future (Mahapatra et al., 2013; Nel et al., 2009; Singh et al., 2010) In environmental technology, ENMs are applied in water treatment and remediation technologies (Bhawana and Fulekar, 2012; Karn et al., 2009; O'Carroll et al., 2013; Patil et al., 2015).

An example of an ENM applied for remediation technologies is NZVI (Cantrell et al., 1995; Chang et al., 2005; Köber et al., 2014; Mueller and Nowack, 2010; Tratnyek and Johnson, 2006; Wang and Zhang, 1997; Zhang, 2003). Like its micro scale counterparts, NZVI is applied for remediation purposes to transform various environmental contaminants (Cantrell et al., 1995; Gillham and O'Hannesin, 1994; Wang and Zhang, 1997). Two example applications are the transformation of heavy metals (e.g. chromium) or organic compounds (e.g. chlorinated hydrocarbons (CHCs)) to non-mobile or non-toxic compounds in aquifers (Ponder et al., 2000; Zhang, 2003). Due to their huge surface nanomaterials possess an increased reactivity compared to their micro scale counterparts (Comba et al., 2011; Lowry and Johnson, 2004; Wang and Zhang, 1997; Zhang, 2003).

Besides the intended pollutant transformation, anaerobic ZVI corrosion leads to the formation of hydrogen, which may result in gas clogging and consequently limited hydraulic permeability of the aquifer. On the other hand, hydrogen is consumed by hydrogenotrophic bacteria, acting as a sink for hydrogen and mitigating the problem of gas clogging. Moreover, hydrogen is an

excellent electron donor for supporting biological reductive dechlorination (Bruton et al., 2015; Lohner et al., 2011; Lohner and Tiehm, 2009; Velimirovic et al., 2015). Biological reductive dechlorination represents an environmental friendly, sustainable and cost-efficient option for removal of e.g. chlorinated compounds (Tiehm and Schmidt, 2011). The formulation ingredients (coatings, suspending agents, stabilization materials) of NZVI preparations can also serve as a source of electron donors supporting biological dechlorination (He et al., 2010; Kirschling et al., 2010; Su et al., 2012; Wei et al., 2012). Despite toxic effects of NZVI on natural microflora and dechlorinating microorganisms (Barnes et al., 2010; Bruton et al., 2015; Kumar et al., 2014b; Velimirovic et al., 2015; Xiu et al., 2010a; Xiu et al., 2010b), the combined use of abiotic dechlorination with NZVI and biological dechlorination can result in synergetic effects, positive for the remediation process (Bruton et al., 2015; He et al., 2010; Kocur et al., 2015; Su et al., 2012). High pH conditions developing during anaerobic ZVI corrosion as well as acidification due to fermentation of formulation ingredients being unfavourable for biological processes have to be taken into account during field applications (Bruton et al., 2015; Velimirovic et al., 2015).

The innovative aspect of the application of NZVI is the remediation of contaminants in areas where classic remediation technologies cannot be applied due to difficulties to reach the subsurface contamination (Li et al., 2006; Su and Puls, 2001). It is possible to inject the NZVI *in situ* directly into the source of contamination (Kanel et al., 2005). This approach can reduce the remediation duration as well as its costs (Li et al., 2006; Mueller et al., 2012).

There are two main problems concerning the possible use of NZVI for remediation purposes: 1) this material is not sufficiently tested for its safety, and 2) varying forms of NZVI are produced and their environmental behaviour and effects cannot directly be compared. The aim of this study was to assess the ecotoxicological potential of a new zero-valent iron nanomaterial and to evaluate its efficiency in eliminating chlorinated pollutants at contaminated sites. The newly developed NZVI used in this study were produced in a cost effective top down process by milling micro scale iron raw material to micrometre and nanometre scale (Köber et al., 2014). It has been applied at a pilot site and injected as a slurry with 10 g/L (Köber et al., 2014). In this study, both reduced and oxidized (referred to as “aged”) materials were tested. A commercial product of reduced NZVI was tested in anaerobic batch experiments and the comparable newly developed reduced NZVI was investigated in column studies to assess its toxic potential onto selected dechlorinating microorganisms as well as synergies between abiotic and biological dechlorination of the model contaminant perchloroethene (PCE). Newly

developed aged NZVI was tested in an ecotoxicological test battery containing methods to investigate its safety at different biological levels (cell tests & organisms).

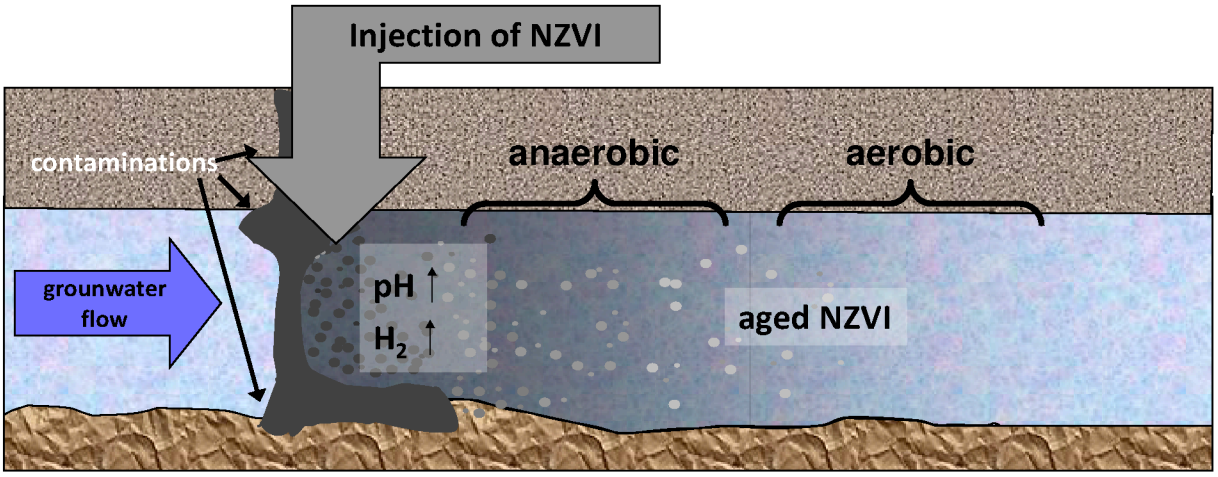

Figure 3.1: A schematic representation of the compartments in which NZVI come in contact with the environment - Figure re-drawn from Schell (2011)

In this study both the reduced and the oxidized referred to as "aged" material was investigated (cf. Figure 3.1). NZVI age instantly under aerobic laboratory conditions, a process that results in a product representing the nanomaterial after its initial reaction in the remediation process. Reduced NZVI was tested in anaerobic batch and column studies to assess its toxic potential onto selected dechlorinating microorganisms as well as synergies between abiotic and biological dechlorination of the model contaminant perchloroethylene (PCE). Aged NZVI was tested in an aerobic ecotoxicological test battery. The test battery included the algae growth inhibition test with *Desmodesmus subspicatus*, the acute crustacean immobilization test with *Daphnia magna*, and the fish embryo toxicity test with *Danio rerio* (Hafner et al., 2015; Peddinghaus et al., 2012; Wyrwoll et al., 2016). Additionally, the Ames fluctuation test with *Salmonella typhimurium* was conducted as a mechanistic test to evaluate a mutagenic potential (Meyer et al., 2014).

The investigations were conducted with the aged i.e. oxidized, iron material to investigate the toxic potential of the nanomaterial after its initial reaction in the remediation process. It was evaluated as an air dried powder in suspension without an additive. The pristine nanomaterial was not included in the aquatic tests through limitations in the laboratory setup and the conflict of physical prerequisites between the aquatic test systems and the nanomaterial: On the one hand all aquatic organisms need a level of oxygen in the medium to survive. The algae produce even oxygen as a product of their photosynthesis. Thus, no experiment can be conducted under the exclusion of oxygen. On the other hand, all NZVI nanomaterials are highly reactive and oxidize quickly. During this exothermic reaction, ferrous nanomaterials can even burn in an

oxygen atmosphere and thus become a concern for occupational safety (Celebi et al., 2007; Frost et al., 2010; Kumar et al., 2014a). Therefore, in a remediation application they are directly injected into the contaminated zone. However, in aquatic media with with circumneutral pH and environmentally relevant oxygen concentrations, NZVI rapidly oxidizes (Mackenzie et al., 2012). The particle concentrations investigated in the aquatic toxicity tests were lower than the concentrations applied at field injection sites for NZVI remediation projects with concentrations up to 10 g/L (Grieger et al., 2010; Köber et al., 2014; Nemecek et al., 2014). However, they were higher than the concentrations of NZVI in the aquatic environment originating as run-off from these remediation sites as the mobility of these nanomaterials is limited (Crane and Scott, 2012). In the study by Köber et al. (2014) the total iron concentration decreased over a length of 0.5 meter 12-fold in a column experiment and the iron material injected at a field site was not detected further than 1.5 m away from the injection point.

3.2. Material and Methods

3.2.1 Effect on anaerobic-reductive biological dechlorination

Batch and column studies were performed under anaerobic conditions to study the interplay between abiotic dechlorination through reduced NZVI and anaerobic-reductive biological dechlorination. The response of the most important anaerobic-reductively dechlorinating microbial groups *Dehalococcoides sp.*, *Desulfitobacterium sp.*, *Desulfomonile tiedjei*, *Dehalobacter sp.*, and *Desulfuromonas sp.* was monitored by nested polymerase chain reaction (PCR) with the method described in Kranzioch et al. (2013). The occurrence of these organohalide-respiring microorganisms can be taken as an indicator for the existence of biological dechlorination (Schmidt et al., 2006). Furthermore, the presence of the gene sequences coding for the four reductively dechlorinating enzymes (dehalogenases) pceA, tceA, bvcA and vcrA from *Dehalococcoides sp.* was assessed by PCR using the primers described in Behrens et al. (2008).

Batch experiments (with commercial NZVI) were conducted under anaerobic conditions in 2L bottles filled with a carbonate buffered mineral medium with 10 mg/L PCE. As reactive agents, the batch assays obtained either 0.5 g/L reduced NZVI Nanofer 25 (NANO IRON, Rajhrad, Czech Republic) or an actively dechlorinating laboratory microbial culture or NZVI plus microbial culture. Each batch assay was sampled for chloroethene analysis (PCE and its degradation products) via gas chromatography (measured as described in Lohner and Tiehm (2009) at several points in time as well as for analysis of anaerobic-reductively dechlorinating microorganisms and enzymes by PCR at the start and the end (day 64) of the experiment.

Column experiments (with our newly developed material) were conducted under anaerobic conditions with sediment and groundwater containing the natural site microflora from a model site in Braunschweig, Germany (Köber et al., 2014). Groundwater with PCE as primary contaminant was obtained at several sampling dates and stored anaerobically at 3 °C. Due to the ongoing NZVI injection at the field site (Köber et al., 2014) the individual groundwater samples differed in their chloroethene composition as well as in their hydrochemical properties (e.g. pH). The column set-up consisted of two parallel column systems (A and B) with two sequentially connected sediment columns (0.05 m diameter, 0.4 m height of packed bed), each. The flow-through of 0.34 L/d of groundwater was upwards from the columns A1 and B1 to the columns A2 and B2. The four columns were filled with a 1:1 mixture of field sediment (sandy material also containing fine grains smaller than 0.1 mm) and sand (Dorsilit 0.1-0.5 mm) resulting in a porosity of 0.4. The first columns additionally contained a 10 cm layer of pure sand at the inflow.

Column A1 was supplied with the newly developed NZVI material as anaerobic NZVI suspension prepared as described (Code MMA01 – B5) in Köber et al. (2014). At day 82 10 g NZVI suspended in 1 L groundwater were injected into column A1 at an injection rate of 6.9 L/d. At day 110 20 g NZVI suspended in 1 L groundwater were injected into column A1 at an injection rate of 12 L/d. For the third delivery at day 236 a gravel-packed pre-column filled with 18 g NZVI in suspension was connected to the inflow of column A1. Column B1 was supplied with the same amounts of suspension without NZVI.

The transport of the NZVI through the column was assessed visually. During 300 days test duration the influent of the whole column system as well as the effluents of each sediment column were regularly analysed for the concentrations of chloroethenes (PCE and its degradation products) and for the presence of anaerobic-reductively dechlorinating microorganisms and enzymes. Results are shown for the influent as well as for the effluents of the second sediment columns (A2 and B2).

3.2.2 Material characterization of the aged nanomaterial

3.2.2.1 Sample preparation for material characterizations and ecotoxicity testing

To prepare oxidized referred to as “aged” NZVI an aliquot of the reduced newly developed NZVI nanomaterial in its original suspension prepared as described (Code MMA01 – B5) in Köber et al. (2014) was transferred into a glass vessel and dried in an oxygen atmosphere at 80 °C in an oven over night.

For the characterizations or the aquatic toxicity tests the air dried iron powder was ground as the material covered the glass surface and formed a homogenous layer. The ground powder was weighed in aluminium weighing pans. Each dilution of the aged NZVI in 100 mL ultrapure water or corresponding test medium was weighed individually with an ultra-balance (XP6U, Mettler-Toledo GmbH, Gießen, Germany) and a maximum tolerance of ± 1 %. The ultrapure water was obtained by an ultra-filtration unit (ZFMQ23004, Millipore SA, Molsheim, France; 18 MΩ, 25°C). Finally, the samples were sonicated. The sonication was conducted with a HD 2200 ultrasonic probe with a VS70T tip (Bandelin, Berlin, Germany) at 200 W. The tip was inserted into the liquid approx. 1 cm above the bottom of the beaker (250 mL, short form). The settings for the ultrasonic probe were 0.8 ″/0.2 ″ (pulse/pause) for 5 min with 100 % power. After sonication, the suspension was introduced in the subsequent test without delay.

3.2.2.2 Dynamic light scattering (DLS)

For DLS investigations a 100 mg/L suspension in ultrapure or artificial water was prepared. A volume of 1 mL was transferred into a DTS0012 or a DTS1060 cuvette and filled according to the manufacturers´ recommendation. The samples were analysed with a DLS instrument (Zetasizer ZS 3600, Malvern Instruments, Malvern, UK) according to Nickel et al. (2014). The measurement parameters were adapted to iron with the following settings: refractive index 2.87, solvent water, automatic mode. The software version was 6.34.

3.2.2.3 Transmission electron microscopy (TEM) and energy dispersive x-ray analysis (EDX)

For the TEM investigations a suspension in ultrapure water with a concentration of 100 mg/L was prepared and 3 µL of this suspension were transferred onto a carbon coated copper TEM grid (Plano, Wetzlar, Germany). Following, it was air dried for storage and analysis. Subsequently, the nanomaterial was investigated with a Philips CM 20 FEG (Philips electronics, Eindhoven, Netherlands) transmission electron microscope operated at 200 kV using a Philips double-tilt sample holder. The images were collected with a CCD camera (Gatan Inc., Pleasanton, CA, USA). Selected objects were tilted with respect to the electron beam and a series of images was collected to estimate the three-dimensional shape and thickness of these objects. Additionally, for selected objects an EDX analysis was conducted using a connected EDAX spectrometer (EDAX Inc., Mahwah, NJ, USA).

3.2.2.4 X-ray diffractometry (XRD)

The XRD investigations were conducted with the aged NZVI with a x-ray diffractometer (MC 9300, HUBER Diffraktionstechnik GmbH & Co. KG, Rimsting, Germany) using Co Kα-radiation produced at 45 kV and 35 mA. The angles were from 20 degrees to 135 degrees. Quantitative phase analysis was performed by Rietveld refinement. The resulting data were analysed with BGMN software 5.1.3.

3.2.2.5 Cell free reactive oxygen species (ROS) detection

A cell free reactive oxygen species (ROS) detection was conducted according to the procedure by Simon et al. (2014b) and Rushton et al. (2010). This assay quantifies the amount of ROS in the medium whereas other assays measure the ROS within animal cells. In this assay, the substrate 2′,7′-dichlorodihydrofluorescin diacetate (DCFDA) is transformed to the sensitive compound 2',7'-dichlorodihydrofluorescin (DCFH). In the presence of ROS this compound is oxidized to 2',7' dichlorofluorescein (DCF). DCFDA (SigmaAldrich, Steinheim, Germany) was solved in ethanol and mixed with 0.01 mM NaOH for 30 min at room temperature in an opaque vessel. Then, it was neutralized with sodium phosphate buffer (pH = 7.2) and stored shaded form light on ice until usage. For measurement, a working reagent was prepared with 1 µM DCFH solution and horseradish peroxidase in a final concentration of 2.2 units/mL as catalyst. The reaction mix was incubated with sonicated aged NZVI suspensions at 10, 100, 450 and 1000 mg/L and sonicated medium as a process control. As a positive control H_2O_2 was applied at concentrations of 1, 2, 5, 10, 20 and 40 µM. Unsonicated medium was used as blank. The samples were incubated in darkness at 37 °C for 15 min in technical triplicates in 6-well plates (TPP Techno Plastic Products AG, Trasadingen, Switzerland). The formation of DCF was detected by excitation at 485 nm and emission at 530 nm with a plate reader Infinite M200 (Tecan Group Ltd., Männedorf, Switzerland).

3.2.3 Ecotoxical test battery of aged NZVI

3.2.3.1 Algae growth inhibition test

The algae growth inhibition test with *Desmodesmus subspicatus* was conducted based on the OECD guideline 201 (2011), Hafner et al. (2015) and Altenburger et al. (2008). The growth medium for the algae was prepared and aerated before usage. The pH value was adjusted to 8.1 and tempered to room temperature. A preculture was started 2 d to 3 d before the test under identical conditions as the final test with algae cultured in a medium prepared according to Bringmann and Kühn (1980). Algae in the exponential growth phase were used for the test. The

test suspensions were prepared by sonicating separately weighed aged NZVI in ultrapure water before the addition of the algae. Afterwards, 10-fold concentrated growth medium was added to obtain a 1-fold concentrated growth medium with the nutrients necessary for the algae. Before the start of the test, the chlorophyll fluorescence of the preculture was determined. The excitation of light with a wavelength of 465 nm and the emission of light with a wavelength of 685 nm were measured with a plate reader (Infinite M200, Tecan Group Ltd., Männedorf, Switzerland). The fluorescence is correlated to algal cell number which was calibrated in advance. The initial cell density in all wells was calculated to be 5000 cells/mL in a volume of 2 mL. The aged NZVI was tested in five concentrations against a negative control. The five concentrations and the negative control were tested in triplicate on a 24-well plate (TPP Techno Plastic Products AG, Trasadingen, Switzerland). The concentrations of the nanomaterial used were 6, 11, 23, 45, 90 mg/L. The setup was incubated in a climate chamber with a continuous illumination between 60 µE/m2s and 120 µE/m2s at 22 ± 2 °C and shaken at 120 rpm for 72 h. Every 24 h, the chlorophyll fluorescence was determined with the plate reader. After 72 h, the pH value of the pooled triplicates was recorded. The cell number was derived from the fluorescence measurements and used to calculate the growth rate. The growth rate inhibition was determined by comparison to the negative control. The validity criteria for the test apply only to the negative control and are defined as following: The pH value of the negative control medium should not increase more than 1.5 units during the test; controls should reach a specific growth rate of at least 0.92 per day; the mean coefficient of variation for section-by-section specific growth rates (day 0-1, 1-2 and 2-3, for 72 h tests) of the negative control cultures should not exceed 35 % and the coefficient of variation of average specific growth rates during the test period in replicate negative controls should not exceed 7 %. Additionally, a microscopic viability evaluation of the algae cells was conducted for selected samples after 72 h. Therefore, the algae were transferred from the selected wells onto a cover glass and microscopically evaluated with a 1000-fold magnification by oil immersion microscopy. A fluorescent light illumination in combination with filters for 485 nm excitation and 685 nm emission were applied.

3.2.3.2 Daphnia acute immobilisation test

The acute crustacean immobilization test with *Daphnia magna* was conducted based on OECD guideline 202 (OECD, 2004) and Wyrwoll et al. (2016). A day before the test, neonate daphnids were separated from the mother animals to ensure that only daphnids younger than 24 h were used in the test. The artificial water was prepared according to the guideline and the pH and oxygen levels recorded. The setup consisted of four replicates per concentration with five

daphnids, in each test beaker. Each animal had a volume of 2 mL medium. The aged NZVI were evaluated at 10, 25, 50, 100, 500 and 1000 mg/L. Additionally, a negative control (NC) with only the artificial water or a sonication treatment control (TC) without aged NZVI was included. The neonates were randomly taken from the total breed of the day and transferred with as little as possible of additional medium into the aged NZVI suspension. The setup was incubated at 20°C in darkness. After 24 h and 48 h, the number of immobile animals was noted. The percentage of immobile daphnids was calculated and effect concentrations (EC) were determined after probit analysis of the data using the ToxRat software package (ToxRat Solutions GmbH, Alsdorf, Germany). At the end of the test the pH value and oxygen saturation of each concentration was determined. The test was valid if the percentage of immobility in the negative control was < 10 % and the oxygen saturation > 2 mg/L.

3.2.3.3 Fish embryo toxicity test

The assay with zebrafish (*Danio rerio*) was carried out based on OECD guideline 236 (OECD, 2013) with modifications given by Peddinghaus et al. (2012) and Schiwy et al. (2015b). The nanomaterials were tested in duplicates in seven concentrations (16, 31, 63, 125, 250, 500 and 1000 mg/L) prepared with artificial water with a static test design. 3,4-dichloroaniline (Sigma–Aldrich GmbH, Steinheim, Germany; 3.7 mg/L) served as a positive control, artificial water as a negative control, and sonicated artificial water as a treatment control (TC). To each test concentration, ten eggs that reached the 8 cell stadium were added. Then, each egg was transferred into a volume of 2 mL on a well of a 24-well plate. Each plate was covered with a gas-permeable foil (Renner, Darmstadt, Germany) and incubated at 26 ± 1 °C for the exposure period of 96 hours post fertilization (hpf). Evaluation of the test was carried out with an inverted microscope at 40-fold and a 100-fold magnifications. Every 24 hpf, the lethal endpoints (coagulation of the embryo, non-detachment of the tail, non-detection of the heartbeat, and lack of somites) were recorded. As an additional endpoint, the hatching of the embryos was included. The percentage of effect was calculated and an EC_{50} was determined using Graphpad Prism 6 with least square fit analysis.

3.2.3.4 Ames fluctuation test

For measurement of the mutagenic potential, a modification of the standard Ames assay was conducted according to ISO guideline 11350 (ISO, 2012), Reifferscheid et al. (2012) and Heger et al. (2012). Mutagenicity was investigated using the *Salmonella typhimurium* strains TA 98 and TA100 with the Ames fluctuation test. Detection of the reverse mutation was realized by using a pH indicator dye in the test media and counting the number of positive wells (wells with

revertant growth). Sensitivity of the test system can be increased by adding a metabolic activation system i.e. the rat liver S9 homogenate. This results either in an increased mutagenicity due to activation of progenotoxic substances or a decreased mutagenicity due to the detoxification of genotoxic compounds. The test strains were inoculated in growth medium 24 h before onset of the test. Prior to seeding into a 24-well test plate, optical density (OD) was measured photometrically at a wave length of 595 nm. The concentration and absorption relationship of the reference compound formazine called Formazine Attenuation Units (FAU) was used as an estimate for bacterial density. The bacterial density was adjusted to 450 FAU. For exposure, either sample or controls were added to a 24-well plate.

As positive controls for the approach without metabolic activation 0.02 mg 4-nitro-*o*-phenylendiamin (4-NOPD; in DMSO) for the strain TA98 and 0.5 µg/mL nitrofurantoin (NF; in DMSO) for the strain TA100 were applied. In the approach with metabolic activation through the S9 mix 0.4 µg/mL and 0.8 µg/mL 2-aminoanthrancene (2-AA; in DMSO) were applied for TA98 and TA100, respectively. The negative control consisted of ultrapure water. For experiments with metabolic activation, the S9 mix was added to each well. The investigated aged NZVI was sonicated in ultrapure water and added to 10x medium. Finally, the bacteria in exposure medium were added. Test concentrations investigated were 5, 10, 20, 40, 50 and 100 mg/L. After 100 min, exposure was terminated by adding the reverse indicator medium to each well. Subsequently, 50 mL of each test concentration with the added reverse indicator medium were added to 48-wells of a 384-well plate and incubated at 30 °C in darkness for 48 h. For evaluation, all wells with revertant growth per concentration were counted. A test was considered valid if the number of revertant wells in the negative control was less than ten and in the positive control was at least 25. Samples are considered mutagenic if a dose response curve can be drawn to the data or if revertants are visible in the consecutive concentrations.

3.3. Results

3.3.1 Effect on anaerobic reductive biological dechlorination

Anaerobic batch studies showed a removal of 28 %, 7.7 % and 24 % of the initial PCE concentration after 64 days for the assays with reduced NZVI, with microbial culture and with reduced NZVI plus microbial culture, respectively (Table 3.1, Figure 3.2). In view of possible variability of the batch assays as well as the unavoidable measuring error the assay with reduced NZVI, and with reduced NZVI plus microbial culture performed equally. These results demonstrated that due to the lack of electron donors, the microbial culture alone was hardly

able to perform anaerobic-reductive dechlorination despite of the presence of *Dehalococcoides sp.*. The other dechlorinating organisms *Desulfitobacterium sp.*, *Desulfomonile tiedjei*, *Dehalobacter sp.*, and *Desulfuromonas sp.* were not detected. The needed electron donors were provided by the addition of reduced NZVI. From the formation of cDCE (Figure 3.2) and the increase of the number of detected dechlorinating enzymes of *Dehalococcoides sp.* (Table 3.1) at the end of the experiment in the batch with reduced NZVI plus microbial culture it can be concluded that i) NZVI was not inhibiting *Dehalococcoides sp.* ii) the dechlorinating microorganisms were proliferating and iii) the microorganisms contributed to the reductive dechlorination observed.

Table 3.1: Anaerobic batch studies - PCR detection of DNA sequences of *Dehalococcoides sp.* and its four enzymes and percent of perchloroethene (PCE) degraded at the start and the end (64 days) of the batch studies, (-: not detected; +: detected)

Batch		*Dehalococcoides* sp.	pceA	tceA	bvcA	vcrA	PCE degraded [%]
NZVI	start	-	-	-	-	-	-
	end	-	-	-	-	-	28
microbial culture	start	+	-	-	-	+	-
	end	+	-	-	-	+	7.7
NZVI + microbial culture	start	-	-	-	-	+	-
	end	+	+	+	-	+	24

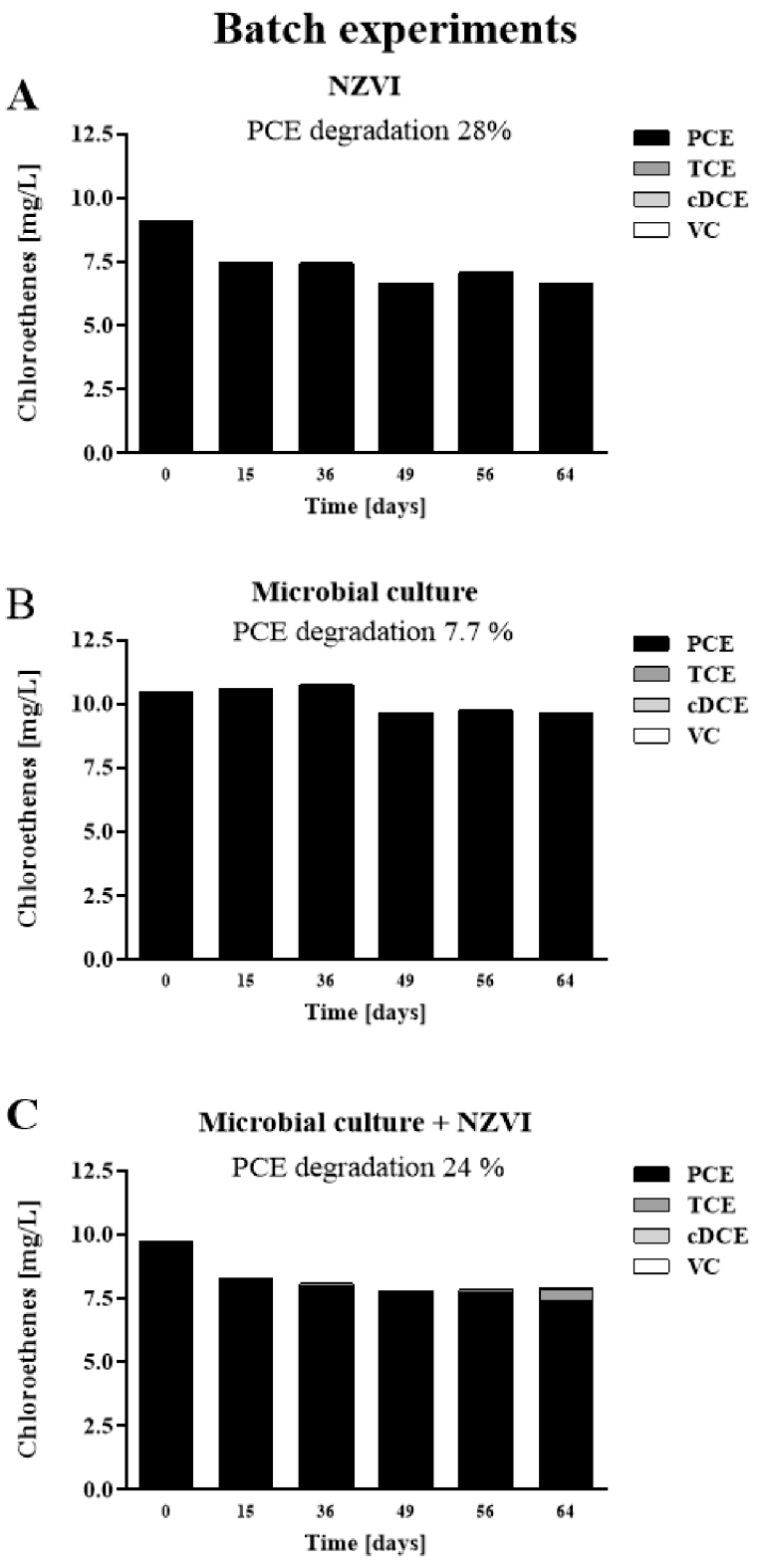

Figure 3.2: Anaerobic batch experiments - Chloroethene composition in the assays with NZVI (A), with microbial culture (B) and with NZVI plus microbial culture (C) (PCE: perchloroethene ; TCE: trichloroethylene; cDCE: cis-1,2-dichloroethene; VC: vinyl chloride)

The transport with the anaerobic column experiments was assessed visually. During the injection with a higher flow rate an uneven distribution of the NZVI was clearly visible in column A1 (Figure 3.3). No further spreading of NZVI was observed during the column experiment with the normal flow rate. At a later stage of the experiment the column was blackened due to the precipitation of iron sulphide thus masking the location of the NZVI.

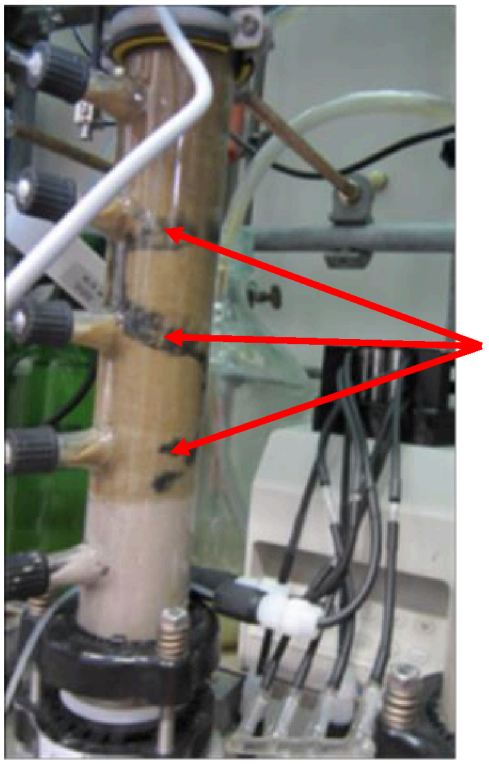

Figure 3.3: Anaerobic column experiments - Photograph of the column A1 after NVZI injection

During the first 100 days of the anaerobic column experiment the effluents showed only minor dechlorination (Figure 3.6) and a lower or equal number of detected groups of dechlorinating microorganisms compared to the influent (Figure 3.7). Due to biodegradation of the organic suspending agents pH values at the field site (influent between day 70 and day 100) as well as in the columns (measurable in the effluents after the NZVI injection at day 110 and 236) dropped (Figure 3.4). This acidification and the formation of ethanol and methanol indicated fermentation processes (Figure 3.4 and Figure 3.5). A pH increase caused by anaerobic ZVI corrosion was not measured.

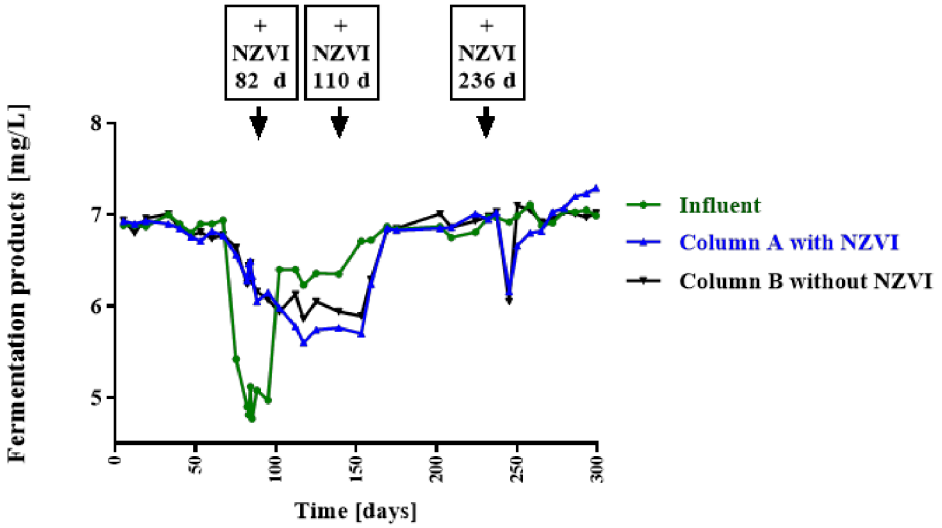

Figure 3.4: Anaerobic column experiments - pH values in the influent and in the effluents of columns without and with NZVI treatment. The groundwater was sampled at different days and was influenced by the field injection of NZVI resulting in changing pH values in the influent.

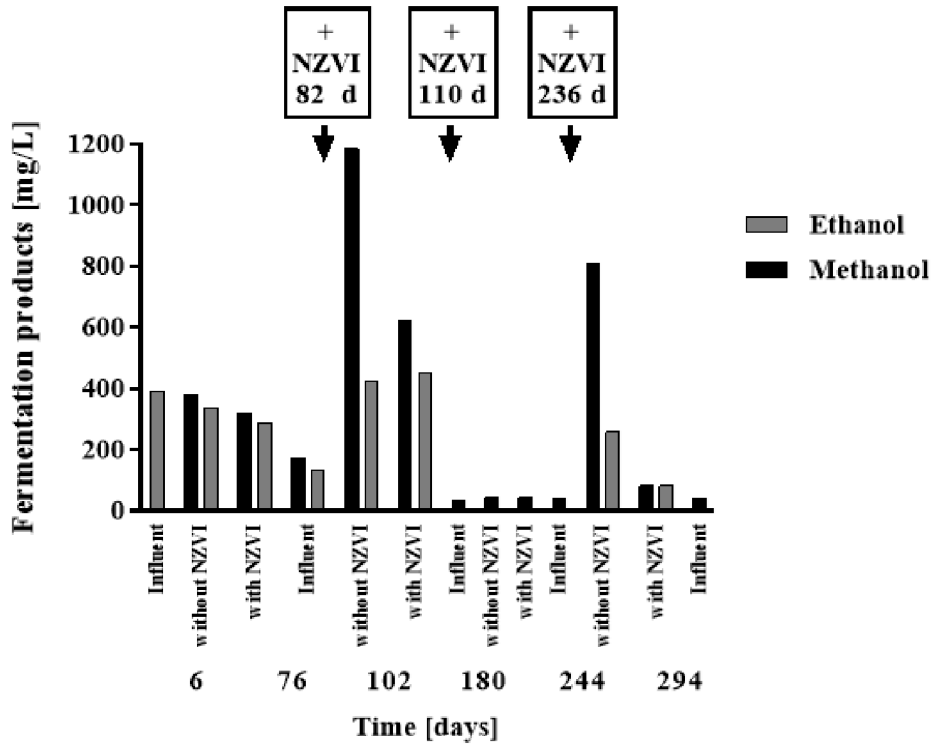

Figure 3.5: Anaerobic column experiments – Fermentation products methanol and ethanol in the effluent from the column experiments

After the acidification declined, biological dechlorination was observed (sampling dates 180, 244 and 294 in Figure 3.6). A corresponding increase of the number of PCR detected DNA sequences of dechlorinating microorganisms (Figure 3.7) and enzymes (Figure 3.8) in the effluents compared to the influent was then observed as well (Figure 3.7 and Figure 3.8).
Due to the changing chloroethene concentrations within the groundwater sampled at different days all effluent results need to be compared to the corresponding influent concentrations as it is done in Figure 3.6. In both column systems, the metabolites trichloroethene and cis-1,2-dichloroethene were formed. Further degradation to vinyl chloride and ethene was not observed. Except for the last sampling date, showing a higher degree of dechlorination for the column A with NZVI, there was no significant difference in dechlorination between the columns with and without NZVI. There was no significant difference in the amount of PCR detected DNA sequences of dechlorinating microorganisms and enzymes between the column system with and without NZVI, neither. Corresponding to the results of the batch studies, the column studies again demonstrated that NZVI did not exert a measurable inhibition of the microbial activity being relevant for biological dechlorination in the subsurface environment.

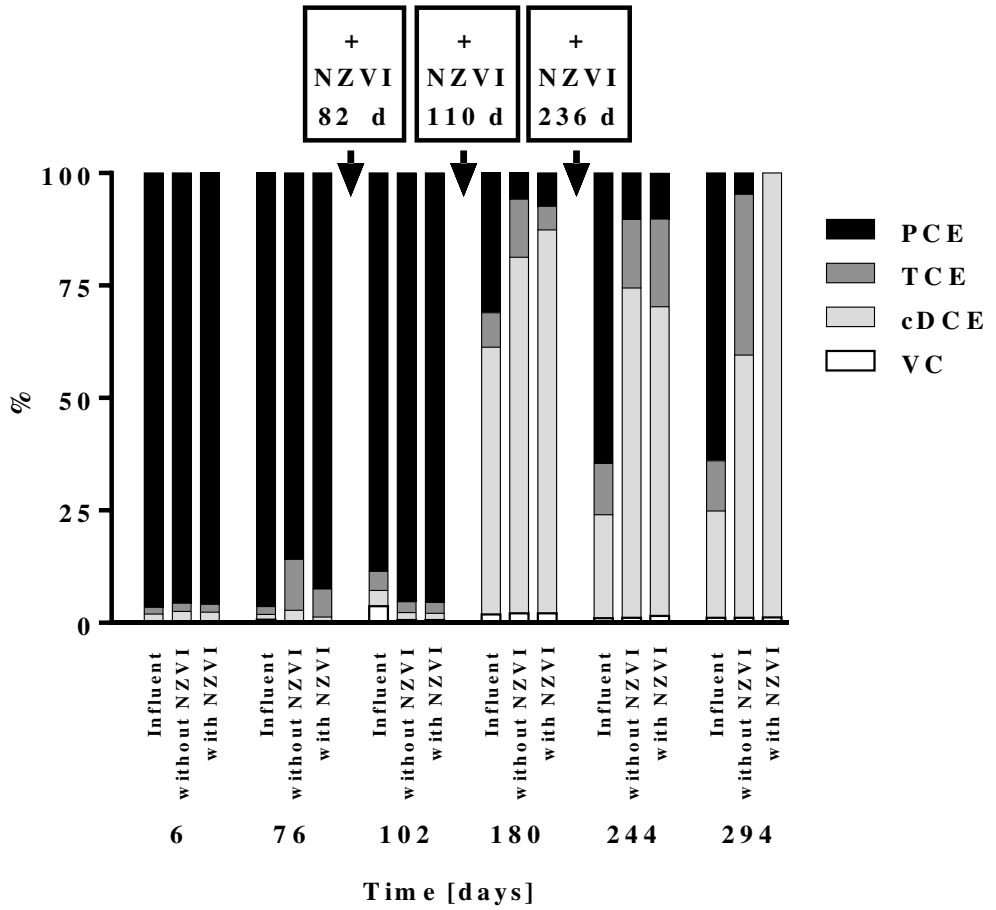

Figure 3.6: Anaerobic column experiments - Chloroethene composition in the influent and in the effluents of columns without and with NZVI treatment (PCE: perchloroethylene; TCE: trichloroethylene; cDCE: cis-1,2-dichloroethene; VC: vinyl chloride)

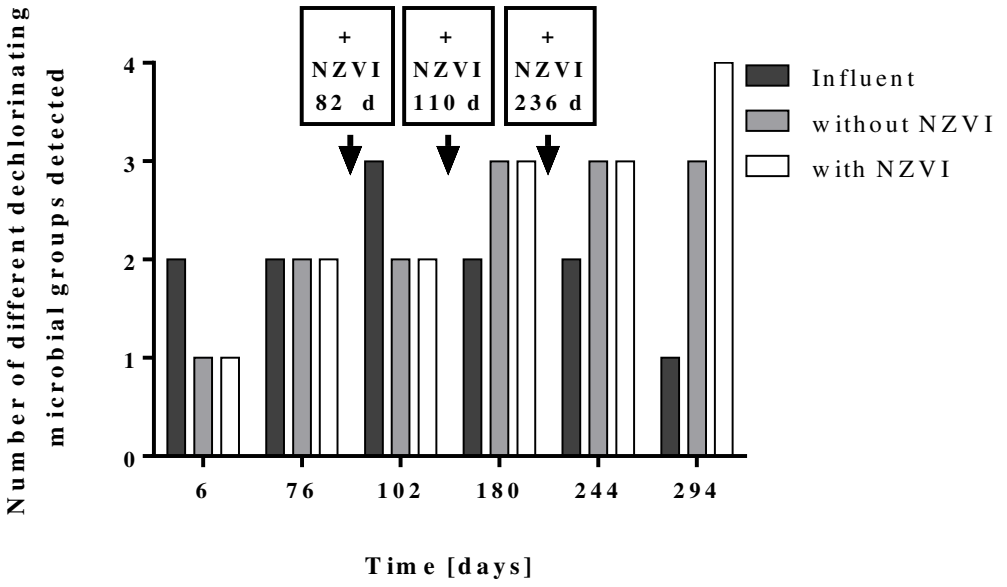

Figure 3.7: Anaerobic column experiments - Number of different anaerobic-reductively dechlorinating microbial groups detected with PCR (five in total tested) in the influent and in the effluents of columns without and with NZVI treatment

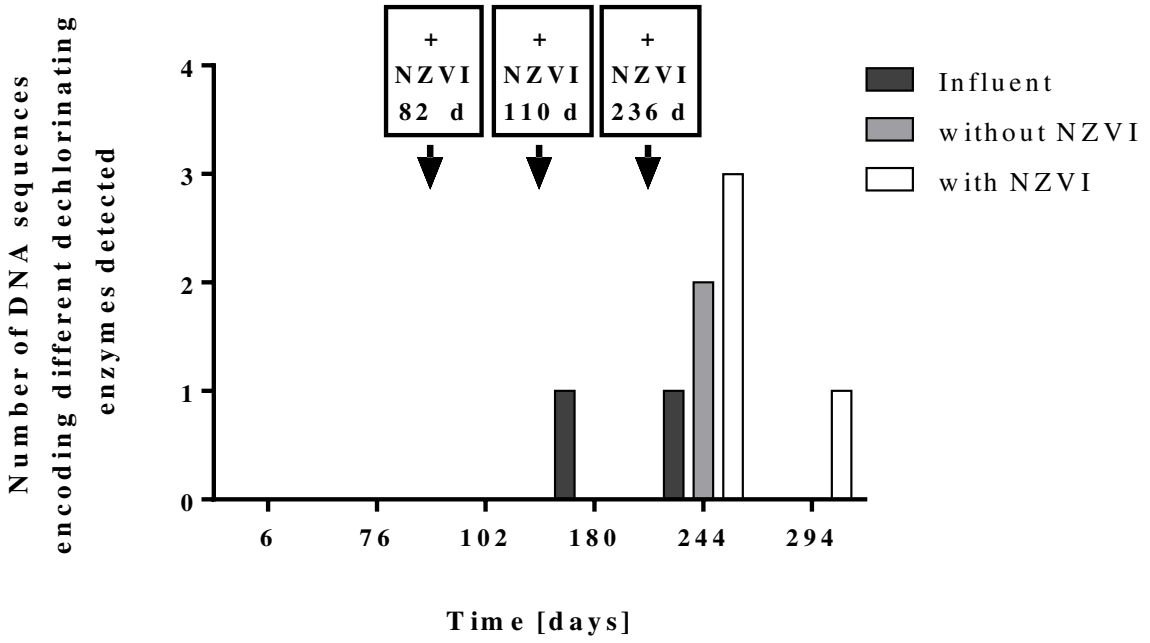

Figure 3.8: Anaerobic column experiments - Number of DNA sequences encoding different anaerobic-reductively dechlorinating enzymes of *Dehalococcoides sp.* detected with PCR (four in total tested) in the influent and in the effluents of columns without and with NZVI treatment

3.3.2 Characterization of aged NZVI

3.3.2.1 Dynamic light scattering

The results for the DLS measurements with the aged nanomaterial did not show any consistent data (data not shown) regarding the particle sizes of the nanomaterials. In ultrapure and artificial water, the results did not meet the quality criteria which consists of 12 tests including check for polydispersity, correlation function intercept value between <0.1 or >1.0, and sufficient data collected. The quality report indicated the possibility of sedimenting particles as the size results varied over time. The values for the polydispersity index for all measurements were above 0.5 (data not shown).

3.3.2.2 Transmission electron microscopy (TEM) and energy dispersive x-ray analysis (EDX)

The micrographs present various particle sizes between some tens of nanometres and some micrometres for the aged nanomaterial (Figure 3.9). No statistical analysis was conducted due to the heterogeneity and no uniform morphology of the aged NZVI. To estimate the thickness of a selected particle, the sample was tilted stepwise and a series of micrographs was subsequently taken (Figure 3.10). The analysis revealed a sample thickness below 100 nm. The composition of the particle was analysed by EDX and the presence of iron was verified (Figure 3.10, right upper graph). A spot on the carbon coated TEM grid was used as a reference which did not show any iron signal (Figure 3.10, right lower graph).

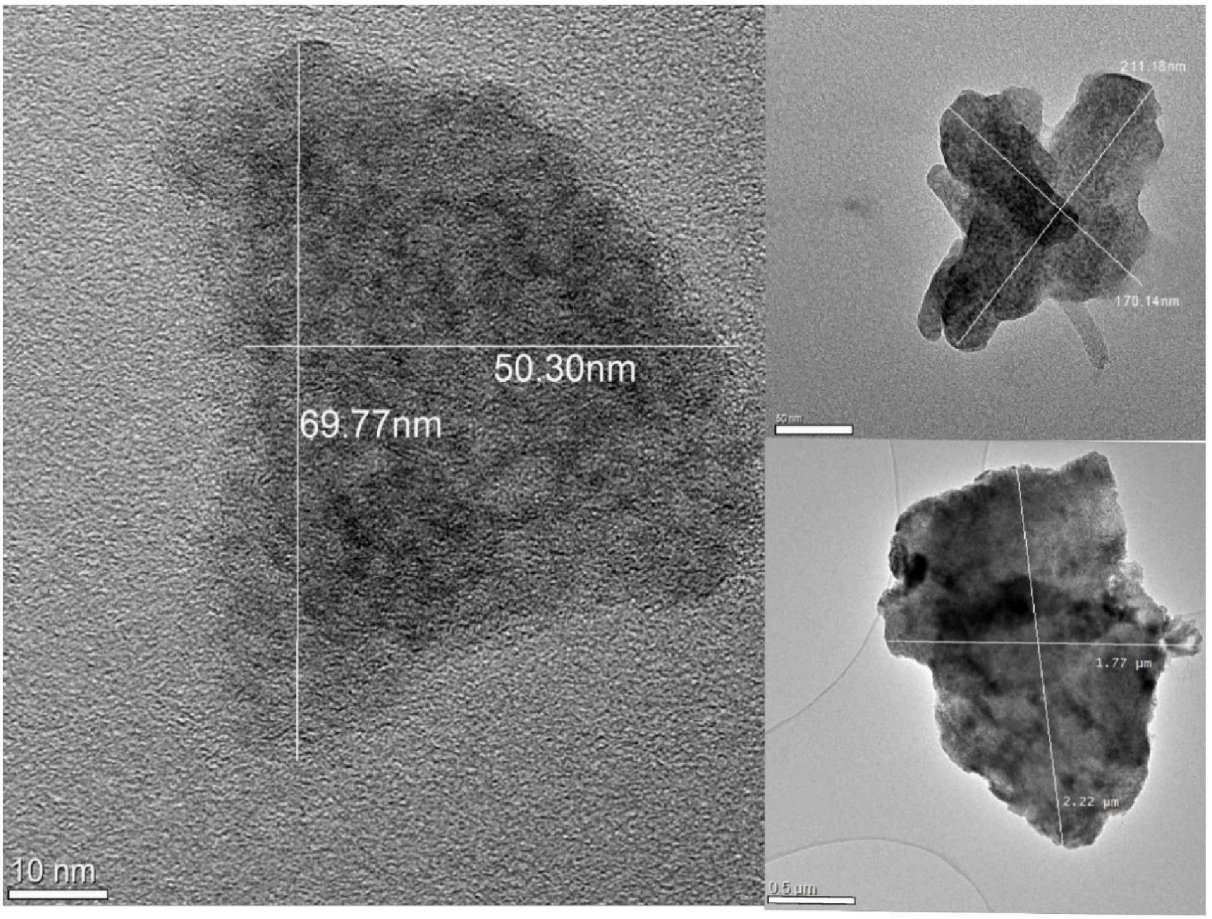

Figure 3.9: TEM micrographs of three different aged NZVI flakes of the aged NZVI

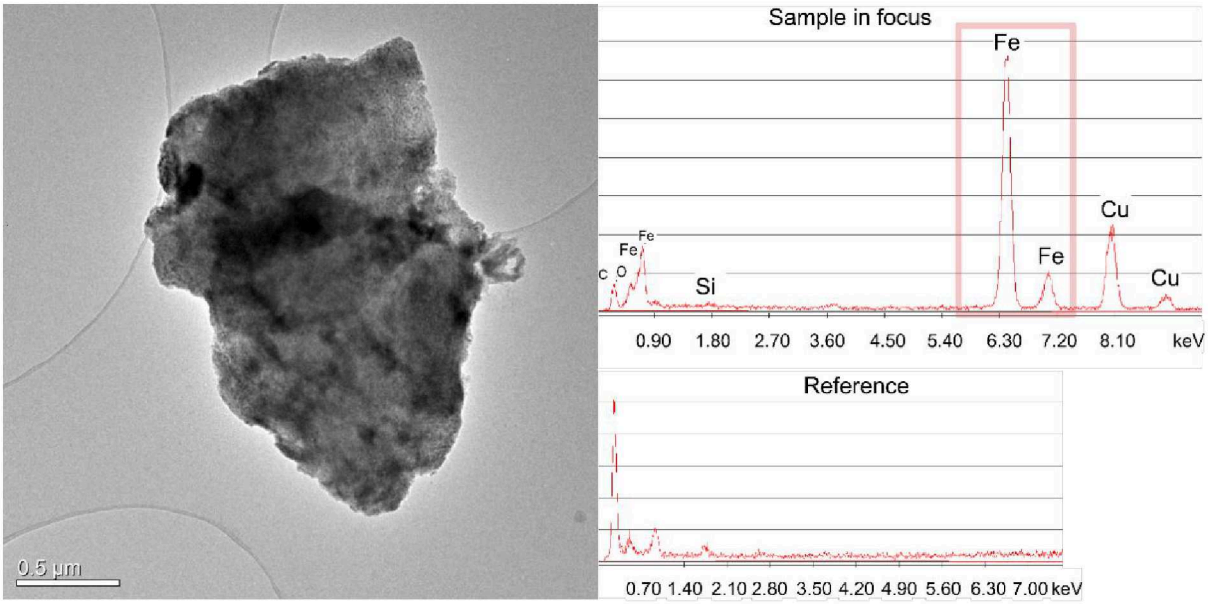

Figure 3.10: TEM micrograph of aged NZVI flake (left) and corresponding EDX spectrum (right, upper graph). An EDX spectrum of the carbon film without any sample is shown as a reference (right, lower graph)

3.3.2.3 X-ray diffractometry (XRD)

The results of the XRD measurement indicate that the aged nanomaterial consist mainly of the allotrope α-Fe (ferrite) with a percentage of over 81 % and the remaining part of 19 % γ-Fe (austenite). Besides these both modifications no additional phases were detected. The broad peaks indicated both size and strain contributions. From the size term mean coherence lengths of 62±22 nm were determined, which corresponds well with the particle dimensions determined by TEM.

3.3.2.4 Cell free reactive oxygen species (ROS) detection

In this assay, the non-fluorescent 2′,7′-dichlorodihydrofluorescin diacetate is transformed to a highly reactive compound that reacts with any ROS in suspension. After the addition of the aged NZVI and horseradish peroxidase (HRP), any ROS in the medium leads to the formation of the fluorogenic dye that indicates the amount of ROS present. The results of the cell free ROS measurement showed a dose response for the positive control H_2O_2 and the aged NZVI (Figure 3.11). The results indicate that high concentrations of the aged NZVI are correlated with the formation of ROS. The treatment control with sonicated medium as well as the aged NZVI concentrations of 10 mg/L and 100 mg/L showed a response comparable to the blank. The response of 450 mg/L and 1000 mg/L NZVI was approximately 4-fold higher.

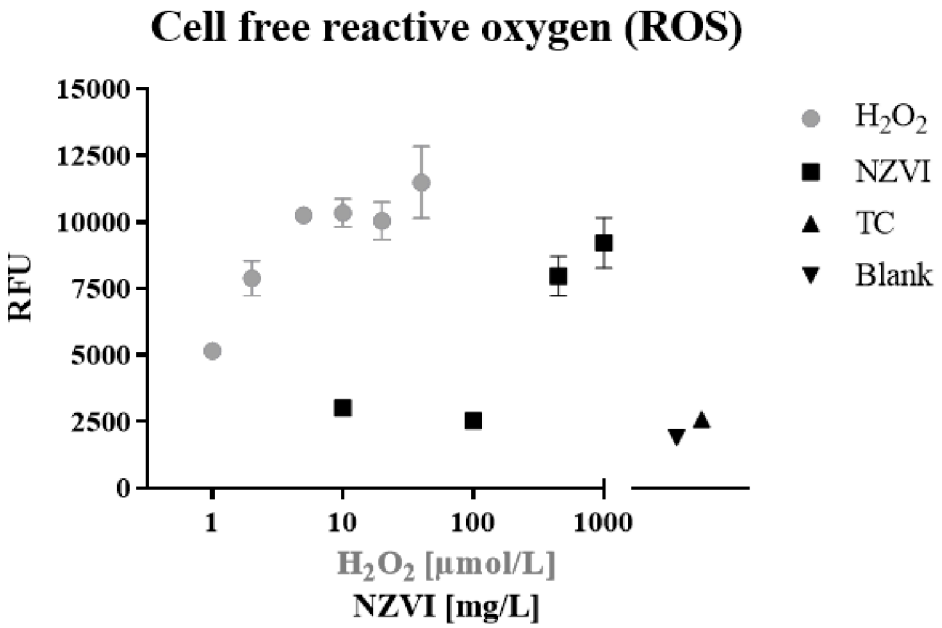

Figure 3.11: ROS detection - Fluorescence response of the cell free ROS DCFDA assay with aged NZVI and H_2O_2 as reference. The whiskers represent the standard deviation on the mean of three technical replicates. (RFU: Relative fluorescence units; TC: Treatment control; Blank: Untreated control; NZVI: Nanoscale zero-valent iron)

3.3.3 Ecotoxicity testing of aged NZVI

3.3.3.1 Algae growth inhibition test

The algae growth inhibition test did not show any evaluable results (data not shown). No growth could be recorded for the aged nanomaterial dilutions by measuring the chlorophyll fluorescence with a plate reader. The nanomaterial associated to algae and sedimented quickly in the initial phase of the experiment forming a layer of sedimented material after 20 min preferentially in the middle of the well plate. A microscopic investigation of the sample showed that the algae were viable (Figure 3.12). The cells were incorporated into a cluster of the aged NZVI and were not visible without fluoroscopic illumination.

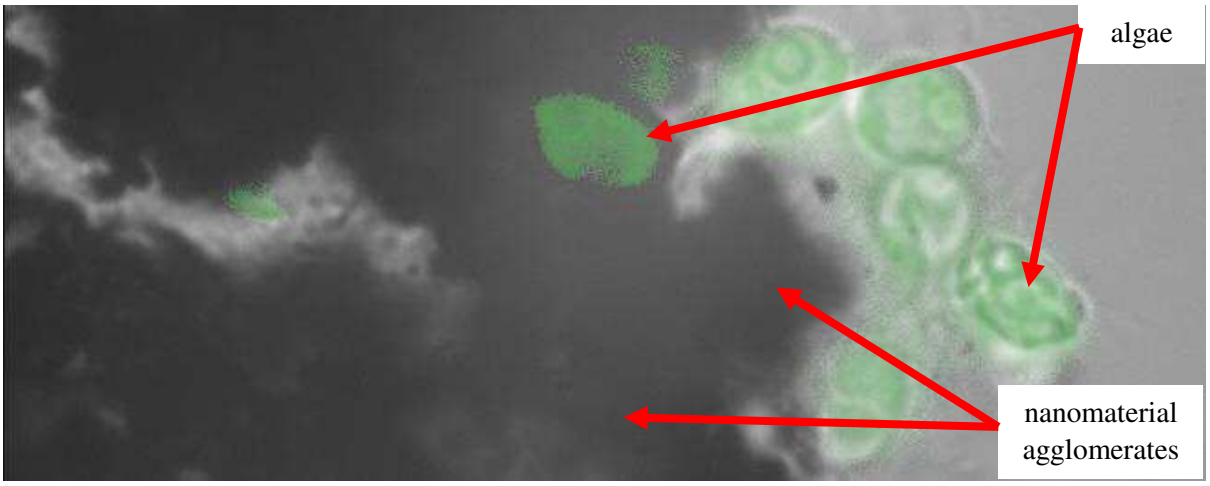

Figure 3.12: Algae growth inhibition test - Algae cells associated with clusters of aged NZVI (1000-fold magnification) with fluorescence filters. Viable algae cells are presented in green

3.3.3.2 Daphnia acute immobilisation test

The results of the Daphnia tests showed a dose response relationship between exposure to the aged NZVI and daphnid immobility. The EC_{50} value for these five tests were determined as 163 mg/L (Figure 3.13). The dissolved oxygen levels at the beginning and end of the tests showed a trend dependent on the aged NZVI concentration (Figure 3.14). The higher the nanomaterial concentration the lower the oxygen levels recorded. The two highest concentrations of 500 mg/L and 1000 mg/L showed dissolved oxygen levels below the recommended minimum value of 2 mg/L in some tests at the time point 0 h. For the concentration of 500 mg/L, the dissolved oxygen measured after 48 h was above the threshold of 2 mg/L whereas for the concentration of 1000 mg/L the oxygen level was below the threshold in all five experiments. This results indicate that the material was not fully oxidized. The pH value of the suspensions in the end of the test did not differ by more than 0.8 from the initial conditions. The nanomaterial sedimented quickly in the initial phase of the experiment. A layer

of sedimented material was visible after 20 min. During the initial phase of exposure, some of the Daphnia were coated with the material. After molting the Daphnia shed their carapax free of the associated nanomaterial and could move without any impairment.

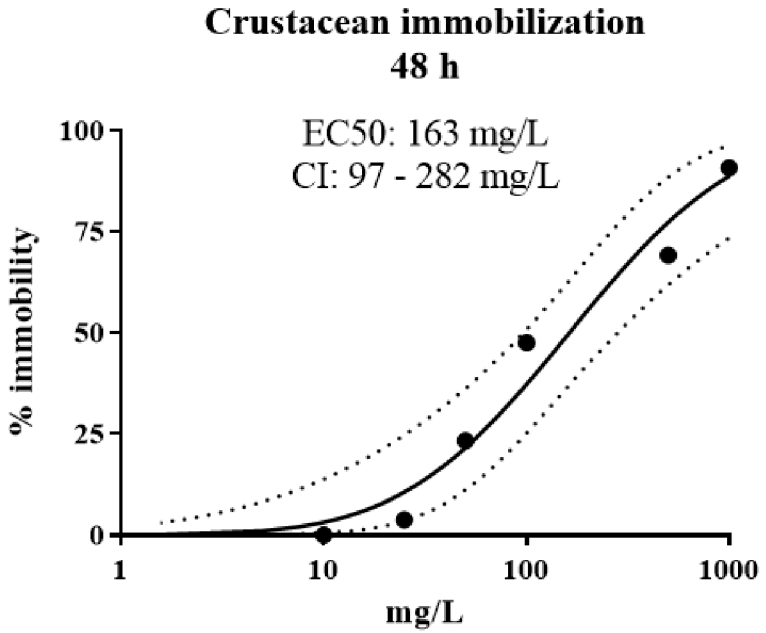

Figure 3.13: Daphnia acute immobilization test - Percentage immobility of *Daphnia magna* after exposure to aged NZVI at concentrations of 10, 25, 50, 100, 500 and 1000 mg/L for 48 h. The 95 % confidence interval is indicated (dashed lines)

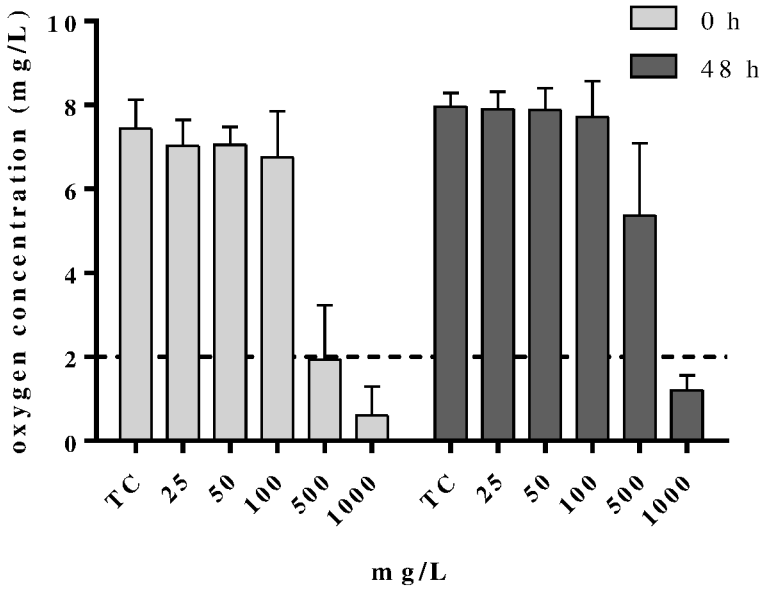

Figure 3.14: Daphnia acute immobilization test - Oxygen saturation in the medium after exposure to aged NZVI with 25, 50, 100, 500 and 1000 mg/L and a sonication treatment control (TC) without the nanomaterial. Bar graphs represent the oxygen concentration in mg/L at the time point of 0 h (left, light grey) and 48 h (right, dark gray). The whiskers represent the standard deviation on the mean of five independent test. The recommended oxygen saturation threshold of 2 mg/L is indicated by a dashed line

3.3.3.3 Fish embryo toxicity test

A dose dependent effect on the fish embryos was observed upon exposure to the aged NZVI. An EC_{50} value of 458 mg/L 96 hpf was determined (Figure 3.15). Again, the nanomaterial sedimented quickly and covered the fish eggs (Figure 3.16). The eggs showed an increasing association with the aged iron nanomaterial throughout the experiment. At concentrations higher than 62 mg/L, the bottom of the wells was completely covered and hindered microscopic evaluation of the heart beat and blood circulation during the first 48 hpf at concentrations beyond 62 mg/L. With the help of an additional light source the investigation could be partially conducted.

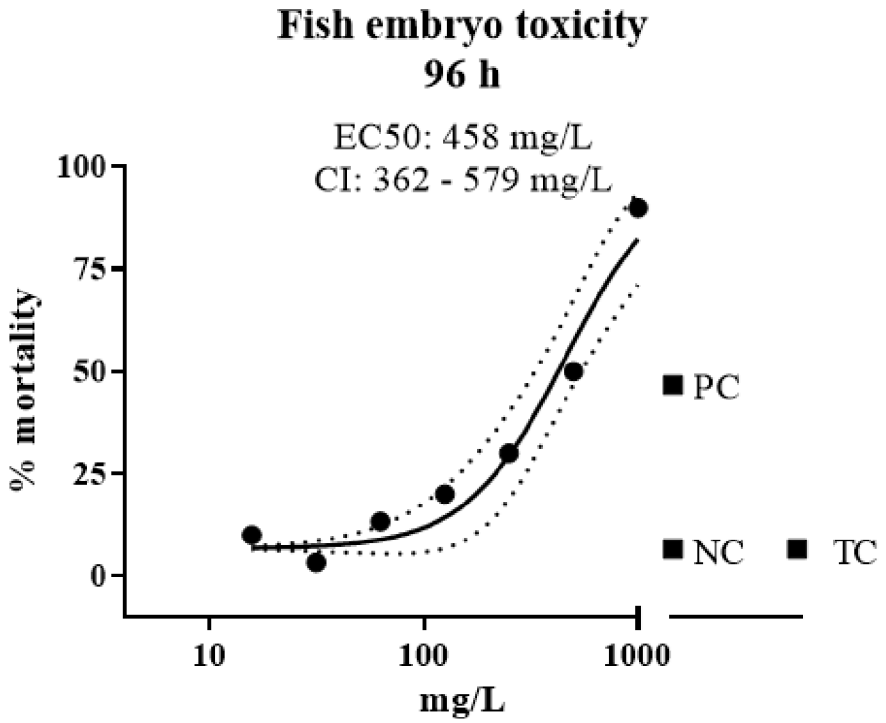

Figure 3.15: Fish embryo toxicity test - Percentage mortality of zebrafish (*Danio rerio*) embryos after exposure to aged NZVI at concentrations of 16, 31, 63, 125, 250, 500 and 1000 mg/L at 96 hpf. The 95 % confidence interval is indicated (dashed lines). TC: sonication treatment control; PC: positive control treatment with 3.7 mg/L 3,4-Dichloranilin ; NC: negative control untreated control

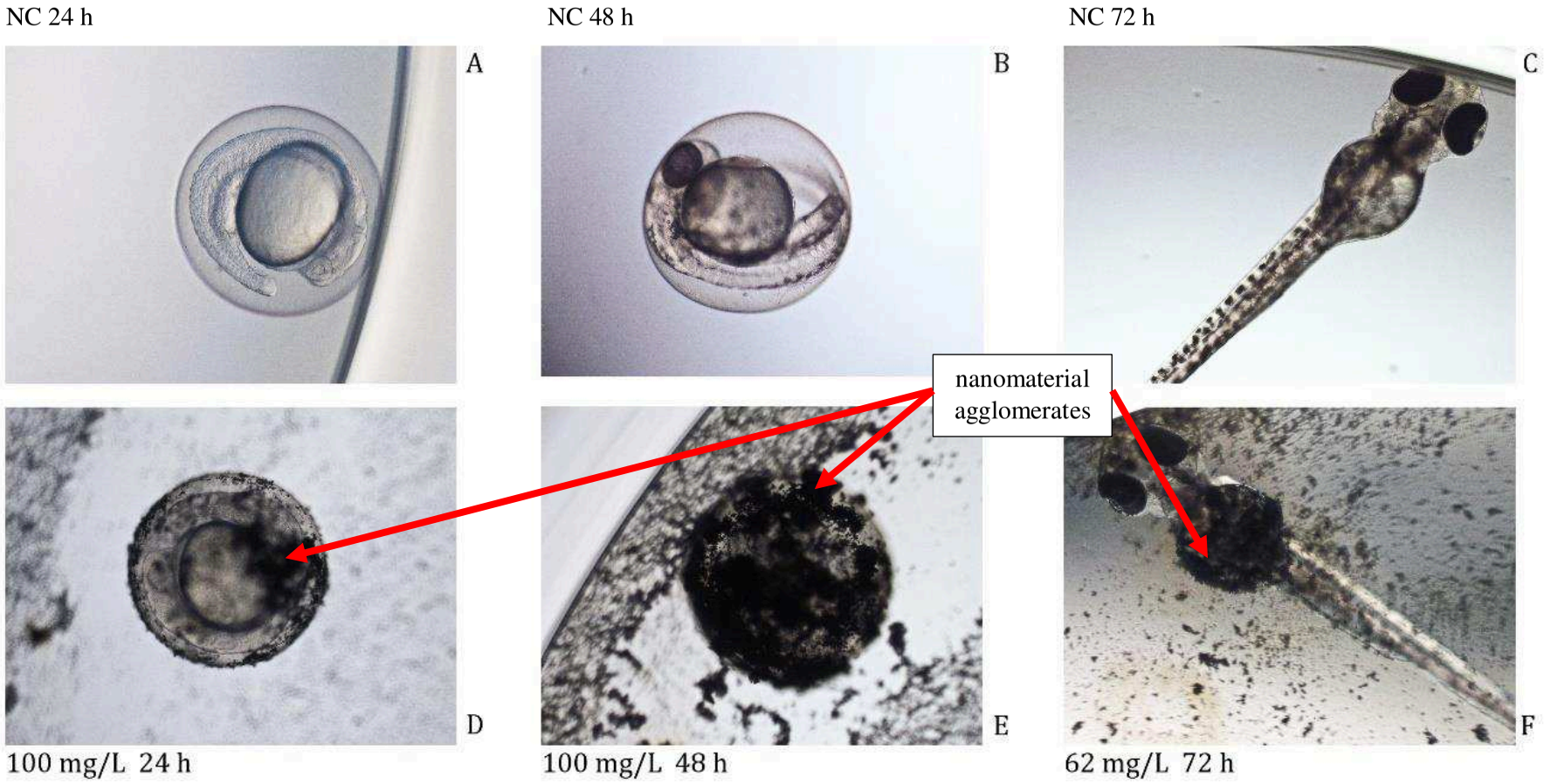

Figure 3.16: Fish embryo toxicity test - Association of the aged NZVI to the chorion and larvae. The upper row depicts the developmental stages of the negative control (NC) at the time points of 24 h (A), 48 h (B) and 72 h (C). The lower row depicts the association of the aged NZVI to the chorion (D,E) and to the larvae (F) at the same time points

3.3.3.4 Ames fluctuation test

The results of the Ames fluctuation assays showed a bacterial toxicity in the TA100 strain at aged NZVI concentrations higher than 50 mg/L. The assay did not indicate any mutagenic potential of the aged NZVI with or without the S9 mix with both tester strains (TA98 and TA100).

3.4. Discussion

3.4.1 Effect on anaerobic-reductive biological dechlorination

The anaerobic laboratory studies showed that biological dechlorination of chloroethenes was stimulated due to the microbial degradation of the suspending agents of NZVI. Long term inhibitory or toxic effects of NZVI on dechlorinating microorganisms were not observed. These findings were corroborated by the results of a field test published by Köber et al. (2014): PCR results as well as metabolite formation pointed to the occurrence of biological dechlorination in the aquifer after NZVI injection despite transient unfavourable pH values due to the fermentation of the suspending agents.

Toxic effects of NZVI on dechlorinating microorganisms were observed in some laboratory studies (Tilston et al., 2013; Zabetakis et al., 2015). Further field applications of NZVI did as well not show any prolonged negative effects on the microbial activity but a stimulation of biological dechlorination (He et al., 2010; Kirschling et al., 2010; Kocur et al., 2015; Su et al., 2012; Wei et al., 2012) supporting the results of our study. Aging of NZVI as well as interaction with natural organic matter was shown to mitigate the toxicity of the NZVI (Baalousha, 2009; Bruton et al., 2015; Jang et al., 2014; Phenrat et al., 2009).

In order to benefit from synergies between the abiotic and biotic processes, biological processes (biodegradation as well as hydrogen consumption) should be considered during field application NZVI materials. Therefore, transient toxic effects as well as unfavourable pH-effects of abiotic and biotic processes have to be taken into account.

3.4.2 Material characterization of aged NZVI

The physical characterization of the aged NZVI was an important aspect of the study, since the physical state of the nanomaterial may have an impact on its behaviour in the aquatic environment.

The nanomaterials were investigated with various analytical methods to gain insight about their morphology. The characterization was conducted with dynamic light scattering (DLS),

transmission electron microscopy (TEM) with energy dispersive x-ray analysis (EDX), and X-ray diffractometry (XRD). Additionally, the reactive oxygen species (ROS) levels were monitored in a cell free assay with 2′,7′-dichlorodihydrofluorescein diacetate (DCFDA) as the fluorogenic probe.

The DLS measurement did not present reproducible data. The form as well as the particle size distribution and agglomeration of the nanomaterial influenced the dynamic light scattering measurement and rendered the data not evaluable. Especially, the agglomeration of the aged NZVI caused by magnetic interactions had a negative impact on the measurement. The larger agglomerates were overrepresented in the size measurement as these particles scatter to the power of 6 more light than smaller particles (Nickel et al., 2014). For a comparable DLS size measurement a stable suspension with spherical objects and a monomodal size distribution is preferred (Hoo et al., 2008). These various aspects that hindered the size measurements by DLS also influenced the zeta-potential measurement by laser Doppler velocimetry and additionally the conductivity of the material added another factor of uncertainty (Gallardo-Moreno et al., 2012).

The investigation by TEM shows an inhomogeneous size distribution of the material consisting of particles and agglomerates in the nanometre unto the micrometre range (Figure 3.9). This heterogeneous size distribution is a result of the milling process (Köber et al., 2014). The product therefore differs from NZVI produced in a chemical process by reducing of iron oxides with borohydride. This process results in spherical particles with a distinct size range (Sun et al., 2008). A milling process is an interplay between forging and breakdown of particles and results in a broad particle size distribution with a multitude of shapes. In this study the predominant form of the milled product were flakes with a thickness below 100 nm as shown in the tilting TEM analysis and the investigations with the same material by Köber et al. (2014).

The results of the XRD measurement showed that the material indicated a ferrite content of 81 % and an austenite content of 19 %. This indicates that this phase is already present in the source material. As of a high carbon content of in raw material (3.2 %) the allotrope austenite is stabilized within the material. The aged NZVI investigated were air dried and hence an iron oxide layer was expected. However, none was detected by XRD. A possible explanation is that the iron oxide layer is too thin for detection. In former studies, it was reported that such a layer can be as thin as 3 nm to 5 nm (Efecan et al., 2009; Kumar et al., 2014a). Hence, the amount of iron oxide in the aged NZVI was not sufficient to be detected with our method. As an alternative method, Mössbauer spectroscopy or a TEM with an electron energy loss spectroscopy (EELS) analysis should be conducted (Cornell and Schwertmann, 2006). Furthermore, the crystal

structure of the iron was highly disordered as a consequence of the milling process. The Rietveld fits refined therefore not only a size term, but included the strain-dependent broadening as well. This is an additional aspect that makes the XRD size calculations difficult to interpret. The size estimation has similar requirements like the DLS measurement, i.e. the shape should be constant in size and spherical for all the elements of the crystal. These prerequisites were shown not to be fulfilled in TEM analysis.

Summarizing, an expensive and elaborate characterization with different complementing methods could give insight on the morphology of a nanomaterial. However, some methods have only a very narrow specificity (e.g. DLS measurement) as they rely on many mathematical assumptions to discriminate particles in the nanometre scale. As a result, none of the applied characterization methods resulted in a robust evaluation of the size distribution. Therefore, we used the nominal concentrations to describe the amounts of NZVI nanomaterial investigated in the different tests.

3.4.2.1 Stability in suspension

Stokes´ law predicts sedimentation times of about a week per centimetre for isolated 60 nm particles. In this study, the nanomaterials agglomerated and sedimented within 60 minutes in the different OECD media indication an agglomerate size of about 0.8 µm. This is a result of the magnetic properties of the nanomaterial as they enhance the agglomeration process (Rosická and Šembera, 2010). This agglomeration process is self-enhancing as the initial agglomerates collide during their vertical sedimentation with further particles. The magnetic properties depend on the domain configuration of the iron nanomaterial (Kittel, 1946). The transition from the superparamagnetic to the single-domain state for alpha-Fe is around 20 nm, true multidomain particles are 80 – 100 nm in size (Dunlop and Özdemir, 2001). This implies that our particles can interact with maximum magnetic forces. The aspect of suspension stabilization through the electrokinetic zeta-potential cannot be applied in this study as the magneticity and conductivity of the nanomaterial as well as the composition of the aquatic media hinder any formation of a strong repulsive force (Gallardo-Moreno et al., 2012; Keller et al., 2012). The extended Derjaguin, Landau, Verwey and Overbeek (DVLO) theory which includes magnetic properties of materials to estimate the agglomeration of particles in suspensions shows that the magnetic properties have the highest impact on the stability of magnetic NZVI suspensions (Hotze et al., 2010; Jiang et al., 2015). In the study by Phenrat et al. (2007), the concentration at which these magnetic interaction dominate the sedimentation process was above 10 mg/L. In this study almost all applied NZVI concentrations were higher.

3.4.3 Ecotoxicity of NZVI

In the present study, the toxicity of the aged NZVI nanomaterial was investigated in aquatic test systems: algae growth inhibition test, acute crustacean immobilization test, fish embryo toxicity test. Additionally, a mechanistic toxicity test to detect mutagenicity was conducted. We compared our results to NZVI and aged NZVI from the literature with the corresponding test systems. In this context the aspect of material coating has to be introduced. The modification of the NZVI surface as well as additives to the NZVI suspension have a modulating effect on the toxicity of nanomaterials both increasing or decreasing their toxicity (Baumann et al., 2014; Cao, 2004; Chen et al., 2012; Chen et al., 2013; Dong et al., 2016; Keller et al., 2012; Romer et al., 2013; Romer et al., 2011; Tejamaya et al., 2012; Zhou et al., 2014). In our study the aged NZVI were investigated without any modifications.

3.4.3.1 Algae growth inhibition test

The algae growth inhibition test was not applicable for testing the iron nanomaterials as the material associated with the algae. The formation of clusters of the material occurred as a result of the particles morphology as well as the salt concentration of the medium. These clusters incorporated the algae and sedimented onto the bottom of the vessel. In other studies e.g. with titanium dioxide nanoparticles, the effect of shading by the nanomaterials or change of light quality could be excluded (Aruoja et al., 2009; Hartmann et al., 2010; Hund-Rinke and Simon, 2006). Thus, the effects on the growth were rather based on the sedimentation and shading than on a toxic mode of action of the titanium nanomaterial. In this study, no EC_{50} values could be determined. In the study by Keller et al. (2012), the uncoated NZVI Nanofer25 showed a similar agglomerating and sedimenting behaviour and was excluded from their investigation with algae. Hence, a validation of the test system for the nanomaterial of interest is crucial to distinguish between physical interaction and toxic effects.

3.4.3.2 Daphnia acute immobilization test

The results of our test with Daphnia indicate a toxicity of our aged NZVI with an EC_{50} value of 163 mg/L. The toxicity recorded was higher than the toxicity to *Daphnia magna* reported by Marsalek et al. (2012) who determined an EC_{50} value for NZVI higher than 1000 mg/L. A study that compared the toxicity of uncoated and coated NZVI to aquatic organism showed that the crustacean *Daphnia magna* was more sensitive to the NZVI that the fish (Keller et al., 2012). Our results are in accordance with our study as *Daphnia magna* showed to be approx. 3-fold more sensitive to aged NZVI than the fish *Danio rerio*.

3.4.3.3 Fish embryo toxicity test

The presented results of the fish embryo toxicity test were comparable to results from former studies with fish and iron nanomaterials. Especially, for oxidized iron nanomaterials Weil et al. (2015) showed no toxicity to the fish *Danio rerio* in a concentration up to 100 mg/L. This result is comparable to our research. In our study, the aged NZVI was more toxic to *Danio rerio* with an EC_{50} value of 458 mg/L than in the study by Marsalek et al. (2012) to the fish *Poecilia reticulate* with an EC_{50} value of 2500 mg/L. In another study with medaka fish 40 % mortality was reported for an iron nanomaterial at a nominal concentration of 100 mg/L (Chen et al., 2012). A full dose response curve was not reached in this study for the iron nanomaterial and thus no EC_{50} value was determined. However, this value showed a higher initial toxicity than our nanomaterial. Li et al. (2009) reported for the same fish and iron nanomaterial deleterious effects on gills and intestine in histological investigations at concentrations of 5 mg/L. These studies reported a comparable behaviour of the nanomaterials as these materials were also agglomerating and sedimenting within minutes to hours. Our evaluation of various endpoints in the fish embryo toxicity test indicate that for this nanomaterial the hatching rate after 72 hpf (EC_{50} 337 mg/L, data not shown) is a more sensitive endpoint than mortality (EC_{50} 458 mg/L). However, more scattering in the hatching data compared to mortality data was observed. This is a consequence of the association of the nanomaterials with the chorion of the embryos. As the embryos were covered, no effects on the embryo could be recorded until the end of the experiment. The average time point of hatching at 72 hpf is 24 h earlier than the end of the test at 96 hpf.

3.4.3.4 Ames fluctuation test

The Ames fluctuation test did not show any mutagenicity of NZVI, which is consistent to the results of a study from Barzan et al. (2014). The possible mode of action for NZVI to elucidate mutagenicity would be due to incorporation in cells and its ROS generating properties (Fu et al., 2014b). However, as shown in Figure 3.11, the concentrations to produce ROS and elucidate toxicity were higher than 450 mg/L. Hence, any ecotoxicological negative effects of the NZVI would act before the onset of mutagenicity.

3.4.4 Modes of NZVI toxicity

In the literature various modes of action of toxicity for iron based nanomaterials were proposed and we structured the discussion accordingly. The factors influencing toxicity are size as well as the reactions of the iron nanomaterial including corrosion and transformation processes, ferrous ions release, oxygen consumption and generation of reactive oxygen species.

3.4.5 Does size matter?

The toxicity of nanomaterials was assumed to be size dependent (Scown et al., 2010; Wyrwoll et al., 2016). Our iron nanomaterial showed a very broad particle size and form. The number of particles with a size smaller than 100 nm in all three dimensions could not be determined. As a consequence, according to definitions our experiments were performed with a nanomaterial rather than with nanoparticles. Potentially, the toxicity in our study was originating from a small fraction of the very broad size distribution. To elucidate the responsible size or form fraction an elaborated field flow fractionation could be applied to separate the different sized particles (Hassellov et al., 2008). However, the magnetic behaviour of the material would result in agglomeration during the separation. Hence, it is a steadily changing system that is difficult to control. The expensive and elaborate characterisation represents data from a particular state and time point only. A cost effective, rapid, and easy to use analytical method is still missing.

3.4.6 Is iron or its transformation products causing toxicity?

Elemental iron reacts in contact with the environment and corrodes in the presence of oxygen and water. Especially, in the context of its application NZVI will undergo various reactions in the soil system and the resulting intermediates will react also in this compartment (El-Temsah and Joner, 2012; Liu and Lowry, 2006). However, if in direct contact with organisms ENM can be a source of toxicity(Zhu et al., 2012). The procedure conducted in this study to prepare an aged NZVI inevitably passivated the iron with an oxide layer (Kim et al., 2010; Wang and Zhang, 1997; Yan et al., 2013b). In this process NZVI oxidizes by dissolved oxygen which results in the production of Fe(II) and H_2O_2 via a two-electron transfer reaction from the NZVI surface to O_2 (Worch et al., 1983). Additional H_2O_2 is produced in the reaction of Fe(II) with O_2 which is followed by a reaction of superoxide with Fe(II). H_2O_2 reacts later with the NZVI to H_2O or is converted to hydroxyl radicals or ferryl ions in a reaction with Fe(II) (Fenton reaction, (LeBel et al., 1992; Stohs and Bagchi, 1995; Winterbourn, 1995). In the neutral pH range as in our test conditions the oxidation of Fe(II) by oxygen is the most prominent reaction and Fe(IV) is the dominant intermediate oxidant (Stumm and Lee, 1961; Sung and Morgan, 1980). During this oxidation processes Fe(III) is formed from Fe(II) and can precipitate as layers of ferric oxides or hydroxides like magnetite, maghemite and/or lepidocrocite on the surface of the NZVI (Auffan et al., 2008; Kanel et al., 2005; Liu et al., 2014; Yan et al., 2013b; Zhang and Huang, 2006). The presence and amount of oxygen available has an impact on what corrosion products are formed and what mobility these products have in the groundwater (Jiang et al., 2015). The magnetic properties of these iron oxidation products determine the mobility

of the NZVI in the groundwater aquifer and thus the probability to come in contact with the aquatic environment. Magnetic and agglomerating products are less likely to come in contact with the aquatic environment than paramagnetic particles (Jiang et al., 2015). A proposed result of this agglomeration process is a reduces specific surface area and the interfacial free energy, which leads to a reduced particle reactivity and showed to have a decreasing effect on the toxicity (Li et al., 2010; Phenrat et al., 2009). However, diffusion controlled processes at the surface of the NZVI could also result in the same effect of reduced toxicity.

Additionally, the salts present in the different test media have an impact on the described processes. By enhancing the ionic strength, the agglomeration rate is accelerated. Moreover, the production of oxidation enhancing entities such as hydroxides, carbonates and sulphates is facilitated (Liu et al., 2015; Stumm and Morgan, 2012). The results of the described reactions are oxygen depletion, soluble Fe(II) ions, reactive oxygen species like O_2^-, H_2O_2 and OH•, and other nanomaterial specific toxicity (Handy et al., 2008b).

The oxygen depletion occurring during the expose to NVZI was shown to last for up to 48 h at the highest concentration of 1000 mg/L aged NZVI in our Daphnia tests. However, this duration of oxygen depletion could be overestimated as the aged NZVI suspension was stirred during the measurement. In this process the surface of the nanomaterial was greatly increased as the material was resuspended whereas during exposure after the material sedimented only a limited surface was available. In a study by Chen et al. (2012) the process of oxygen depletion lasted only for approx. for 1000 min. Additionally, our test systems were open and oxygen was able to diffuse into the exposure media reducing the effects of oxygen depletion.

The ferrous ions were shown to be toxic in various studies (Chen et al., 2012; Keenan et al., 2009; Keller et al., 2012; Vuori, 1995). The concentration of this ion during the reaction of NZVI with the water and oxygen is steadily varying as this ions has a half-life of minutes in an oxygen water environment and is transformed to Fe(III) oxyhydroxides (Jander and Scheele, 1932; Stumm and Morgan, 2012; Vuori, 1995). The release of Fe(II) from Fe(0) is not dependent on the pH value in the pH range from 5 to 10 (Wilson, 1923). Therefore, the surface of the NVZI was the reaction limiting factor (Sarin et al., 2004). In the study by Chen et al. (2012) with NZVI the ratio between NZVI concentration and filterable Fe(II) was 10 to 1. This value was stable for over 1000 min.

Therefore, if in direct contact with animal tissue or incorporated into the organisms this species of iron can cause toxicity (Li et al., 2009). In our test the chorion of the fish embryos could be a barrier for this element of toxicity (Chen et al., 2013). For the Daphnia, where the organisms are in direct contact to the nanomaterial this can be a source of toxicity in the initial moments

of the tests where the nanomaterial is dispersed in the water column. Through filtration the animals can incorporate the nanomaterial. The acute toxicity for Fe(II) ions originating form $FeCl_2$ was determined to be above 50 mg/L for embryos of the fish medaka (Chen et al., 2011; Chen et al., 2012). In the study by Keller et al. (2012) with *Daphnia magna* and NZVI it was described that one part of the reported toxicity to the Daphnia from ferrous ions with a reported concentration of 1 mg/L.

Reactive oxygen species (ROS) can be the cause of toxic effects (Auffan et al., 2008; Keenan et al., 2009; Naqvi et al., 2010; Singh et al., 2010; Zepp et al., 1992). It is known that transition metals participating in one-electron oxidation-reduction reactions like iron lead to the formation of ROS (Schrand et al., 2010; Yan et al., 2013a; Yin et al., 2012). Our findings in the cell free assay (Figure 3.11) show that the sonication process itself is a source of ROS. This phenomenon was reported by Miljevic et al. (2014) and Harada et al. (2013). This amount did not cause any toxicity in the treatment controls. It has to be mentioned that the cell free assay does not detect ROS exclusively but rather the enzyme, horseradish peroxidase (HRP), and Fe(II) ions are known to generate signals in the assay (Bonini et al., 2006; Myhre et al., 2003; Pal et al., 2012; Rota et al., 1999). In our study, we accounted for the effect of HRP by introducing a blank control and by subtracting this value only the remaining ROS effects are considered in the evaluation. However, we did not quantify the contribution of Fe(II) ions. The amount of ions released from NZVI should correlate with the concentration introduced like described before (Chen et al., 2012). In our study acute toxicity was detected at 50 mg/L of aged NZVI exposure. At this concentration no elevated ROS signals levels were recorded. However, various studies reported deleterious effects to organisms originating in direct contact to NZVI or ROS generated by engineered nanomaterials (Chen et al., 2012; Chen et al., 2013; Li et al., 2009; Ma et al., 2013). Summarizing, the combination of oxygen depletion, ferrous ion toxicity, ROS-related toxicity and nanomaterial specific toxicity contribute to the observed toxicity.

3.5. Conclusion

Regarding environmental risk assessment of NZVI applied for groundwater remediation, this nanomaterial will be applied at high (effective) concentrations only in limited areas. Thus, the NZVI will reach a wider environment only at low concentrations that have only transient toxic and pH effects with no prolonged consequences according to our study. Hence, this nanomaterial is probably of no environmental concern not prohibiting its application for groundwater remediation. During field application synergetic effects of abiotic dechlorination and biological dechlorination as well as hydrogen consumption can enhance the efficiency of

NZVI groundwater remediation projects. The results of our investigations can be used in the international discussion on the use of standard test procedures for the testing of nanomaterials.

Acknowledgments

Funding: This work is part of the joint project NAPASAN (Nanoparticles for ground water remediation) which was funded by German Federal Ministry for Education and Research (BMBF) under the Grant Number 03X0097 within the research program NanoNature (Nanotechnologies for Environmental Protection—Value and Impact) which is part of the framework program WING (Material Innovations for Industry and Society).

Chapter 4
Determination of the CYP1A-inducing potential of single substances, mixtures and extracts of samples in the Micro-EROD assay with H4IIE cells

This chapter has been published in the peer-reviewed article:
Schiwy, A., Brinkmann, M., Thiem, I., Guder, G., Winkens, K., Eichbaum, K., Nuszer, L., Thalmann, B., Buchinger, S., Reifferscheid, G., Seiler, T.-B., Thoms, B., Hollert, H., 2015. Determination of the CYP1A-inducing potential of single substances, mixtures and extracts of samples in the micro-EROD assay with H4IIE cells. *Nature Protocols* 10, 1728-1741. DOI: 10.1038/nprot.2015.108

Abstract

This protocol describes a quantitative and robust 96-well plate-reader-based assay for the measurement of ethoxyresorufin-*O*-deethylase (EROD) activity using the rat hepatoma cell line H4IIE. The assay can be applied to determine the CYP1A-inducing potential of single substances, as well as mixtures and extracts of samples. It is based on the aryl hydrocarbon receptor (AhR)-mediated induction of cytochrome P450 enzymes (CYPs, subfamily 1A) in cells following exposure to dioxins and dioxin-like compounds. One enzymatic reaction catalysed by CYP1A is the deethylation of the exogenous substrate 7-ethoxyresorufin to the fluorescent product resorufin, which is measured as EROD activity in the assay. The CYP1A-inducing potential of a sample can be reliably quantified by comparing the EROD activity with the concentration-response curve of the standard substance 2,3,7,8-tetrachlorodibenzo-*p*-dioxin, which can be detected at concentrations down to the pg/L range. A researcher familiar with the procedure can process up to 160 samples with four wells each within 3 days. The series described uses four plates with three concentrations per sample which can be easily scaled to accommodate different sample sizes.

4.1. Introduction

Dioxins and dioxin-like chemicals (DLCs) are of high toxicological and environmental concern. They belong to the class of persistent organic pollutants (POPs) that are characterized by low environmental degradation rates through physical, chemical or biological processes (Sinkkonen and Paasivirta, 2000). Consequently, their environmental half-lives are rather high, ranging from months to over several years and decades meaning they tend to accumulate in soils and sediments (Brack, 2003; Weber et al., 2008). It is due to their high lipophilicity and their low rate of biotransformation, that dioxins and DLCs are highly bioaccumulative. This leads to increased levels in wildlife, feedstuff, meat, and dairy products (La Rocca and Mantovani, 2006; Spagnoli and Skinner, 1977; Theelen et al., 1993). The resulting elevated risk of human exposure through contaminated food is particularly alarming in light of the variety of acute and chronic toxic effects that dioxins and DLCs are known to provoke. These toxic effects include neuro-, immuno- and hepatotoxicity, reproductive toxicity and ultimately even certain types of cancer (Brouwer et al., 1995; Denison and Heath-Pagliuso, 1998; Denison and Nagy, 2003; Giesy et al., 1994; Poland and Knutson, 1982; Van den Berg et al., 1998). Activation of the nuclear aryl hydrocarbon receptor (AhR) and subsequent induction of CYP1A-dependent monooxygenases is a well-studied effect of dioxins and DLCs (Dencker, 1985).

Polychlorinated dibenzo-*p*-dioxins and dibenzofurans (PCDD/Fs often summarized as 'dioxins') are mostly produced unintentionally as by-products of chemical reactions involving chlorine, and during industrial or domestic combustion processes (Huang and Buekens, 1995). Polychlorinated biphenyls (PCBs) had been extensively used in technical applications, such as transformer oil or cutting liquids, because of their favourable physical and chemical properties, i.e. their chemical inertness and high thermal conductivity. Therefore, dioxin-like PCBs (dl-PCBs) are probably the most prevalent class of DLCs in the environment. As their environmental and toxicological impacts became apparent, production of PCBs has been globally restricted and finally banned (Lallas, 2001). Although emissions substantially decreased, dioxins and DLCs are still re-distributed in the environment by processes which are still poorly understood. This became evident during the 'Belgian dioxin and PCB crisis' in 1999 (Covaci et al., 2008) and the extensive contamination of eggs and different types of meat in Germany in 2011 (Abraham et al., 2011) due to contaminated feedstuff. In 2012 and 2013, the European Rapid Alert System for Food and Feed (RASFF) reported a total number of 29 dioxin limit exceedances in feed samples (EC, 2013a; EC, 2014a). As a consequence, national and multinational regulations were implemented or revised to reduce the risk for consumer health. The European Commission proposed a two-step approach for reducing the amount of dioxins, furans and PCBs in food and feed (EC, 2002b; EC, 2006b; EC, 2012a; EC, 2012b; EC, 2013b; EC, 2014b; EC, 2014d).

Instrumental chemical analysis of dioxins and DLCs, which is typically performed using high resolution gas chromatography with high resolution mass spectrometry (HRGC/HRMS), is costly and requires highly specialized personnel. This clearly limits the number of samples that can be investigated and the applicability for developing countries (EC, 2014c; Jordaan et al., 2007; Nieuwoudt et al., 2009). It became quickly evident that more rapid and economic methods are needed to efficiently protect consumer safety and uncover toxicological burden present in the environment.

A powerful and promising solution to the problem is the use of cell-based *in vitro* bioassays for pre-screening of a large number of samples (Keiter et al., 2008; Olsman et al., 2007; Wernersson et al., 2015; Wölz et al., 2008). This type of analytical tool does not allow for exact quantification of single compounds, but greatly facilitates the assessment of a sample's overall CYP1A-inducing potential (Behnisch et al., 2001). Several methods applying different, untransfected or genetically engineered cell lines exist for this purpose, all of which utilize the activation of AhR by agonists which are present in a given sample (Eichbaum et al., 2014). Differences in affinity exist between different Ah receptors, with the rodent AhR showing a

greater affinity to 2,3,7,8-tetrachlorodibenzo-*p*-dioxin (TCDD) than the human receptor (Van den Berg et al., 2006). While this is an advantage in terms of sensitivity of the assay, it does not allow for straightforward extrapolations to effects on human health (Novotna et al., 2011; Van den Berg et al., 2006). Among the most frequently used assays is the commercial DR CALUX® assay. It is based on H4IIE cells that have been stably transfected and thus genetically modified with a luciferase reporter gene that is expressed upon receptor binding (Murk et al., 1996).

4.1.1 Development of the protocol

Here, we describe a protocol for the ethoxyresorufin-*O*-deethylase (EROD) assay using the untransfected rat hepatoma cell line H4IIE which is approx. 10 times more sensitive to TCDD than human cell lines (Pitot et al., 1964; Van den Berg et al., 2006). Our protocol is based on the original method of Schwirzer et al. (1998), as modified and applied by (Thiem and Boehmler, 2011a; Thiem and Boehmler, 2011b); Thiem et al. (2014) for routine dioxin screening, which is based on the pioneering work of Donato et al. (1992); Donato et al. (1993), Safe (1993) and Tillitt et al. (1991b). It is regularly applied at the Institute for Environmental Research, RWTH Aachen University, Aachen, Germany, and at the Food and Veterinary Institute Braunschweig/Hannover, Lower Saxony State Office for Consumer Protection and Food Safety (LAVES), Germany. The method is based on the endogenous AhR-mediated induction of cytochrome P450 enzymes (CYPs) - members of subfamily 1A (CYP1A) in particular - which is triggered by dioxins and dioxin-like compounds. The induced CYP1A-dependent monooxygenases catalyse the deethylation of the exogenous substrate 7-ethoxyresorufin (ETX) to the fluorescent product resorufin. It can be easily quantified fluorometrically in a 96-well plate reader format. The CYP1A-inducing potential of a given sample can be reliably quantified when comparing the activity induced by the sample with the concentration-response curve of a well-characterized standard substance, e.g. 2,3,7,8-tetrachlorodibenzo-*p*-dioxin (TCDD), benzo[*a*]pyrene, or β-naphthoflavone.

It has been shown that the EROD assay is compliant with the regulations of the European Commission for dioxin screening of food and feed (EC, 2012a; Thiem et al., 2014). These include various criteria for dioxin screening, e.g. false-compliant rate with respect to the maximum levels lower than 5 %, repeatability (RSD_r) of < 20 %, and within-laboratory reproducibility (RSD_R) of < 25 % referring to the matrix validation. Other criteria are more bioassay specific, e. g. that the relative standard deviations of technical triplicates shall not exceed 15 %.

4.1.2 Comparison with other methods, applications and potential limitations

Recently, our group published a literature review on the analytical performance of different cell-based bioassays for assessing the CYP1A-inducing potential of chemicals, mixtures and extracts of environmental samples (Eichbaum et al., 2014). Although the commercially available DR CALUX® achieved the lowest limits of detection, the Micro-EROD bioassay described here showed the highest sensitivity to TCDD, i.e. the lowest effective concentrations, out of all compared assays. An advantage in comparison to the reporter gene assays is that it utilizes untransfected H4IIE cells, often referred to as "wild-type" (Figure 4.1a). Therefore, it can be carried out in laboratories without containment level for genetically modified cells. Furthermore, the cell line is readily available, e.g. *via* the American Type Culture Collection (ATCC). Additionally, the assay procedure has been economically optimized as expensive substrates, e.g. for determination of luciferase activity, or the addition of co-substrates such as NADPH, are not required.

The assay can be applied to various sample types, including single substances, mixtures, and extracts of environmental samples, food, and feed. It had been used to assess soils, sediments, exhaust from domestic and industrial combustion processes, fish, eggs, meat and dairy products, plant materials, and sewage sludge (Table 4.1). It is important to note that different matrices require different extraction and clean-up procedures to prepare samples for the bioassay. Expert knowledge is necessary as some matrix components can drastically influence the results of the bioassay. The removal of fat from biological samples is especially required. Depending on the analytical aim readily degradable inducers can be extracted.

Table 4.1: Examples of typical applications for the Micro-EROD assay with H4IIE cells with exemplary references.

Sample matrix	Exemplary references
Single substances and technical mixtures	Hanberg et al. (1991), Peters et al. (2004), Sanderson et al. (1996), Schmitz et al. (1996)
Soils and sediment	Behnisch et al. (2002), Gale et al. (2000), Li et al. (1999), Schwirzer et al. (1998)
Sewage sludge	Schwirzer et al. (1998)
Plant materials	Li et al. (1999)
Fish	Hanberg et al. (1991), Hewitt et al. (2000), Jiang et al. (2005)
Feed	Behnisch et al. (2002), Summer et al. (1996)
Meat and dairy products	Thiem et al. (2014), (Thiem et al., 2006), Valdovinosa et al. (2013)
Fly ash, industrial and domestic emissions	Behnisch et al. (2002), Li et al. (1999), Schramm et al. (2001), Schwirzer et al. (1998)
Transformer PCB-oil	Behnisch et al. (2002)

For the analysis of stable inducers like dioxins the oxidation of these degradable inducers is recommended. Such compounds might be transformed by xenobiotic metabolizing enzymes during the assay within 24 h to 48 h. Depending on their receptor affinity they can significantly alter the assay result. The exposure time of 72 h reduces the contribution to the results to the most stable inducers like dioxins and dl-PCBs. A number of suitable clean-up procedures can be found in the literature, e.g. in Schwirzer et al. (1998).

4.2. Experimental design

Overview: A flow-chart of the assay procedure is shown in Figure 4.1**b**. After seeding of the cells and incubation for 2 h to 16 h, samples and standards are added directly to the wells. After an incubation period of 68 h to 72 h, the exposure medium is removed and a solution of the substrate ETX is added. During the subsequent incubation step (30 min, 37 °C), ETX is converted by EROD to the fluorescent product resorufin. To avoid reductive degradation of resorufin, the reductase inhibitor dicoumarol is added to the incubation mixture. After incubation, methanol is added to terminate the reaction and the amount of resorufin in each well is determined by means of fluorescence spectroscopy. Thereafter, the corresponding protein concentration is measured. It can be used as a validity criterion in comparison with wells containing solvent and negative controls (≥ 80 %), to exclude any cytotoxicity or contaminations as well as erroneous handling. Furthermore, it can be used to calculate the

specific EROD activity relative to the protein content of the wells. A concentration-response curve can be plotted for the standard and sample, from which biological TCDD equivalents (BEQs) can be calculated (Figure 4.1c).

Controls: The Micro-EROD bioassay has been optimized with special emphasis on a high sample throughput and economic considerations. The assay is performed in a 96-well format with H4IIE cells (Figure 4.1a), and requires mostly basic cell culture. To meet the requirement for improved sample throughput, only the most necessary standards and controls are included, i.e. TCDD and protein standards, as well as a negative control consisting of the same lot and concentrations of solvent as the TCDD standard. Where required solvent controls from the sample clean-up should be included. Unlike with many other EROD assays, the protocol does not include a resorufin standard curve, since it is not necessary for comparative analysis of samples and standard (Sanderson et al., 1996; Whyte et al., 2004). Furthermore, no sample transfer to a second plate is necessary as described in former methods (Schwirzer et al., 1998).

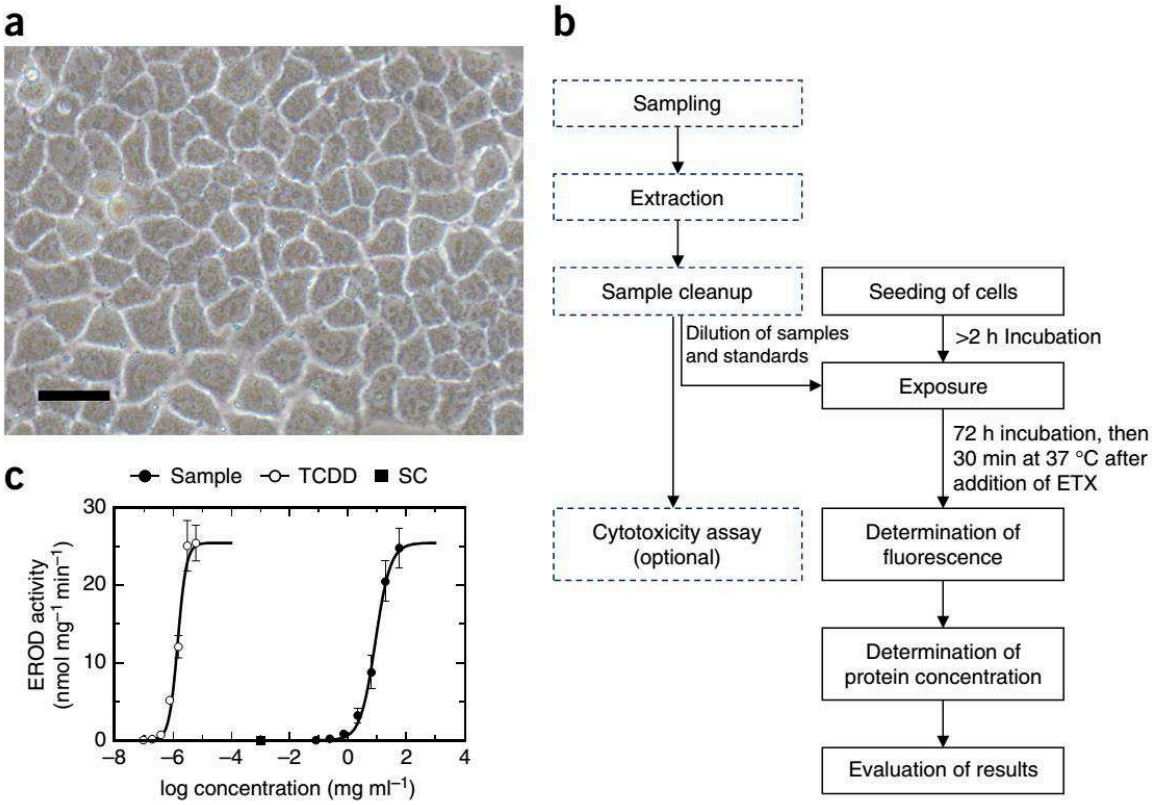

Figure 4.1: Summary of the micro-EROD bioassay with H4IIE cells . **(a)** Confluent H4IIE rat hepatoma cells in culture. Scale bar: 50 µm. **(b)** Flowchart of the micro-EROD bioassay. The corresponding steps are described in detail in the PROCEDURE section of the protocol. Optional steps or steps that are only necessary for certain sample matrices are indicated by a dashed outline and not detailed in this protocol. **(c)** Exemplary result for the solvent control (SC), the TCDD standard, and the PCDD/F fraction of a sediment extract from the Elbe River (Zollelbe, Magdeburg, Germany) following treatment with sulphuric acid, as well as multilayer and carbon/celite fractionation

Sample preparation: Depending on the nature of the tested samples, different sample preparation steps will be necessary. Single substances need to be dissolved in appropriate solvents, e.g. a mixture of DMSO and isopropanol (4:1, v./v.). Always choose the same solvent for standards and samples. Keep the final solvent concentration constant for all wells. The compatibility and a suitable concentration range of any unknown solvent needs to be verified beforehand in the assay. We have had a good experience with a mixture of DMSO and isopropanol (4:1, v./v.). For environmental, food and feed samples, adequate extraction and clean-up techniques, e.g. pressurized liquid extraction, liquid-liquid extraction, multilayer column chromatography, treatments with sulphuric acid, gel permeation chromatography or high performance liquid chromatography (HPLC) fractionation, need to be applied. These procedures should be evaluated with appropriate recovery controls. If different lots of solvent are used for the sample clean-up than for standards, a solvent control for the sample should be included. An exemplary clean-up scheme for the preparation of food and feed samples with a

maximum of 1 g fat content according to Gizzi et al. (2005) and Thiem et al. (2014) is provided in Box 1 and Figure 4.2.

Box 1: Exemplary acidic silica column clean-up procedure for the clean-up of up to 1 g fat (e.g. fish oil or food and feed samples) according to Gizzi et al. (2005) and Thiem et al. (2014).

The protocol required for extraction and a subsequent clean-up before processing a sample in the micro-EROD bioassay highly depends on the matrix of the sample and the compounds of interest. Figure 4.2 presents a clean-up procedure for samples with a maximum of 1 g fat content. This clean-up is optimized for samples with low cytotoxicity and comparably low content of CYP1A inducers. For matrices anticipated to exhibit higher cytotoxicity or content of inducers, a modification of this procedure is necessary e.g., the amounts of column components (sulphuric silica gel, solvent, column dimensions) can be scaled and the final volume of DMSO can be increased. Alternatively, other extraction and clean-up methods such as pressurized solvent extraction with in-cell clean-up might be more suitable.

In summary, the procedure is designed to remove components that interfere with the bioassay and to concentrate the persistent inducers. A sulphuric acid treatment is used to remove fat and readily degradable inducers such as PAHs. The sequence of two separate sulphuric acid silica gel layers with different acid concentrations helps to reduce the formation of an impermeable layer within the column. The volatile solvent *n*-hexane is used to elute the CYP1A inducers. *N*-hexane or dichloromethane can be used to transfer the extract to a sample vial. DMSO is applied as a non-volatile keeper and as the final solvent for the bioassay. For reliable results all components of the clean-up process have to be evaluated in the micro-EROD bioassay to exclude any induction originating in the process itself. For each batch of solvents, chemicals or chromatography materials, a control needs to be implemented. Furthermore, a procedure blank and preferably a recovery control should be included. Additionally, all chemicals have to be of high purity and all materials in contact with the sample must be specially prepared and cleaned.

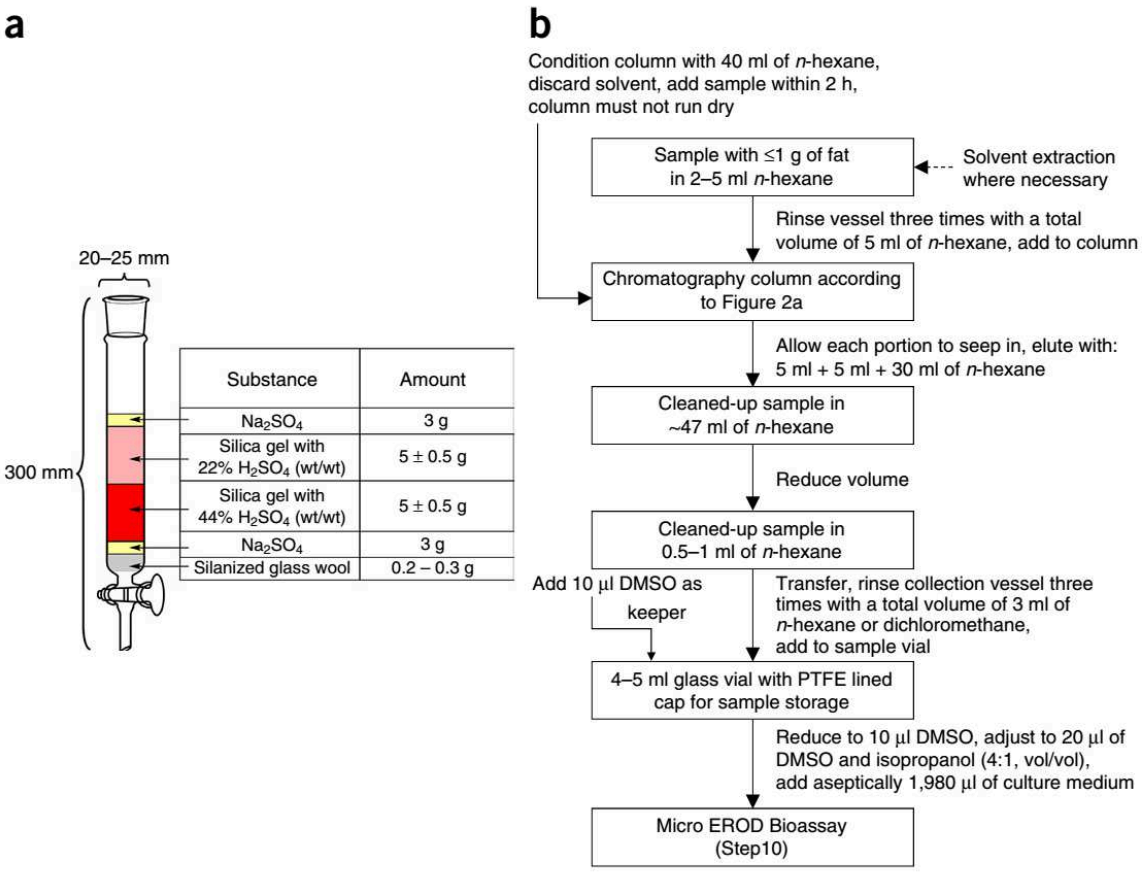

Figure 4.2: Clean-up procedure for removal of up to 1 g fat content and instable CYP1A inducers preceding analysis in the micro-EROD bioassay (**a**) Dimensions and composition of the chromatography column; (**b**) Workflow of steps necessary for the clean-up procedure

Data evaluation: The current data evaluation strategy described in the procedure (steps 33 to 38) has been optimized for use of the H4IIE micro-EROD in the assessment of food or feed samples, i.e. to conform to the needs of maximum sample throughput and thus a low number of tested concentrations. Please be aware that different sample matrices and management criteria will require other data evaluation strategies, e.g. for mass-balance analyses of sediments. Good starting points are the reviews of Safe et al. (1995), Whyte et al. (2004), Thiem and Boehmler (2011a) and Eichbaum et al. (2014), as well as the general considerations by Villeneuve et al. (2000) and Hädrich et al. (2012).

4.2.1 Materials

4.2.2 Reagents

H4IIE rat hepatoma cell line (ATCC, cat. no. CRL 1548)

CRITICAL The cell passage number has to be recorded and the cell quality should be regularly verified microscopically. Contamination with mycoplasma must be excluded and the cultures should be screened regularly.

2,3,7,8-tetrachlorodibenzo-*p*-dioxin (TCDD) standard stock solutions, 50 µg ml^{-1} (CIL, cat. no. ED-901-B). Alternatively, working solutions in the appropriate range can be obtained directly from the manufacturer after consultation.

CAUTION TCDD is a known human carcinogen and a developmental toxicant in animals. It should be handled with care. As for any other chemicals used in this protocol, appropriate institutional and national guidelines need to be followed. Please refer to the respective Material Safety Datasheets (MSDSs).

Bicinchoninic acid (BCA) assay kit for protein determination (Sigma-Aldrich, cat. no. BCA1)

Dicoumarol (Sigma-Aldrich, cat. no. M1390)

TRIS (Sigma-Aldrich, cat. no. 252859)

Sodium hydroxide (NaOH; Sigma-Aldrich, cat. no. 38210)

DMEM cell culture medium, low glucose, without glutamine, without phenol red (Life Technologies, cat. no. 11054-020)

Fetal bovine serum (FBS; BioWest, cat.no. S1810-500)

L-glutamine 200 mM, sterile, suitable for cell culture (Life Technologies, cat. no 25030-081) or GlutaMAX solution, 200 mM, sterile, suitable for cell culture (Life Technologies, cat. no. 35050-061)

HEPES buffer, 1 M, sterile, suitable for cell culture (Sigma-Aldrich, cat. no. H0887)

Dimethyl sulfoxide (DMSO), cell culture tested, >97.5 % (Sigma-Aldrich, cat. no. D2650)

Methanol, laboratory reagent (Sigma-Aldrich, cat. no. 179957)

Isopropanol, reagent grade (Sigma-Aldrich, cat. no. 190764)

7-ethoxyresorufin (ETX; Sigma-Aldrich, cat. no. E3763)

Dulbecco's phosphate-buffered saline (DPBS) solution, with calcium, magnesium, without phenol red (Life Technologies, cat.no. 14040-091)

10x Trypsin/EDTA solution (0.5 % Trypsin; 0.2 % EDTA; BIOCHROM, cat. no. L2153)

Sterile water suitable for cell culture (Life Technologies, cat. no. A1287301)

4.2.3 Equipment

4.2.3.1 Apparatus

CO_2-incubator for tissue culture (37 °C, 5 % to 7 % CO_2, > 95 % rel. humidity)

Microplate spectrofluorometer and spectrophotometer

Liquid handling and aspiration apparatus with appropriate accessories

Inverted phase-contrast microscope for inspection of cells

Sterile workbench suitable for cell culture

Pipette 10 µl

Refrigerator (2 °C to 8 °C)

Freezer (≤ -18 °C)

Ultrasonic bath for volumes of at least 50 ml (approx. 35 kHz)

Electronic multichannel pipette 20-300 µl

Electronic multichannel pipette 50-1200 µl

Electronic pipetting aid (pipettor)

Shaker suitable for multiwell plates

Water bath 30 °C to 37 °C

Hemocytometer according to Neubauer or automated cell counter

4.2.3.2 General equipment and consumables

Disposable laboratory gloves (nitrile or latex)

Standard tissue and cell culture flasks (TPP, cat. no. 90026 or 90076)

Sterile 96-well tissue culture plates (Sarstedt, cat. no. 83.1835.300)

Pipette tips: 2-20 µl, 10-300 µl and 50-1200 µl, sterile or autoclaved

Sterile serological pipettes: 1, 5, 10, 25 ml

Sterile reaction tubes 2 ml (VWR, cat. no. 2112165)

Sterile Reagent reservoirs min. 50 ml suitable for 12-channel pipettes (VWR, cat. no. 612-6572)

Paper towels and 70 % ethanol

Glass vials with polytetrafluoroethylene (PTFE) lined caps (volume of 4 ml to 5 ml)

4.2.4 Reagent setup

4.2.4.1 Complemented DMEM cell culture medium (culture medium)

Complement 500 ml DMEM-Medium without phenol red with 50 ml FBS and 9.9 ml 200 mM L-Glutamine or 200 mM GlutaMAX solution and 12.5 ml 1 M HEPES buffer under aseptic conditions. Culture medium should be stored refrigerated at 2 °C to 8 °C for no longer than 4 weeks. Additionally, the number of warming and cooling cycles shall not exceed 12 and a sterility control should be conducted weekly. To avoid partial media component degradation, each warming period shall not exceed 30 min.

4.2.4.2 TCDD standard working stock solutions (30-1200 pg ml^{-1}) (optional)

The preparation is described exemplarily for the concentrations shown in Table 2. Depending on the test setup other solvents or mixtures with different concentrations may be chosen. Pre-dilute the original TCDD solution (50 µg ml^{-1}) with DMSO to a concentration of 3000 pg ml^{-1} in a 1 ml volume. This parent solution is stable at 2 °C to 8 °C for the storage life of DMSO (2 years). We recommend using a mixture of DMSO and isopropanol (4:1, v./v.) as solvent. Prepare the stock solution by adding 250 µl isopropanol to 1 ml of the parent solution, resulting in a TCDD stock concentration of 2400 pg ml^{-1}. This stock solution ca be stored at 2 °C to 8 °C for 12 months. Prepare the different concentrations of TCDD working stock solutions according to Table 4.2 by diluting the stock solution with the solvent mixture (DMSO and isopropanol; 4:1, v./v.). Only experienced staff should conduct this procedure under a laboratory hood. Apply sufficient precautionary measures. Store at 2 °C to 8 °C in glass vials with polytetrafluoroethylene (PTFE) lined caps for up to 12 months. To reduce concentration artefacts due to evaporation dilute parent or original solution with volatile solvents in volumes smaller than the annual consumption. Choose storage vessel with minimal volume.

Table 4.2: Sequence of preparation and storage of the TCDD standard solution in the solvent of choice , exemplary for a mixture of DMSO and isopropanol (4:1, v./v.= D/I) (see REAGENT SETUP)

Name of solution	**Concentration**								**Storage**
Original ↓	50 µg ml^{-1} TCDD in DMSO								As recommended by manufacturer
Parent ↓	3000 pg ml^{-1} TCDD in DMSO								Up to storage life of DMSO at 2 °C to 8 °C
Stock ↓	2400 pg ml^{-1} TCDD in DMSO and isopropanol (4:1, v./v.)								12 month at 2 °C to 8 °C
Working stock[a] ↓	No	1	2	3	4	5	6	7	12 month at 2 °C to 8 °C
	pg ml^{-1} in D/I	1200	800	400	240	120	60	30	
Ready to use[b]	pg ml^{-1} in culture medium	1.200	0.800	0.400	0.240	0.120	0.060	0.030	Max. 15 minutes in reaction tubes
per well[c]	pg $well^{-1}$ in culture medium	0.600	0.400	0.200	0.120	0.060	0.030	0.015	-

[a] *annual preparation of working stock, solution in DMSO and isopropanol (4:1, v./v.)*

[b] *10 µl of each working stock solution in 990 µl culture medium*

[c] *addition of 50 µl of each ready to use standard to wells containing 50 µl of culture medium and cells, resulting in final solvent concentration of 0.5 % DMSO and isopropanol (4:1, v./v.)*

4.2.4.3 Solvent mixture (DMSO and isopropanol; 4:1, v./v.)

Prepare a mixture of DMSO and isopropanol (4:1, v./v.). As an example mix 400 µl DMSO with 100 µl isopropanol. This solvent mixture can be stored at 2 °C to 8 °C for the storage life of DMSO. Use same lot as for preparation of TCDD standards.

4.2.4.4 ETX stock solution (800 µM)

Dissolve 5 mg ETX in 25.5 ml methanol. Close quickly to prevent evaporation of solvent. Store ETX stock solutions in glass vials with PTFE lid at 2 °C to 8 °C and protected from direct light for up to 36 months. Contamination of the ETX stock solution or a spontaneous conversion to resorufin should be regularly excluded by means of fluorescence spectroscopy (Radenac et al., 2004).

4.2.4.5 Dicoumarol stock solution (1 mM)

Dissolve 16.5 mg dicoumarol in 50 µl of 0.1 M NaOH solution and add 48 ml 50 mM TRIS. Dissolution can be accelerated by ultrasonication. Do not exceed temperatures > 40 °C for the solution. Store aliquots of 2 ml to 5 ml at ≤ -18 °C for a maximum time of 12 months. Thaw each aliquot not more than three times.

4.2.4.6 ETX working solution (8 µM ETX and 10 µM dicoumarol in DPBS, with calcium, magnesium)

For each 96-well plate, 9.6 ml of ETX working solution is required. For a typical set of four plates with sufficient reserve volume, combine the following volumes freshly each day and use the solution within 2 h after preparation: 410 µl dicoumarol stock solution (1 mM), 410 µl ETX stock solution (800 µM), and 40.18 ml DPBS. Use an ultrasonic bath to dissolve any particles under dimmed light for approx. 15 min. Verify before proceeding if particles remain visible. If necessary, prolong ultrasonication. Keep the solution at room temperature protected from direct light. The excess volume will be needed for the protein standard.

4.2.4.7 BCA working solution

Prepare fresh BCA working solution according to the manufacturer's protocol and use within 12 h.

Protein standard (bovine serum albumin, BSA) diluted in ETX working solution

Store the BSA stock standard supplied within the BCA kit according to the manufacturer's specifications. Higher concentrated protein solutions can be diluted to 1 mg/ml with sterile water and stored at 2 °C to 8 °C for up to 3 months. Freezing is not recommended.

Prepare the BCA standard dilutions according to Table 4.3 freshly each day. Use excess volume of ETX working solution from step 18 of the same day.

CRITICAL The BSA protein standard supplied with the BCA kit contains a preservative. It can interfere with other protein determination methods than the BCA method.

Table 4.3: Dilution of the BSA standard in ETX working solution (see REAGENT SETUP)

Protein standard	Well	Concentration per well (µg well^{-1})[a]	Stock concentration (µg ml^{-1})[b]
1	A1	50.00	500.00
2	B1	25.00	250.00
3	C1	12.50	125.00
4	D1	6.25	62.50
5	E1	3.13	31.25
6	F1	1.56	15.63
7	G1	0.78	7.81
8	H1	0	ETX working solution

[a]*This concentration per well results from the addition of 100 µl of the corresponding BSA standard concentration to each well.*

[b]*This is the concentration that needs to be prepared as a serial dilution in ETX working solution.*

4.2.4.8 Trypsin/EDTA working solution (0.05 % Trypsin, 0.02 % EDTA)

Dilute stock solution 1:10 (v./v.) with sterile water. After opening, Trypsin/EDTA solutions should be stored frozen in sterile 10 ml aliquots at -20 °C no longer than the expiration date. Thawed ready-to-use solutions should be stored at 2 °C to 8 °C for no longer than 2 weeks.

4.2.4.9 Dilution medium (culture medium with solvent mixture)

Add 1 % v./v. of the solvent mixture to the culture medium freshly each day, e.g. for four plates (16 samples with three concentrations): Add 100 µl of the solvent mixture to 9.9 ml culture medium, to result in the dilution medium.

CRITICAL DMSO tends to sink to the bottom due to its higher density. Shake vials before processing the responding solution. Do not prepare larger volumes for storage.

4.2.5 Equipment setup

4.2.5.1 Equipment preparation

Prepare the cell culture bench and clean it thoroughly with 70 % ethanol. All materials shall be cleaned with 70 % ethanol and where possible sterile/autoclaved to reduce the risk of contamination. Temper cell culture medium and trypsin/EDTA solution to 30 °C to 37 °C. Adjust the electronic pipette for the various liquid handling steps like pipetting, dispensing, and

mixing. The use of electronic pipettes reduces the handling time and results in an improved accuracy.

4.3. Procedure

4.3.1 Sample preparation, TIMING 1 day to 3 days

1 | Prepare single substance or biological (e.g. environmental, food, or feed) samples for analysis. The preparation procedure will depend on the sample of interest. Refer to the experimental design section for more information.

CRITICAL STEP Fat or other matrix compounds might have a negative effect on the performance of the bioassay and need to be removed using appropriate protocols (see experimental design and Box 1).

4.3.2 Cytotoxicity evaluation, TIMING 3 days

2 | (Optional) Depending on the test design and the chosen matrix cytotoxicity, investigated samples may be evaluated prior to conducting the micro-EROD bioassay to exclude potential masking of the dioxin-like effects of interest. If required, follow the recommended procedure as previously described by Repetto et al. (2008).

CRITICAL STEP Cytotoxicity of a sample can alter the results of the micro-EROD bioassay. It causes a reduced response and leads to potentially false negative results. The maximum concentration applied in the micro-EROD bioassay should not cause any cytotoxicity. Alternatively, check for cytotoxicity of a given sample in step 33 and excluded it from further calculations.

4.3.3 Seeding of cells into tissue culture plates, TIMING 1 h to1 h 30 min

3 | Verify the quality of the cells with an inverted phase-contrast microscope. Exclude contaminations before proceeding with the assay. The cell monolayer should reach a desired confluence of 60 % to 90 %. Select appropriate flasks with cells and transfer into the laminar flow cabinet.

CRITICAL STEP All following procedures of the first day (Steps 3 – 9) must be performed under aseptic conditions in the sterile environment of a laminar flow cabinet. Flasks exceeding 90 % confluence are not recommended for the bioassay as they show a lower metabolic rate.

4 | Aspirate the medium of a cell culture flask preferably with a liquid handling apparatus and add 1 ml of the trypsin/EDTA working solution. Gently agitate the solution over the monolayer of cells and carefully remove it.

5 | Add another 1 ml of trypsin/EDTA working solution and incubate the cell culture flask at 33 °C to 37 °C for 4 min to 8 min.

6 | Tap the flask to detach the cells and add 5 ml of culture medium. Mechanically dissociate the cell layer into a suspension of single cells by gently aspirating and expelling the cells into the flask with a serological pipette. Repeat five to ten times until all macroscopically visible clusters of cells have dissociated.

CRITICAL STEP Proceed quickly to avoid recurring adhesion of the cells to the flask.

!TROUBLESHOOTING

7 | Determine the cell density within the suspension using a hemocytometer or an automated cell counter. During manual counting, the viability of the cells can be verified using trypan blue staining. The cell viability shall be > 95 %.

8 | Dilute the cell suspension to 200,000 cells per ml with culture medium in a sterile reagent reservoir. Immediately dispense 50 µl of the cell suspension into wells A2 to H12 (Figure 4.3). The resulting cell density is 10,000 cells per well. Each plate requires approx. 5 ml of the cell suspension.

CRITICAL STEP Thoroughly mix the cell suspension in the reagent reservoir before addition into the tissue culture plates to ensure an even distribution of the cells throughout all wells. Repeat periodically at least between every two plates and dispense quickly using an electronic multichannel pipette.

!TROUBLESHOOTING

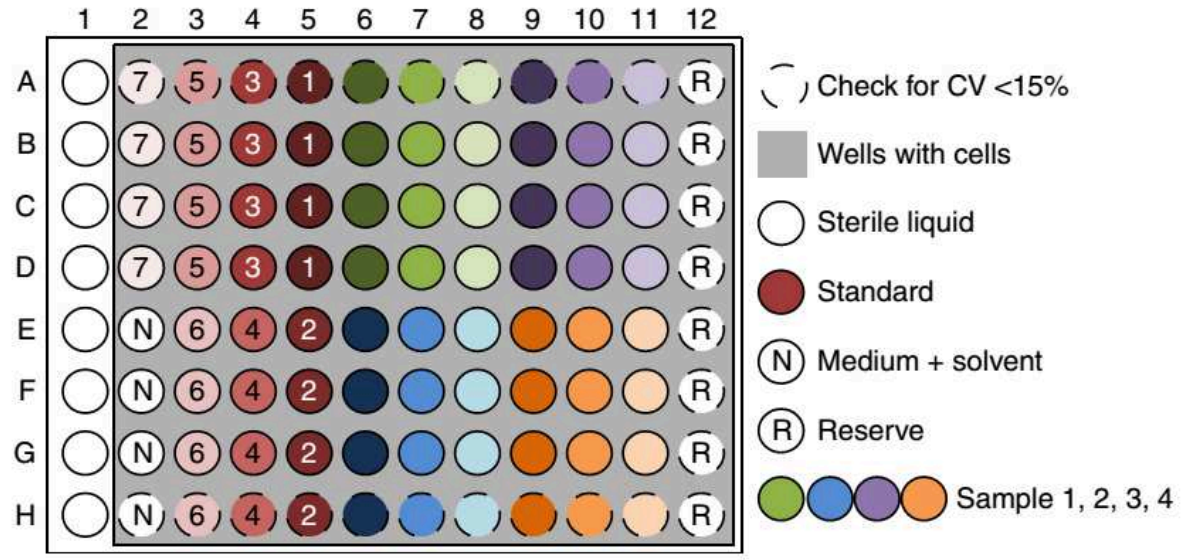

Figure 4.3: Layout for exposure of H4IIE cells in 96-well tissue culture plates . In the current example seven concentrations (S1 to S7) for the standard and a negative control (N) containing the solvent of the standard are presented. Additionally four different samples can be tested in three different dilutions (indicated by the colour gradient) with *n*=4 technical replicates. The wells labelled with R can be additionally used, e.g. additional solvent controls. Outer well on the plate shall be used with caution as edge effect can occur (check for CV <15 %). The wells in column 1 are filled with a sterile liquid. Subsequently, in step 27 the protein standard (Table 4.3) is located in these wells. All wells highlighted in grey contain cells. Depending on the study design, schemes with less samples and more tested concentrations could be applied.

9 | After addition of the cells, gently tilt the well plates to ensure an even distribution of cells within the wells. Cover the plates with a lid, label, and transfer the plates into an incubator (33 °C to 37 °C, 5 % to 7 % CO_2, 95 % humidity). During this incubation step, the cells are supposed to attach to the bottom of the tissue culture plates and grow a monolayer.

CRITICAL STEP Do not circularly agitate the plates, this will result in a central cell cluster.

!TROUBLESHOOTING

PAUSE POINT Samples and standards should be added not earlier than after 2 h, and latest after 16 h.

4.3.4 Preparation of samples and standards, TIMING 1 h 40 min

10 | Prepare the dilutions of samples and standards freshly before exposure of the cells in the solvent of choice. This procedure describes the use of a mixture of DMSO and isopropanol (4:1, v./v.) as a solvent for all samples and controls. The dilution scheme for the samples must be individually developed according to the study design. Here we present an example for three sample concentrations: a sample stock and two further dilutions.

First, prepare 2 ml of a sample stock solution in sterile conditions by adjusting the sample or sample extract (see Box 1) to 20 µl with a 4:1 DMSO and isopropanol volumetric ratio. Then,

add 1980 µl of culture medium to the sample and agitate for at least 10 min on a shaker at 300 rpm to 600 rpm to mix all compounds without touching the cap of the vials.

Next, fill two reaction tubes per sample with 250 µl dilution medium containing 1 % solvent mixture (see REAGENT SETUP). These tubes will be used for a subsequent serial dilution of the samples (see step 12) and can be prepared up to 4 h in advance. Close all tubes until use.

CRITICAL STEP A contact time of 15 min to 30 min of dioxins to plastic tubes causes a significant reduction in the cell response. When applying this protocol, the contact time is shorter than 2 min per concentration.

11 | For each standard concentration (S1 to S7) and the negative control, dispense 990 µl culture medium into 8 reaction tubes. Stock solutions will be added just before pipetting onto the plate. This volume is sufficient for four tissue culture plates and can be prepared up to 4 h in advance.

CRITICAL STEP The volume of standard and negative control dilution depends on the number of samples investigated. For each plate, 200 µl are needed. To reduce pipetting errors a minimum of 990 µl culture medium for 1 ml of final solution should be dispensed. Hence the maximum dilution is 100-fold. When different lots of solvents for standards and samples are used, include an additional solvent control for the samples.

4.3.5 Dosing of cells with the samples, TIMING 1 h

12 | Perform sample dilutions using tubes prepared in step 10. Dilute 250 µl of the sample stock in one of the reaction tubes containing 250 µl dilution medium to create dilution 1. Then, take 250 µl of dilution 1, and add to the second tube to create dilution 2.

Dispense a volume of 50 µl of sample stock, dilution 1 and dilution 2 to four wells each. For an exemplary plate layout, see Figure 4.3. Add the sample stock and the two dilutions to the cells before proceeding with the next sample or the standards. Standards should subsequently be added to all plates at once (step 13). Do not exceed the time span of 1 h between the first sample and the last standard. If this cannot be guaranteed, e.g. due to a high sample number, subdivide the sample set and prepare separate standards for each subset.

CRITICAL STEP We recommend using an electronic multichannel pipette for this step. The dilution and dispensing process per concentration can be combined and furthermore be performed for two samples in parallel for quick succession.

CRITICAL STEP As already 50 µl of the cell suspension are inside the wells, all sample concentrations are diluted during this step. Calculate concentrations accordingly (step 10). For the chosen example the resulting final solvent concentration is 0.5 % within all wells.

!TROUBLESHOOTING

4.3.6 Dosing of cells with TCDD standard and negative control, TIMING 15 min

13 | Add 10 µl of the corresponding standard working stock solutions and negative control to the reaction tubes with 990 µl culture medium (step 11). Mix the resulting standard dilution immediately. Dispense 50 µl into the four corresponding wells per concentration of all previously prepared plates (step 9) as indicated in Figure 4.3.

CRITICAL STEP Prepare a maximum of four reaction tubes with standard dilution at once as TCDD shows a strong sorption to plastics. Handle the standards quickly to reduce the contact time in the tubes to less than 2 min. As already 50 µl of the cell suspension are inside the wells, standards are diluted during this step. For the chosen example the resulting final solvent concentration is 0.5 % within all wells.

!TROUBLESHOOTING

14 | To avoid extensive evaporation, fill all wells without sample or controls with 100 µl culture medium or excess solvent control.

15 | Verify that the addition of all components was successful. Each well should now contain 100 µl liquid.

CRITICAL STEP In case drops of liquids are not mixed and adhere to the well, carefully tip the plates to ensure successful addition of the components.

!TROUBLESHOOTING

16 | Cover the plates with lids, label and record the exact time. Transfer the plates into the incubator for 68 h to 72 h.

CAUTION Collect all remaining standard solutions and discard them properly as toxic waste. Handle with care and adhere to all national and institutional regulations.

!TROUBLESHOOTING

PAUSE POINT Depending on the test design the plates can be incubated for different periods. In the protocol, 68 h to 72 h are chosen to measure stable inducers of the AhR. Shorter periods give different results as instable compounds may be still measurable. When using sample extracts procedure blanks and samples, they usually showed higher EROD activity after 24 h or 48 h of incubation.

4.3.7 Preparation of the EROD activity measurement, TIMING 1 h

17 | Cool methanol, pipette tips and a reagent reservoir at 2 °C to 8 °C. The following parts of the protocol do not require sterile conditions.

18 | Prepare the ETX working solution freshly prior to use according to the REAGENT SETUP.

CRITICAL STEP All steps handling the ETX working solution (18 to 25) should be conducted under dimmed light conditions. The required time can be reduced when performing the visual plate examination (step 19) and the ultrasonication of the ETX working solution (step 18 cf. REAGENT SETUP) in parallel.

19 | After 68 h to 72 h, verify proper cell growth and sterility for each plate and at least one well per sample with an inverted phase-contrast microscope. Record any problems.

20 | Carefully aspirate the medium from each well of all plates including the wells which were filled with liquid only. Do no damage the cell layer.

CRITICAL STEP Accidental aspiration or damage of cells will result in reduced EROD activity and protein concentration, thus falsifying the results of the assay. Uneven distribution of medium leftovers results in higher coefficients of variation. Tilt the plate to 40 degrees to 70 degrees and aspirate the liquid out of the corner to achieve best results. Use aspiration rake for quick procession through parallel handling of several rows.

CAUTION Collect all aspirated media and discard them properly as toxic waste. Handle with care and adhere to all national and institutional regulations.

!TROUBLESHOOTING

21 | Dispense 100 µl of room-temperature ETX working solution to each well containing cells (spare column A1 to H1). Cover the plates with lids and transfer them into an incubator at 33 °C to 37 °C for 30 min.

CRITICAL STEP Exact incubation timing for each plate is vital for an accurate result. Use a timer and work at constant speed.

!TROUBLESHOOTING

4.3.8 Addition of methanol, TIMING 10 min

22 | Remove the tempered methanol, pipette tips and reagent reservoir (step 17) from the refrigerator. Add methanol into the reservoir and aspirate with the multichannel pipette. Aspirate and dispense the complete volume a few times and verify that the methanol does not leak or drip from the tips. Quickly add 75 µl methanol to all wells of the incubated plates including column A1 to H1 to stop the reaction and cover the plate with a lid.

CRITICAL STEP Keep the concentration gradient in mind and avoid cross contamination. For the chosen layout (see Figure 4.3) dispensing from row D to row A, and from row E to row H is recommended. Change tips after the first half of the plate or rinse them with methanol, discarding one full aspiration of methanol into a second reservoir.

!TROUBLESHOOTING

23 | Transfer the plates to a shaker and shake for at least 2 min at 300 rpm in darkness, e.g. by covering the plate shaker with a box.

PAUSE POINT Plates can be covered with polyolefin film for storage. The film is transmissible for fluorescence and almost impermeable for methanol. The loss of fluorescence intensity when measuring through the film is approx. 15 %. At ambient temperature the results are stable for at least three days (Thiem et al., 2014). Cooling can result in condensed water inside the wells and thus increase the coefficient of variation. Adjust amplification in the plate reader, if applicable.

4.3.9 Determination of resorufin using fluorescence spectroscopy, TIMING 30 min

24 | Prepare the fluorescence spectrometer for the measurement. The following settings should be applied: excitation wavelength 544 nm to 572 nm, emission wavelength 584 nm to 590 nm, 10 flashes, position delay 0.2 s.

CRITICAL STEP The excitation and emission wavelengths might require adjustments for the particular fluorometer used. Resorufin has an excitation maximum at 572 nm and an emission maximum at 584 nm. 7-ethoxyresorufin has an excitation maximum at 494 nm and an emission maximum at 576 nm (Radenac et al., 2004). Adjust the settings to achieve the highest ratio between the values of the negative control and the highest TCDD standard induction. Especially for devices with variable amplification (also referred to as gain, zoom, etc.) and a dynamic range, further adjustment shall be conducted. The outer well with the highest TCDD standard shall be adjusted to 75 % to 90 % of the working range of the device. Too high amplification will result in an overflow of the photomultiplier and the data for this measurement point will be lost. If applicable, the measurement setting “optimal gain” can be used to determine the best parameters. Verify the setting before a measurement.

25 | Measure the fluorescence units (FU) in each well of all plates with the corresponding settings.

CRITICAL STEP Until this step, all plates and solutions should have been handled under dimmed light conditions.

4.3.10 Measurement of protein amount, TIMING 1 h to 1 h 40 min

26 | Prepare the BCA working solution freshly prior to use according to REAGENT SETUP. Freshly prepare dilutions of protein standard (BSA, see REAGENT SETUP) to result in the concentrations given in Table 4.3. There should be sufficient ETX working solution left from step 18 of the same day for use.

27 | Add 100 µl of each concentration of the protein standard to the corresponding wells without cells (column A1 to H1, see Figure 4.3.

28 | Add 100 µl of the BCA working solution to all wells of the plate. Now all wells contain a volume of 275 µl.

CRITICAL STEP Take care that the reagent reservoir is clean and does not contain any proteins or tissue fibres. Do not cross contaminate wells containing cells with protein standard. Rinse tips with BCA working solution between samples and protein standard.

!TROUBLESHOOTING

29 | Cover the plates with lids. Incubate the plates at temperatures below 40 °C in well ventilated areas or under a laboratory hood. Incubation at room temperature for 45 min to 90 min.

CAUTION Methanol is a flammable and toxic liquid, avoid overheating and inhalation. Do not use an incubator for this step.

!TROUBLESHOOTING

PAUSE POINT Incubation at room temperature takes 45 min to 90 min. Covering the plates with the lid is sufficient. After firmly sealing the plates, e. g. with polyolefin film, plates can be stored at 2 °C to 8 °C overnight. Before measurement allow plates to reach room temperature. Be aware of condensed water inside the wells.

30 | Measure the absorbance units (AU) in each well at the wavelength of 550 nm to 570 nm by means of a microplate spectrophotometer.

CRITICAL STEP The absorption wavelength might require adjustments for the particular microplate spectrophotometer used. The measured BCA/copper complex of the BCA protein assay has an absorption maximum at 562 nm (Smith et al., 1985). The ratio between the absorbance of protein negative control and wells with cells should be at least 2. The ratio between the protein negative control and the highest value of the protein standard should be approx. 3. If these ratios are not met, a prolonged incubation is recommended. Evaporation can be minimized by sealing the plates.

31 | Store all measurements in a proper file format for subsequent data analysis.

32 | Properly discard the solutions as toxic waste according to national and institutional guidelines as the BCA working solution contains copper, and discard the plates.

PAUSE POINT Evaluation of the previously documented results can be performed at any time following the measurement.

4.3.11 Data evaluation; TIMING 15 min

33 | Calculate the protein content in each well by interpolation from the BSA standard curve using linear regression. To verify the quality of the curve, slope, position of the single values along the curve, as well as the coefficient of determination have to be evaluated. The coefficient of determination (R^2) should be above 0.975. The protein content in each well with sample should be at least 80 % of the mean value from wells with standard and negative control (row 2 to row 5).

CRITICAL STEP If the protein content of a single well is conspicuous, it can be assumed to be a bacterial contamination or a handling artefact. The value should be removed from analysis. Increasing protein content with higher dilution can be observed with toxic sample compounds.

34 | Evaluate the fluorescence values of the four technical replicates of each concentration of standards and samples if the coefficient of variation (CV) is below 15 %. If needed, one of the four values can be excluded, which typically affects the outer wells (evaporation and growth differences). If the CV of the remaining three wells still exceeds 15 % that concentration must be disregarded from further calculation.

CRITICAL STEP Calculate the data using FU or specific EROD activity (step 35) depending on the chosen evaluation strategy. The following steps describe the latter.

35 | For all individual wells, calculate the specific EROD activity (FU min^{-1} mg $protein^{-1}$) according to Equation 4.1, where *FU* is the fluorescence intensity, *t* the time of incubation (i.e., 30 min), $c_{protein}$ the protein content within the well (step 33).

$$\mathrm{EROD} = \frac{\mathrm{FU}}{t \cdot c_{\mathrm{Protein}}}$$

Equation 4.1: Specific EROD activity

36 | Plot the TCDD standard curve using four-parameter logistic regression (Hill function) of the data points using Equation 4.2, where *top* is the y-value of the upper asymptote, *bottom* the y-value of the lower asymptote, EC_{50} the point of inflection, and *slope* the slope factor which corresponds to the steepness of the curve at EC_{50}. The x-axis corresponds to the concentration (pg $well^{-1}$), the y-axis to the specific EROD activity (step 35). If the curve is plotted with

logarithmic x-axis, it will result in a sigmoidal shape. For a good representation of the curve the value of at least one of the two highest standard concentrations has to be higher than EC_{80}.

$$y=\frac{\text{bottom-top}}{1+\left(\frac{x}{EC_{50}}\right)}\cdot\text{slope}+\text{top}$$

Equation 4.2: Four-parameter logistic regression (Hill function)

37 | Subtract the average specific EROD activity of the negative control from the activities of the standards. The *bottom* value is then equal to zero. Fit curves by means of least squares fit between expected and measured values of the standard concentrations. For a better fit of the curve especially at lower concentrations, perform weighting of the values through variances. Calculate the weighted sum of squared residuals (WSSR) according to Hädrich et al. (2012) using Equation 4.3, where y_i is the measured value, $\hat{y}_i$ the corrected value, $i = 1$ to N the different concentrations of the standard, and w_i the weighting factor that equals the inverse of the variance of y_i.

$$WSSR=\sum_{i=1}^{N} w_i\left(y_i-\hat{y}_i\right)^2$$

Equation 4.3: Weighted sum of squared residuals (WSSR)

CRITICAL STEP When using different lots of solvents for standards and samples, include an additional solvent control for the samples and correct data accordingly.

38 | Subtract the average specific EROD activity of the corresponding solvent control from the activities of the samples (step 35). Use the resulting values to interpolate the corresponding TCDD concentration from the standard curve. Express the results as pg BEQ per well and then back-calculated to the corresponding concentration within the original sample.

4.4. Troubleshooting

Table 4.4: Troubleshooting table

Step	Problem	Possible Reason	Solution
Steps 6, 8, 9	Unevenly distributed fluorescence and/or Unevenly distributed protein content CV within one concentration >15 %	Cell aggregates	Separate cells with higher pressure, but keep vitality above 95 %
			Microscopically verify separation into single cells
		Unevenly distributed cells due to a. Pipetting error b. Sedimentation of cells c. Central cell cluster	a. Differently operate the pipette, the pipette might need maintenance b. Frequently agitate suspension, dispense in less steps c. Do not agitate plate circularly
Steps 12, 13, 15	Fluorescence different within samples/concentrations	Time idle or pipetting different between different samples	Time needed for addition of samples should be minimized to less than 12 min per plate, keep contact time of sample and standard solution in reaction vessel below two minutes.
	Unevenly distributed fluorescence at comparable protein content	Different distribution of sample or standard liquids by the pipette	The pipette might need maintenance, use optical pattern to keep track of the dosed wells.
	Values are erroneously distributed	Plate layout not followed properly	If possible allocate samples to correct sample, repeat bioassay
Steps 16, 21, 22, 29	Activity in outer wells higher than in inner wells	Evaporation of media	Ventilation too high, relative humidity too low, cover plates
Step 20	Unevenly distributed fluorescence Unevenly distributed protein content CV within one concentration >15 %	Residual liquids within wells, dilution effects	Visually inspect if residues are present, if applicable aspirate medium from corresponding wells individually
		Damage of the cell layer	Microscopically evaluate if damage occurred, if applicable aspirate more gently
Step 21	Fluorescence systematically lower or higher in one row per plate	positive displacement before first full volume for dispensing added	If applicable expel positive displacement before dispensing.
Step 22	Unevenly distributed fluorescence and absorbance, seemingly correlated	Temperature gradient between methanol, pipette and tips with uneven methanol distribution	Rinse tips with cool methanol directly before dispensing at least twice to cool down air inside the pipette. Ensure no dripping occurs and full volumes are dispensed. Then proceed quickly

Step 28	Protein concentration systematically higher or lower in one row per plate	positive displacement before first full volume for dispensing added	Expel residual substrate solution before dispensing
	Unevenly distributed protein values	BCA solution cloudy or impure	Mix properly and avoid dust from paper towels. Use room-temperature solution.
	Protein concentrations decreases with column number 2>3>4…	Carryover of protein standard	Row 1 should receive the BCA solution last, rinse tips with BCA working solution

4.5. Timing

Day 1-3

Step 1: Sample preparation

Allow 3 days for complete chromatography column preparation, sample clean-up and cleaning. The column chromatography with subsequent volume reduction and solvent transfer can be performed within 8 h. Pure chemicals can be dissolved in a solvent of choice within a few minutes.

Day 4-6

Step 2: Cytotoxicity evaluation (optional)

The recommended protocol by Repetto et al. (2008) requires 3 days to obtain results. The total handling time for this protocol is 4 h 15 min.

Day 7

Steps 3 - 9: Seeding of cells into tissue culture plates: 1 h to 1 h 30 min

Step 10 - 11: Preparation of samples and standards: 1 h 40 min

Step 12: Dosing of cells with the samples: 1 h

Steps 13 - 16: Dosing of cells with TCDD standard and solvent control: 15 min

Day 9

Steps 17 - 21: Preparation of the EROD activity measurement: 1 h

Steps 22 - 23: Addition of methanol: 10 min

Steps 24 - 25: Determination of resorufin using fluorescence spectroscopy: 30 min

Steps 26 – 32: Measurement of protein amount: 1 h to 1 h 40 min

Steps 33 – 38: Data evaluation: 15 min

4.6. Anticipated results

TCDD standard curves show a characteristic shape. Its parameters have proven to be useful as quality criteria (QC, Table 4.5, Figure 4.4). If applicable the requirements of the European Commission should be regarded as well (EC, 2012a; EC, 2014c). The exemplary TCDD concentrations, shown in Table 4.2, result in S-shaped concentration-response-curves with lower and upper asymptotes. For a well-defined upper asymptote the EC_{80} must be reached by at least one of the two highest standard concentrations (Hädrich et al., 2012).

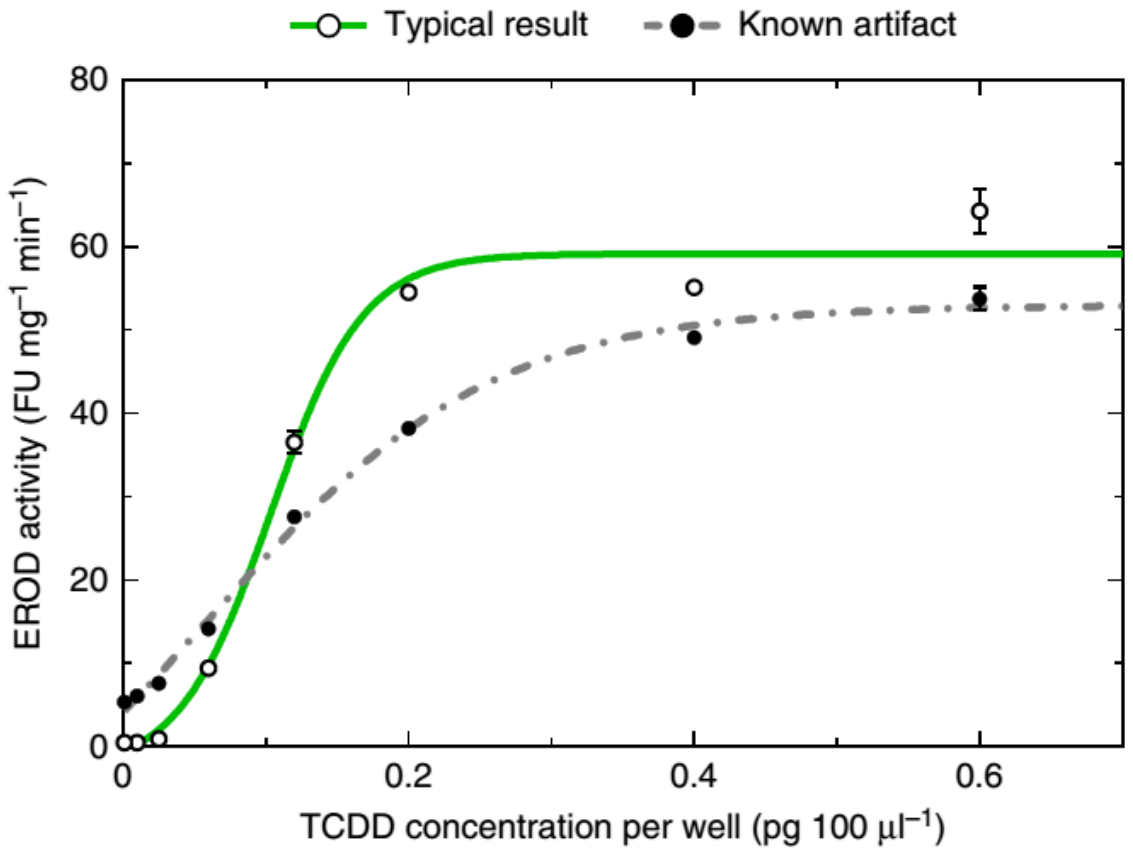

Figure 4.4: Specific EROD activity for TCDD with typical curve shape and parameters. The Typical result plot represents a curve of TCDD (EC_{50}=0.11 pg TCDD well-1, slope=3.11, FU-ratio = 118). The plot for known artefact represents a curve from a mycoplasma infected cell line (EC_{50}=0.15 pg TCDD well-1, slope=1.72, FU-ratio = 11). Error bars represent standard deviation of n=4 replicates

Table 4.5: Typical curve parameters and quality criteria for TCDD after incubation for 68 h to 72 h in the micro-EROD bioassay

Criterion	Acceptable performance	Comments
FU-ratio (FU_{max}* to FU_N**)	> 15	Good cell lines show values of 60 to 120
EC_{50} in pg BEQ $well^{-1}$	0.12 ±0.06	Observed for FU and specific EROD activity respectively
Slope	3.00 ±1.00	
Ratio $EC_{50\ TCDD}$ to $EC_{50\ PCB\text{-}126}$	0.08 ±0.03	
CV of triplicates	<15 %	In routine approx. 5 % are typical

* FU_{max} = Highest measured fluorescence for a standard concentration, alternatively upper asymptote of curve

**FU_N = Fluorescence for the negative control

During a pre round robin test curves without upper asymptotes occurred leading to erroneous sample results (Figure 4.5**,** 0.5 % DMSO+I, artefact). A change of the lot of cells resulted in a regular shape.

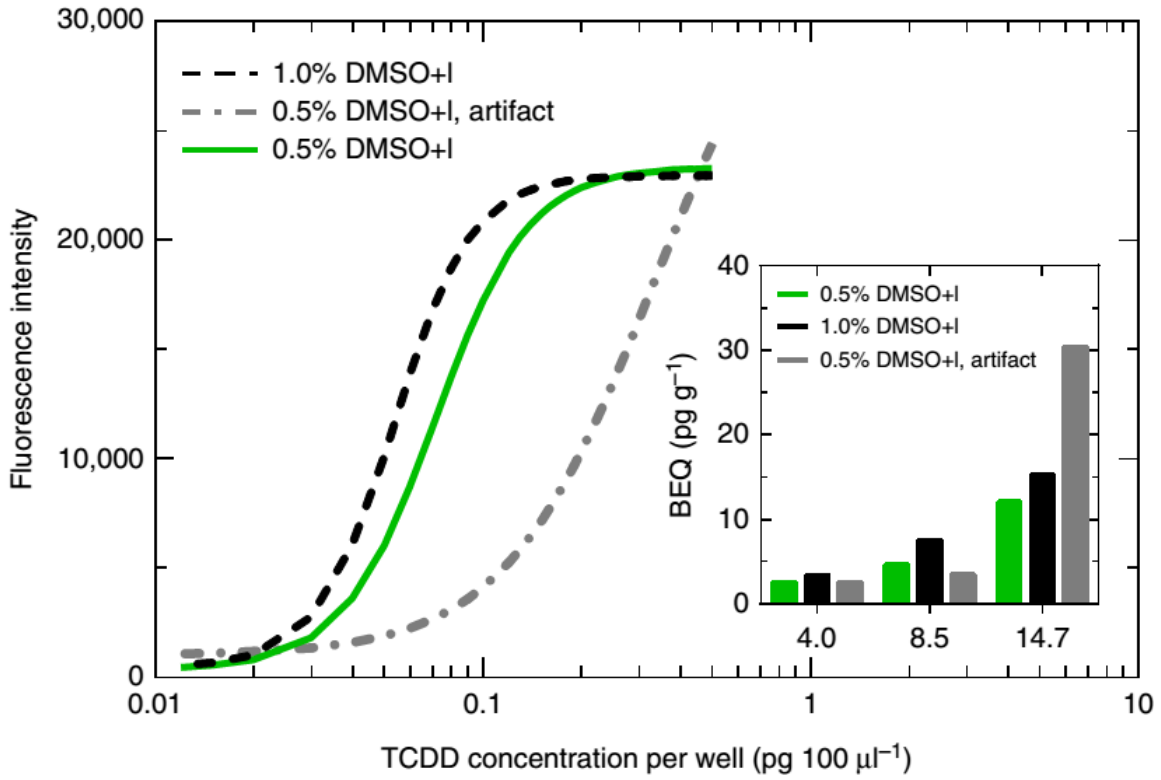

Figure 4.5: Exemplary result from pre round robin test . Fluorescence intensity for TCDD using a final solvent concentration in the well of 0.5 % and 1 %, respectively. Sample results are from fish oil after clean up with sulphuric acid. The artefact represents an incomplete standard curve (missing upper asymptote). This resulted in an overestimation of the sample's potency for the highest contamination level but in an underestimation for the medium contamination level. Error bars represent standard deviation of *n*=4 replicates.

Higher background fluorescence resulting in decreasing slopes and FU-ratios, respectively, can be observed for aged or stressed cells. Possible stressors are cryopreservation, infection with

mycoplasma and too high solvent concentrations or confluence before seeding. Other reasons for similar results are suboptimal measurement conditions, e. g. filter settings, degraded or contaminated ETX stock solution, and incubation with ETX below 30 °C (step 21). Changes in EC_{50} can be signs of alterations in the TCDD standard stock solutions.

Within one test, solvent composition and concentrations should be equal in all wells. Differences can result in varying substance uptake into the cells. Thus, misinterpretation of sample results could be possible (Figure 4.5). For several substances other curve shapes compared to TCDD are known (Behnisch et al., 2001; Thiem and Boehmler, 2011b). Very high amounts of AhR active compounds may lead to cytotoxicity, competing receptor activity or other artefacts. Higher dilution of samples may prove necessary.

When choosing standard substance concentrations the following criteria should be considered: A minimum of seven concentrations should be included. Two of these concentrations should define the asymptotes of the curves with values of $< EC_{20}$ and $> EC_{80}$, respectively. One of these concentrations should represent the EC_{50}. At least one concentration should be between EC_{20} and EC_{50}. A negative control representing the solvent of the same lot and concentration as for the standard dilution should be included.

For a curve calculation via four-parameter-fit at least six valid concentrations are needed. Make sure the former QC parameters are valid. Always check data from newly prepared standards with a verified working stock. The relative difference between identical concentrations should be below 15 %.

Author contributions

All authors contributed extensively to the work presented in this paper, read and edited it and gave their final approval for publication. AS and MB have contributed equally to the work and share first authorship. AS has adopted the protocol from an initial version of IT, GG, and BT, and established it together with KW, LN and KE in our laboratory. MB and AS wrote the manuscript and compiled the protocol. TBS, BT, SB, GR and HH gave technical support and conceptual advice.

Acknowledgements

This protocol was applied within the §64-LFGB working group “Wirkungsbezogene Analytik” (effect directed analysis) for a pre round-robin test. The authors would like to acknowledge the federal office of Consumer Protection and Food Safety (BVL) for their support in this project. The protocol was used and further adopted in context of the project “DioRAMA - Assessment of the dioxin-like activity in sediments and fish for sediment evaluation” that received funds from the German Federal Ministry of Transport and Digital Infrastructure. The authors acknowledge the German National Academic Foundation (“Studienstiftung des deutschen Volkes”) for a personal scholarship granted to MB.

Chapter 5
Development of a high throughput *in vitro* bioassay for determination of the CYP1A-inducing potential of samples using chemically defined media – Efficiency meets ethical cell culture

This research article will be submitted to an international peer-reviewed journal:

Schiwy, A., Nüßer, L., Vorreier, K., Xiao, H., Thalmann, B., Hollert, H., Development of a high throughput in vitro bioassay for determination of the CYP1A-inducing potential of samples using chemically defined media – Efficiency meets ethical cell culture.

Abstract

Cell lines adapted to animal component-free chemically-defined media in suspensions show various benefits compared to cell lines maintained adherent with media containing serum. In this proof-of-concept study we present for the three analytic cell lines H4IIE, H4IIE-luc and HEPG2 the adaptation to these new culturing conditions and their evaluation in bioassays. Resulting, the cells showed high maximal cell densities and a high viability. The change in mode of action resulted in a high throughput and cost efficiency for the bioassays. Additionally, two of the tree cell lines benefit from a high repeatability and process stability in a serum-free medium. This new approach with analytical cell lines allows for new applications as well a new level of automatization.

Keywords: high throughput, bioassay, chemically define, animal alternative, *in vitro*

5.1. Introduction

The development of *in vitro* technology in the 1910s was a driving force of innovation in the past decades for many disciplines in biology and biotechnology (Harrison, 1910; Harrison et al., 1907). It offered many benefits for the scientific community to investigate cellular processes and allowed for new production and diagnostic applications (Fasinu et al., 2012; Geyer et al., 2012; Michael C. Alley et al., 1988; Reiners et al., 1990; Skehan et al., 1990). Additionally, it had many positive effects on other disciplines of experimental research like toxicology or ecotoxicology (Adler et al., 2011; Eisenbrand et al., 2002; Liebsch and Spielmann, 2002). The application of *in vitro* test systems to reduce or replace animal experiments is an excellent example (Adler et al., 2011; Basketter et al., 2012; Leist, 2014; Liebsch and Spielmann, 2002; Ranganatha and Kuppast, 2012). With the rise of *in vitro* technology, various *in vivo* test systems for activity (drug candidates) and toxicity could be replaced with cell-based test systems (Basketter et al., 2012; Ranganatha and Kuppast, 2012). However, *in vitro* techniques can be further improved by means of efficiency and sustainability (Adler et al., 2011; Basketter et al., 2012; van der Valk et al., 2010). One main aspect that leaves room for optimization is the culture media, the composition of which is generally non-optimized and which are essentially supplemented with complex animal-sourced components in utterly all cases. For their growth, cells require media that appropriately replicate the conditions within the living organism (Brunner et al., 2010; Taub, 1990). This includes nutrients, amino acids, vitamins, salts, trace elements, buffers, growth factors, protective substances and many other components (Barnes and Sato, 1980a; Brunner et al., 2010; Riebeling et al., 2011; van der Valk et al., 2010). Hence,

a comprehensive source for these many components are natural and highly complex additives such as human or animal sera (Brindley et al., 2012; Brunner et al., 2010). Up to date, these animal-sourced supplements are essential for many cell culture systems. They stimulate the proliferation and differentiation of the cells with hormonal factors (van der Valk et al., 2004). Additionally, they are a source of adhesions factors which favour or facilitate the adhesion of the cells to the culturing vessels (Taub, 1990). Furthermore, they contain transport and binding proteins that deliver hormones, minerals and lipids to the cells (Rauch et al., 2011). As an additional positive aspect, serum proteins scavenge toxic compound that are formed during cell proliferation. The most common source of these cell culture supplements is fetal calf serum (FCS) (Brindley et al., 2012). It contains high concentrations of the required compounds alongside with low concentrations of immunoglobulins (Brindley et al., 2012). Apart from these advantages, the use of FCS in *in vitro* technology has a bitter aftertaste (Brunner et al., 2010). Most importantly, its animal origin reduces the positive aspects of the *in vitro* technology as an animal alternative (Gstraunthaler, 2003; Gstraunthaler et al., 2013b). Additionally, its composition is not constant and varies with the age, origin, diet of the foetus and even with the season of production (Siegel and Foster, 2013; van der Valk et al., 2010). Therefore, each new serum lot needs to be tested for compliance. Using sera for *in vitro* testing often leads to difficulties in independent replicate comparability due to its variable and non-defined composition (Tekkatte et al., 2011; van der Valk et al., 2004; Wappler et al., 2013). The risk of contamination is high as sera can contain bacteria, fungi, mycoplasma and viruses (Jochems et al., 2002; Tekkatte et al., 2011). Additionally, the contamination with transmissible spongiform encephalopathy cannot be completely ruled out (Jochems et al., 2002). There is a risk of impurities in the final product originating from serum proteins or pyrogens (Biaggio et al., 2015; van der Valk et al., 2004). The downstream processing and clean-up methods for products with therapeutic purpose is more elaborate and cost intensive in serum based production processes (Barnes and Sato, 1980a; Iscove, 1984; Léry and Fédière, 1990). The production process for serum itself requires specialized facilities and the quantity of available serum is finite (Brindley et al., 2012; Brunner et al., 2010). FCS is a side-product of meat industry; it is harvested form extensively farmed cattle and not from animals farmed specifically for serum production (Gstraunthaler et al., 2013b; Siegel and Foster, 2013). In free roaming herds like in Mexico, Argentina, Brazil, South Africa, Canada, New Zealand, Australia and the U.S., gravid cows are directed to slaughter and – from their unborn calf – FCS is harvested by punctuation with a cannula into the beating hearth (Gstraunthaler et al., 2013b; Häusl, 2008). The approximate volume is half a litre per calf and the production volume of serum fluctuates as it depends on

various factors, e.g. beef price and weather (Siegel and Foster, 2013).

It is an alarming fact that it is anticipated that the maximal production volume of FCS has already been reached. The term "peak serum" (as an analogy to the term "peak oil", which refers to the point in time when the maximum rate of fossil oil extraction is reached) was been used to describe this situation (Brindley et al., 2012). Hence, the cost of serum can be expected to further increase in the next years (Brindley et al., 2012; Häusl, 2008); especially in light of the recent developments to apply *in vitro* technology for generation of therapeutics (e.g. insulin, growth factors, vaccines, monoclonal antibodies, clotting factors and etc.). It is important to note that only traceable serum without any contaminations can be used for this purpose and its volume is limited to an estimated 200,000 litres per year (Brindley et al., 2012). Furthermore, *in vitro* technology is even expected to replace animals for meat production (Bhat and Bhat, 2011; Bhat and Fayaz, 2010; Bhat et al., 2015). The first hamburger patty produced *in vitro* has already been eaten in 2013 (Mattick et al., 2015). However, this alternative has its own technical and ethical challenges and implications (Bhat and Fayaz, 2010; Bhat et al., 2015; Chiles, 2013; Driessen and Korthals, 2012; Heale, 2012; Mattick et al., 2015). With breakthroughs in these two fields, a significantly higher serum demand is expected (Biaggio et al., 2015; Brindley et al., 2012). With an increasing price, serum-related crime may be attracted and fraud has already been reported (Gstraunthaler et al., 2013a; Gstraunthaler et al., 2013b). These developments can have devastating effects for application of *in vitro* technology in any field.

To overcome these obstacles, medium additives that help to reduce the serum concentrations without negative effects as well as serum-free media are being developed (Brunner et al., 2010; Rauch et al., 2011). As a proactive move to this development, the vaccination industry switched to serum-free media or alternative processes and other should follow (Brindley et al., 2012). In compliance with the principle of the 3 R´s (reduction, refinement and replacement) that was developed in the 1950s, the substitution of animal sera is the most crucial element to develop *in vitro* technology into a true animal-free alternative with good cell culture practice (Flecknell, 2002; Gstraunthaler et al., 2013b; Russell et al., 1959). Interestingly, it is predicted that the source of transition to serum-free media will not occur as a result of new regulations but out of economic reasons (Brindley et al., 2012). Chemically-defined animal component-free media improve the technical and ethical aspects of *in vitro* technology (Brunner et al., 2010). The most important technical benefits are the reduction of variability and increase of productivity (Brunner et al., 2010). In addition, the use of optimized and fully enriched chemically-defined media massively reduces the limitations in growth as well as productivity including reporter gene expression (Li et al., 2007; Page et al., 2014; Schlaeger and Christensen, 1999). It enables

higher quality biotechnology products that readily meet the regulatory requirements for medical products (Biaggio et al., 2015; Swamynathan et al., 2014). Not only a higher quality but also a higher product quantity is feasible as clean-up procedures are facilitated by reducing the number of components in the medium (Biaggio et al., 2015; Brunner et al., 2010; Zhang et al., 2013). The final product has a reduced risk of impurities, which could affect the production and analytical outcome (Swamynathan et al., 2014). For analytical purposes, this aspect can facilitate the analysis of metabolites and by-products. Undesired processes such as sorption to serum components and contamination with viruses, fungi, bacteria and mycoplasma are reduced or, as in the case of prions, eliminated entirely (Brunner et al., 2010; Swamynathan et al., 2014; van der Valk et al., 2010). Better defined and reproducible formulations allow for research with a higher relevance and reproducibility (Swamynathan et al., 2014; van der Valk et al., 2010). As a result of the constant composition of serum-free media, no elaborate testing of new lots is necessary (Eske et al., 2009). In summary, different elements of media used for the *in vitro* culture of cells are standardized and improved with chemically-defined animal component-free media with subsequent technical, ethic and economic benefits (Biaggio et al., 2015; Gstraunthaler et al., 2013b).

The first research conducted to replace serum in cell culture media was conducted in the 1960s (Pumper, 1958; Shitamura et al., 2005). However, most of these attempts to elucidate the components of the serum necessary for cell proliferation were not very successful (Taub, 1990). Another approach was the supplementation of a basal medium with a varying number of essential components according to each cell line. This approach also had a high failure rate of 80 % or more (Pazos et al., 2004). The work by Hayashi and Sato (1976) has to be specially highlighted as it helped to replace serum with selected hormones that promote growth and differentiation of specific cells (Barnes and Sato, 1980a; Barnes and Sato, 1980b; Bottenstein and Sato, 1979). Their work led to chemically-defined, serum-free media (Taub, 1990). In the past fifteen years, research on cell functions was fruitful and identified a growing number of components that are applied in modern serum-free cell culture media (van der Valk et al., 2010). More than three hundred different serum-free media formulations are now commercially available and the number is steadily growing (Brunner et al., 2010). However, the process of development is elaborate and time- and cost-demanding. Custom-made media cost approx. 250k € for each cell line (Greulich et al., 2011). As more and more serum-free media formulations become available, it appears possible to develop own media with reduced costs and in a reasonable timeframe (Zhang et al., 2013). In the literature various protocols are described (Gstraunthaler, 2003; Gstraunthaler and Lindl, 2013; van der Valk et al., 2010).

One of the various applications for *in vitro* cell systems that will benefit from serum-free media are cell-based bioassays. With such bioassays, different aspect of cellular physiology and metabolic activity may be monitored for the purpose of toxicity testing or drug discovery (Adler et al., 2011; Coecke et al., 2013). They are good alternatives to animal experiments as they combine some of the properties of animals such as their specific metabolic activity and receptor composition in animal-free methods with reduced time-, space- and cost-requirements. The sensitivity of some bioassays is very high and comparable to or even exceeding that of instrumental analysis (Eichbaum et al., 2014; Hilscherova et al., 2000). Viability or cytotoxicity tests are a straight-forward approach but not very representative for whole organism (Astashkina et al., 2012). Bioassays that utilize receptor-mediated processes are more complex but far more sensitive as they investigate receptor-mediated signalling cascades and signal induction. These bioassays can simulate organ-specific reactions such as the metabolic activity of the liver or the endocrine regulation of the gonads (Fasinu et al., 2012; Hilscherova et al., 2000). As an example, metabolically-active hepatoma cell lines originating from the liver react to dioxin-like compounds (DLCs) *via* the aryl hydrocarbon receptor (AhR) pathway (Sawyer and Safe, 1982). At the end of the signalling cascade, the metabolic activity of CYP1A enzymes is induced. Especially, the induction of the ethoxyresorufin-*O*-deethylase (EROD) activity has been used to quantify DLCs in various sample matrices (Eichbaum et al., 2014; Thiem et al., 2014; Whyte et al., 2004). In a recent publication, we presented a protocol to conduct a bioassay to quantify the induction of CYP1A using the rat hepatoma cell line H4IIE (Schiwy et al., 2015a). This micro-EROD bioassay is able to detect one of the strongest inducers and the most toxic compound in this class, namely 2,3,7,8-tetrachlorodibenzo-*p*-dioxin (TCDD) in the low pg/L range (Schiwy et al., 2015a). Alternatively, bioassays have been developed with genetically-modified cells that coupled AhR-binding with the reporter enzyme luciferase (Behnisch et al., 2002; Bovee et al., 1998; Eichbaum et al., 2014; Murk et al., 1996).

We selected these two bioassays to perform a proof-of-concept study for the application of chemically-defined media and suspension cell culture for high-throughput screening of various sample matrices.

5.2. Aims

The aim of this study was to advance the established *in vitro* bioassay technology. We want to showcase a suspension cell culture test system with serum-free animal component-free chemically-defined media (Figure 5.1). The wild-type H4IIE, HEPG2 and the recombinant H4IIE-luc cell lines were adapted to chemically-defined media and suspension cell culture. The newly developed cell lines H4IIE-S, HEPG2-S and H4IIE-luc-S were then used for conducting the micro-EROD bioassay and a luciferase assay, respectively, to investigate their performance with well-characterized reference compounds (Figure 5.2). Modifications to the established protocols to adapt to the new culturing conditions were evaluated.

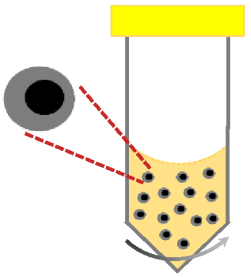

Figure 5.1: A schematic representation of the suspension culturing conditions

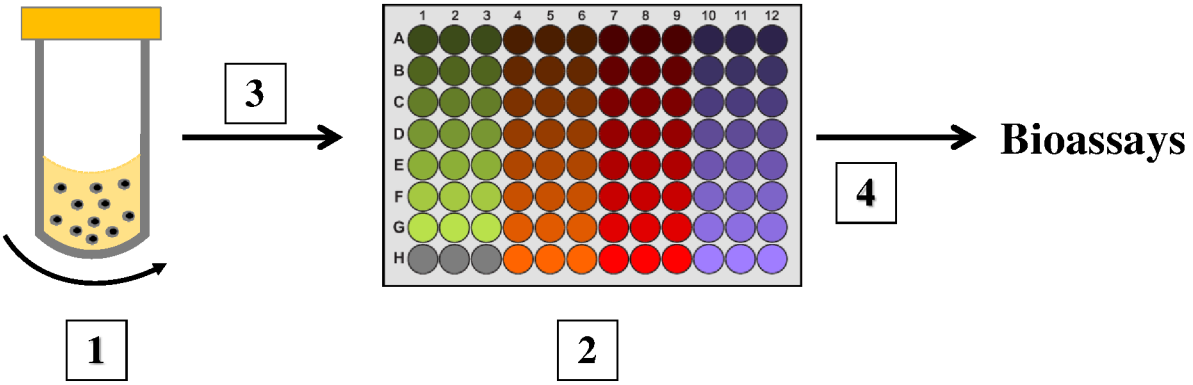

Figure 5.2: Process scheme of the newly developed suspension cell culture bioassay system . 1 – The cells are cultivated in suspension; 2 – Sample preparation is conducted in a well plate format; 3 – The cells are transferred onto the plate to start the incubation; 4- The incubated cells are transferred into other plates to conduct various bioassays

5.3. Material and Methods

5.3.1 Chemicals

All chemicals were supplied in analytical reagent quality and cell culture-tested by Sigma-Aldrich unless specifically indicated.

5.3.2 Adherent cell culture

The culture of H4IIE (ATCC® CRL-1548™), H4IIE-luc and HEPG2 (ATCC® HB-8065™) cells was conducted according to the recommendations of ATCC and the protocols published by Hinger et al. (2011), Keiter et al. (2006), Sanderson et al. (1996), as well as Schiwy et al. (2015a) at 37 °C, 5 % CO_2 and > 95 % humidity. H4IIE cells were maintained in Dulbecco´s Modified Eagle Medium (DMEM) medium (Gibco, Darmstadt, Germany) with low glucose, without phenol red and supplemented with 10 % FCS (Biowest, Nuaillé, France), 10 mM GlutaMAX (Gibco, Darmstadt, Germany) and 1 mM HEPES (Gibco, Darmstadt, Germany). H4IIE-luc and HEPG2 cells were maintained in DMEM with low glucose, without phenol red and supplemented with 10 % FCS. Cells were passaged after visual investigation with an inverse light microscope (Nikon Instruments Europe BV GmbH, Amsterdam, Netherlands) at a confluence of 70 % to 90 %.

5.3.3 Adaptation to animal component-free chemically-defined media and suspension culture

H4IIE, H4IIE-luc and HEPG2 cells were adapted to a continuous suspension cell culture in an animal component-free chemically-defined medium CDM5 (GE Healthcare Life Sciences HyClone Laboratories, Freiburg, Germany). The cells were cultured in 50 ml tubes (TPP, Trasadingen, Switzerland) with a filter lid under constant shaking at 37 °C, 5 % CO_2 and > 95 % humidity and 220 rpm with an amplitude of 20 mm. Cell densities were monitored by cell counting using a hemocytometer and cell viability was monitored by trypan blue staining with an inverse light microscope. Percentage of viable cells was calculated. At a cell concentration of approx. $2•10^6$ - $5•10^6$ cells/ml the cells were passaged by dilution to $2.5•10^5$ - $5.0•10^5$ cells/ml with the culturing medium. The newly developed suspension cell lines were named H4IIE-S, H4IIE-luc-S and HEPG2-S.

5.3.4 Bioassays with H4IIE-S, HEPG2-S and H4IIE-luc-S cells

The suspension cell lines were investigated with in different bioassays. The protocols of the respective bioassays were adapted for use of suspension-cultured cells. For H4IIE-S and HEPG2-S cells, the dioxin-like activity and the viability were measured using a modified micro-EROD protocol according to Schiwy et al. (2015a) and the resazurin bioassay according to Czekanska (2011), respectively. The genetically modified H4IIE-luc-S cells were investigated in the two mentioned bioassays, and additionally in a modified luciferase bioassay according to Hinger et al. (2011) and Keiter et al. (2006).

5.3.5 Reference compounds and bioassay adaptation to suspension conditions

The procedures for the bioassays were adapted to the suspension cell culture. First, sample dilutions were prepared in the corresponding medium and plates, and subsequently the cells were added. To evaluate the performance and suitability of the new cells lines, the established positive control 2,3,7,8-tetrachlorodibenzo-*p*-dioxin (TCDD, Sigma Aldrich, Steinheim, Germany) dissolved in dimethyl sulfoxide (DMSO, Sigma Aldrich, Steinheim, Germany) was applied in various concentrations ranging from 20 µM to 12945 mM. The highest TCDD concentration was adjusted to 1 % (v./v.) DMSO, and a serial dilution was conducted. Subsequently, the cells were added in a medium without DMSO. This resulted in a 3-fold dilution of the DMSO concentration. The plates were sealed with a sealing membrane for multiwell plates (Breathe Easier, Sigma, Darmstadt, Germany) and incubated on an orbital plate shaker Unimax 1010 (Heidolph, Schwabach, Germany) for 22 h to 24 h in an incubator at 37 °C, 5 % CO2, > 95 % humidity and 450 rpm with an amplitude of 10 mm. After incubation the plates were centrifuged for 1 min at 209 g to remove any cells from the well walls. Following, the foil was removed and the cells were resuspended.

5.3.6 Dioxin-like activity assay – H4IIE-S, H4IIE-luc-S and HEPG2-S

The EROD measurement was conducted in a modified protocol according to Schiwy et al. (2015a). The artificial substrate 7-ethoxyresorufin (ETX) in PBS without bivalent ions was added under dimmed light conditions to the wells containing cells at a concentration of 2 µM. After incubation for 30 min at 37 °C, 5 % CO_2 and > 95 % humidity, 90 µl methanol was added to stop the reaction. Finally, the fluorescence signal of resorufin was recorded as relative fluorescence units (RFUs) with the plate reader Infinite M200 at 560 nm excitation and 590 nm emission wavelength (Radenac et al., 2004).

5.3.7 Luciferase assay - H4IIE-luc-S

The luciferase assay was conducted with the Steadylite plus (PerkinElmer, Baesweiler Germany) reagent solution. The solution was prepared according to the manufacturer's recommendation and 20 µl were transferred into the wells with 40 µl cell suspension. The plates were incubated under constant shaking in darkness for 10 min at room temperature. Following, the luminescence signal was measured with an Infinite M200 plate reader (Infinite M200, Tecan Group Ltd., Männedorf, Switzerland) or GloMax-96 Microplate (Promega, Mannheim, Germany).

5.3.8 Data evaluation

The results of the fluorescence measurements for the EROD induction were used to calculate the fold change of induction compared to the untreated solvent control from here on called negative control (Equation 5.1). A non-linear regression was conducted and all graphs were calculated and plotted with GraphPad Prism 6 (GraphPad Software, La Jolla, USA). As non-linear regression the function 'log agonist vs response – Find ECanything' with least squares regression was chosen (Equation 5.2).

$$fold\ change\ compared\ to\ NC = \frac{RFU\ signal}{RFU\ NC}$$

Equation 5.1: Fold change calculation compared to negative control NC= negative control; RFU= relative fluorescence units

$$logEC50 = logECF\ -\ (\frac{1}{HillSlope}) * log(\frac{F}{100 - F})$$

$$Y = \frac{Bottom\ +\ (Top - Bottom)}{(1 + 10^{((LogEC_{50} - X) * HillSlope))}}$$

Equation 5.2: Non-linear regression log agonist vs response – Find ECanything x= log of concentration; y= response; F= constant value between 0 and 100 for EC_{25} the value is 25; Bottom = lowest response value divided by the mean response of the negative control; Top = the highest response value as fold change compared to negative control; LogECX= same log units as x; X= concentration at EC_{50}; Hill slope= slope factor or Hill slope, unitless

5.3.9 Demethylation of DNA by 5-azacytidine treatment

To assess the influence of DNA methylation the H4IIE-luc-S cells were treated with 5 µM 5-azacytidine (AZA) solution for 24 h as a demethylation agent in an additional experiment for the passages P3.3.27, P3.3.32 and P3.3.35. After this period of time the cells were investigated in the EROD and luciferase assay, respectively.

Modified cultivation of the H4IIE-S cells for improved sensitivity in the micro-EROD bioassay

The H4IIE-S cell line was selected to conduct additional investigations. The cultivation and bioassay conditions were optimized for sensitivity. The CDM5 medium was supplemented with 10 mg/L bovine insulin. Additionally, a second reference compound, β-naphthoflavone, in addition to TCDD was evaluated in multi well plates with polystyrene or polypropylene as plate material. The polypropylene plates were obtained from three manufactures (TPP, Trasadingen, Switzerland; Thermo Fisher Scientific Germany; Braunschweig, Germany; Greiner Bio-One, Frickenhausen, Germany). The three different manufacturers were chosen to evaluate any differences originating in the manufacturing process. The polystyrene plates were obtained from one manufacturer (Thermo Fisher Scientific Germany; Braunschweig, Germany).

5.4. Results

The results of the experiments are divided into two sections. In the first section we present the results of the adaptation of adherent cell lines to the animal component-free chemically-defined medium and suspension culturing conditions (Figure 5.1). In the second section we present the results of the bioassays conducted with the adapted cell lines.

Section 1

5.4.1 Adaptation to chemically defined medium and suspension cell culture

Table 5.1 shows the maximum cell densities, doubling time and viability of the adapted cell lines. The cell densities were $5.5 \cdot 10^6$ cells/ml for HEPG2-S and $6 \cdot 10^6$ cells/ml for H4IIE-S and H4IIE-luc-S, respectively. All cell lines showed a doubling time of 3 days and a viability of 99 %.

Table 5.1: Cell densities and cell viability of the newly developed cell lines H4IIE-S, HE4IIEluc-S and HEPG2-S

	H4IIE-S & H4IIE-luc-S	**HEPG2-S**
Max. cell density [cells/ml]	$6 \cdot 10^6$	$5.5 \cdot 10^6$
Doubling time [h]	22-26	22-26
Viable cells [%]	99	99

Section 2

5.4.2 Results of micro-EROD and luciferase bioassays with the adapted cell lines

The bioassays conducted with the newly developed cell lines showed concentration-response relations for the reference compound TCDD. The viability of the cell lines was not influenced by the concentrations of the reference compound; therefore the data of the viability assays are not shown.

5.4.3 Micro-EROD bioassay with the HEPG2-S cells

Figure 5.3 presents the dose response curve for a serial dilution of the reference compound TCDD with the HEPG2-S cell line after incubation for 24 h in the micro-EROD bioassay. The x-axis presents the pM TCDD on a logarithmic scale. The y-axis presents the fold change of signal induction compared to the response of the negative control. A nonlinear regression was performed for the response in the concentration range from 0.19 pM to 12945 pM TCDD. The EC_{25} value was 518 pM.

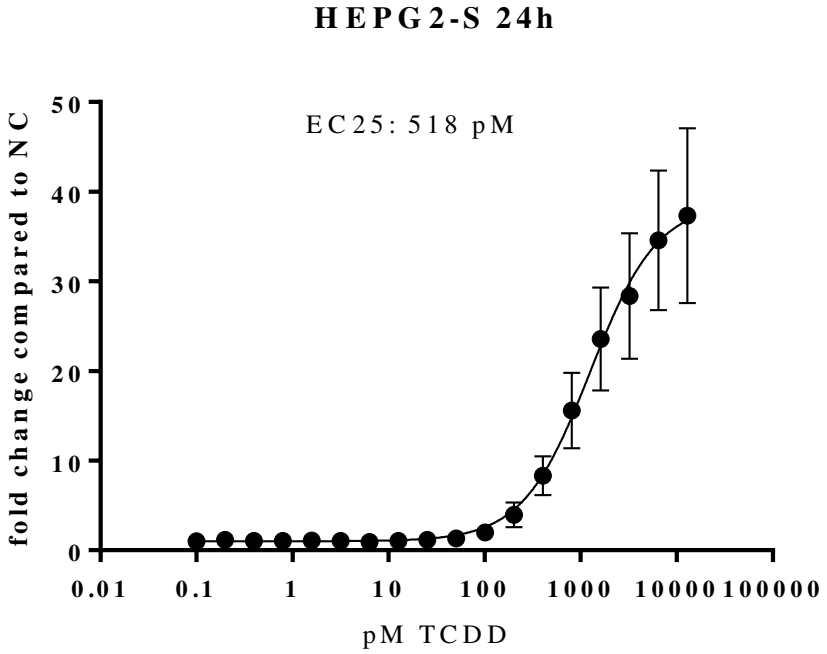

Figure 5.3: Dose response curves of the HepG2-S cells after exposure to a serial dilution of TCDD in the micro-EROD bioassay, n=3

5.4.4 Micro-EROD and luciferase bioassay with the H4IIE-luc-S cells

Figure 5.4 presents the dose response curve for a serial dilution of the reference compound TCDD with H4IIE-luc-S cell line after an incubation time of 24 h in the micro-EROD (**A**) and luciferase (**B**) bioassay . The x-axis presents the pM TCDD on a logarithmic scale. The y-axis presents the fold change of signal induction compared to the response of the negative control. A nonlinear regression was performed for the response in the concentration range from 0.26 pM to 1000 pM TCDD for the micro-EROD and from 0.32 pM to 161 pM TCDD for the luciferase bioassay. For TCDD the EC_{25} value was 41 pM in the micro-EROD (**A**) and 13 pM in the luciferase (**B**) bioassay.

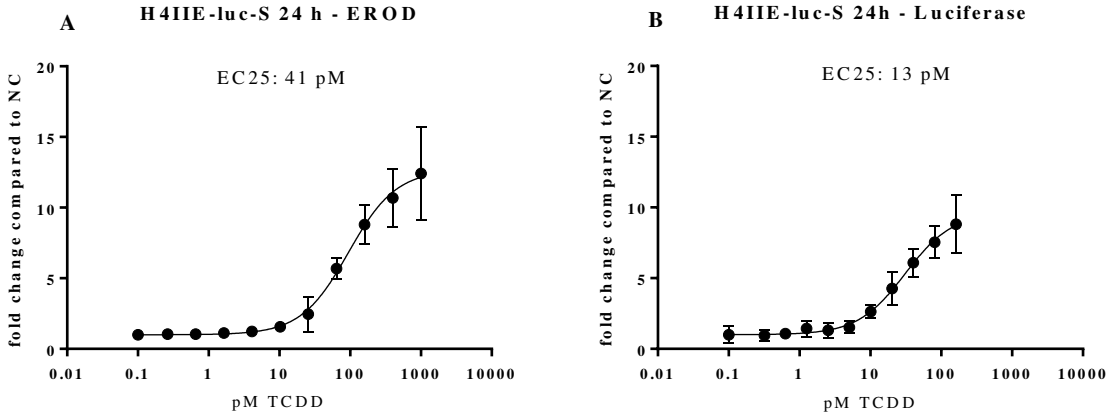

Figure 5.4: Dose response curves of the H4IIE-luc-S cells after exposure to a serial dilution of TCDD in the micro-EROD (**A**) and luciferase (**B**) bioassay, n=2

Figure 5.5 presents the dose response curves for the reference compound TCDD with the H4IIE-luc-S cell line after an incubation time of 24 h in the Luciferase (**left**) and micro-EROD (**right**) bioassay over multiple passages. The x-axis presents the pM TCDD on a logarithmic scale. The y-axis presents the fold change of signal induction compared to the response of the negative control. A nonlinear regression was performed for the response in the concentration range from 0.26 pM to 1000 pM TCDD. The EC_{25} values for the different passage numbers and treatments are presented within the graphs.

5.4.5 Luciferase bioassays (left column)

The luciferase bioassay with the H4IIE-luc-S cells was conducted to investigate a silencing of the reporter genes by DNA methylation. In the initial test (Figure 5.4) with the adapted H4IIE-luc-S cell line the cells showed an EC_{25} value of 13 pM. For the passage P3.5.28 no reliable EC_{25} values could be determined in the luciferase bioassay with or without 5-azacytidine treatment. In the following passages P3.5.32 an EC_{25} value of 87 pM was determined after 5-azacytidine treatment and an EC_{25} value of 286 pM after 4 passages without treatment. The last passage P3.5.35 showed an EC_{25} value of 435 pM TCDD after 5- azacytidine treatment and an EC_{25} value of 1569 after 7 passages without treatment. The treatment with 5-azacytidine results in an approx. 3-fold lower EC_{25} value compared to the control.

5.4.6 Micro-EROD bioassay (right column)

The micro-EROD bioassay was performed with the H4IIE-luc-S cells as a control of the intrinsic EROD activity. The initial EC_{25} value of 43 pM TCDD (Figure 5.4) was not reproduced in the control group P3.5.28. The cells showed an decreased sensitivity with an EC_{25} value of 482 pM TCDD. After a single treatment with 5-azacytidine the sensitivity was increased to an EC_{25} value of 70 pM TCDD. Incubated for 3 passage the sensitivity reduced to an EC_{25} value of 421 pm TCDD. The repeated treatment with 5-azacytidine gained an sensitivity increase for the cells between 1.5-fold and 7.4-fold compared to the cells after a single treatment. The most sensitive passage was P3.5.32 with an EC_{25} value of 41 pM after 5-azacytidine treatment. With increasing passage number the sensitivity to TCDD decreased to an EC_{25} value of 296 pM even after 5-azacytidine treatment.

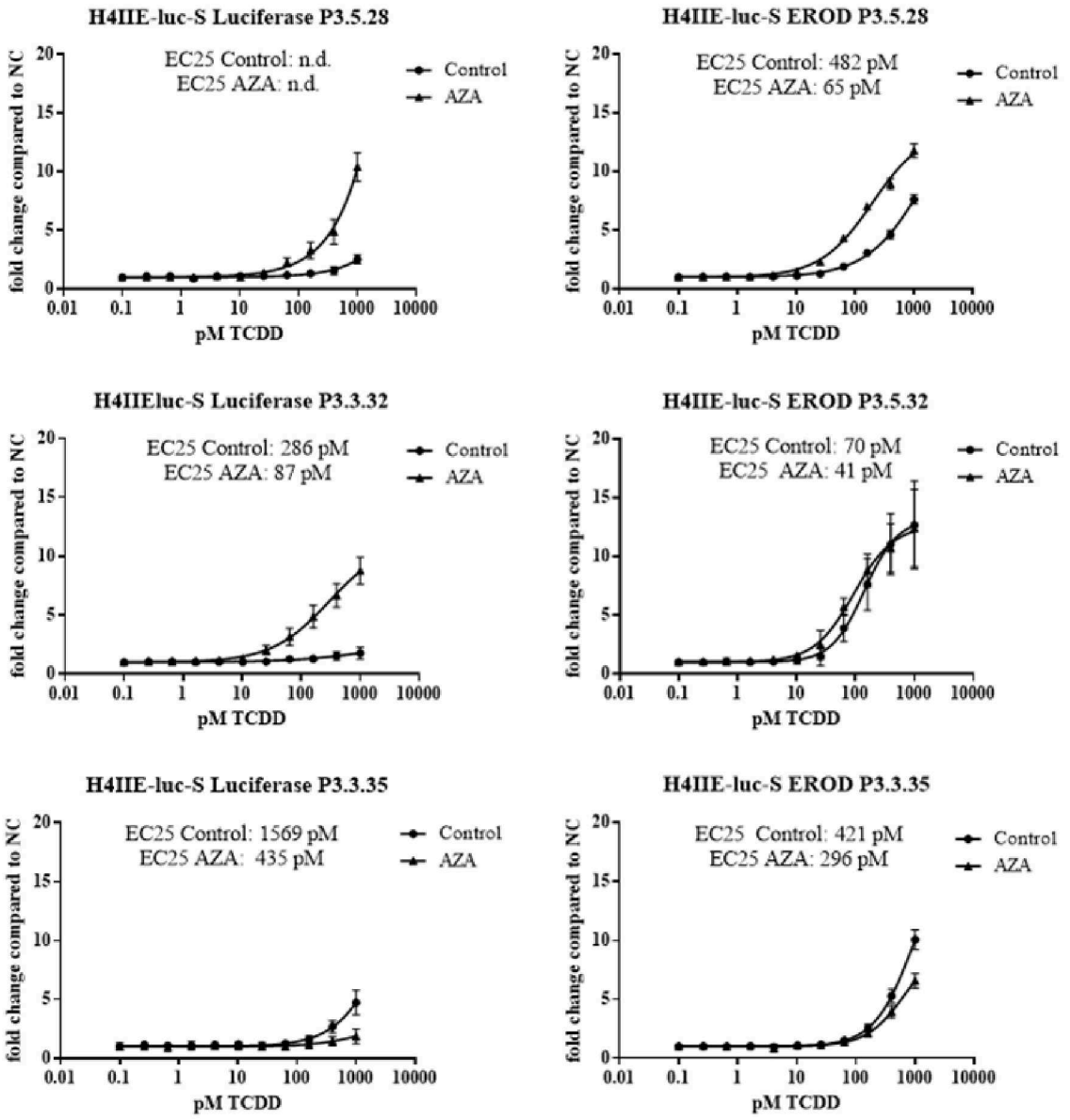

Figure 5.5: Dose response curves of the H4IIE-luc-S cells after exposure to a serial dilution of TCDD and treatment with or without 5-azacytidine (AZA) in the luciferase (**left**) and micro-EROD bioassays (**right**), n=3

5.4.7 Micro-EROD bioassay with the H4IIE-S cells

Figure 5.6 presents the dose response curve for the reference compound TCDD with the H4IIE-S cell line after an incubation time of 24 h in the micro-EROD bioassay. The x-axis presents the pM TCDD on a logarithmic scale. The y-axis presents the fold change of signal induction compared to the response of the negative control. A nonlinear regression was performed for the response in the concentration range from 0.2 pM to 1618 pM TCDD. The EC_{25} value was 13 pM TCDD.

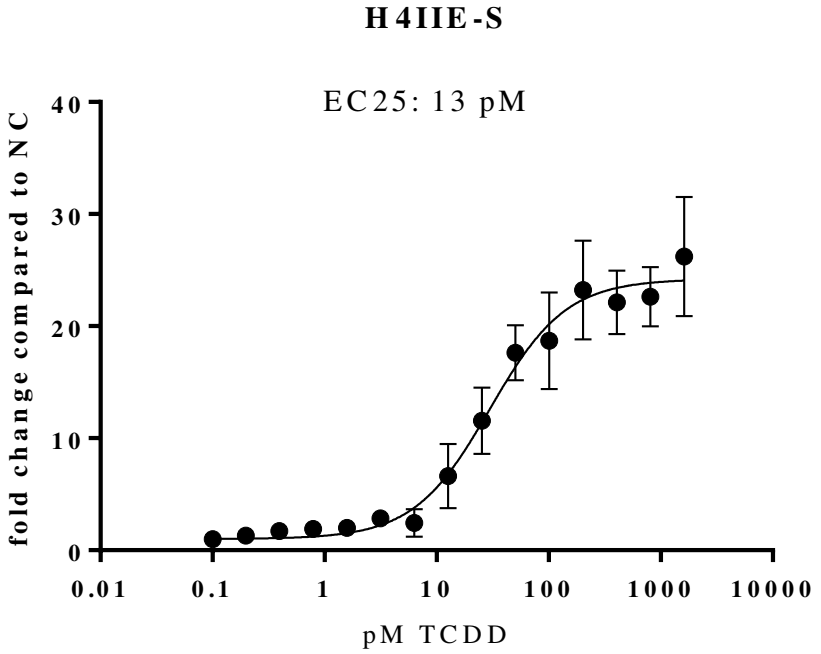

Figure 5.6: Dose response curves of the H4IIE-S cells after exposure to a serial dilution of TCDD in the micro-EROD bioassay, n=4

Figure 5.7 presents the dose response curves for the reference compounds TCDD (**A**) and β-naphthoflavone (**B**) for H4IIE-S cells with optimized culturing and bioassay conditions after an incubation time of 24 h in polystyrene (PS) or polypropylene (PP) plates for the micro-EROD bioassay. Figure 5.7 (**A**) shows the response of the H4IIE-S cells to TCDD in the concentration range of 0.06 pM to 1000 pM. Figure 5.7 (**B**) shows the response of the H4IIE-S cells to β-naphthoflavone in the concentration range of 2.4 nM to 36724 nM. The EC_{25} values for TCDD were 6 pM for PS and 217 pM for PP. For β-naphthoflavone the EC_{25} values were 94 nM for PP and 634 nM for PS.

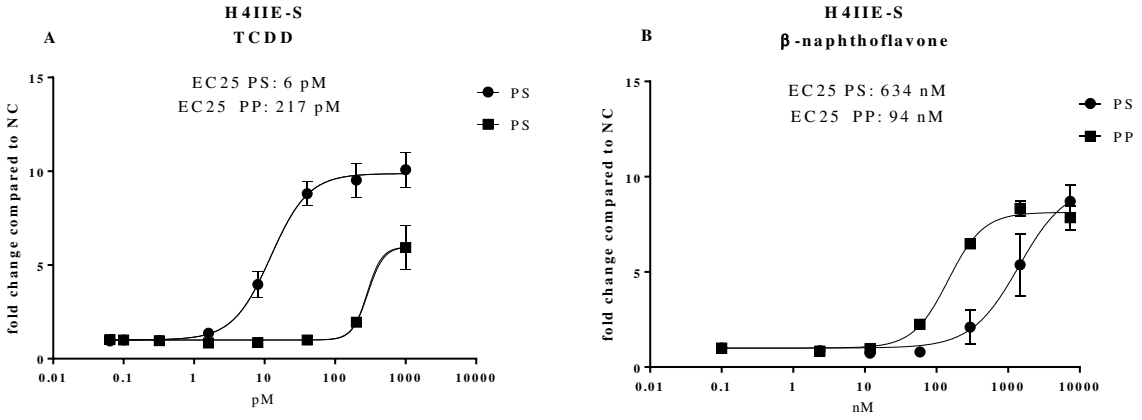

Figure 5.7: Micro-EROD bioassay with H4IIE-S cells with improved culturing conditions in 96-well plates composed of polystyrene (PS) or polypropylene (PP) material. The cells were exposed to a serial dilution of TCDD from 0.06 pM to 1000 pM (**A**) and β-naphthoflavone from 2.4 nM to 36724 nM (**B**). The EC_{25} values are presented in table included above the graphs. TCCD n=18 ;β-naphthoflavone n=6

5.5. Discussion

5.5.1 Serum-free adaptation

The adherent cell lines H4IIE, H4IIE-luc and HEPG2 were successfully adapted to a serum-free chemically-defined medium. Additionally, these cells were adapted to suspension culture conditions. These adapted cell lines have been named H4IIE-S, H4IIE-luc-S and HEPG2-S. The doubling time of 22-26 hours for each cell line is comparable or improved compared to the adherent cell lines using the cultivation procedure with FCS. The cells showed a 99 % viability which is comparable or higher than in the adherent cell culture. The viable batch culture duration (>95% Viability) is 6–7 days without subcultivation. These elements of FCS substitution and change of cultivation process have a major impact on the cost of these *in vitro* systems. Based on our calculations with a FCS price in the time period of August 2013 to July 2015 it is four times more cost-efficient than the classic cell culture methods. The major aspect

is the reduced need of components, handling steps and the higher cell number per cultivation vessel. The number of handling steps and components is reduced as no cell detachment step is needed and the cells are passaged by dilution. This also results in a reduced risk of contamination. An additional benefit of the suspensions culture is that the complete volume of a cultivation vessel can be used to maintain the cells. By comparison to adherent cell culture this gains an improvement of approx. three orders of magnitudes. The price of a chemically-defined medium is higher than that of DMEM or a comparable medium. However, without the need for the supplement FCS and trypsin for cell detachment the costs are comparable. Additionally, through mass-production the price per litre for chemically-defined medium can be reduced. Nevertheless, the price of FCS is essential for this positive calculation in favour of the chemically-defined media. Only if the price for FCS remains at an elevated level can the chemically-defined media technology achieve a wide acceptance. The political initiatives to substitute FCS from *in vitro* technology are beneficial but their impact is not as strong as a financial incentive (Brindley et al., 2012).

5.5.2 Bioassays

The conducted bioassays show the compatibility of animal component-free chemically-defined media with mammalian liver cell lines. The adapted cells lines show various attributes of the adherent cells. The results in Figure 5.3 to Figure 5.7 show the concentration-response curves in the bioassays. All bioassays were conducted with an incubation time of 24 h as a prolonged incubation time of 48 h did not show any improved results for any cell lines (data not shown). Our newly adapted cells lines show results in the bioassay that are comparable to previously described cell lines and methods (Eichbaum et al., 2014; Hilscherova et al., 2000).

5.5.3 HEPG2-S – micro-EROD

For the HEPG2-S cell line we calculated a concentration-response curve with the assumption that the maximal response was reached at 10000 pM. These levels were shown for this cells line in literature (Anderson et al., 1995; Sato et al., 2010; Zeiger et al., 2001). The reported EC_{50} were in these studies between 680 pM and 1000 pM and were lower than the determined EC_{50} value of 1254 pM for our cell line (Anderson et al., 1995; Sato et al., 2010; Zeiger et al., 2001). For an analytical use of these cells lines a complete concentration-response curve of a standard substance like TCDD is mandatory to calculate bioanalytical equivalents (BEQs) (Kojima et al., 2015; Thiem and Boehmler, 2011a; Villeneuve et al., 2000). As a plateau is not depicted in Figure 5.3, the EC_{50} value could misinterpret the sensitivity of the cell line (Villeneuve et al., 2000). We have chosen to compare the cell lines according to their EC_{25} value as this value is

more robust than the EC_{50} especially, if the dose-response curves might not be complete (Eichbaum et al., 2014; Villeneuve et al., 2000).The comparison of the HEPG2-S cell line to the other cells shows with an EC_{25} value of 518 pM that this cell line is one magnitude less sensitive to TCDD than the H4IIE-S and H4IIE-luc-S cells (Anderson et al., 1995; Eichbaum et al., 2014; Thiem et al., 2014; Zeiger et al., 2001). This difference of sensitivity holds also true for the adherent HEPG2 cell line.

5.5.4 H4IIE-luc-S Luciferase & micro-EROD

In the luciferase bioassay the H4IIE-luc-S cells showed an EC_{25} value of 13 pM TCDD (Figure 5.4). However, with an increasing passage number the sensitivity to TCDD for the cell line declined. In Figure 5.5 the sensitivity of the H4IIE-luc-S cell line to TCDD is presented for the luciferase and as a control for the micro-EROD bioassay. This figure shows that the genetically introduced dioxin response elements and the luciferase gene responsible for the reaction of the cells are downregulated or silenced by prolonged cultivation as a suspension cell culture. The treatment with 5-azacytidine was conducted to remove methyl groups from GC rich DNA regions in close connection to these genes and hence remove silencing. As a result the sensitivity to TCDD increased approx. 3-fold compared to the control and the EC_{25} value recovered to approx. 87 pM TCDD. However, this is approx. 7-fold less sensitive than the initial value. Any other luciferase bioassay with these cell lines shows even less sensitive EC_{25} values. Furthermore, the sensitivity of the cell line could not be recovered with the 5-azacytidine treatment as through prolonged cultivation the EC_{25} value declined. This behaviour is known in literature (Chiang et al., 2015; van der Burg et al., 2010). A solution for this problem is to limit the passage number to 40 or 50 passages for the CALUX protocols (Pieterse et al., 2013; van der Burg et al., 2010). A similar behaviour showed the cell line in the micro-EROD bioassay. The sensitivity decreased approx. 12-fold compared to the initial value of 41 pM (Figure 5.4). After treatment with 5-azacytidine the sensitivity was restored to the initial levels but not for a prolonged number of passages (Figure 5.5). After a few passages the sensitivity was reduced to the initial levels of this test series with an EC_{25} value of 421 pM TCDD. We concluded, that to maintain a high sensitivity of this cell line a recurring 5-azacytidine treatment would be necessary as the genetic sequence of dioxin response elements were methylated and silenced. Alternatively, a limitation of the passage number, as recommended for the CALUX cell lines, should be implemented. In summary, the H4IIE-luc-S cell line showed no stable and prolonged sensitivity to dioxin-like compounds. Hence, we concentrated on the more promising

H4IIE-S cell line as this cell line did not show any decrease of sensitivity in the course of passages.

5.5.5 H4IIE-S – micro-EROD

The H4IIE-S cell line showed an EC_{25} value of 5 pM for TCDD in the micro-EROD bioassay that was comparable to the H4IIE-luc-S cells in the luciferase bioassay (Figure 5.7). This sensitivity is also comparable to values reported in the literature for this cells line (Eichbaum et al., 2014). Bioassays in the 96-well plate format presented in this publication showed EC_{50} values ranging from 5 pM to 64 pM TCDD. The most sensitive bioassay with H4IIE cells is approx. 6-fold more sensitive than the initial EC_{50} values (30 pM) of the H4IIE-S cell line. By optimizing the chemically defined medium composition for the H4IIE-S cells a more sensitive reaction was developed. To achieve this goal various medium additives were investigated to improve the sensitivity of the H4IIE-S cell line (data not shown). The addition of insulin to the medium resulted in a 3-fold increase in sensitivity. After optimization the cells showed an EC_{50} value of 11 pM TCDD after incubation for 24 h. This exceeds the results from Murk et al. (1996) and Sanderson et al. (1996) for adherent H4IIE cells that showed an EC_{50} value of 16 pM and 20 pM TCDD after an incubation time of 48 h and 72 h, respectively. Thiem et al. (2014) and Behnisch et al. (2002) showed for the same cells an EC_{50} value of 5 pM TCDD after an incubation time of 72 h. These cells represent one of the most sensitive analytic cell lines for dioxin-like compounds (Eichbaum et al., 2014). Only the genetically modified DR-EcoScreen cells are more sensitive with an EC_{50} value of 2.8 pM TCDD and an incubation time of 24 h (Kojima et al., 2015). To sum up the newly developed H4IIE-S cells are highly comparable to established methods with the additional benefits of easier handling, improved reproducibility, short incubation time and cost-effectiveness.

5.5.6 Evaluation of polystyrene and polypropylene as well plate material for bioassays

The evaluation of the two cell culture plate materials with H4IIE-S cells in the micro-EROD bioassay showed that material compositions are important for comparable results. The results of the bioassay differed in the two plate materials. Bioassays conducted in plates manufactured from polypropylene showed a shifted dose response curve compared to polystyrene plates and the EC_{25} value for TCDD was approx. 36-fold less sensitive. The other compound tested, β-naphthoflavone, showed the opposite behaviour. For β-naphthoflavone the polypropylene plates were more suitable and resulted in approx. 7-fold more sensitive EC_{25} values. An explanation for these behaviours can be the sorption of the compounds of interest to the

materials. This aspect has been investigated in literature for various plastics materials (Cseh et al., 1989; Goebel-Stengel et al., 2011; Pascall et al., 2005; Teuten et al., 2009; Wielgosinski, 2010). As described by Pascall et al. (2005) several factors influence the uptake like (1) the physical and chemical nature of the sorbent, (2) the physical and chemical nature of the sorbate, (3) the sorbate concentration in contact with the sorbent phase, (4) the characteristics of the phase in contact with the adsorbent, (5) the environmental temperature, and (6) the contact time of the system. In our study, TCDD and β-naphthoflavone represent hydrophobic compounds with a *log* K_{OW} of 6.8 and 4.7, respectively. Hence, both tend to adsorb to organic surfaces. Their different behaviour can be explained by the structural differences of the plate materials and compounds. Polypropylene (PP) is formed by a matrix that only contains a hydrocarbon framework which results in a highly hydrophobic material. It interacts with other compounds only *via* van-der-Waals forces. Polystyrene (PS) is composed of a hydrocarbon framework and aromatic rings which make it highly hydrophobic, too. It interacts with compounds *via* van-der-Waals forces and donor-acceptor interactions between the π-bonds of the aromatic groups of PS. The polymeric backbone of the styrene polymer has a benzene molecule in place of hydrogen. As a result, segmental mobility within the polystyrene chains is restricted and the presence of benzene increases the distance between adjacent polymeric chains. The greater the segmental mobility and the greater the distance between the polymeric chains, the easier it is for a diffusing chemical to transverse the matrix of a given polymer (all other factors being constant) (Pascall et al., 2005). In a study by Cseh et al. (1989) the adsorption and desorption of a polychlorinated biphenyls mixture (PCBs) Aroclor 1254 was investigated for various polymers including polypropylene. After an incubation time of 24 h, polypropylene adsorbed 82 % of the initial Aroclor 1254 concentration. Furthermore, a patent and further research papers describe the application of PP as sorbents for dioxins or other hydrophobic organic pollutants (Kreisz et al., 2000; Lee et al., 2004; Teuten et al., 2009; Wielgosinski, 2010). In another study by Pascall et al. (2005) the behaviour of PCBs was investigated to polymers including polystyrene. This material showed a selective behaviour: the uptake decreased from tri to penta congeners, but showed an increase for the hexa congeners, and then a decrease of uptake until the deca-chlorinated congeners. PS removed the higher chlorinated congeners more efficiently that the lower chlorinated analogues (Pascall et al., 2005). As the chemical structure and the *log* K_{OW} of PCBs are similar to the investigated compounds the adsorption effects should be comparable. In summary, for TCDD the polypropylene plates and for β-naphthoflavone the polypropylene plates are more suitable for bioassays. Additionally, it has to be mentioned that polypropylene is more resistant to solvents. Therefore, for application that

requires solvent-resistance a substitution to polystyrene is not feasible and alternatives such as glass plates or glass-coated well plates should be considered.

5.5.7 Benefits of bioassays in chemically defined media and cells in suspension

The implementation of a chemically-defined medium in analytical *in vitro* bioassays results in many benefits. One of them is that the serum components do not interfere with the compounds of interest. In a study by Hestermann et al. (2000) it was shown that the presence of serum led to a reduced bioavailability of TCDD. The EC_{50} value was reduced 20-fold in the presence of 10 % FCS compared to cells assayed without serum. However, the relative potencies within the same assay were not changed for various compounds. The conclusion was that the medium composition and especially the concentration of FCS leads to artificial differences between bioassays if they differ in this aspect (Hestermann et al., 2000). Another benefit of a serum-free chemically-defined medium in analytical bioassays is the possibility to conduct innovative studies that were not feasible before. The chemically-defined medium allows to investigate metabolites in the supernatant of the cells (Dietmair et al., 2012; Issaq et al., 2002). Compounds can be monitored more easily through instrumental analyses as no undefined background of serum components is present (Issaq et al., 2002). A further improvement results from the culturing in suspension. This culturing condition allows for automated cell maintenance. With the application of a liquid handling robot it is possible to monitor the growth rate and viability of the cells online as well as to conduct the cell maintenance by transferring and diluting the cells with medium. The components necessary are a liquid handling robot with a cell counting add-on, an incubator, a shaker and medium. With classic adherent cell systems an automated system requires additional elements and the complexity is higher as an additional detachment of the cells from the bottom of the cultivation flask is necessary. Therefore, our system should be much more cost-effective in these applications. Beyond an automated maintenance of the cells it is possible to implement an automated procedure to distribute the cells on a plate in which samples were prepared manually. By using analytic cells in suspensions it is possible to implement cost-effective fully automated systems that incorporate the culturing of cells, sample preparation, distribution of cells on the prepared samples, bioassay incubation and evaluation in one system. One element that can improve this system and reduce cost is the substitution to a CO_2-feed free incubation system. As the incubation time of 24 h in the bioassays is short, it will be evaluated if a CO_2 free incubation is feasible. A preferred approach is the implementation of an artificial source of CO_2 like 2-[4-(2-hydroxyethyl)piperazin-1-yl]ethanesulfonic acid (HEPES). Experiments are planned to

verify its performance. This improvement would allow to conduct the bioassay without the need for an incubator and finally reduce the cost for this system further. The main benefit of this system is the reduction of laborious steps. With these automation steps the time necessary for a skilled technician to perform this bioassays can be reduced by half or more as the working steps are reduced to the preparation, dilution of sample and reagents. This improvement gains significant monetary benefits as manual work is very cost-intensive.

This system can be combined with instrumental analyses like high performance liquid chromatography (HPLC) to analyse and fractionate a sample. In combination with an HPLC system with a fraction collector our serum-free suspension bioassays can be applied onto the samples with minimal sample pre-treatment. As a proof-of-concept our group conducted a study with an environmental sample that was extracted by pressurized solvent extraction (PSE) and fractionated by means of HPLC into a 96-well polypropylene plate (Xiao et al., 2016). The polypropylene material was chosen as it is more solvent resistant than polystyrene. After solvent removal by nitrogen flow only the sample compounds remained. Following, the micro-EROD bioassay with H4IIE-S cells was conducted. This combined application of instrumental analysis and fractionation with bioassays has already been conducted (Suzuki et al., 2004; Suzuki et al., 2006). The benefit of our system is streamlining of this process. The fractionation is conducted directly into the assay plate which results in less handling steps. With this integrated approach an effect directed analysis (EDA) is accelerated and its cost reduced. In our study the use of polypropylene as plate material showed to be problematic as some compounds of interest adsorbed onto this material (Figure 5.7). Therefore a study with glass coated polypropylene microplates is planned to verify it as an alternative material.

5.6. Conclusion

Our study shows the possibilities and benefits of implementing animal component-free chemically-defined media in diagnostic/analytic *in vitro* bioassays with the additional feature of a continuous suspension cell culture. This feature enables results with many practical benefits. First, it enables an easier maintenance of the cell culture by reducing manipulation steps needed which consequently reduces the sources of contamination. Consequently, it results also in a cost-reduction for the bioassays. Additionally, it allows for new applications and modifications of the bioassays. These systems can easily be implemented into an automated system, combined with instrumental analyses and implemented as high-throughput systems. Moreover, by removal of serum for the culturing medium it is easier to conduct metabolism studies as an undefined background and adsorption to serum components is removed. This

system with cells in an animal component-free chemically-defined medium and cultured in suspension has the prospect to advance analytical *in vitro* bioassays onto a new level as a complete animal alternative with miscellaneous applications.

Acknowledgements

We would like to thank Dr. Ines Thiem from the Lower Saxony State Office for Consumer Protection and Food Safety for their development of the micro-EROD protocol for the adherent H4IIE-S cells. Additionally, we would like to thank her for the provision of the H4IIE cells. The authors would like to acknowledge the federal office of Consumer Protection and Food Safety (BVL) for their support in this project. Furthermore, we would like Prof. Dr. John P. Giesy for the generous provision of the H4IIE-luc cells.

Chapter 6
Discussion

6.1. Introduction

In this thesis different aspects of environmental toxicity have been investigated. On the one hand the toxicity of a newly developed nanoscale zero-valent iron flakes for groundwater remediation. It has been investigated in its pristine with batch and column experiments as well as in an aged state with an ecotoxicological test battery including the acute Daphnia immobilization test, algae growth inhibition test, fish embryo toxicity test (FET) and the Ames fluctuation test (Chapter 3). Additionally, in this chapter the nanomaterial has been characterized with various material analysis techniques like DLS, TEM with EDX, and XRD which gave further insight into the morphology and composition of the material. The generation of ROS was investigated with a cell-free assay. On the other hand *in vitro* bioassays were developed. This technology is aims to substitute animal experiments with cell based test systems. It is the next step in the process of obtain an improved chemical safety. These cells derived from different species and organs can under favourable conditions maintain their unique properties and can be applied as effect-based tools (Wernersson et al., 2015). Through their size and rapid reaction time *in vitro* systems are an excellent tool to reduce animal tests or aid in the process of pre-screening of compounds. In a recent study by Escher et al. (2014) bioassays were used to monitor 18 different modes of action for complex mixtures in recycled water. This showed how many *in vitro* bioassays are already available and a trend can be deducted that the number is increasing. In chapter 4 of this thesis a protocol for the micro-EROD bioassay with H4IIe cells to monitor dioxins and dioxin-like compounds at the picomolar level has been presented (Schiwy et al., 2015a). The bioassays protocol presented can be applied to investigate various environmental samples. It is performed with a license free cell line and can be performed with moderate experience. Additionally, in chapter 4 new analytic cell lines have been developed to investigate dioxin-like activity in environmental samples. Evolving the analytic *in vitro* technology the adaptation of adherent analytic cells lines to suspension culturing conditions and chemically defined animal component free media has been has been developed. The advantages of this development are a higher throughput, reduced handling steps and the independence of FCS as a media supplement. Hence, with the *in vitro* technology in the upcoming future a replacement of animal test by *in vitro* bioassay or at least their reduction is feasible. Therefore, we decided to apply *in vitro* bioassays to evaluate the NAPASAN NZVI as a nanoremediation tool in co-exposure with an organic dioxin-like active compound. This chapter is here to unify the various aspects of nanotechnology and *in vitro* bioassays. In literature these two technologies have been combined to investigate nanomaterials toxicity (directly) and the effects of nanomaterials on model compounds (indirectly). Studies with *in*

vitro bioassays have been conducted to detect direct toxic effects of NZVI on the cellular level (Auffan et al., 2006; Li et al., 2010; Macé et al., 2006; Sun et al., 2015). However, the application of *in vitro* studies to investigate nanomaterials has been discussed critically in literature as the dosimetry for this system and the translation to *in vivo* results are challenging (Cohen et al., 2014; Hussain et al., 2015). The effective concentration that causes the effects is not comparable to the introduced concentration in the exposure media as many processes influence the transport of the nanomaterial to the cells (Cohen et al., 2014; DeLoid et al., 2014). Medium components like albumins originating from FCS were identified as a source of uncertainty (Schulze et al., 2008). These proteins have an influence on the stability of nanomaterials in the cells systems. Particles that agglomerate and sediment in media consisting of salts show a different behaviour in cell culture media supplemented with serum. In serum containing systems nanomaterials were more stable (Cohen et al., 2013; Schulze et al., 2008) Additionally, albumins can bind nanomaterials and act as vehicles to deliver them into the cells (Elzoghby et al., 2012). These various interactions have to be accounted for to determine the active concentration of nanomaterials in cell based systems and make dosimetry challenging. However, studies like from Cohen et al. (2014) propose alternatives. This approach could not be applied to this study as through the manufacturing process by milling for the NAPASAN NZVI no uniform product could be obtained and hence no dispersion characteristics could be determined.

The indirect effects of nanomaterials in co-exposure with model compounds or environmental pollutants have also been assessed by *in vitro* techniques (Hernandez-Moreno et al., 2016; Jarošová et al., 2015; Lammel et al., 2015; Li et al., 2015; Simon et al., 2014b; Vannuccini et al., 2015; Yu et al., 2015). In these studies bioassays have not been applied to directly measure the toxicity of a nanomaterial but to assess the effect of the nanomaterial on a model compound. These studies have investigated the nanomaterial, the model compound and the combination of both. This approach was applied also in this thesis. The NZVI developed in the NAPASAN project as a remediation tool has been applied to the model compound acridine. It is a heterocyclic PAH that occurs at creosote contaminated sites and can be distributed into groundwater (Blum et al., 2011). As reported in literature this compound elucidates aquatic toxicity and dioxin-like activity (Hinger et al., 2011; Peddinghaus et al., 2012). NZVI have been propose as a technology to remediate heterocyclic PAHs (Gosu and Gurjar, 2013).

6.2. Co-exposure of acridine with NZVI

The co-exposure of NZVI and acridine was investigated to elucidate the remediation efficiency of this approach. To elucidate the effects an organism based fish embryo toxicity test as well as the cell based micro-EROD bioassays with H4IIe cells (cf. Chapter 4) have been applied.

6.2.1 Acridine and NZVI in the FET bioassay complemented by HPLC analysis

The FET was complemented with high pressure liquid chromatography (HPLC) to monitor the concentration of acridine sampled direct for the medium according the method by Mundt and Hollender (2005). In preliminary experiments a reference concentration series of acridine has been investigated and a limit of detection (LOD) and limit of quantification (LOQ) were determined for the HPLC system with values of 0.01 mg/L and 0.04 mg/L (Figure 6.1), respectively. The concentrations series of acridine showed a good linearity up to a concentration of 2.5 mg/L. In comparison to the study by Mundt and Hollender (2005) the limit of detection was not as sensitive (0.0 µg/L). However, it was more than sufficient for our investigations in a range of interest between 0.1 mg/L and 2 mg/L.

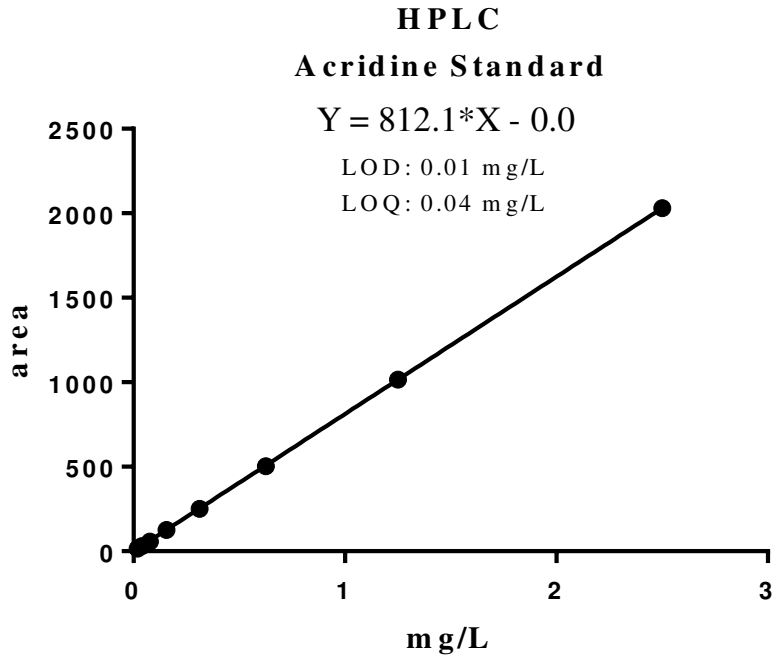

Figure 6.1: HPLC – Standard curve for acridine determined from 0.08, 0.04, 0.02, 0.16, 0.31, 0.63, 1.25 and 2.50 mg/L. LOD: limit of detection; LOQ: limit of quantification

Furthermore, the suitability of polystyrene or fused quartz glass as a vessel material for the exposure of fish embryos and cells with acridine have been investigated. In both vessel materials the acridine concentration declined over time. After 96 h the initial concentration was

reduced about 25 % in fused quartz glass and 28 % in polystyrene, respectively (data not shown). As the difference was minor we concluded that these two materials do not have an influence on the concentration of acridine. Therefore, all experiments were conducted in polystyrene plastic material which was beneficial for the cell culture.

To investigate the interaction of the NZVI nanomaterial with the organic pollutant the non-toxic or low toxic NZVI concentrations of 10 mg/L (EC_0) and 100 mg/L (approx. EC_6) have been chosen (Figure 3.15). Preliminary test with acridine showed an EC_{50} value of 1.3 mg/L acridine (Figure 6.2) which is approx. 2-fold higher than reported in the study by Peddinghaus et al. (2012) of 0.7 mg/L. However, in combination with the HPLC analysis this value had to be corrected. The actual concentration measured after 24 h was 1 mg/L. Within this timeframe the total toxicity was detected and a prolonged incubation did not result in an increased toxicity. Hence, the toxicity of acridine is narcotic. The remaining difference in the determined values could result from different strains of *Danio rerio* utilized. The fish strain in this study originated from the Frauenhofer Institute in Schmallenberg, Germany whereas the study by Peddinghaus et al. (2012) investigated acridine with a *Danio rerio* strain obtained from the Environmental protection agency (UBA) in Germany. However, it has to be added that this FET test system like all bioassays has some intrinsic variability. It is estimated to be approx. 30 % variance which results in negligible differences between the two studies (Belanger et al., 2012).

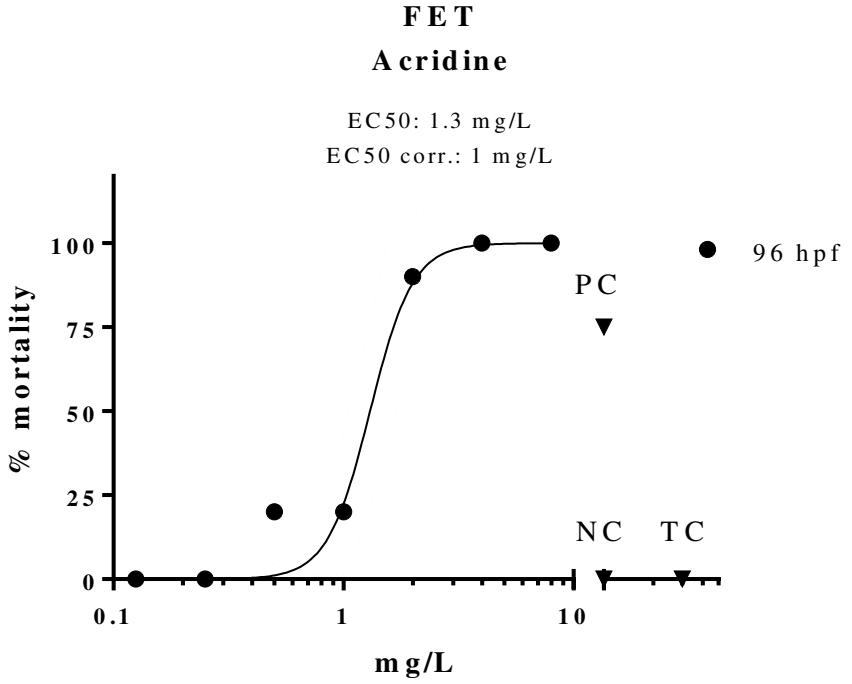

Figure 6.2: Fish embryo toxicity - Percentage mortality of zebrafish (*Danio rerio*) embryos after exposure to acridine at concentrations of 0.13, 0.25, 0.5, 1, 2, 4 and 8 mg/L at 96 hpf. The 95 % confidence interval is indicated (dashed lines). NC: negative control; PC: positive control; TC: treatment control

The EC_{50} value of 1.3 mg/L has been applied as the reference concentration to investigate the effects of the two non-toxic NZVI concentrations of 10 mg/L and 100 mg/L. The co-exposure of 1.3 mg/L acridine and 10 mg/L or 100 mg/L NZVI did not show any correlations in the FET assay (data not shown). One experiment showed a decline of toxicity for the setup with 100 mg/L NZVI and acridine. The mortality was reduced at this concentration to a level comparable to the negative control. In the same experiment the setup with 10 mg/L presented 40 % mortality. Hence, the higher NZVI concentration resulted in a reduction of toxicity and the lower concentration was not sufficient to have any effects. In a follow up experiment both concentrations of NZVI did not show any reducing effect on the toxicity of acridine. On the opposite, both experimental treatments showed a very high mortality of 100 %. The last experiment with the same setup showed 30 % mortality for 10 mg/L NZVI and 80 % mortality for 100 mg/L NZVI after 96 h. Hence, every possible effect of NZVI is represented in the experiments. The first represents a reducing effect of NZVI on the toxicity of acridine. The second and third show either no effect of NZVI on acridine or that NZVI is a vehicle to increase toxicity. The combination with instrumental analysis was able to shed some light on the results. It showed that both NZVI treatments did not have a reducing effect on the acridine concentration. The reduction detected was comparable to the spontaneous reduction without

NZVI. Only the second experiment showed an increased reduction of acridine (>46 %) for both NZVI concentrations. However, in this experiment the mortality for both NZVI concentration was at 100 % mortality which excludes any toxicity reducing effects. This comparable high loss of acridine could be a result of a sampling error or problems during the HPLC analysis. We concluded that NZVI in the FET system has no reducing effects on the toxicity of acridine and all effects reported for the FET are within its natural variability to acridine. However, in comparable studies like the study by Gosu and Gurjar (2013) the hetero-PAHs quinolone was successfully reduced with NZVI at similar concentrations like in our study. In another study by Chang et al. (2005) a hetero-PAH pyrene treated with ZVI and NZVI showed reduced concentrations after a reaction time of 60 minutes in contaminated soil. Thus, the NZVI are suitable to remediate the hetero-PAHs and that in an aquatic environment the interaction of NZVI and a hetero-PAH should be rapid as the pollutant is solved in the medium and comes into direct contact with the remediating agent. A possible explanation for the lack of effect on acridine in our study could be that the NZVI oxidized too rapidly under aerobic conditions of the FET and lost all its remediating activity (Jiang et al., 2015). However, an x-ray diffractometry (XRD) analysis showed an alpha-iron content of 81 % for the applied NZVI. This discrepancy can be explained by the fact that the passivating layer around the NZVI is only a few nanometres thick and was not detected with the XRD (Kumar et al., 2014a). As the financial possibilities were scare in the project further investigation could not be conducted to elucidate the reason for the deviation with the former studies. In a follow up study the interaction of acridine with a pristine or additionally coated NZVI should be investigated to elucidate the impact of passivation on the reaction.

6.2.2 Acridine and NZVI in the micro-EROD bioassay

The second aim of this investigation was suitability of cell based bioassays to monitor organic pollutants in interaction with nanomaterials. The cell based micro-EROD bioassays was evaluated as a tool to gain further insight about the dioxin-like activities of the hetero-PAH acridine. The improved micro-EROD bioassay was applied to investigate acridine alone and in interaction with NZVI. This indirect approach was chosen as bioassays can monitor various compounds with comparable or even exceeding instrumental analysis sensitivity. Additionally, bioassays provide insight about the mode of action in contrast to instrumental analysis which is applied for monitoring of predefined compounds.

The results of the micro-EROD bioassay showed no dioxin-like activity for acridine up to a concentration of 2.5 mg/L. At this concentration cytotoxicity was detected by investigating the

cells with light microscopy. In the study by Hinger et al. (2011) acridine was reported to show dioxin-like activity but only in one of the two applied bioassay. The RTL-W1 assay did not show any dioxin-like toxicity whereas the DR-CALUX® reported an EC_{25} value of 1.72 mg/L. The difference between these two *in vitro* bioassays (RTL-W1 vs. DR-CALUX®) is explained in the study by Hinger et al. (2011) through different receptor affinities for the compound. However, the micro-EROD and the DR-CALUX® bioassay apply both the rat cell line H4IIE. The micro-EROD bioassay used in this study investigates the dioxin-like activity with the wild-type intrinsic rat aryl hydrocarbon receptor (AhR) and the EROD enzyme as the reporter element (Tillitt et al., 1991a; Tillitt et al., 1991b). In contrast to this the DR-CALUX® bioassays uses a genetically modified H4IIE cell line with a pGudLuc1.1 receptor construct that has luciferase as its final reporter element (Aarts et al., 1995; Garrison et al., 1996; Sonneveld et al., 2007). Thus, the difference of these two reporter elements could the source of different results for the dioxin-like activity of acridine (Giesy and Kannan, 1998; Jamsa et al., 2001; Van den Berg et al., 2006; van den Berg et al., 2013). The EROD pathway could be influence by acridine not only by binding to the AhR but also to the EROD enzyme itself. This effect was shown for different halogenated aromatic compounds (Chen and Bunce, 2004). Hence, not displaying the dioxin-like potential of acridine. This effect is circumvent in the DR-CALUX® as the luciferase enzyme does not interact with these compounds (Eichbaum et al., 2014). As no dioxin-like activity could be detected the effect of NZVI on acridine could also not be evaluated. However, due to the results from the FET it can be assumed the NZVI would show similar results in the cell based bioassay and no reduction of acridine toxicity would be recorded. By comparison of the bioassays with instrumental analysis the bioassays were not detecting acridine or showed a limit of quantification of approx. 0.32 mg/L (Hinger et al., 2011) which is 10-fold lower when compared to the limit of quantification of 0.04 mg/L (Figure 6.1) for the instrumental analysis. This is contradicting the statement that bioassays are comparable sensitive to instrumental analysis. However, it has to be verified on a case by case basis. In this case acridine seems like a weak agonist of the AhR receptor and through its structure (Figure 1.6) well detectable with a diode array detector. Other compounds like TCDD are stronger agonists and have a limit of detection in the micro-EROD bioassay of 0.78 ng/L (Eichbaum et al., 2014). Therefore, in a follow up study, another organic pollutant to circumvent the substrate inhibition and an improved NZVI that remains its remediation potential in the aquatic environment should be investigated. Therefore, PCB-126 or TCDD should be applied as model compounds. Alternatively, an investigation with *beta*-naphthoflavone and the serum-free suspension bioassays could be applied (cf. Chapter 5). This experimental setup could result in

a better mixing of the NZVI with the organic pollutant of interest and a reduced interaction of the NZVI with albumins originating in FCS. Furthermore, a combined approach with analytic cell based bioassays and an effect directed analysis could be applied. Instead of using mono substances environmental groundwater samples could be investigated. By fractionating and analysing by HPLC for example according the hydrophobicity of the compounds present in the groundwater sample a comprehensive view on the contaminant situation and the remediation efficiency can be achieved. The fractions collected into 96-well plates could be investigated with the newly developed cell lines (cf. Chapter 5) directly after evaporation of the solvent. Especially, as the new cell lines do not require adherence solvent resistant plate materials can be applied. A publication discussion this approach is under preparation and will be published by Xiao et al. (2016). The benefits of such a strategy are on the one hand the dioxin-like activity of the groundwater sample can be monitored if the nanoremediation was successful. On the other hand the remaining dioxin-like active compounds can be elucidated by fractionating the groundwater sample. With this information appropriate methods can be applied to reduce the remaining dioxin-like acting compounds whether by injecting additional NZVI or applying another remediation technology. Summarizing, bioassays are a useful tool to detect and quantify environmental pollutants as they represent biological pathways. With the development of modern tools like the serum-free and suspensions cultivation of analytical cells new applications can be obtained for this technology as it is efficient, cost-effective and flexible.

Chapter 7
Conclusion

Within this thesis various aspects of nanotoxicology have been investigated and a characterization of the nanomaterial was conducted. The material composition of the aged NZI was determined by a XRD measurement (Chapter 3). However, the result for the aged NZVI nanomaterial was unexpected as only alpha-iron and gamma-iron could be detected for an aged sample. No iron oxides could be detected with this techniques. Here further investigation would benefit a comprehensive view. However, due to limited founding of the project no further investigation could be performed. Additional investigations could have gain more insight about the material composition of the aged NVZI nanomaterial. Especially, the fact that only two iron phases were detected in the XRD is not plausible as iron oxides are expected to be present. However, as presented before the oxide layer could be too thin to be detected by the XRD measurement. Therefore, Mössbauer spectroscopy could be applied to elucidate the presence of it. This aspect is of importance as it could explain the observed oxygen depletion in the Daphnia acute immobilization test with aged NZVI (cf. Figure 3.14). Furthermore, investigation could have been conducted to elucidate the presence of solved iron species in the media. As shown in literature these iron ions can elucidate toxicity and Fe(II) is the most toxic. The presence of these ions could have been detected with a photometric method with ferrozine or phenanthroline. However, its presence in the aquatic systems is not long as it reacts with the components of the system. By adding hydrochloric acid to the sample and hence reducing the pH below 4 this reactions are stopped and the Fe(II) remains in the system for a prolonged time and could be measured.

As for the material morphology of the aged nanomaterial various techniques have been applied to elucidate it (Chapter 2 & 3). The TEM investigation in combination with EDX gave an insight to the morphology of the nanomaterial. It presented an inhomogeneous particle morphology and size composition. Especially, a tiling experiment help to elucidate that the nanomaterial is very thin with a particles thickness below 100 nm. This is a result of the milling process. Therefore, the NZVI nanomaterial has been named NVZI flakes. This morphology proved to be even beneficial in the experiments conducted within the NAPASAN consortium. Through their morphology the flakes could be further transported in a 2-D column than spherical NZVI materials. The understanding of the morphology helped to understand the results obtained with the DLS technique. This ready-to-use method and is less costly than a TEM instrument. It can give insight into a wide particle size range and report their hydrodynamic diameters and zeta-potential. However, it has some prerequisites for a successful measurement that could not be met with the aged NVZI nanomaterial. The most important one is a uniform particles, preferentially monomodal, size distribution. It could not be met as shown with the TEM

investigations. These two techniques, TEM and DLS, complement each other. However, in the case of the aged NZVI the DLS did not give any useful input. With a nanomaterial with a size exclusive manufacturing method that results in a homogenous spherical particle with an uniform size range the DLS technique would presents it strengths. The main benefit is it moderate costs and immediate measurement technique. In comparison the TEM technique is elaborate and requires expensive instruments which results in high costs.

The next element investigated concerning the NZVI nanotoxicity was its mode of toxicity. The results from the cell-free ROS assay showed that the ROS release from the aged NZVI does not contribute significantly to the toxicity of the nanomaterial. The levels are very low and only at elevated concentrations ROS levels higher than the treatment control could be recorded (Figure 3.11; 450 mg/L and 1000 mg/L). The toxicity manifested at lower concentrations with an EC_{50} value of 163 mg/L in the acute Daphnia immobilization test. As the toxicity of the nanomaterial is low additional studies should focus to elucidate the main mode of toxicity. Different modes of toxicity like oxygen depletion and iron ions release have been proposed for iron nanomaterials. Therefore, investigations with the NZVI and iron salts could be conducted to account for iron ions specify toxicity.

However, the environmental relevance of this nanoremediation technology has taken into account. This is crucial to present the toxicity of the nanomaterial in comparison with other nanomaterials as well as with other organic environmental pollutants. As presented in chapter 2 and 3 the NZVI nanomaterial is applied for nanoremediation. For this special purpose it will be injected into the subsurface at high injection volumes and concentrations. However, this will be limited to already contaminated areas. A drift off of this nanomaterial is no probable as the mobility of this nanomaterial is limited (cf. Chapter 2). The presented toxicity investigations within this thesis applied concentrations up to 1 g/L of NZVI and hence exceed the recommended limit test concentrations of 100 mg/L for the OECD and DIN test guidelines. This was performed due to that during nanoremediation procedures concentrations of up to 20 g/L will be applied. Nevertheless, as described before only a small fraction of this concentration or no NZVI will reach the aquatic environment. Therefore, we have concluded in consideration of the anaerobic batch, anaerobic column experiments and the aerobic bioassay battery that this NZVI does not represent a hazard to the environment. Compared to other nanomaterials the toxicity of aged NZVI is comparable low with an EC_{50} value of 163 mg/L in the acute Daphnia immobilization test which is comparable to other studies with aged NZVI. Additionally, studies with nanoscale iron oxides showed a comparable toxicity to the aged NZVI. The reported EC_{50} value for coated iron oxides nanomaterials to *Daphnia magna* vary

between a not detected EC_{50} value in the concentration range up to 100 mg/L and EC_{50} values in the range between 30 mg/L and >100 mg/L (Baumann et al., 2014; Filser et al., 2013). For carbon nanotubes (CNTs) the literature does not present a consistent view on the toxicity of this nanomaterial. One study presented an EC_{50} value of 2 mg/L for CNTs (Edgington et al., 2010) whereas another reported no acute toxicity up to a concentration of 100 mg/L (Sohn et al., 2015). The studies by Wyrwoll et al. (2016) and Amiano et al. (2012) showed for nanoscale titanium dioxide that the toxicity can be influence by the surrounding conditions. Especially, the interaction with ultra violet (UV) light leads to a higher toxicity (Amiano et al., 2012; Wyrwoll et al., 2016). For this nanomaterial an EC_{50} value in the Daphnia acute test was reported in the range between 30 mg/L and 80 mg/L in dark conditions or laboratory light (Amiano et al., 2012; Wyrwoll et al., 2016). However, when UV light was added the toxicity increased in this test system and EC_{50} values of approx. 1 mg/L were reported (Amiano et al., 2012; Wyrwoll et al., 2016). Hence, the toxic potential to Daphnia is much lower for NZVI than for nanoscale titanium dioxide. At last, in comparison to nanoscale silver nanomaterials this low acute toxicity is even more evident as this nanomaterial showed an acute toxicity in the Daphnia test with an EC_{50} value of approx. 10 µg/L (Volker et al., 2013a). The study by Baumann et al. (2013) showed an EC_{50} value of approx. 35 µg/L for this nanomaterial. This is an up to 16000-fold higher toxicity than for the aged NZVI. Summarizing, the aged NZVI showed a comparable low toxicity even at elevated concentrations. Especially, as this material is designated for special remediation applications a low environmental hazard is to be expected for this new remediation tool.

In this thesis the development of a license free protocol for the determination of the CYP1A-inducing potential was presented. The procedure is very detailed and allows the protocol to be adapted to various sample types like single compounds and environmental samples. The main advantage of this protocol is that it is optimized to be cost effective. Therefore, wild-type cells are used that provide for the measurement of the inducing potential their intrinsic NADPH. This reduces the assay cost as no additional NADPH as an energy source for the reaction is necessary. Additionally, the protocol is flexible as criteria are provided how to handle the results of outer wells. According to these criteria the user can decide whether to include or exclude the results (cf. Chapter 4). This element expands the available space on the well-plate and increases hence the throughput of this bioassays. The method is described in detail and includes many troubleshooting elements. Hence, it is a method that can be recommended for routine testing as well as single experiments.

The adaptation of analytical cell lines to serum-free media and suspension culturing conditions was another element of this thesis. It was success full for cell lines like the HEPG2 that were presented in literature to be problematic to adapt to this conditions (Biaggio et al., 2015). This development allows for various new applications of bioassays. It causes economic benefits as it allows to cultivate the cells with a highly reduced maintenance as the cells are constantly in suspension the passaging requires just a dilution of the cells. Moreover, through this mode of cultivation much higher cell densities are feasible as the growth is not limited to the surface but to the volume of the culturing vessel. Therefore, even continuous testing procedures are feasible with this technology. To achieve this the passaging would have to be automatized. An application would be to have a constant cell density on-hand maintained by an automatized cell counting and dilution system. This constant cell density could be applied for online measurements.

The evaluation of the analytical cell lines in serum-free medium and suspension cell culture showed that the newly developed cell lines are comparable to adherent cell lines. The EC_{50} value of 11 pM for the H4IIE-S cells is comparable to established adherent cell lines (Eichbaum et al., 2014). For the HEPG2-S cell the EC_{50} value of 1254 pM is approx. 1.5 to 2-fold less sensitive than the adherent cells but this bioassay has not been optimized like the H4IIE-S cell line. It is feasible to achieve with this cell line also the higher sensitivity in suspension. However, as it is not as sensitive as the H4IIE-S cells this optimization has not been conducted in this thesis and should be performed in a follow-up study. As for the genetically modified H4IIE.Luc-S cells the transgenic element composed of dioxin response elements and the genetic information for luciferase was silenced by methylation during the cultivation in suspensions. Hence, the cells were less sensitive than the adherent version of this cell line. A treatment with an agent that demethylated the DNA could reserve this silencing effect (Jones and Takai, 2001). However, after a few passages without the treatment the transgenic DNA element was silenced again. This is an interesting effect that should be further investigated in a follow-up study.

The investigations in combination between NZVI and acridine showed that within this setup the NZVI did not show any effects on the model compound acridine. For this experiments the instrumental analysis was crucial as it could give insight about the concentrations within the fish embryo toxicity test (Mundt and Hollender, 2005; Peddinghaus et al., 2012). It could be elucidated that the concentration of acridine was not affected by the treatment with NZVI. Additionally, the dioxin-like activity of acridine could not be detected with the micro-EROD bioassays. Hence, the two elements of acridine reduction by NZVI and its detection with an *in*

vitro bioassays were not successful. For a follow up study a more readily reducible model compound or a stronger reducing agent should be used. Bimetallic (iron and palladium) nanomaterial could be applied as they showed to be even more reactive than NZVI (Hildebrand et al., 2009). Otherwise, a treatment of the NZVI could be applied to obtain as much as possible of the reactive material by thoroughly washing of the nanomaterial under anaerobic conditions. This procedure could remove the additive MEG and result in a higher reactive surface. Nevertheless, the application of a dioxin-like activity monitoring *in vitro* bioassay to elucidate the remediation efficiency was not successful. The dioxin-like activity of the model compound acridine could not be elucidated. Therefore, another compound should be applied as the model groundwater pollutant. Possible candidate substances are PAHs or β-naphthoflavone or TCDD as they are stronger CYP1-inducer. Nevertheless, *in vitro* bioassays can be applied as monitoring tools for remediation applications. Especially, for effect directed analysis *in vitro* bioassays are suitable to elucidate the fraction with a specific toxicity (Xiao et al., 2016). Therefore, the newly developed cell lines in suspension should be used to investigate extracts and fraction of extracts of environmental samples. For a remediation applications this technology could assist in the characterization of a potentially contaminated site. It could be applied to determine the toxic fractions and thus to elucidate the toxic compounds. With this knowledge the optimal remediation technique can be planed.

Danksagung

„Es reicht das kurze Wort „Danke!“, um anderen Menschen ein Lächeln zu schenken“

Mit diesen Zeilen möchte ich all den Personen danken, die mich während der Zeit meiner Promotion begleitet haben. Es war eine spannende und ereignisreiche Zeit. Seit dem Jahr 2009 bin ich am Institut für Umweltforschung involviert und konnte dort eine tolle Zeit meines Studiums wie auch meines Privatlebens erfahren. Ich traf dort tolle Wissenschaftler, Kollegen, Freunde und meine Liebe. Deshalb möchte ich Ihnen aus ganzen Herzen danken.

Zuerst möchte ich Prof. Dr. Henner Hollert, meinem Doktorvater, für das Vertrauen mir vielfältige Aufgaben zu übertragen, danken. Ich konnte an ihnen wachsen und viel dazulernen. Besonders möchte ich für die gemeinsamen Dienstreisen wie auch Abende danken, bei denen nicht nur Wissenschaft gemacht wurde, sondern auch getanzt oder Karaoke gesunden wurde. Ich möchte Dir außerdem für Deine Unterstützung und Dein Verständnis danken besonders auf dem erlebnisreichen Weg der Familiengründung.

Prof. Dr. Andreas Schäffer danke ich für die Übernahme des Koreferats. Zudem danke ich für die Unterstützung durch die ich neue Türen geöffnet bekommen und neue Bekanntschaften gemacht habe.

Zu diesen Bekanntschaften zählen Prof. Rafal Dunin-Borokowski und Dr. Marc Heggen, mit denen eine tolle wissenschaftliche Zusammenarbeit entstanden ist. Mit Dr. Marc Heggen habe ich Stunden vor einem TEM gesessen und so faszinierende Einblicke in die Nano-Welt bekommen.

Dr. Hanna Maes möchte ich für die wissenschaftliche Zusammenarbeit als Arbeitsgruppenleiterin und die große Hilfe beim Schreiben und Reviewen von Papern danken.

Dr. Thomas-Benjamin Seiler möchte ich für das stets offene Ohr, die vielen Tipps und Ratschläge danken. An die Zeit im IT-Team werde ich mich gerne erinnern, als wir uns gemeinsam das Institut mit Spiceworks Tickets und Kaspersky unterstützt haben.

Den Kollegen vom Technologie Zentrum Wasser in Karlsruhe Prof. Andreas Tiehm, Dr. Kathrin Schmitt und Heico Schell möchte ich für die gute Zusammenarbeit im Projekt NAPASAN danken. Mein Dank gilt auch den weiteren Kollegen aus dem Verbundprojekt NAPASAN Prof. Martin Jekel, PhD Jürgen Braun, Dr. Norbert Klaas, Dr. Ralf Köber, Dr. Andre Kamptner, Silke Thümmler, Tessa Strutz, Andre Matheis, Hendrik Paar. Mit ihnen hatte ich tollen wissenschaftlichen Austausch und immer freundliche Begegnungen.

Ich danke Prof. Helge Stanjek für die herzliche und hilfsbereite Kooperation. Sie sind der Experte, der mir half die doch verworrene Welt des Eisens besser zu verstehen.

Meinen Freunden, Kollegen und Erfindungs-/Paper-partnern Dr. Markus Brinkmann und Dr. Beat Thalmann, danke ich für die tollen wissenschaftlichen Ideen und Träumereien, die wir verwirklichen konnten. Mit Euch kann man immer was erleben, ob auf Tagungen oder im Urlaub in Spanien, Italien oder in Deutschland.

Dr. Tilman Floehr möchte ich für die tolle Freundschaft und die stete Bereitschaft uns zu helfen danken. Du hast mir schon einen Anzug organisiert und so für mich Feuerwehr gespielt. Dafür möchte ich Dir vom ganzen Herzen danken.

Dr. Sibylle Maletz und Kerstin Bluhm danke ich für tolle Zeit, besonders danke ich euch für die herzliche Hilfe im privaten.

Meinen Container-Biologen Dr. Anne Simon, Dr. Anne Wyrwoll, Dr. Stefan Rhiem, Jochen Kuckelkorn, Julia Lörks und Matthias Findeiß danke ich für die gemeinsame „Sardinen-Zeit". Wir konnten auf engsten Raum zusammenarbeiten und privat gemeinsam kochen, Nikolaus-Schinkenwurst-Essen und uns gegenseitig unterstützen.

Dr. Christian Pfaff danke ich für die lustigen Augenblicke während der Doktorarbeit. Mit Dir konnte man immer einen neuen Blick auf die Dinge bekommen und auch wunderliche Sachen mit ihnen anstellen.

Den Abschlusskandidaten und UROP-Praktikanten M.Sc. Kerstin Winkens, M.Sc. Markus Kurth, M.Sc. Mirkko Flecken, M.Sc. Daniel Koske und M.Sc. Gunnar Lehmann, die ich in meiner Zeit im Institut auf ihrem Weg begleiten konnte. Danke für die vielen positiven gemeinsam Erfahrungen. Es hat Spaß gemacht euch etwas zu vermitteln und auch von euch etwas zu lernen.

Meinem besten Freund Dr. Sung Han danke ich für das immer offene Ohr und die Worte der Ermutigung. Ich bin so froh so einen Seelenverwandten wie Dich gefunden zu haben.

Meiner Familie danke ich für die wunderbare und vom Herzen kommende Unterstützung. Ihr seid eine Stütze in meinen Leben und begleitet mich überallhin auf meinem Lebensweg. Besonders danke ich Euch, dass Ihr mir vorlebt wie man sein Leben erfüllt gestalten kann.

Ich widme diese Arbeit meiner Familie: Meiner Liebe Dr. Sabrina Schiwy und unseren gemeinsamen Kindern. Ich danke euch für eure selbstlose Unterstützung und die Geduld, die ihr mir in dieser Zeit entgegengebracht habt. Danke Emilia, dass Du immer an mich geglaubt hast und mich mit folgenden Worten motiviert hast „Mama ist schlau und Papa ist stark!".

Curriculum vitae

Name	Andreas Herbert Schiwy
Date of birth	January 5th, 1982
Place of birth	Tarnowitz
Nationality	German
04/2011-2016	PhD student at the Institute for Environmental Research, RWTH Aachen University, Germany
08/2010	Diploma in Biology
10/2002-08/2010	Studies of Biology at the RWTH Aachen University, Germany
05/2002	Abitur
08/1993-05/2002	Bischöfliches Pius-Gymnasium Aachen, Germany

Scientific contributions

Research articles in international peer-reviewed journals

Schiwy, A., Maes, H.M., Koske, D., Flecken, M., Schmidt, K.R., Schell, H., Tiehm, A., Kamptner, A., Thümmler, S., Stanjek, H., Heggen, M., Dunin-Borkowski, R.E., Braun, J., Schäffer, A., Hollert, H., 2016. The ecotoxic potential of a new zero-valent iron nanomaterial, designed for the elimination of halogenated pollutants, and its effect on reductive dechlorinating microbial communities. Environmental Pollution.

Schiwy, A. & Brinkmann, M., Thiem, I., Guder, G., Winkens, K., Eichbaum, K., Nuszer, L., Thalmann, B., Buchinger, S., Reifferscheid, G., Seiler, T.-B., Thoms, B., Hollert, H., 2015. Determination of the CYP1A-inducing potential of single substances, mixtures and extracts of samples in the micro-EROD assay with H4IIE cells. Nat. Protocols 10, 1728-1741.

Nickel, C., Angelstorf, J., Bienert, R., Burkart, C., Gabsch, S., Giebner, S., Haase, A., Hellack, B., Hollert, H., Hund-Rinke, K., Jungmann, D., Kaminski, H., Luch, A., Maes, H.M., Nogowski, A., Oetken, M., Schaeffer, A., Schiwy, A., Schlich, K., Stintz, M., von der Kammer, F., Kuhlbusch, T.A.J., 2014. Dynamic light-scattering measurement comparability of nanomaterial suspensions. J Nanopart Res 16, 1-12.

Köber, R., Hollert, H., Hornbruch, G., Jekel, M., Kamptner, A., Klaas, N., Maes, H., Mangold, K.M., Martac, E., Matheis, A., Paar, H., Schäffer, A., Schell, H., Schiwy, A., Schmidt, K.R., Strutz, T.J., Thümmler, S., Tiehm, A., Braun, J., 2014. Nanoscale zero-valent iron flakes for groundwater treatment. Environ Earth Sci 72, 3339-3352.

Hollert, H., Filser, J., Häußling, R., Hein, M., Matthies, M., Oehlmann, J., Ratte, H.-T., Roß-Nickoll, M., Schäffer, A., Scheringer, M., Schiwy, A., 2011. Financial Research Support for Ecotoxicology and Environmental Chemistry in Germany - Results of an Online Survey. Environmental Sciences Europe 23, 24.

Research articles to be submitted in international peer-reviewed journals

Schiwy, A., Nüßer, L., Vorreier, K., Xiao, H., Thalmann, B., Hollert, H., Development of a high throughput in vitro bioassay for determination of the CYP1A-inducing potential of samples using chemically defined media – Efficiency meets ethical cell culture.

Scientific Reports

Nickel, C., Hellack, B., Gartiser, S., Flach, F., Schiwy, A., Maes, H., Schaeffer, A., Gabsch, S., Stintz, M., Erdinger, L., Kuhlbusch, T.A.J., 2012. Fate and behaviour of TiO2 nanomaterials in the environment, influenced by their shape, size and surface area, in: Federal Environment Agency (Germany) (Ed.), p. 163.

Plattform presentations

Schiwy, A., Maes, H.M., Schaffer, A., Hollert, H., 2012. Aquatische Toxikologie von Eisennanopartikeln, YoungNano Workshop, DECHEMA, Frankfurt am Main.

Schiwy, A., Seiler, T.-B., Thiem, I., Hollert, H., 2010. Comparison of bioassays for screening dioxin-like activities in food samples, 4. Gemeinsame Jahrestagung der GDCh-Fachgruppe Umweltchemie und Ökotoxikologie der Society of Environmental Toxicology and Chemistry Europe (German-Language Branch) e.V. (SETAC GLB) Umwelt 2010 Von der Erkenntnis zur Entscheidung, Dessau, Germany.

Poster proceedings

Schell, H., Schiwy, A., Maes, H.M., Schäffer, A., Schmidt, K.R., Hollert, H., Tiehm, A., 2013. Wechselwirkungen zwischen mikrobieller und abiotischer CKW-Dechlorierung – Synergien

und toxische Effekte, DaNa-Clustertreffen zu BMBF-Förderungsmaßnahmen NanoCare und NanoNature, DECHEMA, Frankfurt am Main, pp. 1-1.

Flecken, M., Schiwy, A., Maes, H.M., Peddinghaus, S., Schäffer, A., Hollert, H., Schmidt, K., Schell, H., Tiehm, A., 2012. Ecotoxic evaluation of iron nanomaterials with the fish embryo toxicity test (*Danio rerio*), Gemeinsame Jahrestagung von SETAC GLB und Fachgruppe Umweltchemie und Ökotoxikologie der GDCh "Erkennen, Untersuchen, Modellieren - Vom Nutzen des Verstehens", Helmholz-Zentrum für Umweltforschung, Leipzig, Germany.

Schiwy, A., Maes, H.M., Schaffer, A., Hollert, H., 2012. Ecotoxic evaluation of zero-valent iron nanomaterials in the aquatic environment, 6th SETAC World Congress/ SETAC Europe 22nd Annual Meeting "Securing a sustainable future: Integrating science, policy and people", Estrel Convention Center, Berlin, Germany, pp. 1-1.

Schell, H., Schiwy, A., Maes, H.M., Schäffer, A., Schmidt, K.R., Hollert, H., Tiehm, A., 2012. Wechselwirkungen zwischen mikrobieller und abiotischer CKW-Dechlorierung - Synergien und toxische Effekte, DaNa-Clustertreffen zu BMBF-Förderungsmaßnahmen NanoCare und NanoNature, DECHEMA, Frankfurt am Main.

Schiwy, A., Seiler, T.-B., Thiem, I., Hollert, H., 2011a. Comparison of bioassays for screening dioxin-like activities in food samples, Young Environmental Scientists Meeting (YES-Meeting) "Environmental challenges in a changing world", Aachen, Germany.

Schiwy, A., Seiler, T.-B., Thiem, I., Hollert, H., 2011b. Comparison of bioassays for screening dioxin-like activities in food samples, SETAC Europe 21st Annual Meeting, Milano Convention Centre, Milan, Italy.

Schell, H., Schiwy, A., Maes, H.M., Schäffer, A., Schmidt, K.R., Hollert, H., Tiehm, A., 2011. Wechselwirkungen zwischen mikrobieller und abiotischer CKW-Dechlorierung - Synergien und toxische Effekte, DaNa-Clustertreffen zu BMBF-Förderungsmaßnahmen NanoCare und NanoNature, DECHEMA, Frankfurt am Main, p. 1.

References

9227:1995, I., Determination of the specific surface area of solids by gas adsorption using the BET method.

11348-1, D. E. I., 2009. Water quality - Determination of the inhibitory effect of water samples on the light emission of *Vibrio fischeri* (Luminescent bacteria test) - Part 1: Method using freshly prepared bacteria (ISO 11348-1:2007); German version EN ISO 11348-1:2008.

Aarts, J. M., et al., 1995. Species-specific antagonism of Ah receptor action by 2,2',5,5'-tetrachloro- and 2,2',3,3'4,4'-hexachlorobiphenyl. Eur J Pharmacol. 293**,** 463-74.

Abraham, K., et al., 2011. Review: Incidents regarding dioxin in feedstuff in Germany 2011 - a consumer health risk? Arch Lebensmittelhyg. 62**,** 108-115.

Adler, S., et al., 2011. Alternative (non-animal) methods for cosmetics testing: Current status and future prospects-2010. Arch Toxicol. 85**,** 367-485.

Ahlborg, U. G., et al., 1994. Toxic equivalency factors for dioxin-like PCBs. Chemosphere. 28**,** 1049-1067.

Aktas, O., et al., 2012. Effect of chloroethene concentrations and granular activated carbon on reductive dechlorination rates and growth of *Dehalococcoides spp.* Bioresour Technol. 103**,** 286-92.

Altenburger, R., et al., 2008. Bioassays with unicellular algae: Deviations from exponential growth and its implications for toxicity test results. J Environ Qual. 37**,** 16-21.

Ames, B. N., et al., 1973. Carcinogens are mutagens: A simple test system combining liver homogenates for activation and bacteria for detection. Proceedings of the National Academy of Sciences. 70**,** 2281-2285.

Ames, B. N., Gold, L. S., 1997. Environmental pollution, pesticides, and the prevention of cancer: misconceptions. FASEB J. 11**,** 1041-52.

Ames, B. N., et al., 1975. Methods for detecting carcinogens and mutagens with the *Salmonella*/mammalian-microsome mutagenicity test. Mutation Research/Environmental Mutagenesis and Related Subjects. 31**,** 347-363.

Amiano, I., et al., 2012. Acute toxicity of nanosized TiO_2 to *Daphnia magna* under UVA irradiation. Environ Toxicol Chem. 31**,** 2564-6.

Ammann, M., et al., 1990. Monitoring volcanic activity by characterization of ultrafine aerosol emissions. J Aerosol Sci. 21**,** S275-S278.

Anderson, J. W., et al., 1995. A biomarker, P450 RGS, for assessing the induction potential of environmental samples. Environ Toxicol Chem. 14**,** 1159.

Arlt, V. M., et al., 2015. Pulmonary inflammation impacts on CYP1A1-mediated respiratory tract DNA damage induced by the carcinogenic air pollutant benzo[*a*]pyrene. Toxicol Sci.

Aruoja, V., et al., 2009. Toxicity of nanoparticles of CuO, ZnO and TiO_2 to microalgae *Pseudokirchneriella subcapitata*. Sci Total Environ. 407**,** 1461-8.

Astashkina, A., et al., 2012. A critical evaluation of *in vitro* cell culture models for high-throughput drug screening and toxicity. Pharmacol Ther. 134**,** 82-106.

Auerbach, C., 1949. Chemical mutagenesis. Biological Reviews. 24**,** 355-391.

Auffan, M., et al., 2006. *In vitro* interactions between DMSA-coated maghemite nanoparticles and human fibroblasts: A physicochemical and cyto-genotoxical study. Environ Sci Technol. 40**,** 4367-73.

Auffan, M. l., et al., 2008. Relation between the redox state of iron-based nanoparticles and their cytotoxicity toward *Escherichia coli*. Environ Sci Technol. 42**,** 6730-6735.

Baalousha, M., 2009. Aggregation and disaggregation of iron oxide nanoparticles: Influence of particle concentration, pH and natural organic matter. Sci Total Environ. 407**,** 2093-101.

Banwart, W. L., et al., 1982. Sorption of nitrogen-heterocyclic compounds by soils and sediments. Soil Science. 133**,** 42-47.

Barnes, D., Sato, G., 1980a. Methods for growth of cultured cells in serum-free medium. Anal Biochem. 102**,** 255-70.

Barnes, D., Sato, G., 1980b. Serum-free cell culture: A unifying approach. Cell. 22**,** 649-55.

Barnes, R. J., et al., 2010. Inhibition of biological TCE and sulphate reduction in the presence of iron nanoparticles. Chemosphere. 80**,** 554-62.

Barzan, E., et al., 2014. Antimicrobial and genotoxicity effects of zero-valent iron nanoparticles. Jundishapur J Microbiol. 7**,** e10054.

Basketter, D., et al., 2012. A roadmap for the development of alternative (non-animal) methods for systemic toxicity testing. ALTEX. 29**,** 3-91.

Baumann, J., et al., 2014. The coating makes the difference: Acute effects of iron oxide nanoparticles on *Daphnia magna*. Sci Total Environ. 484C**,** 176-184.

Baumann, J., et al., 2013. Adaptation of the *Daphnia sp.* acute toxicity test: Miniaturization and prolongation for the testing of nanomaterials. Environ Sci Pollut Res Int.

Baun, A., et al., 2008. Ecotoxicity of engineered nanoparticles to aquatic invertebrates: A brief review and recommendations for future toxicity testing. Ecotoxicology. 17**,** 387-95.

Baun, A., et al., 2009. Setting the limits for engineered nanoparticles in European surface waters - Are current approaches appropriate? J Environ Monit. 11**,** 1774-81.

Baviere, M., et al., *In-situ* remediation of oil-contaminated soils with surfactants: Laboratory and pilot studies. International Symposium on Oilfield Chemistry, 1997.

Behnisch, P. A., et al., 2002. Screening of dioxin-like toxicity equivalents for various matrices with wildtype and recombinant rat hepatoma H4IIE cells. Toxicol Sci. 69**,** 125-130.

Behnisch, P. A., et al., 2001. Combinatorial bio/chemical analysis of dioxin and dioxin-like compounds in waste recycling, feed/food, humans/wildlife and the environment. Environ Int. 27**,** 495-519.

Behra, R., Krug, H., 2008. Nanoecotoxicology: Nanoparticles at large. Nat Nanotechnol. 3**,** 253-4.

Behrens, S., et al., 2008. Monitoring abundance and expression of "*Dehalococcoides*" species chloroethene-reductive dehalogenases in a tetrachloroethene-dechlorinating flow column. Appl Environ Microbiol. 74**,** 5695-703.

Belanger, S. E., et al., An update to the fish embryo toxicity-Acute fish toxicity relationship and prospects for support of the use of the FET as an animal alternative. Document prepared for the 2012 OECD ad hoc Expert Meeting Group on the Fish Embryo Test, 2012, pp. 1-156.

Belanger, S. E., et al., 2013. Use of fish embryo toxicity tests for the prediction of acute fish toxicity to chemicals. Environ Toxicol Chem. 32**,** 1768-83.

Benedict, W. F., et al., 1973. Aryl hydrocarbon hydroxylase induction in mammalian liver cell culture. IV. Stimulation of the enzyme activity in established cell lines derived from rat or mouse hepatoma and from normal rat liver. Biochem Pharmacol. 22**,** 2766-9.

Bhat, Z. F., Bhat, H., 2011. Tissue engineered meat - Future meat. J. Stored Prod. Postharvest Res. 2**,** 1-10.

Bhat, Z. F., Fayaz, H., 2010. Prospectus of cultured meat—advancing meat alternatives. Int J Food Sci Tech. 48**,** 125-140.

Bhat, Z. F., et al., 2015. *In vitro* meat production: Challenges and benefits over conventional meat production. J Integr Agr. 14**,** 241-248.

Bhawana, P., Fulekar, M., 2012. Nanotechnology: Remediation technologies to clean up the environmental pollutants. Res. J. Chem. Sci. 2231**,** 606X.

Biaggio, R. T., et al., 2015. Serum-free suspension culturing of human cells: Adaptation, growth, and cryopreservation. Bioprocess Biosyst Eng. 38**,** 1495-507.

Birkholz, M., 2006. Thin film analysis by X-ray scattering. John Wiley & Sons.

Bittner, M., et al., 2006. Activation of Ah receptor by pure humic acids. Environ Toxicol. 21**,** 338-42.

Blum, P., et al., 2011. Importance of heterocylic aromatic compounds in monitored natural attenuation for coal tar contaminated aquifers: A review. J Contam Hydrol. 126**,** 181-94.

BMBF, Werkstoffinnovationen für Industrie und Gesellschaft – WING. In: Bundesministerium für Bildung und Forschung, (Ed.), 2003.

Bokare, A. D., et al., 2007. Effect of surface chemistry of Fe-Ni nanoparticles on mechanistic pathways of azo dye degradation. Environ Sci Technol. 41**,** 7437-43.

Bolin, S., et al., 1991. Methods for detection and frequency of contamination of fetal calf serum with bovine viral diarrhea virus and antibodies against bovine viral diarrhea virus. J Vet Diagn Invest. 3**,** 199-203.

Bonder, M. J., et al., 2007. Controlling synthesis of Fe nanoparticles with polyethylene glycol. Journal of Magnetism and Magnetic Materials. 311**,** 658-664.

Bonini, M. G., et al., 2006. The oxidation of 2',7'-dichlorofluorescin to reactive oxygen species: A self-fulfilling prophesy? Free Radic Biol Med. 40**,** 968-75.

Borden, R. C., et al., 1997. Intrinsic biodegradation of MTBE and BTEX in a gasoline-contaminated aquifer. Water Resour Res. 33**,** 1105-1115.
Bottenstein, J. E., Sato, G. H., 1979. Growth of a rat neuroblastoma cell line in serum-free supplemented medium. Proc Natl Acad Sci U S A. 76**,** 514-7.
Bovee, T. F., et al., 1998. Validation and use of the CALUX-bioassay for the determination of dioxins and PCBs in bovine milk. Food Addit Contam. 15**,** 863-75.
Brack, W., 2003. Effect-directed analysis: A promising tool for the identification of organic toxicants in complex mixtures? Anal Bioanal Chem. 377**,** 397-407.
Bradford, S. A., et al., 2003. Modeling colloid attachment, straining, and exclusion in saturated porous media. Environ Sci Technol. 37**,** 2242-2250.
Bradford, S. A., et al., 2009. Modeling the coupled effects of pore space geometry and velocity on colloid transport and retention. Water Resources Research. 45.
Bradford, S. A., et al., 2011. Modeling colloid transport and retention in saturated porous media under unfavorable attachment conditions. Water Resources Research. 47.
Bradford, S. A., et al., 2002. Physical factors affecting the transport and fate of colloids in saturated porous media. Water Resources Research. 38**,** 63-1-63-12.
Bradlaw, J., Casterline Jr, J., 1979. Induction of enzyme activity in cell culture: A rapid screen for detection of planar polychlorinated organic compounds. J Assoc Off Anal Chem. 62**,** 904-916.
Braunbeck, T., et al., 2005. Towards an alternative for the acute fish LC (50) test in chemical assessment: The fish embryo toxicity test goes multi-species—An update. Altex. 22**,** 87-102.
Brennan, J. C., et al., 2015. Development of species-specific Ah receptor-responsive third generation CALUX cell lines with enhanced responsiveness and improved detection limits. Environ Sci Technol. 49**,** 11903-12.
Brindley, D. A., et al., 2012. Peak serum: Implications of serum supply for cell therapy manufacturing. Regen Med. 7**,** 7-13.
Bringmann, G., Kühn, R., 1980. Comparison of the toxicity thresholds of water pollutants to bacteria, algae, and protozoa in the cell multiplication inhibition test. Water Res. 14**,** 231-241.
Brinkmann, M., et al., 2014a. Genotoxicity of heterocyclic PAHs in the micronucleus assay with the fish liver cell line RTL-W1. PLoS One. 9**,** e85692.
Brinkmann, M., et al., 2014b. Heterocyclic aromatic hydrocarbons show estrogenic activity upon metabolization in a recombinant transactivation assay. Environ Sci Technol. 48**,** 5892-901.
Brouwer, A., et al., 1995. Functional aspects of developmental toxicity of polyhalogenated aromatic hydrocarbons in experimental animals and human infants. Eur. J. Pharmacol. Environ. Toxicol. Pharm. 293**,** 1-40.
Brunner, D., et al., 2010. Serum-free cell culture: The serum-free media interactive online database. ALTEX. 27**,** 53-62.
Bruton, T. A., et al., 2015. Effect of nanoscale zero-valent iron treatment on biological reductive dechlorination: A review of current understanding and research needs. Crit Rev Environ Sci Technol. 45**,** 1148-1175.
Burke, M. D., Mayer, R. T., 1974. Ethoxyresorufin: Direct fluorimetric assay of a microsomal *O*-dealkylation which is preferentially inducible by 3-methylcholanthrene. Drug Metab Disposition. 2**,** 583-588.
Caliman, F. A., et al., 2010. Soil and groundwater cleanup: Benefits and limits of emerging technologies. Clean Technol Envir. 13**,** 241-268.
Cantrell, K. J., et al., 1995. Zero-valent iron for the *in situ* remediation of selected metals in groundwater. J Hazard Mater. 42**,** 201-212.
Cao, G., 2004. Nanostructures and nanomaterials: Synthesis, properties and applications.
Carr, B., Malloy, A., NanoParticle Tracking Analysis–The NANOSIGHT system. www.nanosight.co.uk, 2006.
Carvalho, R. N., et al., 2014. Mixtures of chemical pollutants at European legislation safety concentrations: How safe are they? Toxicol Sci. 141**,** 218-33.
Carvan, M. J., 3rd, et al., 2000. Activation of transcription factors in zebrafish cell cultures by environmental pollutants. Arch Biochem Biophys. 376**,** 320-7.
Castell, J. V., et al., *In vitro* investigation of the molecular mechanisms of hepatotoxicity. Arch Toxicol Suppl. Springer, 1997, pp. 313-321.

Celebi, O., et al., 2007. A radiotracer study of the adsorption behavior of aqueous Ba^{2+} ions on nanoparticles of zero-valent iron. J Hazard Mater. 148**,** 761-7.
Chang, M.-C., et al., 2005. Using nanoscale zero-valent iron for the remediation of polycyclic aromatic hydrocarbons contaminated soil. J Air Waste Manage Assoc. 55**,** 1200-1207.
Chen, G., Bunce, N. J., 2004. Interaction between halogenated aromatic compounds in the Ah receptor signal transduction pathway. Environ Toxicol. 19**,** 480-9.
Chen, J., et al., 2011. Effect of natural organic matter on toxicity and reactivity of nano-scale zero-valent iron. Water Res. 45**,** 1995-2001.
Chen, P. J., et al., 2012. Stabilization or oxidation of nanoscale zerovalent iron at environmentally relevant exposure changes bioavailability and toxicity in medaka fish. Environ Sci Technol. 46**,** 8431-9.
Chen, P. J., et al., 2013. The zerovalent iron nanoparticle causes higher developmental toxicity than its oxidation products in early life stages of medaka fish. Water Res. 47**,** 3899-909.
Chen, X., Mao, S. S., 2007. Titanium dioxide nanomaterials: Synthesis, properties, modifications, and applications. Chem Rev. 107**,** 2891-959.
Chiang, H.-c., et al., 2015. Reliable and sensitive adenovirus-based reporter system for high-throughput screening of dioxins. Environmental Technology & Innovation. 4**,** 8-16.
Chiles, R. M., 2013. If they come, we will build it: *In vitro* meat and the discursive struggle over future agrofood expectations. Agric Human Values. 30**,** 511-523.
Choi, S. J., Choy, J. H., 2011. Effect of physico-chemical parameters on the toxicity of inorganic nanoparticles. J Mater Chem. 21**,** 5547-5554.
Christian, P., et al., 2008. Nanoparticles: Structure, properties, preparation and behaviour in environmental media. Ecotoxicology. 17**,** 326-43.
Chu, L., Robinson, D. K., 2001. Industrial choices for protein production by large-scale cell culture. Curr Opin Biotechnol. 12**,** 180-187.
Cleuvers, M., 2003. Aquatic ecotoxicity of pharmaceuticals including the assessment of combination effects. Toxicol Lett. 142**,** 185-94.
Clewell, R. A., Andersen, M. E., 2016. Approaches for characterizing threshold dose-response relationships for DNA-damage pathways involved in carcinogenicity in vivo and micronuclei formation in vitro. Mutagenesis.
Clift, M. J., et al., 2013. Can the Ames test provide an insight into nano-object mutagenicity? Investigating the interaction between nano-objects and bacteria. Nanotoxicology. 7**,** 1373-85.
Coecke, S., et al., 2013. Toxicokinetics as a key to the integrated toxicity risk assessment based primarily on non-animal approaches. Toxicol In Vitro. 27**,** 1570-7.
Cohen, J., et al., 2013. Interactions of engineered nanomaterials in physiological media and implications for *in vitro* dosimetry. Nanotoxicology. 7**,** 417-431.
Cohen, J. M., et al., 2014. An integrated approach for the *in vitro* dosimetry of engineered nanomaterials. Particle and Fibre Toxicology. 11**,** 20.
Cohen, R. M., et al., DNAPL site evaluation. CK. Smoley, Boca Raton, Florida, 1993.
Colvin, V. L., 2003. The potential environmental impact of engineered nanomaterials. Nat Biotechnol. 21**,** 1166-70.
Comba, S., et al., 2011. A comparison between field applications of nano-, micro-, and millimetric zero-valent iron for the remediation of contaminated aquifers. Water Air Soil Pollut. 215**,** 595-607.
Corbett, J., et al., 2000. Nanotechnology: International developments and emerging products. Cirp Ann-Manuf Techn. 49**,** 523-545.
Cornell, R. M., Schwertmann, U., 2006. The iron oxides: Structure, properties, reactions, occurrences and uses. John Wiley & Sons.
Covaci, A., et al., 2008. The Belgian PCB/dioxin crisis-8 years later. Environ Toxicol Pharmacol. 25**,** 164-70.
Crane, R. A., Scott, T. B., 2012. Nanoscale zero-valent iron: Future prospects for an emerging water treatment technology. J Hazard Mater. 211-212**,** 112-25.
Crebelli, R., 2000. Threshold-mediated mechanisms in mutagenesis: implications in the classification and regulation of chemical mutagens. Mutation Research/Genetic Toxicology and Environmental Mutagenesis. 464**,** 129-135.
Cseh, T., et al., 1989. Adsorption-desorption characteristics of polychlorinated biphenyls on various polymers commonly found in laboratories. Appl Environ Microbiol. 55**,** 3150–3154.

Cullen, E., et al., 2010. Simulation of the subsurface mobility of carbon nanoparticles at the field scale. Advances in Water Resources. 33**,** 361-371.

Czekanska, E. M., 2011. Assessment of cell proliferation with resazurin-based fluorescent dye. Methods Mol Biol. 740**,** 27-32.

de Boer, C., 2007. Characteristics and mobility of zero-valent nano-iron in porous media.

De Boer, K., 2006. Grundlagenuntersuchungen zum hydraulischen Verhalten von Nano-Eisen im Aquifer. Heft 150 Hrsg.: J. Braun, H.-P. Koschitzky, M. Stuhrmann VEGAS–Statuskolloquium 2006. 88.

Delescluse, C., et al., 2000. Is CYP1A1 induction always related to AHR signaling pathway? Toxicology. 153**,** 73-82.

DeLoid, G., et al., 2014. Estimating the effective density of engineered nanomaterials for *in vitro* dosimetry. Nat Commun. 5**,** 3514.

Dencker, L., 1985. The role of receptors in 2,3,7,8-tetrachlorodibenzo-*p*-dioxin (TCDD) toxicity. Arch Toxicol Suppl. 8**,** 43-60.

Denison, M. S., Heath-Pagliuso, S., 1998. The Ah receptor: A regulator of the biochemical and toxicological actions of structurally diverse chemicals. Bull Environ Contam Toxicol. 61**,** 557-68.

Denison, M. S., Nagy, S. R., 2003. Activation of the aryl hydrocarbon receptor by structurally diverse exogenous and endogenous chemicals. Annu Rev Pharmacol Toxicol. 43**,** 309-34.

Di Paolo, C., et al., 2015. The value of zebrafish as an integrative model in effect-directed analysis - A review. Env Sci Eur. 27.

Di Sotto, A., et al., 2009. Multi-walled carbon nanotubes: Lack of mutagenic activity in the bacterial reverse mutation assay. Toxicol Lett. 184**,** 192-7.

Dietmair, S., et al., 2012. Metabolite profiling of CHO cells with different growth characteristics. Biotechnol Bioeng. 109**,** 1404-1414.

Dietrich, P., Leven, C., Direct Push-Technologies. In: R. Kirsch, (Ed.), Groundwater Geophysics. Springer Berlin Heidelberg, 2006, pp. 321-340.

DIN, Water quality - Determination of the acute toxicity of waste water to zebrafish eggs (*Danio rerio*) (ISO 15088:2007). DIN EN ISO 15088. DIN German Institute for Standardization, 2008, pp. 20.

DIN, Water quality - Determination of the inhibition of the mobility of *Daphnia magna* Straus (Cladocera, Crustacea) - Acute toxicity test (ISO/DIS 6341:2010). DIN EN ISO 6341. DIN German Institute for Standardization, 2010a, pp. 33.

DIN, Water quality - Fresh water algal growth inhibition test with unicellular green algae (ISO 8692:2010). DIN EN ISO 8692. DIN German Institute for Standardization, 2010b, pp. 30.

Donato, M. T., et al., 1992. A rapid and sensitive method for measuring monooxygenase activities in hepatocytes cultured in 96-well plates. J Tissue Cult Methods. 14**,** 153-157.

Donato, M. T., et al., 1993. A microassay for measuring cytochrome P450IA1 and P450IIB1 activities in intact human and rat hepatocytes cultured on 96-well plates. Anal Biochem. 213**,** 29-33.

Donato, M. T., et al., 1998. Human hepatocyte growth factor down-regulates the expression of cytochrome P450 isozymes in human hepatocytes in primary culture. J Pharmacol Exp Ther. 284**,** 760-7.

Dong, H., et al., 2016. The dual effects of carboxymethyl cellulose on the colloidal stability and toxicity of nanoscale zero-valent iron. Chemosphere. 144**,** 1682-1689.

Doong, R. A., Lai, Y. L., 2006. Effect of metal ions and humic acid on the dechlorination of tetrachloroethylene by zerovalent iron. Chemosphere. 64**,** 371-8.

Driessen, C., Korthals, M., 2012. Pig towers and *in vitro* meat: Disclosing moral worlds by design. Soc Stud Sci. 42**,** 797-820.

DTU Environment, The nanodatabase. Vol. 2014, 2014.

Dunkel, V. C., et al., 1985. Reproducibility of microbial mutagenicity assays: II. Testing of carcinogens and noncarcinogens in *Salmonella typhimurium* and *Escherichia coli*. Environmental Mutagenesis. 7**,** 1-19.

Dunlop, D. J., Özdemir, Ö., 2001. Rock magnetism: Fundamentals and frontiers. Cambridge university press.

Ebert, D., 2005. Introduction to the ecology, epidemiology, and evolution of parasitism in Daphnia.

EC, 2002a. Communication of 16 April 2002 from the Commission to the Council, the European parliament, the Economic and Social Committee and the Committee of the regions: Towards a thematic strategy for soil protection. COM (2002) 179. 179.

EC, 2002b. Directive 2002/32/EC of the European Parliament and of the Council of 7 May 2002 on undesirable substances in animal feed - Council statement OJ L. 140.

EC, 2006a. Commision Regulation (EC) No 1907/2006 of the European Parliament and of the Council of 18 December 2006 concerning the Registration, Evaluation, Authorisation and Restriction of Chemicals (REACH), establishing a European Chemicals Agency, amending Directive 1999/45/EC and repealing Council Regulation (EEC) No 793/93 and Commission Regulation (EC) No 1488/94 as well as Council Directive 76/769/EEC and Commission Directives 91/155/EEC, 93/67/EEC, 93/105/EC and 2000/21/EC. OJ L. 396.

EC, 2006b. Commission Regulation (EC) No 1881/2006 of 19 December 2006 setting maximum levels for certain contaminants in foodstuffs (Text with EEA relevance) OJ L. 364.

EC, 2008. Commission Regulation (EC) No 1272/2008 of the European Parliament and of the Council of 16 December 2008 on classification, labelling and packaging of substances and mixtures, amending and repealing Directives 67/548/EEC and 1999/45/EC, and amending Regulation (EC) No 1907/2006. OJ L. 353.

EC, 2011. Commission Recommendation of 18 October 2011 on the definition of nanomaterial (2011/696/EU). OJ L. 275.

EC, 2012a. Commission Regulation (EC) No 278/2012 of 28 March 2012 amending Regulation (EC) No 152/2009 as regards the determination of the levels of dioxins and polychlorinated biphenyls. OJ L. 91.

EC, 2012b. Commission Regulation (EU) No 277/2012 of 28 March 2012 amending Annexes I and II to Directive 2002/32/EC of the European Parliament and of the Council as regards maximum levels and action thresholds for dioxins and polychlorinated biphenyls. OJ L. 91.

EC, 2012c. Commission staff working paper: Types and uses of nanomaterials, including safety aspects OJ C. 288.

EC, 2012d. Communication from the Commission to the European Parliament, the Council and the European Economic and Social Committee second regulatory review on nanomaterials OJ C. 572.

EC, 2012 - Annual Report. In: E. Union, (Ed.), The Rapid Alert System for Food and Feed, OP, 2013a.

EC, 2013b. Commission Recommendation (EC) No 711/2013 of 3 December 2013 on the reduction of the presence of dioxins, furans and PCBs in feed and food. OJ L. 323.

EC, 2013 - Annual Report. In: E. Union, (Ed.), The Rapid Alert System for Food and Feed, OP, 2014a.

EC, 2014b. Commission Recommendation (EC) No 663/2014 of 11 September 2014 amending the Annex to Recommendation 2013/711/EU on the reduction of the presence of dioxins, furans and PCBs in feed and food. OJ L. 272.

EC, 2014c. Commission Regulation (EC) No 589/2014 of 2 June 2014 laying down methods of sampling and analysis for the control of levels of dioxins, dioxin-like PCBs and non-dioxin-like PCBs in certain foodstuffs and repealing Regulation (EU) No 252/2012. OJ L. 164.

EC, 2014d. Commission Regulation (EU) No 589/2014 of 2 June 2014 laying down methods of sampling and analysis for the control of levels of dioxins, dioxin-like PCBs and non-dioxin-like PCBs in certain foodstuffs and repealing Regulation (EU) No 252/2012 (Text with EEA relevance). OJ L. 164.

EC, Definition of nanomaterial. In: E. Directorate-General, (Ed.), Definition of nanomaterial, Vol. 2016. EC, 2016.

ECHA, Guidance on information requirements and chemical safety assessment - Chapter R.7b: Endpoint specific guidance. 2016.

Edgington, A. J., et al., 2010. The influence of natural organic matter on the toxicity of multiwalled carbon nanotubes. Environ Toxicol Chem. 29**,** 2511-8.

Efecan, N., et al., 2009. Characterization of the uptake of aqueous Ni^{2+} ions on nanoparticles of zero-valent iron (nZVI). Desalination. 249**,** 1048-1054.

Ehling, U. H., et al., 1983. Review of the evidence for the presence or absence of thresholds in the induction of genetic effects by genotoxic chemicals. Mutation Research/Reviews in Genetic Toxicology. 123**,** 281-341.

Eichbaum, K., et al., 2014. *In vitro* bioassays for detecting dioxin-like activity - Application potentials and limits of detection, a review. Sci Total Environ. 487**,** 37-48.

Eisenbrand, G., et al., 2002. Methods of *in vitro* toxicology. Food Chem Toxicol. 40**,** 193-236.

Eisentraeger, A., et al., 2008. Heterocyclic Compounds: Toxic Effects Using Algae, Daphnids, and the *Salmonella*/Microsome Test Taking Methodical Quantitative Aspects into Account. Environ Toxicol Chem. 27**,** 1590.

El-Temsah, Y. S., Joner, E. J., 2012. Ecotoxicological effects on earthworms of fresh and aged nano-sized zero-valent iron (nZVI) in soil. Chemosphere. 89**,** 76-82.

El Fantroussi, S., et al., 1997a. Introduction and PCR detection of *Desulfomonile tiedjei* in soil slurry microcosms. Biodegradation. 8**,** 125-33.

El Fantroussi, S., et al., 1997b. Introduction of anaerobic dechlorinating bacteria into soil slurry microcosms and nested-PCR monitoring. Appl Environ Microbiol. 63**,** 806-11.

Elliott, D. W., Zhang, W.-X., 2001. Field assessment of nanoscale bimetallic particles for groundwater treatment. Environ Sci Technol. 35**,** 4922-4926.

Elzoghby, A. O., et al., 2012. Albumin-based nanoparticles as potential controlled release drug delivery systems. J Controlled Release. 157**,** 168-182.

Escher, B. I., et al., 2014. Benchmarking organic micropollutants in wastewater, recycled water and drinking water with *in vitro* bioassays. Environ Sci Technol. 48**,** 1940-56.

Eske, K., et al., 2009. Generation of murine bone marrow derived macrophages in a standardised serum-free cell culture system. J Immunol Methods. 342**,** 13-9.

Fako, V. E., Furgeson, D. Y., 2009. Zebrafish as a correlative and predictive model for assessing biomaterial nanotoxicity. Adv Drug Deliv Rev. 61**,** 478-86.

Falkner, R., Jaspers, N., 2012. Regulating nanotechnologies: Risk, uncertainty and the global governance gap. Global Environ Polit. 12**,** 30-55.

Fasinu, P., et al., 2012. Liver-based *in vitro* technologies for drug biotransformation studies - A review. Curr Drug Metab. 13**,** 215-224.

Feldmannova, M., et al., 2006. Effects of N-heterocyclic polyaromatic hydrocarbons on survival, reproduction, and biochemical parameters in *Daphnia magna*. Environ Toxicol. 21**,** 425-31.

Felix, L. C., et al., 2013. Physicochemical characteristics of polymer-coated metal-oxide nanoparticles and their toxicological effects on zebrafish (*Danio rerio*) development. Environ Sci Technol. 47**,** 6589-96.

Feynman, R. P., 1960. There's plenty of room at the bottom. Eng Sci. 23**,** 22-36.

Fiedler, H., Dioxins and furans (PCDD/PCDF). The Handbook of Environmental Chemistry Vol. 3, 2003, pp. 123-201.

Filser, J., et al., 2013. Intrinsically green iron oxide nanoparticles? From synthesis via (eco-)toxicology to scenario modelling. Nanoscale. 5**,** 1034-46.

Flecken, M., et al., Ecotoxic evaluation of iron nanomaterials with the fish embryo toxicity test (*Danio rerio*). 2012.

Flecknell, P., 2002. Replacement, reduction and refinement. ALTEX. 19**,** 73-8.

Forró, L., et al., Global diversity of cladocerans (Cladocera; Crustacea) in freshwater. Freshwater Animal Diversity Assessment. Springer, 2008, pp. 177-184.

Franklin, R. E., Gosling, R. G., 1953. The structure of sodium thymonucleate fibres. I. The influence of water content. Acta Crystallogr. 6**,** 673-677.

Frost, R. L., et al., 2010. Synthesis, characterization of palygorskite supported zero-valent iron and its application for methylene blue adsorption. J Colloid Interface Sci. 341**,** 153-61.

Fu, F., et al., 2014a. The use of zero-valent iron for groundwater remediation and wastewater treatment: A review. J Hazard Mater. 267**,** 194-205.

Fu, P. P., et al., 2014b. Mechanisms of nanotoxicity: Generation of reactive oxygen species. J Food Drug Anal. 22**,** 64-75.

Gale, R. W., et al., 2000. Evaluation of planar halogenated and polycyclic aromatic hydrocarbons in estuarine sediments using ethoxyresorufin-*O*-deethylase induction of H4IIE cells. Environ Toxicol Chem. 19**,** 1348-1359.

Gallardo-Moreno, A. M., et al., 2012. The zeta potential of extended dielectrics and conductors in terms of streaming potential and streaming current measurements. Phys Chem Chem Phys. 14**,** 9758.

Garrison, P. M., et al., 1996. Species-specific recombinant cell lines as bioassay systems for the detection of 2,3,7,8-tetrachlorodibenzo-*p*-dioxin-like chemicals. Fundam Appl Toxicol. 30**,** 194-203.

Gatica, S. M., et al., 2005. Designing van der Waals forces between nanocolloids. Nano Lett. 5**,** 169-173.

Geyer, C. R., et al., 2012. Recombinant antibodies and *in vitro* selection technologies. Methods Mol Biol. 901**,** 11-32.

Gheju, M., 2011. Hexavalent chromium reduction with zero-valent iron (ZVI) in aquatic systems. Water, Air, Soil Pollut. 222**,** 103-148.

Ghosh Chaudhuri, R., Paria, S., 2012. Core/shell nanoparticles: Classes, properties, synthesis mechanisms, characterization, and applications. Chem Rev. 112**,** 2373-433.

Giesy, J. P., Kannan, K., 1998. Dioxin-like and non-dioxin-like toxic effects of polychlorinated biphenyls (PCBs): Implications for risk assessment. Crit Rev Toxicol. 28**,** 511-69.

Giesy, J. P., et al., 1994. Deformities in birds of the Great Lakes region. Environ Sci Technol. 28**,** 128A-135A.

Gillham, R. W., O'Hannesin, S. F., 1994. Enhanced degradation of halogenated aliphatics by zero-valent iron. Ground Water. 32**,** 958-967.

Gizzi, G., et al., 2005. Determination of dioxins (PCDDs/PCDFs) and PCBs in food and feed using the DR CALUX® bioassay: Results of an international validation study. Food Addit Contam. 22**,** 472-81.

Goebel-Stengel, M., et al., 2011. The importance of using the optimal plasticware and glassware in studies involving peptides. Anal Biochem. 414**,** 38-46.

Goldstein, J., Safe, S., 1989. CHAPTER 9 – Mechanism of action and structure-activity relationships for the chlorinated dibenzo-*p*-dioxins and related compounds.

Gosu, V., Gurjar, B. R., 2013. Removal of nitrogenous heterocyclic compounds (NHCs) by nano zero valent iron. Int J ChemTech Res. 5**,** 634-639.

Gosu, V., et al., 2016. Oxidative degradation of quinoline using nanoscale zero-valent iron supported by granular activated carbon. J Environ Eng. 142**,** 04015047.

Gottschalk, F., Nowack, B., 2011. The release of engineered nanomaterials to the environment. J Environ Monit. 13**,** 1145-55.

Greulich, B., et al., Cell line development using the SEFEX system. BMC Proc, Vol. 5 Suppl 8, 2011, pp. P43.

Grieger, K. D., et al., 2010. Environmental benefits and risks of zero-valent iron nanoparticles (nZVI) for *in situ* remediation: Risk mitigation or trade-off? J Contam Hydrol. 118**,** 165-83.

Griffiths, A. J., 2005. An introduction to genetic analysis. Macmillan.

Grosvenor, A. P., et al., 2004. Examination of the oxidation of iron by oxygen using X-ray photoelectron spectroscopy and QUASES™. Surf Sci. 565**,** 151-162.

Gstraunthaler, G., 2003. Alternatives to the use of fetal bovine serum: Serum-free cell culture. ALTEX. 20**,** 275-281.

Gstraunthaler, G., Lindl, T., 2013. Zell-und Gewebekultur: Allgemeine Grundlagen und spezielle Anwendungen. Springer-Verlag.

Gstraunthaler, G., et al., 2013a. FBS production problems demand to call for serum-free media. ALTEX. 30**,** 560-561.

Gstraunthaler, G., et al., 2013b. A plea to reduce or replace fetal bovine serum in cell culture media. Cytotechnology. 65**,** 791-3.

Hädrich, J., et al., 2012. Considerations on the working range in bioassays dose-response curves: Curve fit and assay background response. Organohalogen Compd. 74**,** 177-181.

Hafner, C., et al., 2015. Investigations on sediment toxicity of German rivers applying a standardized bioassay battery. Environ Sci Pollut Res Int. 22**,** 16358-70.

Hahn, D. W., 2006. Light scattering theory. Department of Mechanical and Aerospace Engineering, Florida.

Halder, M. E., et al., EURL ECVAM recommendation on the zebrafish embryo acute toxicity test method (ZFET) for acute aquatic toxicity testing. Health and consumer protection, Publications Office of the European Union, 2014.

Hammond, D., Strobel, H., 1992. Ethoxyresorufin *O*-deethylase activity in intact human cells. Toxicol In Vitro. 6**,** 41-46.

Hanberg, A., et al., 1991. Swedish dioxin survey: Evaluation of the H4IIE bioassay for screening environmental samples for dioxin-like enzyme induction. Pharmacol Toxicol. 69**,** 442-449.
Handy, R. D., et al., 2008a. The ecotoxicology of nanoparticles and nanomaterials: Current status, knowledge gaps, challenges, and future needs. Ecotoxicology. 17**,** 315-25.
Handy, R. D., et al., 2008b. The ecotoxicology and chemistry of manufactured nanoparticles. Ecotoxicology. 17**,** 287-314.
Hankinson, O., 1995. The aryl hydrocarbon receptor complex. Annu Rev Pharmacol Toxicol. 35**,** 307-40.
Hannink, R. H., Hill, A. J., 2006. Nanostructure control of materials. Woodhead Publishing.
Hansch, C., et al., 1995. Exploring QSAR: Hydrophobic, electronic, and steric constants American Chemical Society
Harada, A., et al., 2013. Titanium dioxide nanoparticle-entrapped polyion complex micelles generate singlet oxygen in the cells by ultrasound irradiation for sonodynamic therapy. Biomater Sci. 1**,** 65-73.
Harrison, R. G., 1910. The outgrowth of the nerve fiber as a mode of protoplasmic movement.
J Exp Zool. 9**,** 787-846.
Harrison, R. G., et al., 1907. Observations of the living developing nerve fiber. Anat Rec. 1**,** 116-128.
Hartmann, N. B., et al., 2010. Algal testing of titanium dioxide nanoparticles- Testing considerations, inhibitory effects and modification of cadmium bioavailability. Toxicology. 269**,** 190-7.
Hasegawa, G., et al., 2012. Differential genotoxicity of chemical properties and particle size of rare metal and metal oxide nanoparticles. J Appl Toxicol. 32**,** 72-80.
Hasegawa, S., et al., 2007. Vertical profiles of ultrafine to supermicron particles measured by aircraft over Osaka metropolitan area in Japan. Atmos Environ (1994). 41**,** 717-729.
Hassellov, M., et al., 2008. Nanoparticle analysis and characterization methodologies in environmental risk assessment of engineered nanoparticles. Ecotoxicology. 17**,** 344-61.
Häusl, P., 2008. Fetal bovine serum running short. EuroBiotechNews. 7**,** 26.
Hawkes, P. W., 2015. Fetal bovine serum: geographic origin and regulatory relevance of viral contamination. Bioresources and Bioprocessing. 2.
Hayashi, I., Sato, G. H., 1976. Replacement of serum by hormones permits growth of cells in a defined medium. Nature. 259**,** 132-4.
He, F., et al., 2010. Field assessment of carboxymethyl cellulose stabilized iron nanoparticles for *in situ* destruction of chlorinated solvents in source zones. Water Res. 44**,** 2360-70.
Heale, T., 2012. Synthetic steak: The benefits of multiplying meat.
Heger, S., et al., 2012. Biotests for hazard assessment of biofuel fermentation. Energy Environ. Sci. 5**,** 9778.
Heintzmann, R., Ficz, G., 2006. Breaking the resolution limit in light microscopy. Brief Funct Genomic Proteomic. 5**,** 289-301.
Henn, K. W., Waddill, D. W., 2006. Utilization of nanoscale zero-valent iron for source remediation—A case study. Remediation. 16**,** 57-77.
Hernandez-Moreno, D., et al., 2016. Mechanisms underlying the enhancement of toxicity caused by the Co-incubation of ZnO and Cu nanoparticles in a fish hepatoma cell line. Environ Toxicol Chem.
Heron, G., et al., 1998. Soil heating for enhanced remediation of chlorinated solvents: A laboratory study on resistive heating and vapor extraction in a silty, low-permeable soil contaminated with trichloroethylene. Environ Sci Technol. 32**,** 1474-1481.
Hestermann, E. V., et al., 2000. Serum alters the uptake and relative potencies of halogenated aromatic hydrocarbons in cell culture bioassays. Toxicol Sci. 53**,** 316-25.
Hewitt, L. M., et al., 2000. Characteristics of ligands for the Ah receptor and sex steroid receptors in hepatic tissues of fish exposed to bleached kraft mill effluent. Environ Sci Technol. 34**,** 4327-4334.
Hildebrand, H., et al., 2009. Highly active Pd-on-magnetite nanocatalysts for aqueous phase hydrodechlorination reactions. Environ Sci Technol. 43**,** 3254-3259.
Hill, A. J., et al., 2005. Zebrafish as a model vertebrate for investigating chemical toxicity. Toxicol Sci. 86**,** 6-19.
Hilscherova, K., et al., 2000. Cell bioassays for detection of aryl hydrocarbon (AhR) and estrogen receptor (ER) mediated activity in environmental samples. Environ Sci Pollut Res Int. 7**,** 159-71.

Hinger, G., et al., 2011. Some heterocyclic aromatic compounds are Ah receptor agonists in the DR-CALUX assay and the EROD assay with RTL-W1 cells. Environ Sci Pollut R. 18**,** 1297-1304.
Hollert, H., et al., 2003. A new sediment contact assay to assess particle-bound pollutants using zebrafish (*Danio rerio*) embryos. J Soils Sed. 3**,** 197-207.
Honn, K. V., et al., 1975. Fetal bovine serum: A multivariate standard. Exp Biol Med. 149**,** 344-347.
Hoo, C. M., et al., 2008. A comparison of atomic force microscopy (AFM) and dynamic light scattering (DLS) methods to characterize nanoparticle size distributions. J Nanopart Res. 10**,** 89-96.
Hornbruch, G., et al., in prep. Simulation of NZVI transport in porous media under variable injection conditions.
Hotze, E. M., et al., 2010. Nanoparticle aggregation: Challenges to understanding transport and reactivity in the environment. J Environ Qual. 39**,** 1909-24.
Howe, K., et al., 2013. The zebrafish reference genome sequence and its relationship to the human genome. Nature. 496**,** 498-503.
http://www.napasan.de/, NAPASAN - Nanopartikel zur Grundwassersanierung. 2011.
Hu, W., et al., 2007. Induction of Cyp1a1 is a nonspecific biomarker of aryl hydrocarbon receptor activation: Results of large scale screening of pharmaceuticals and toxicants *in vivo* and *in vitro*. Mol Pharmacol. 71**,** 1475-86.
Huang, H., Buekens, A., 1995. On the mechanisms of dioxin formation in combustion processes. Chemosphere. 31**,** 4099-4117.
Hund-Rinke, K., et al., 2015. Test strategy for assessing the risks of nanomaterials in the environment considering general regulatory procedures. Env Sci Eur. 27.
Hund-Rinke, K., Schlich, K., 2014. The potential benefits and limitations of different test procedures to determine the effects of Ag nanomaterials and $AgNO_3$ on microbial nitrogen transformation in soil. Env Sci Eur. 26.
Hund-Rinke, K., Simon, M., 2006. Ecotoxic effect of photocatalytic active nanoparticles (TiO_2) on algae and daphnids. Environ Sci Pollut Res Int. 13**,** 225-32.
Hussain, S. M., et al., 2015. At the crossroads of nanotoxicology *in vitro*: Past achievements and current challenges. Toxicol Sci. 147**,** 5-16.
Ioannides, C., Lewis, D. F., 2004. Cytochromes P450 in the bioactivation of chemicals. Curr Top Med Chem. 4**,** 1767-1788.
Iscove, N. N., 1984. Culture of lymphocytes and hemopoietic cells in serum-free medium. A.R.Liss, N.Y. .
ISO, 13321 - Particle size analysis - Photon correlation spectroscopy. DIN German Institute for Standardization, Beuth Verlag GmbH, 1996.
ISO, 11350 - Water quality - Determination of the genotoxicity of water and waste water - *Salmonella*/microsome fluctuation test (Ames fluctuation test). ISO 11350. ISO International Organization for Standardization, 2012, pp. 42.
Issaq, H. J., et al., 2002. The SELDI-TOF MS approach to proteomics: Protein profiling and biomarker identification. Biochem Biophys Res Commun. 292**,** 587-92.
Jackson, R. E., Dwarakanath, V., 1999. Chlorinated decreasing solvents: Physical-chemical properties affecting aquifer contamination and remediation. Ground Water Monit Remediat. 19**,** 102-110.
Jamsa, T., et al., 2001. Effects of 2,3,7,8-tetrachlorodibenzo-*p*-dioxin on bone in two rat strains with different aryl hydrocarbon receptor structures. J Bone Miner Res. 16**,** 1812-20.
Jander, G., Scheele, W., 1932. Über amphotere Oxydhydrate, deren wäßrige Lösungen und kristallisierende Verbindungen. XIV. Mitteilung. Über Hydrolyseprodukte und Aggregationsvorgänge in den Salzlösungen dreiwertiger Metalle, insbesondere in wäßrigen Chromisalzlösungen. Z Anorg Allg Chem. 206**,** 241-251.
Jang, M. H., et al., 2014. Potential environmental implications of nanoscale zero-valent iron particles for environmental remediation. Environ Health Toxicol. 29**,** e2014022.
Jarošová, B., et al., 2015. Can zero-valent iron nanoparticles remove waterborne estrogens? J Environ Manage. 150**,** 387-392.
Jiang, D., et al., 2015. Oxidation of nanoscale zero-valent iron under sufficient and limited dissolved oxygen: Influences on aggregation behaviors. Chemosphere. 122**,** 8-13.
Jiang, J., et al., 2009. Characterization of size, surface charge, and agglomeration state of nanoparticle dispersions for toxicological studies. J Nanopart Res. 11**,** 77-89.

Jiang, Q. T., et al., 2005. Human health risk assessment of organochlorines associated with fish consumption in a coastal city in China. Environ Pollut. 136**,** 155-65.

Joachim, C., 2005. To be nano or not to be nano? Nat Mater. 4**,** 107-109.

Jochems, C. E., et al., 2002. The use of fetal bovine serum: Ethical or scientific problem? ATLA. 30**,** 219-228.

Johnson, P. R., Elimelech, M., 1995. Dynamics of colloid deposition in porous media: Blocking based on random sequential adsorption. Langmuir. 11**,** 801-812.

Johnson, P. R., et al., 1996. Colloid transport in geochemically heterogeneous porous media: Modeling and measurements. Environ Sci Technol. 30**,** 3284-3293.

Joner, E., et al., Environmental fate and ecotoxicity of engineered nanoparticles. Norwegian Pollution Control Authority Report no. TA 2304, 2007, pp. 1-64.

Jones, P. A., Takai, D., 2001. The role of DNA methylation in mammalian epigenetics. Science. 293**,** 1068-70.

Jordaan, I., et al., 2007. The contribution of dioxin-like compounds from platinum mining and processing samples. Miner Eng. 20**,** 191-193.

Joshi, M., et al., 2008. Characterization techniques for nanotechnology applications in textiles. Indian J Fibre Text Res. 33**,** 304-317.

Kahru, A., Dubourguier, H. C., 2010. From ecotoxicology to nanoecotoxicology. Toxicology. 269**,** 105-19.

Kahru, A., Ivask, A., 2013. Mapping the dawn of nanoecotoxicological research. Acc Chem Res. 46**,** 823-33.

Kalin, R. M., 2004. Engineered passive bioreactive barriers: Risk-managing the legacy of industrial soil and groundwater pollution. Curr Opin Microbiol. 7**,** 227-38.

Kanel, S. R., et al., 2008. Two dimensional transport characteristics of surface stabilized zero-valent iron nanoparticles in porous media. Environ Sci Technol. 42**,** 896-900.

Kanel, S. R., et al., 2005. Removal of arsenic(III) from groundwater by nanoscale zero-valent iron. Environ Sci Technol. 39**,** 1291-8.

Karlsson, H. L., et al., 2009. Size-dependent toxicity of metal oxide particles-A comparison between nano- and micrometer size. Toxicol Lett. 188**,** 112-8.

Karn, B., et al., 2009. Nanotechnology and *in situ* remediation: A review of the benefits and potential risks. Environ Health Perspect. 117**,** 1813-31.

Kearns, P., et al., The safety of nanotechnologies at the OECD. Nanomaterials: Risks and benefits. Springer Netherlands, 2009, pp. 351-358.

Keenan, C. R., et al., 2009. Oxidative stress induced by zero-valent iron nanoparticles and Fe(II) in human bronchial epithelial cells. Environ Sci Technol. 43**,** 4555-60.

Keiter, S., et al., 2008. Activities and identification of aryl hydrocarbon receptor agonists in sediments from the Danube river. Anal Bioanal Chem. 390**,** 2009-2019.

Keiter, S., et al., 2006. Ecotoxicological assessment of sediment, suspended matter and water samples in the upper Danube river. Environ Sci Pollut Res Int. 13**,** 308-319.

Keller, A. A., et al., 2012. Toxicity of nano-zero valent iron to freshwater and marine organisms. PLoS One. 7**,** e43983.

Khan, F. I., et al., 2004. An overview and analysis of site remediation technologies. J Environ Manage. 71**,** 95-122.

Kim, H. J., et al., 2012. Effect of kaolinite, silica fines and pH on transport of polymer-modified zero valent iron nano-particles in heterogeneous porous media. J Colloid Interface Sci. 370**,** 1-10.

Kim, H. S., et al., 2010. Atmospherically stable nanoscale zero-valent iron particles formed under controlled air contact: Characteristics and reactivity. Environ Sci Technol. 44**,** 1760-6.

Kirkland, D., et al., 2014. Can *in vitro* mammalian cell genotoxicity test results be used to complement positive results in the Ames test and help predict carcinogenic or *in vivo* genotoxic activity? I. Reports of individual databases presented at an EURL ECVAM Workshop. Mutat Res Genet Toxicol Environ Mutagen. 775-776**,** 55-68.

Kirsch-Volders, M., et al., 2000. Concepts of threshold in mutagenesis and carcinogenesis. Mutation Research/Genetic Toxicology and Environmental Mutagenesis. 464**,** 3-11.

Kirschling, T. L., et al., 2010. Impact of nanoscale zero valent iron on geochemistry and microbial populations in trichloroethylene contaminated aquifer materials. Environ Sci Technol. 44**,** 3474-80.

Kittel, C., 1946. Theory of the structure of ferromagnetic domains in films and small particles. Phys Rev. 70**,** 965-971.
Klaine, S. J., et al., 2012. Paradigms to assess the environmental impact of manufactured nanomaterials. Environ Toxicol Chem. 31**,** 3-14.
Knie, J., 1978. Der dynamische Daphnientest-Ein automatischer Biomonitor zur Überwachung von Gewässern und Abwässern. Wasser Boden. 12**,** 310-312.
Ko, C.-H., Elimelech, M., 2000. The "shadow effect" in colloid transport and deposition dynamics in granular porous media: Measurements and mechanisms. Environ Sci Technol. 34**,** 3681-3689.
Köber, R., et al., 2014. Nanoscale zero-valent iron flakes for groundwater treatment. Environ Earth Sci. 72**,** 3339-3352.
Kocur, C. M., et al., 2015. Contributions of abiotic and biotic dechlorination following carboxymethyl cellulose stabilized nanoscale zero valent iron injection. Environ Sci Technol. 49**,** 8648-56.
Kojima, H., et al., 2015. A sensitive, rapid, and simple DR-EcoScreen bioassay for the determination of PCDD/Fs and dioxin-like PCBs in environmental and food samples. Environ Sci Pollut Res Int.
Kolditz, O., et al., 2012. OpenGeoSys: An open-source initiative for numerical simulation of thermo-hydro-mechanical/chemical (THM/C) processes in porous media. Environmental Earth Sciences. 67**,** 589-599.
Komar, P. D., Reimers, C. E., 1978. Grain shape effects on settling rates. The Journal of Geology. 86**,** 193-209.
Kong, M., et al., 2011. Tuning the relative concentration ratio of bulk defects to surface defects in TiO_2 nanocrystals leads to high photocatalytic efficiency. J Am Chem Soc. 133**,** 16414-7.
Kovalev, A., 2013. Trends of the nanomaterial market. Mediterr J Soc Sci.
Kranzioch, I., et al., 2013. Dechlorination and organohalide-respiring bacteria dynamics in sediment samples of the Yangtze Three Gorges Reservoir. Environ Sci Pollut Res Int. 20**,** 7046-56.
Kreisz, S., et al., 2000. Polypropylene as regenerable absorber for PCDD/F emission control. Chemosphere. 40**,** 1029-1031.
Krug, H. F., Wick, P., 2011. Nanotoxicology: An interdisciplinary challenge. Angew Chem Int Ed Engl. 50**,** 1260-78.
Krysanov, E. Y., et al., 2010. Effect of nanoparticles on aquatic organisms. Biol Bull. 37**,** 406-412.
Kühnel, D., et al., 2014. Environmental impacts of nanomaterials: Providing comprehensive information on exposure, transport and ecotoxicity - the project DaNa2.0. Env Sci Eur. 26**,** 21.
Kühnel, D., Nickel, C., 2014. The OECD expert meeting on ecotoxicology and environmental fate-Towards the development of improved OECD guidelines for the testing of nanomaterials. Sci Total Environ. 472**,** 347-53.
Kuiken, T., 2010. The project on emerging nanotechnologies and nanoremediation. Environmental Earth Sciences. 60**,** 903-907.
Kulacki, K. J., Cardinale, B. J., 2012. Effects of nano-titanium dioxide on freshwater algal population dynamics.
Kumar, A., et al., 2011. Cellular uptake and mutagenic potential of metal oxide nanoparticles in bacterial cells. Chemosphere. 83**,** 1124-32.
Kumar, N., et al., 2014a. Molecular insights of oxidation process of iron nanoparticles: Spectroscopic, magnetic, and microscopic evidence. Environ Sci Technol. 48**,** 13888-94.
Kumar, N., et al., 2014b. Inhibition of sulfate reducing bacteria in aquifer sediment by iron nanoparticles. Water Res. 51**,** 64-72.
La Rocca, C., Mantovani, A., 2006. From environment to food: The case of PCB. Ann Ist Super Sanita. 42**,** 410-416.
Laasch, T., Laasch, E., Trinkwasserversorgung. Haustechnik. Springer Fachmedien Wiesbaden, 2013, pp. 81-161.
LABO, Bundesweite Kennzahlen zur Altlastenstatistik. Bund/Länder-Arbeitsgemeinschaft Bodenschutz ALA-Ständiger Ausschuss Altlasten, 2012.
Lallas, P. L., 2001. The stockholm convention on persistent organic pollutants. Am J Int Law. 95**,** 692.
Lammel, T., et al., 2015. Potentiating effect of graphene nanomaterials on aromatic environmental pollutant-induced cytochrome P450 1A expression in the topminnow fish hepatoma cell line PLHC-1. Environ Toxicol. 30**,** 1192-204.

Lammer, E., et al., 2009. Is the fish embryo toxicity test (FET) with the zebrafish (*Danio rerio*) a potential alternative for the fish acute toxicity test? Comp Biochem Physiol C Toxicol Pharmacol. 149**,** 196-209.

Landsiedel, R., et al., 2009. Genotoxicity investigations on nanomaterials: Methods, preparation and characterization of test material, potential artifacts and limitations-Many questions, some answers. Mutat Res. 681**,** 241-58.

Lead, J. R., Wilkinson, K. J., 2006. Aquatic colloids and nanoparticles: Current knowledge and future trends. Environ Chem. 3**,** 159-171.

LeBel, C. P., et al., 1992. Evaluation of the probe 2',7'-dichlorofluorescin as an indicator of reactive oxygen species formation and oxidative stress. Chem Res Toxicol. 5**,** 227-231.

Lee, S.-H., et al., Catalyst for removing dioxin and preparation method thereof. Google Patents, 2004.

Leist, M., 2014. Consensus report on the future of animal-free systemic toxicity testing. ALTEX. 31**,** 341-356.

Léry, X., Fédière, G., 1990. A new serum-free medium for lepidopteran cell culture. J Invertebr Pathol. 55**,** 342-349.

Li, H., et al., 2009. Effects of waterborne nano-iron on medaka (*Oryzias latipes*): Antioxidant enzymatic activity, lipid peroxidation and histopathology. Ecotoxicol Environ Saf. 72**,** 684-92.

Li, L., et al., 2015. The potentiation effect makes the difference: Non-toxic concentrations of ZnO nanoparticles enhance Cu nanoparticle toxicity *in vitro*. Sci Total Environ. 505**,** 253-260.

Li, W., et al., 1999. A new enzyme immunoassay for PCDD/F TEQ screening in environmental samples: Comparison to micro-EROD assay and to chemical analysis. Chemosphere. 38**,** 3313-8.

Li, W. C., et al., 2007. Keratinocyte serum-free medium maintains long-term liver gene expression and function in cultured rat hepatocytes by preventing the loss of liver-enriched transcription factors. Int J Biochem Cell Biol. 39**,** 541-54.

Li, X.-q., et al., 2006. Zero-valent iron nanoparticles for abatement of environmental pollutants: Materials and engineering aspects. Crit Rev Solid State. 31**,** 111-122.

Li, Z., et al., 2010. Adsorbed polymer and NOM limits adhesion and toxicity of nano scale zerovalent iron to *E. coli*. Environ Sci Technol. 44**,** 3462-7.

Liebsch, M., Spielmann, H., 2002. Currently available *in vitro* methods used in the regulatory toxicology. Toxicol Lett. 127**,** 127-134.

Lin, D., et al., 2010. Fate and transport of engineered nanomaterials in the environment. J Environ Qual. 39**,** 1896-908.

Liu, A., et al., 2014. Formation of lepidocrocite (γ-FeOOH) from oxidation of nanoscale zero-valent iron (nZVI) in oxygenated water. RSC Adv. 4**,** 57377-57382.

Liu, A., et al., 2015. Transformation and composition evolution of nanoscale zero valent iron (nZVI) synthesized by borohydride reduction in static water. Chemosphere. 119**,** 1068-74.

Liu, Y., et al., 2005. Trichloroethene hydrodechlorination in water by highly disordered monometallic nanoiron. Chemistry of Materials. 17**,** 5315-5322.

Liu, Y., Lowry, G. V., 2006. Effect of particle age (fe^0 content) and solution pH on NZVI reactivity: H_2 evolution and TCE dechlorination. Environ Sci Technol. 40**,** 6085-6090.

Loffler, F. E., et al., 2000. 16s rRNA gene-based detection of tetrachloroethene-Dechlorinating *Desulfuromonas* and *Dehalococcoides* species. Appl Environ Microbiol. 66**,** 1369-1374.

Lohner, S. T., et al., 2011. Sequential reductive and oxidative biodegradation of chloroethenes stimulated in a coupled bioelectro-process. Environ Sci Technol. 45**,** 6491-7.

Lohner, S. T., Tiehm, A., 2009. Application of electrolysis to stimulate microbial reductive PCE dechlorination and oxidative VC biodegradation. Environ Sci Technol. 43**,** 7098-104.

Londergan, J. T., et al., 2001. DNAPL removal from a heterogeneous alluvial aquifer by surfactant-enhanced aquifer remediation. Ground Water Monit Remediat. 21**,** 57-67.

Longnecker, M. P., et al., 1997. The human health effects of DDT (dichlorodiphenyltrichloroethane) and PCBS (polychlorinated biphenyls) and an overview of organochlorines in public health. Annu Rev Public Health. 18**,** 211-44.

Loveland, J. P., et al., 2003. Colloid transport in a geochemically heterogeneous porous medium: Aquifer tank experiment and modeling. Journal of Contaminant Hydrology. 65**,** 161-182.

Lowry, G. V., Johnson, K. M., 2004. Congener-specific dechlorination of dissolved PCBs by microscale and nanoscale zerovalent iron in a water/methanol solution. Environ Sci Technol. 38**,** 5208-16.

Ma, X., et al., 2013. Phytotoxicity and uptake of nanoscale zero-valent iron (nZVI) by two plant species. Sci Total Environ. 443**,** 844-9.
Macé, C., et al., 2006. Nanotechnology and groundwater remediation: A step forward in technology understanding. Remediation. 16**,** 23-33.
Mackay, D. M., Cherry, J. A., 1989. Groundwater contamination: Pump-and-treat remediation. Environ Sci Technol. 23**,** 630-636.
Mackenzie, K., et al., 2012. Carbo-Iron – An Fe/AC composite – As alternative to nano-iron for groundwater treatment. Water Res. 46**,** 3817-3826.
Mahapatra, I., et al., 2013. Potential environmental implications of nano-enabled medical applications: Critical review. Environ Sci Process Impacts. 15**,** 123-44.
Maron, D. M., Ames, B. N., 1983. Revised methods for the *Salmonella* mutagenicity test. Mutation Research/Environmental Mutagenesis and Related Subjects. 113**,** 173-215.
Marsalek, B., et al., 2012. Multimodal action and selective toxicity of zerovalent iron nanoparticles against cyanobacteria. Environ Sci Technol. 46**,** 2316-23.
Masarovičová, E., Kráľová, K., 2013. Metal Nanoparticles and Plants / Nanocząstki Metaliczne I Rośliny. Ecological Chemistry and Engineering S. 20.
Matheson, L. J., Tratnyek, P. G., 1994. Reductive dehalogenation of chlorinated methanes by iron metal. Environ Sci Technol. 28**,** 2045-53.
Mattick, C. S., et al., 2015. A case for systemic environmental analysis of cultured meat. J Integr Agric. 14**,** 249-254.
Mattison, K., et al., 2003. A primer on particle sizing using dynamic light scattering. Am Biotechnol Lab. 21**,** 20-22.
Maynard, A., Michelson, E., The nanotechnology consumer products inventory. Woodrow Wilson International Center for Scholars, Washington, DC, , Vol. 2006, 2006.
Maynard, A. D., 2011. Don't define nanomaterials. Nature. 475**,** 31-31.
Maynard, A. D., et al., 2006. Safe handling of nanotechnology. Nature. 444**,** 267-9.
McCann, J., et al., 1975. Detection of carcinogens as mutagens in the *Salmonella*/microsome test: Assay of 300 chemicals. Proc. Natl. Acad. Sci. U. 75**,** 5135–5139.
McDowell-Boyer, L. M., et al., 1986. Particle transport through porous media. Water Resources Research. 22**,** 1901-1921.
McGeough, K. L., et al., 2007. Carbon disulfide removal by zero valent iron. Environ Sci Technol. 41**,** 4607-12.
Meyer, W., et al., 2014. Mutagenicity, dioxin-like activity and bioaccumulation of alkylated picene and chrysene derivatives in a German lignite. Sci Total Environ. 497**,** 634-641.
Meylan, W. M., Howard, P. H., 1991. Bond contribution method for estimating henry's law constants. Environ Toxicol Chem. 10**,** 1283-1293.
Meylan, W. M., Howard, P. H., 1993. Computer estimation of the Atmospheric gas-phase reaction rate of organic compounds with hydroxyl radicals and ozone. Chemosphere. 26**,** 2293-2299.
Michael C. Alley, et al., 1988. Feasibility of drug screening with panels of human tumor cells lines using a microculture tetrazolium assay. Cancer Res. 48**,** 589-601.
Miljevic, B., et al., 2014. To sonicate or not to sonicate PM filters: Reactive oxygen species generation upon ultrasonic irradiation. Aerosol Sci Technol. 48**,** 1276-1284.
Moir, D., et al., 1997. The subchronic toxicity of acridine in the rat. J Environ Sci Health B. 32**,** 545-64.
Moore, M. N., 2006. Do nanoparticles present ecotoxicological risks for the health of the aquatic environment? Environ Int. 32**,** 967-76.
Mortelmans, K., Zeiger, E., 2000. The Ames *Salmonella/*microsome mutagenicity assay. Mutation Research/Fundamental and Molecular Mechanisms of Mutagenesis. 455**,** 29-60.
Mueller, N. C., et al., 2012. Application of nanoscale zero valent iron (NZVI) for groundwater remediation in Europe. Environ Sci Pollut Res Int. 19**,** 550-8.
Mueller, N. C., Nowack, B., 2008. Exposure modeling of engineered nanoparticles in the environment. Environ Sci Technol. 42**,** 4447-53.
Mueller, N. C., Nowack, B., 2010. Nanoparticles for remediation: Solving big problems with little particles. Elements. 6**,** 395-400.
Müller, C., et al., 2006a. Sanierung mit Nano-Eisen Stand der Technik. altlasten spektrum. 2**,** 2006.
Müller, C., et al., 2006b. Nano-Eisen Feldversuch: Strategie, Durchführung, Ergebnisse und Auswertung. altlasten spektrum. 3**,** 137-147.

Müller, N. C., Nowack, B., 2010. Nano zero valent iron—The solution for water and soil remediation. Report of the ObservatoryNANO. 1-34.

Mundt, M., Hollender, J., 2005. Simultaneous determination of NSO-heterocycles, homocycles and their metabolites in groundwater of tar oil contaminated sites using LC with diode array UV and fluorescence detection. J Chromatogr. 1065**,** 211-218.

Murk, A. J., et al., 1996. Chemical-activated luciferase gene expression (CALUX): A novel *in vitro* bioassay for Ah receptor active compounds in sediments and pore water. Fundam Appl Toxicol. 33**,** 149-60.

Myhre, O., et al., 2003. Evaluation of the probes 2′,7′-dichlorofluorescin diacetate, luminol, and lucigenin as indicators of reactive species formation. Biochem Pharmacol. 65**,** 1575-1582.

Nagai, T., et al., 2013. Application of a fluorometric microplate algal toxicity assay for riverine periphytic algal species. Ecotoxicol Environ Saf. 94**,** 37-44.

Naqvi, S., et al., 2010. Concentration-dependent toxicity of iron oxide nanoparticles mediated by increased oxidative stress. Int J Nanomedicine. 5**,** 983-9.

Nebert, D. W., et al., 2004. Role of aryl hydrocarbon receptor-mediated induction of the CYP1 enzymes in environmental toxicity and cancer. J Biol Chem. 279**,** 23847-50.

Nel, A., et al., 2006. Toxic potential of materials at the nanolevel. Science. 311**,** 622-7.

Nel, A. E., et al., 2009. Understanding biophysicochemical interactions at the nano-bio interface. Nat Mater. 8**,** 543-57.

Nemecek, J., et al., 2014. Nanoscale zero-valent iron application for *in situ* reduction of hexavalent chromium and its effects on indigenous microorganism populations. Sci Total Environ. 485-486**,** 739-47.

Neuwoehner, J., et al., 2009. Ecotoxicity of quinoline and hydroxylated derivatives and their occurrence in groundwater of a tar-contaminated field site. Ecotoxicol Environ Saf. 72**,** 819-27.

Ng, C. T., et al., 2010. Current studies into the genotoxic effects of nanomaterials. J Nucleic Acids. 2010.

Nichols, G., et al., 2002. A review of the terms agglomerate and aggregate with a recommendation for nomenclature used in powder and particle characterization. J Pharm Sci. 91**,** 2103-9.

Nickel, C., et al., 2014. Dynamic light-scattering measurement comparability of nanomaterial suspensions. J Nanopart Res. 16**,** 1-12.

Nieuwoudt, C., et al., 2009. Dioxin-like chemicals in soil and sediment from residential and industrial areas in central South Africa. Chemosphere. 76**,** 774-83.

Novotna, A., et al., 2011. Novel stably transfected gene reporter human hepatoma cell line for assessment of aryl hydrocarbon receptor transcriptional activity: Construction and characterization. Environ Sci Technol. 45**,** 10133-9.

Nowack, B., et al., 2014. How to consider engineered nanomaterials in major accident regulations? Env Sci Eur. 26**,** 2.

O'Carroll, D., et al., 2013. Nanoscale zero valent iron and bimetallic particles for contaminated site remediation. Adv Water Resour. 51**,** 104-122.

Oberdörster, G., et al., 2005. Nanotoxicology: An emerging discipline evolving from studies of ultrafine particles. Environ Health Perspect. 113**,** 823-839.

Oberdörster, G., et al., 2007. Toxicology of nanoparticles: A historical perspective. Nanotoxicology. 1**,** 2-25.

OECD, 1997. Test No. 471: Bacterial Reverse Mutation Test.

OECD, 2004. Test No. 202: *Daphnia sp.* Acute Immobilisation Test.

OECD, 2011. Test No. 201: Freshwater Alga and Cyanobacteria, Growth Inhibition Test.

OECD, 2012. Guidance on sample preparation and dosimetry for the safety testing on manufactured nanomaterials. ENV/JM/Mono. 2012.

OECD, 2013. Test No. 236: Fish Embryo Acute Toxicity (FET) Test.

OECD, 2014a. Draft Guidance Document on the use of OECD Test Guidelines on genotoxicity testing for manufactured nanomaterials.

OECD, 2014b. Report of the OECD expert meeting on the physical chemical properties of manufactured nanomaterials and test guidelines. ENV/JM/MONO. 15.

Olsman, H., et al., 2007. Relative differences in aryl hydrocarbon receptor-mediated response for 18 polybrominated and mixed halogenated dibenzo-*p*-dioxins and -furans in cell lines from four different species. Environ Toxicol Chem. 26**,** 2448-54.

Page, P., et al., 2014. Effect of serum and oxygen concentration on gene expression and secretion of paracrine factors by mesenchymal stem cells. Int J Cell Biol. 2014**,** 601063.

Pal, A. K., et al., 2012. Screening for oxidative stress elicited by engineered nanomaterials: Evaluation of acellular DCFH assay. Dose Response. 10**,** 308-30.

Pan, X., et al., 2010. Mutagenicity evaluation of metal oxide nanoparticles by the bacterial reverse mutation assay. Chemosphere. 79**,** 113-6.

Pan, Y., et al., 2013. High-sensitivity real-time analysis of nanoparticle toxicity in green fluorescent protein-expressing zebrafish. Small. 9**,** 863-9.

Pankow, J. F., Cherry, J. A., 1996. Dense chlorinated solvents and other DNAPLs in groundwater: History, behavior, and remediation. Waterloo Press Portland Oregon.

Park, J. Y. K., et al., 1996. Induction of cytochrome P4501A1 by 2,3,7,8-tetrachlorodibenzo-*p*-dioxin or indolo(3,2-b)carbazole is associated with oxidative DNA damage. Proceedings of the National Academy of Sciences of the United States of America. 93**,** 2322-2327.

Parkhurst, B. R., et al., 1981. The chronic toxicity to *Daphnia magna* of acridine, a representative azaarene present in synthetic fossil fuel products and wastewaters. Environmental Pollution Series A, Ecological and Biological. 24**,** 21-30.

Parkinson, D., et al., 2004. Remediation of a chlorinated solvent-contaminated site using steam injection and extraction. Environ Geosci. 11**,** 239-253.

Pascall, M. A., et al., 2005. Uptake of polychlorinated biphenyls (PCBs) from an aqueous medium by polyethylene, polyvinyl chloride, and polystyrene films. J Agric Food Chem. 53**,** 164-9.

Patil, S. S., et al., 2013. Site-specific pre-evaluation of bioremediation technologies for chloroethene degradation. Int J Environ Sci Technol (Tehran). 11**,** 1869-1880.

Patil, S. S., et al., 2015. Nanoparticles for environmental clean-up: A review of potential risks and emerging solutions. Environmental Technology & Innovation.

Pazos, P., et al., 2004. Culturing cells without serum: Lessons learnt using molecules of plant origin. ALTEX 21**,** 67-72.

Peddinghaus, S., et al., 2012. Quantitative assessment of the embryotoxic potential of NSO-heterocyclic compounds using zebrafish (*Danio rerio*). Reprod Toxicol. 33**,** 224-32.

Pennell, K. D., et al., 1994. Surfactant enhanced remediation of soil columns contaminated by residual tetrachloroethylene. J Contam Hydrol. 16**,** 35-53.

Perrin, D., Dissociation constants of organic bases in aqueous solution. In: Butterworths, (Ed.), London, 1965.

Perry, R., Green, D., 1984. Perry's chemical handbook. Physical and chemical data. McGraw-Hill, New York.

Persoone, G., et al., 2009. Review on the acute *Daphnia magna* toxicity test – Evaluation of the sensitivity and the precision of assays performed with organisms from laboratory cultures or hatched from dormant eggs. Knowledge and Management of Aquatic Ecosystems. 01.

Peters, A. K., et al., 2004. Effects of polybrominated diphenyl ethers on basal and TCDD-induced ethoxyresorufin activity and cytochrome P450-1A1 expression in MCF-7, HepG2, and H4IIE cells. Toxicol Sci. 82**,** 488-96.

Petosa, A. R., et al., 2010. Aggregation and deposition of engineered nanomaterials in aquatic environments: Role of physicochemical interactions. Environ Sci Technol. 44**,** 6532-49.

Phenrat, T., et al., 2010. Transport and deposition of polymer-modified Fe0 nanoparticles in 2-D heterogeneous porous media: Effects of particle concentration, Fe0 content, and coatings. Environ Sci Technol. 44**,** 9086-93.

Phenrat, T., et al., 2011. Polymer-modified Fe0 nanoparticles target entrapped NAPL in two dimensional porous media: Effect of particle concentration, NAPL saturation, and injection strategy. Environ Sci Technol. 45**,** 6102-9.

Phenrat, T., et al., 2009. Partial oxidation ("aging") and surface modification decrease the toxicity of nanosized zerovalent iron. Environ Sci Technol. 43**,** 195-200.

Phenrat, T., et al., 2008. Stabilization of aqueous nanoscale zerovalent iron dispersions by anionic polyelectrolytes: Adsorbed anionic polyelectrolyte layer properties and their effect on aggregation and sedimentation. Journal of Nanoparticle Research. 10**,** 795-814.

Phenrat, T., et al., 2007. Aggregation and sedimentation of aqueous nanoscale zerovalent iron dispersions. Environ Sci Technol. 41**,** 284-90.

Pieterse, B., et al., 2013. PAH-CALUX, an optimized bioassay for AhR-mediated hazard identification of polycyclic aromatic hydrocarbons (PAHs) as individual compounds and in complex mixtures. Environ Sci Technol. 47**,** 11651-9.

Pitot, H. C., et al., 1964. Hepatomas in tissue culture compared with adapting liver *in vivo*. J. Natl. Cancer Inst. Monogr. 13**,** 229-245.

Poland, A., Knutson, J. C., 1982. 2,3,7,8-tetrachlorodibenzo-*p*-dioxin and related halogenated aromatic hydrocarbons: Examination of the mechanism of toxicity. Annu Rev Pharmacol Toxicol. 22**,** 517-54.

Ponder, S. M., et al., 2000. Remediation of Cr(VI) and Pb(II) aqueous solutions using supported, nanoscale zero-valent iron. Environ Sci Technol. 34**,** 2564-2569.

Powers, K. W., et al., 2006. Research strategies for safety evaluation of nanomaterials. Part VI. Characterization of nanoscale particles for toxicological evaluation. Toxicol Sci. 90**,** 296-303.

Pumper, R. W., 1958. Adaptation of tissue culture cells to a serum-free medium. Science. 128**,** 363.

Quigg, A., et al., 2013. Direct and indirect toxic effects of engineered nanoparticles on algae: Role of natural organic matter. ACS Sustainable Chemistry & Engineering. 130603131533006.

Radenac, G., et al., 2004. Measurement of EROD activity: Caution on spectral properties of standards used. Mar Biotechnol. 6**,** 307-11.

Rajendran, S., et al., 2002. Synergistic corrosion inhibition by the sodium dodecylsulphate–Zn2+ system. Corros Sci. 44**,** 2243-2252.

Rana, S., Kalaichelvan, P. T., 2013. Ecotoxicity of nanoparticles. ISRN Toxicol. 2013**,** 574648.

Ranganatha, N., Kuppast, I. J., 2012. A review on alternatives to animal testing methods in drug development. Int J Pharm Pharm Sci. 4**,** 28-32.

Rauch, C., et al., 2011. Alternatives to the use of fetal bovine serum: Human platelet lysates as a serum substitute in cell culture media. ALTEX. 28**,** 305-316.

Reifferscheid, G., et al., 2012. International round-robin study on the Ames fluctuation test. Environ Mol Mutagen. 53**,** 185-97.

Reimer, L., 1984. Transmission Electron Microscopy.

Reiners, J. J., Jr., et al., 1990. Fluorescence assay for per-cell estimation of cytochrome P-450-dependent monooxygenase activities in keratinocyte suspensions and cultures. Anal Biochem. 188**,** 317-24.

Repetto, G., et al., 2008. Neutral red uptake assay for the estimation of cell viability/cytotoxicity. Nat Protoc. 3**,** 1125-31.

Riebeling, C., et al., 2011. Defined culture medium for stem cell differentiation: Applicability of serum-free conditions in the mouse embryonic stem cell test. Toxicol In Vitro. 25**,** 914-21.

Roco, M. C., 1999a. Nanoparticles and nanotechnology research. J Nanopart Res. 1**,** 1-6.

Roco, M. C., 1999b. Towards a US national nanotechnology initiative. J Nanopart Res. 1**,** 435-438.

Roco, M. C., 2003. Nanotechnology: Convergence with modern biology and medicine. Curr Opin Biotechnol. 14**,** 337-46.

Roco, M. C., 2007. Possibilities for global governance of converging technologies. J Nanopart Res. 10**,** 11-29.

Roco, M. C., et al., 2011. Nanotechnology research directions for societal needs in 2020: Summary of international study. J Nanopart Res. 13**,** 897-919.

Rodrigo-Moreno, A., et al., 2013. Transition metals: A double edge sward in ROS generation and signaling. Plant Signal Behav. 8**,** e23425.

Rodrigo, L., et al., 2001. Immunohistochemical evidence for the expression and induction of paraoxonase in rat liver, kidney, lung and brain tissue. Implications for its physiological role. Chem-Biol Interact. 137**,** 123-137.

Römbke, J., et al., 2006. Handlungsempfehlung für die ökotoxikologische Beurteilung von Böden. Sidus-Verlag.

Romer, I., et al., 2013. The critical importance of defined media conditions in *Daphnia magna* nanotoxicity studies. Toxicol Lett. 223**,** 103-8.

Romer, I., et al., 2011. Aggregation and dispersion of silver nanoparticles in exposure media for aquatic toxicity tests. J Chromatogr A. 1218**,** 4226-33.

Roos, W. P., Kaina, B., 2006. DNA damage-induced cell death by apoptosis. Trends Mol Med. 12**,** 440-50.

Rosická, D., Šembera, J., 2010. Assessment of influence of magnetic forces on aggregation of zero-valent iron nanoparticles. Nanoscale Res Lett.

Rota, C., et al., 1999. Evidence for free radical formation during the oxidation of 2'-7'-dichlorofluorescin to the fluorescent dye 2'-7'-dichlorofluorescein by horseradish peroxidase: Possible implications for oxidative stress measurements. Free Radic Biol Med. 27**,** 873-81.

Rushton, E. K., et al., 2010. Concept of assessing nanoparticle hazards considering nanoparticle dosemetric and chemical/biological response metrics. J Toxicol Environ Health, A. 73**,** 445-461.

Ruska, E., 1987. The development of the electron microscope and of electron microscopy. Rev Mod Phys. 59**,** 627-638.

Russell, W. M. S., et al., 1959. The principles of humane experimental technique.

Safe, S., 1990. Polychlorinated biphenyls (PCBs), dibenzo-*p*-dioxins (PCDDs), dibenzofurans (PCDFs), and related compounds: Environmental and mechanistic considerations which support the development of toxic equivalency factors (TEFs). Crit Rev Toxicol. 21**,** 51-88.

Safe, S., 1993. Development of bioassays and approaches for the risk assessment of 2,3,7,8-tetrachlorodibenzo-*p*-dioxin and related compounds. Environ Health Perspect. 101 Suppl 3**,** 317-25.

Safe, S., et al., 1995. Toxic equivalency factor approach for risk assessment of combustion by-products. Toxicol Environ Chem. 49**,** 181-191.

Sanderson, J. T., et al., 1996. Comparison of Ah receptor-mediated luciferase and ethoxyresorufin-*O*-deethylase induction in H4IIE cells: Implications for their use as bioanalytical tools for the detection of polyhalogenated aromatic hydrocarbons. Toxicol Appl Pharmacol. 137**,** 316-25.

Sarin, P., et al., 2004. Iron release from corroded iron pipes in drinking water distribution systems: Effect of dissolved oxygen. Water Res. 38**,** 1259-69.

Sato, W., et al., 2010. Construction of a system that simultaneously evaluates CYP1A1 and CYP1A2 induction in a stable human-derived cell line using a dual reporter plasmid. Drug Metab Pharmacokinet. 25**,** 180-189.

Sawyer, T., Safe, S., 1982. PCB isomers and congeners: Induction of aryl hydrocarbon hydroxylase and ethoxyresorufin-*O*-deethylase enzyme activities in rat hepatoma cells. Toxicol Lett. 13**,** 87-93.

Schecter, A., et al., 2006. Dioxins: An overview. Environ Res. 101**,** 419-28.

Schell, H., Compariments in which zero valent iron materials occur after injection. 2011.

Schell, H., et al., Wechselwirkungen zwischen mikrobieller und abiotischer CKW-Dechlorierung – Synergien und toxische Effekte. DaNa Meeting 2013, Frankfurt am Main, 2013, pp. 1-1.

Scherer, M. M., et al., 2000. Chemistry and microbiology of permeable reactive barriers for *in situ* groundwater clean up. Crit Rev Microbiol. 26**,** 221-64.

Scheringer, M., 2008. Nanoecotoxicology: Environmental risks of nanomaterials. Nat Nanotechnol. 3**,** 322-3.

Schipper, C. A., et al., 2013. Protocol for measuring dioxin-like activity in environmental samples using *in vitro* reporter gene DR-Luc assays.

Schiwy, A., et al., 2015a. Determination of the CYP1A-inducing potential of single substances, mixtures and extracts of samples in the micro-EROD assay with H4IIE cells. Nat. Protocols. 10**,** 1728-1741.

Schiwy, A., et al., Ecotoxic evaluation of zero-valent iron nanomaterials in the aquatic environment. 2012, pp. 1-1.

Schiwy, S., et al., 2015b. A novel contact assay for testing aryl hydrocarbon receptor (AhR)-mediated toxicity of chemicals and whole sediments in zebrafish (*Danio rerio*) embryos. Environ Sci Pollut Res Int. 1-14.

Schlaeger, E. J., Christensen, K., 1999. Transient gene expression in mammalian cells grown in serum-free suspension culture. Cytotechnology. 30**,** 71-83.

Schlag, S., et al., Nanoscale chemicals and materials applications and market overview. International Conference on Nanoscience Engineering and Technology ICONSET 2011 IEEE, 2011, pp. 308-313.

Schlanges, I., et al., 2008. Identification, quantification and distribution of Pac-metabolites, heterocyclic Pac and substituted Pac in groundwater samples of tar-contaminated sites from germany. Polycyc Aromatic Compounds. 28**,** 320-338.

Schlich, K., et al., 2013. Hazard assessment of a silver nanoparticle in soil applied via sewage sludge. Env Sci Eur. 25**,** 17.
Schmidt, K., et al., Synergies between abiotic (zero valent iron) and biological reductive dechlorination of chloroethenes. AquaConSoil 2013, Barcelona, Spain, 2013.
Schmidt, K. R., et al., Nanopartikel zur Sanierung von Grundwasserschadensfällen. TZW-Kolloqium, Vol. Innovation und Praxisforschung für das Wasserfach, Karlsruhe, 2011.
Schmidt, K. R., et al., 2006. Evaluation of 16S-PCR detection of *Dehalococcoides* at two chloroethene-contaminated sites. Water Sci Technol. 6**,** 129.
Schmidt, K. R., Tiehm, A., 2008. Natural attenuation of chloroethenes: Identification of sequential reductive/oxidative biodegradation by microcosm studies. Water Sci Technol. 58**,** 1137-45.
Schmitz, H. J., et al., 1996. CYP1A1-inducing potency in H4IIE cells and chemical composition of technical mixtures of polychlorinated biphenyls. Environ Toxicol Pharmacol. 1**,** 73-9.
Scholz, S., et al., 2008. The zebrafish embryo model in environmental risk assessment-Applications beyond acute toxicity testing. Environ Sci Pollut Res Int. 15**,** 394-404.
Schramm, K. W., et al., 2001. Comparison of dioxin-like-response *in vitro* and chemical analysis of emissions and materials. Chemosphere. 42**,** 551-7.
Schrand, A. M., et al., 2010. Metal-based nanoparticles and their toxicity assessment. Wiley Interdiscip Rev Nanomed Nanobiotechnol. 2**,** 544-68.
Schulze, C., et al., 2008. Not ready to use – Overcoming pitfalls when dispersing nanoparticles in physiological media. Nanotoxicology. 2**,** 51-61.
Schummer, J., 2004. Multidisciplinarity, interdisciplinarity, and patterns of research collaboration in nanoscience and nanotechnology. Scientometrics. 59**,** 425-465.
Schwab, F., et al., 2011. Are carbon nanotube effects on green algae caused by shading and agglomeration? Environ Sci Technol. 45**,** 6136-44.
Schwirzer, S. M., et al., 1998. Establishment of a simple cleanup procedure and bioassay for determining 2,3,7,8-tetrachlorodibenzo-*p*-dioxin toxicity equivalents of environmental samples. Ecotoxicol Environ Saf. 41**,** 77-82.
Scown, T. M., et al., 2010. Review: Do engineered nanoparticles pose a significant threat to the aquatic environment? Crit Rev Toxicol. 40**,** 653-70.
Seitz, F., et al., 2013. Nanoparticle toxicity in *Daphnia magna* reproduction studies: The importance of test design. Aquat Toxicol. 126**,** 163-8.
Shindo, D., Oikawa, T., Energy dispersive X-ray spectroscopy. Analytical electron microscopy for materials science. Springer Japan, Tokyo, 2002, pp. 81-102.
Shitamura, A., et al., 2005. Bioassay-based screening of microorganisms that degrade dioxin using substrate-immobilized microtubes. Anal Biochem. 347**,** 135-43.
Siegel, W., Foster, L., 2013. Fetal bovine serum: The impact of geography. Bioprocessing. 12**,** 28-30.
Siehoff, S., et al., 2009. Periphyton as alternative food source for the filter-feeding cladoceran *Daphnia magna*. Freshwat Biol. 54**,** 15-23.
Simon, A., et al., Chapter 4. Assessment of uptake and toxicity of multiwalled carbon nanotubes and triclocarban in zebrafish (*Danio rerio*) early life stages. At the End of the Life Cycle of Carbon Nanotubes: An Ecotoxicological Point of View, 2014a.
Simon, A., et al., 2014b. Effects of multiwalled carbon nanotubes and triclocarban on several eukaryotic cell lines: Elucidating cytotoxicity, endocrine disruption, and reactive oxygen species generation. Nanoscale Res Lett. 9**,** 396.
Singh, N., et al., 2010. Potential toxicity of superparamagnetic iron oxide nanoparticles (SPION). Nano Rev. 1.
Singh, N., et al., 2009. NanoGenotoxicology: The DNA damaging potential of engineered nanomaterials. Biomaterials. 30**,** 3891-914.
Singh, R., et al., 2012. Removal of Cr(VI) by nanoscale zero-valent iron (nZVI) from soil contaminated with tannery wastes. Bull Environ Contam Toxicol. 88**,** 210-4.
Sinkkonen, S., Paasivirta, J., 2000. Degradation half-life times of PCDDs, PCDFs and PCBs for environmental fate modeling. Chemosphere. 40**,** 943-9.
Skehan, P., et al., 1990. New colorimetric cytotoxicity assay for anticancer-drug screening. J Natl Cancer Inst. 82**,** 1107-12.
Smith, P. K., et al., 1985. Measurement of protein using bicinchoninic acid. Anal Biochem. 150**,** 76-85.

Smits, T. H., et al., 2004. Development of a real-time PCR method for quantification of the three genera *Dehalobacter*, *Dehalococcoides*, and *Desulfitobacterium* in microbial communities. J Microbiol Methods. 57**,** 369-78.

Snyder, R. L., X-ray diffraction. Materials Science and Technology. Wiley-VCH Verlag GmbH & Co. KGaA, 2006.

Sohn, E. K., et al., 2015. Acute toxicity comparison of single-walled carbon nanotubes in various freshwater organisms. Biomed Res Int. 2015**,** 323090.

Sonneveld, E., et al., 2007. Glucocorticoid-enhanced expression of dioxin target genes through regulation of the rat aryl hydrocarbon receptor. Toxicol Sci. 99**,** 455-69.

Sorensen, S. N., Baun, A., 2015. Controlling silver nanoparticle exposure in algal toxicity testing- A matter of timing. Nanotoxicology. 9**,** 201-9.

Spagnoli, J. J., Skinner, L. C., 1977. PCB's in fish from selected waters of New York state. Pestic Monit J. 11**,** 69-87.

Stelzer, E. H., 2002. Beyond the diffraction limit? Nature. 417**,** 806-7.

Stieber, M., et al., 2011. Treatment of pharmaceuticals and diagnostic agents using zero-valent iron--kinetic studies and assessment of transformation products assay. Environ Sci Technol. 45**,** 4944-50.

Stohs, S. J., Bagchi, D., 1995. Oxidative mechanisms in the toxicity of metal ions. Free Radical Biol Med. 18**,** 321-336.

Strahle, U., et al., 2012. Zebrafish embryos as an alternative to animal experiments- A commentary on the definition of the onset of protected life stages in animal welfare regulations. Reprod Toxicol. 33**,** 128-32.

Stroo, H. F., et al., 2003. Remediating chlorinated solvent source zones. Environ Sci Technol. 37**,** 224A-230A.

Stumm, W., Lee, G. F., 1961. Oxygenation of ferrous iron. Ind Eng Chem. 53**,** 143-146.

Stumm, W., Morgan, J. J., 2012. Aquatic chemistry: Chemical equilibria and rates in natural waters. John Wiley & Sons.

Stupp, H. D., et al., 2007. Biologische Verfahren zur Sanierung von CKW-Grundwasserschäden - Systematik und Beschreibung der In-Situ-Techniken. altlasten spektrum.

Su, C., Puls, R. W., 2001. Arsenate and arsenite removal by zerovalent iron: Kinetics, redox transformation, and implications for *in situ* groundwater remediation. Environ Sci Technol. 35**,** 1487-92.

Su, C., et al., 2012. A two and half-year-performance evaluation of a field test on treatment of source zone tetrachloroethene and its chlorinated daughter products using emulsified zero valent iron nanoparticles. Water Res. 46**,** 5071-84.

Summer, C. L., et al., 1996. Effects induced by feeding organochlorine-contaminated carp from Saginaw Bay, Lake Huron, to laying White Leghorn hens. I. Effects on health of adult hens, egg production, and fertility. J Toxicol Environ Health. 49**,** 389-407.

Sun, J., et al., 2011. Cytotoxicity, permeability, and inflammation of metal oxide nanoparticles in human cardiac microvascular endothelial cells. Cell Biol Toxicol. 27**,** 333-342.

Sun, N., et al., 2001a. A novel two-dimensional model for colloid transport in physically and geochemically heterogeneous porous media. Journal of Contaminant Hydrology. 49**,** 173-199.

Sun, N., et al., 2001b. Sensitivity analysis and parameter identifiability for colloid transport in geochemically heterogeneous porous media. Water Resources Research. 37**,** 209-222.

Sun, Q., et al., 2008. Comparison of the reactivity of nanosized zero-valent iron (nZVI) particles produced by borohydride and dithionite reduction of iron salts. Nano. 03**,** 341-349.

Sun, Z., et al., 2015. Nano zerovalent iron particles induce pulmonary and cardiovascular toxicity in an *in vitro* human co-culture model. Nanotoxicology. 1-10.

Sung, W., Morgan, J. J., 1980. Kinetics and product of ferrous iron oxygenation in aqueous systems. Environ Sci Technol. 14**,** 561-568.

Suzuki, G., et al., 2004. Evaluation of mixture effects in a crude extract of compost using the CALUX bioassay and HPLC fractionation. Environ Int. 30**,** 1055-66.

Suzuki, G., et al., 2006. Time-course changes of mixture effects on AhR binding-dependent luciferase activity in a crude extract from a compost sample. Toxicol Lett. 161**,** 174-87.

Swamynathan, P., et al., 2014. Are serum-free and xeno-free culture conditions ideal for large scale clinical grade expansion of Wharton's jelly derived mesenchymal stem cells? A comparative study. Stem Cell Res Ther. 5**,** 88.

Szalay, B., et al., 2012. Potential toxic effects of iron oxide nanoparticles in *in vivo* and *in vitro* experiments. J Appl Toxicol. 32**,** 446-53.

Taghavy, A., et al., 2010. Effectiveness of nanoscale zero-valent iron for treatment of a PCE-DNAPL source zone. J Contam Hydrol. 118**,** 128-42.

Taniguchi, N., On the basic concept of nanotechnology. Proc Intl Conf Prod Eng Tokyo, Part II, Japan Society of Precision Engineering, Tokyo, 1974, pp. 18-23.

Tatarazako, N., Oda, S., 2007. The water flea *Daphnia magna* (Crustacea, Cladocera) as a test species for screening and evaluation of chemicals with endocrine disrupting effects on crustaceans. Ecotoxicology. 16**,** 197-203.

Taub, M., 1990. The use of defined media in cell and tissue culture. Toxicol In Vitro. 4**,** 213-225.

Tejamaya, M., et al., 2012. Stability of citrate, PVP, and PEG coated silver nanoparticles in ecotoxicology media. Environ Sci Technol. 46**,** 7011-7.

Tejs, S., 2008. The Ames test: A methodological short review. Environmental Biotechnology. 4**,** 7-14.

Tekkatte, C., et al., 2011. "Humanized" stem cell culture techniques: The animal serum controversy. Stem Cells Int. 2011**,** 504723.

Teuten, E. L., et al., 2009. Transport and release of chemicals from plastics to the environment and to wildlife. Philos Trans R Soc Lond B Biol Sci. 364**,** 2027-45.

Theelen, R. M. C., et al., 1993. Intake of 2,3,7,8 chlorine substituted dioxins, furans, and planar PCBs from food in the Netherlands: Median and distribution. Chemosphere. 27**,** 1625-1635.

Thiem, I., Boehmler, G., 2011a. Model for interpretation of coupled data from biotests based on the dioxin-like response of Ah-receptors. Organohalogen Compd. 73**,** 2124-2127.

Thiem, I., Boehmler, G., 2011b. Step by step analysis of recovery rates of dioxin like compounds in beef using the Micro-EROD-bioassay. Organohalogen Compd. 73**,** 2128-2131.

Thiem, I., et al., 2014. Modification of the Micro EROD-bioassay and validation for routine analysis demonstrated for beef and milk. Organohalogen Compd. 76**,** 161-164

Thiem, I., et al., 2006. Nachweis von Dioxinen und dioxinähnlichen Substanzen mit dem Micro-EROD-Bioassay: Untersuchungen von Milch und Rinderfett. Journal für Verbraucherschutz und Lebensmittelsicherheit. 1**,** 310-316.

Tiede, K., et al., 2008. Detection and characterization of engineered nanoparticles in food and the environment. Food Addit Contam Part A Chem Anal Control Expo Risk Assess. 25**,** 795-821.

Tiehm, A., et al., Hydrogenotrophic bioprocesses during chloroethene elimination in zero valent iron (ZVI) permeable reactive barriers (PRB). Contaminated Site Management in Europe, Gent, Belgium, 2009.

Tiehm, A., Schmidt, K. R., 2011. Sequential anaerobic/aerobic biodegradation of chloroethenes-Aspects of field application. Curr Opin Biotechnol. 22**,** 415-21.

Tiehm, A., et al., Microbial hydrogen consuming processes in ZVI permeable reactive barriers used for chloroethene elimination. ConSoil 2010, Salzburg, Austria, 2010.

Tiehm, A., et al., 2007. Assessment of natural microbial dechlorination. Ital. J. Eng. Geol. Environ. 1**,** 71-77.

Tillitt, D. E., et al., 1991a. H4IIE rat hepatoma cell bioassay-derived 2,3,7,8-tetrachlorodibenzo-*p*-dioxin equivalents in colonial fish-eating waterbird eggs from the Great Lakes. Arch Environ Contam Toxicol. 21**,** 91-101.

Tillitt, D. E., et al., 1991b. Characterization of the H4IIE rat hepatoma cell bioassay as a tool for assessing toxic potency of planar halogenated hydrocarbons in environmental samples. Environ Sci Technol. 25**,** 87-92.

Tilston, E. L., et al., 2013. Nanoscale zerovalent iron alters soil bacterial community structure and inhibits chloroaromatic biodegradation potential in Aroclor 1242-contaminated soil. Environ Pollut. 173**,** 38-46.

Tiraferri, A., et al., 2010. Transport and retention of microparticles in packed sand columns at low and intermediate ionic strengths: Experiments and mathematical modeling. Environmental Earth Sciences. 63**,** 847-859.

Todd, D. K., Mays, L. W., 1980. Groundwater Hydrology. Wileys.

Tosco, T., Sethi, R., 2009. MNM1D: A Numerical Code for Colloid Transport in Porous Media: Implementation and Validation. American Journal of Environmental Sciences. 5**,** 517-525.

Tosco, T., Sethi, R., 2010. Transport of non-newtonian suspensions of highly concentrated micro- and nanoscale iron particles in porous media: A modeling approach. Environ Sci Technol. 44**,** 9062-8.

Tratnyek, P. G., Johnson, R. L., 2006. Nanotechnologies for environmental cleanup. Nano Today. 1**,** 44-48.

Tue, N. M., et al., 2013. Dioxin-related compounds in house dust from New York State: Occurrence, *in vitro* toxic evaluation and implications for indoor exposure. Environ Pollut. 181C**,** 75-80.

UN, 2015. Globally harmonized system of classification and labelling of chemicals (GHS) - sixth revised edition. United Nations. New York and Geneva. 521.

United States International Trade Commission, Remediation and nature and landscape protection services: An examination of US and foreign markets. USITC Publication. Washington, DC, Washington, DC, 2004.

Upton, A. C., 1989. The question of thresholds for radiation and chemical carcinogenesis. Cancer Invest. 7**,** 267-276.

Valdovinosa, C., et al., 2013. Application of the EROD-H4IIE bioassay for the determination of dioxins in pork in comparison to high resolution gas chromatography coupled to high resolution mass spectrometry. Arch Med Vet. 45**,** 173-181.

Van den Berg, M., et al., 1998. Toxic equivalency factors (TEFs) for PCBs, PCDDs, PCDFs for humans and wildlife. Environ Health Perspect. 106**,** 775-92.

Van den Berg, M., et al., 2006. The 2005 World Health Organization reevaluation of human and mammalian toxic equivalency factors for dioxins and dioxin-like compounds. Toxicol Sci. 93**,** 223-41.

van den Berg, M., et al., 2013. Polybrominated dibenzo-*p*-dioxins, dibenzofurans, and biphenyls: Inclusion in the toxicity equivalency factor concept for dioxin-like compounds. Toxicol Sci. 133**,** 197-208.

van der Burg, B., et al., 2010. Optimization and prevalidation of the *in vitro* ERalpha CALUX method to test estrogenic and antiestrogenic activity of compounds. Reprod Toxicol. 30**,** 73-80.

van der Valk, J., et al., 2010. Optimization of chemically defined cell culture media - Replacing fetal bovine serum in mammalian *in vitro* methods. Toxicol In Vitro. 24**,** 1053-63.

van der Valk, J., et al., 2004. The humane collection of fetal bovine serum and possibilities for serum-free cell and tissue culture. Toxicol In Vitro. 18**,** 1-12.

Vannuccini, M. L., et al., 2015. Combination effects of nano-TiO2 and 2,3,7,8-tetrachlorodibenzo-*p*-dioxin (TCDD) on biotransformation gene expression in the liver of European sea bass *Dicentrarchus labrax*. Comparative Biochemistry and Physiology Part C: Toxicology & Pharmacology. 176–177**,** 71-78.

Velimirovic, M., et al., 2015. Use of CAH-degrading bacteria as test-organisms for evaluating the impact of fine zerovalent iron particles on the anaerobic subsurface environment. Chemosphere. 134**,** 338-45.

Villeneuve, D. L., et al., 2000. Derivation and application of relative potency estimates based on *in vitro* bioassay results. Environ Toxicol Chem. 19**,** 2835-2843.

Voelker, D., et al., 2015. Approach on environmental risk assessment of nanosilver released from textiles. Environ Res. 140**,** 661-72.

Volker, C., et al., 2013a. Comparative toxicity assessment of nanosilver on three *Daphnia* species in acute, chronic and multi-generation experiments. PLoS One. 8**,** e75026.

Volker, C., et al., 2013b. The biological effects and possible modes of action of nanosilver. Rev Environ Contam Toxicol. 223**,** 81-106.

von der Kammer, F., et al., 2012. Analysis of engineered nanomaterials in complex matrices (environment and biota): General considerations and conceptual case studies. Environ Toxicol Chem. 31**,** 32-49.

von der Ohe, P. C., et al., 2012. Triclosan-The forgotten priority substance? Environ Sci Pollut Res Int. 19**,** 585-91.

Vuori, K.-M., 1995. Direct and indirect effects of iron on river ecosystems. Ann Zool Fenn. 32**,** 317-329.

Wang, C.-B., Zhang, W.-x., 1997. Synthesizing nanoscale iron particles for rapid and complete dechlorination of TCE and PCBs. Environ Sci Technol. 31**,** 2154-2156.
Wang, C., et al., 2012. Toxicity effects of four typical nanomaterials on the growth of *Escherichia coli*, *Bacillus subtilis* and *Agrobacterium tumefaciens*. Environmental Earth Sciences. 65**,** 1643-1649.
Wang, L. M., et al., 2011. Effect and toxic mechanism of nanoparticles to algae. Advanced Materials Research. 343-344**,** 81-84.
Wappler, J., et al., 2013. Eliminating the need of serum testing using low serum culture conditions for human bone marrow-derived mesenchymal stromal cell expansion. Biomed Eng Online. 12**,** 15.
Warheit, D. B., 2008. How meaningful are the results of nanotoxicity studies in the absence of adequate material characterization? Toxicol Sci. 101**,** 183-185.
Warheit, D. B., et al., 2007. Pulmonary bioassay studies with nanoscale and fine-quartz particles in rats: Toxicity is not dependent upon particle size but on surface characteristics. Toxicol Sci. 95**,** 270-80.
Watson, J. D., Crick, F. H., 1953. Molecular structure of nucleic acids; a structure for deoxyribose nucleic acid. Nature. 171**,** 737-8.
Weber, R., et al., 2008. Dioxin- and POP-contaminated sites - Contemporary and future relevance and challenges. Environ. Sci. Pollut. Res. 15**,** 363-393.
Wei, Y. T., et al., 2012. Biodegradable surfactant stabilized nanoscale zero-valent iron for *in situ* treatment of vinyl chloride and 1,2-dichloroethane. J Hazard Mater. 211-212**,** 373-80.
Weil, M., et al., 2015. The oxidized state of the nanocomposite Carbo-Iron(R) causes no adverse effects on growth, survival and differential gene expression in zebrafish. Sci Total Environ. 530-531**,** 198-208.
Wernersson, A.-S., et al., 2015. The European technical report on aquatic effect-based monitoring tools under the water framework directive. Env Sci Eur. 27**,** 7.
Wessman, S. J., Levings, R. L., Collective experiences of adventitious viruses of animal-derived raw materials and what can be done about them. Cell Culture Engineering VI. Springer, 1998, pp. 43-48.
Westerfield, M., 2000. The zebrafish book: A guide for the laboratory use of zebrafish (*Danio rerio*). University of Oregon Press.
Westerfield, M., 2007. The zebrafish book: A guide for the laboratory use of zebrafish (*Danio rerio*), 5th edition. University of Oregon Press.
Whyte, J. J., et al., 2004. The H4IIE cell bioassay as an indicator of dioxin-like chemicals in wildlife and the environment. Crit Rev Toxicol. 34**,** 1-83.
Wiedemeier, T. H., et al., 1996. Approximation of biodegradation rate constants for monoaromatic hydrocarbons (BTEX) in ground water. Ground Water Monit Remediat. 16**,** 186-194.
Wielgosinski, G., 2010. The possibilities of reduction of polychlorinated dibenzo-*p*-dioxins and polychlorinated dibenzofurans emission. International Journal of Chemical Engineering. 2010**,** 1-11.
Wiersum, U. E., 1996. The formation of polycyclic aromatics, fullerenes and soot in combustion. The mechanism and the environmental connection. Polycyc Aromatic Compounds. 11**,** 291-300.
Williams, D. B., Carter, C. B., 2009. The transmission electron microscope. Springer.
Wilson, R. E., 1923. The mechanism of the corrosion of iron and steel in natural waters and the calculation of specific rates of corrosion. Ind Eng Chem. 15**,** 127-133.
Winterbourn, C. C., 1995. Toxicity of iron and hydrogen peroxide: The Fenton reaction. Toxicol Lett. 82-83**,** 969-974.
Wittevrongel, C., 2013. The three Rs—Do we need a new principle? ATLA. 41**,** 18.
Wixon, J., 2000a. *Danio rerio*, the zebrafish. Yeast. 1**,** 225-231.
Wixon, J., 2000b. Featured organism: *Danio rerio*, the zebrafish. Yeast. 17**,** 225-31.
Wölz, J., et al., 2008. Changes in toxicity and Ah receptor agonist activity of suspended particulate matter during flood events at the rivers Neckar and Rhine - A mass balance approach using *in vitro* methods and chemical analysis. Environ. Sci. Pollut. Res. 15**,** 536-553.
Worch, H., et al., 1983. Rust formation on iron - A model. Materials and corrosion. 34**,** 402-410.
Wyrwoll, A. J., et al., 2016. Size matters - The phototoxicity of TiO_2 nanomaterials. Environ Pollut. 208**,** 859-67.

Wyrwoll, A. J., et al., 2013. Environmental hazard of selected TiO2 nanomaterials under consideration of relevant exposure scenarios.
Xiao, H., et al., 2016. Optimized work-flow for identification of dioxin-like compounds in environmental samples combining high-throughput fractionation and bioassays. to be published.
Xiu, Z. M., et al., 2010a. Effect of bare and coated nanoscale zerovalent iron on *tce*A and *vcr*A gene expression in *Dehalococcoides* spp. Environ Sci Technol. 44**,** 7647-51.
Xiu, Z. M., et al., 2010b. Effects of nano-scale zero-valent iron particles on a mixed culture dechlorinating trichloroethylene. Bioresour Technol. 101**,** 1141-6.
Xu, R., 2001. Particle characterization: Light scattering methods. Springer Science & Business Media.
Yan, L., et al., 2013a. Chemical mechanisms of the toxicological properties of nanomaterials: Generation of intracellular reactive oxygen species. Chem Asian J.
Yan, W., et al., 2013b. Iron nanoparticles for environmental clean-up: Recent developments and future outlook. Environ Sci Process Impacts. 15**,** 63.
Yao, K.-M., et al., 1971. Water and waste water filtration. Concepts and applications. Environ Sci Technol. 5**,** 1105-1112.
Yeh, K.-J., et al., 2013. Competitive removal of two contaminants in a goethite-catalyzed fenton process at neutral pH. Environ Eng Sci. 30**,** 47-52.
Yin, J.-J., et al., 2012. Dual role of selected antioxidants found in dietary supplements: Crossover between anti- and pro-oxidant activities in the presence of copper. J Agric Food Chem. 60**,** 2554-2561.
Yu, Y., et al., 2015. Combined toxicity of amorphous silica nanoparticles and methylmercury to human lung epithelial cells. Ecotoxicol Environ Saf. 112**,** 144-52.
Yuan, B., et al., 2013. Laboratory-scale column study for remediation of TCE-contaminated aquifers using three-section controlled-release potassium permanganate barriers. J Environ Sci (China). 25**,** 971-977.
Zabetakis, K. M., et al., 2015. Toxicity of zero-valent iron nanoparticles to a trichloroethylene-degrading groundwater microbial community. J Environ Sci Health A Tox Hazard Subst Environ Eng. 50**,** 794-805.
Zeiger, E., 1998. Identification of rodent carcinogens and noncarcinogens using genetic toxicity tests: Premises, promises, and performance. Regul Toxicol Pharmacol. 28**,** 85-95.
Zeiger, M., et al., 2001. Inducing effects of dioxin-like polychlorinated biphenyls on CYP1A in the human hepatoblastoma cell line HepG2, the rat hepatoma cell line H4IIE, and rat primary hepatocytes: Comparison of relative potencies. Toxicol Sci. 63**,** 65-73.
Zepp, R. G., et al., 1992. Hydroxyl radical formation in aqueous reactions (pH 3-8) of iron(II) with hydrogen peroxide: The photo-Fenton reaction. Environ Sci Technol. 26**,** 313-319.
Zhang, H., et al., 2013. Rational development of a serum-free medium and fed-batch process for a GS-CHO cell line expressing recombinant antibody. Cytotechnology. 65**,** 363-78.
Zhang, M., Zhao, D., *In situ* dechlorination in soil and groundwater using stabilized zero-valent iron nanoparticles: Some field experience on effectiveness and limitations. Novel Solutions to Water Pollution. American Chemical Society, 2013, pp. 79-96.
Zhang, T. C., Huang, Y. H., 2006. Profiling iron corrosion coating on iron grains in a zerovalent iron system under the influence of dissolved oxygen. Water Res. 40**,** 2311-20.
Zhang, W.-x., 2003. Nanoscale iron particles for environmental remediation: An overview. J Nanopart Res. 5**,** 323-332.
Zhang, W.-x., Elliott, D. W., 2006. Applications of iron nanoparticles for groundwater remediation. Remediation. 16**,** 7-21.
Zhao, Z., et al., 2013. Degrading perchloroethene at ambient conditions using Pd and Pd-on-Au reduction catalysts. Appl Catal B. 140-141**,** 468-477.
Zhou, L., et al., 2014. Carboxymethyl cellulose coating decreases toxicity and oxidizing capacity of nanoscale zerovalent iron. Chemosphere. 104**,** 155-61.
Zhu, X., et al., 2012. Toxicity assessment of iron oxide nanoparticles in zebrafish (*Danio rerio*) early life stages. PLoS One. 7**,** e46286.
Zhuang, Y., et al., 2012. Kinetics and pathways for the debromination of polybrominated diphenyl ethers by bimetallic and nanoscale zerovalent iron: effects of particle properties and catalyst. Chemosphere. 89**,** 426-32.